Development of sustainable ground improvement methods using biochemical techniques

Laboratory of Biotechnology for Resources Engineering,
Division of Sustainable Resources Engineering,
Graduate School of Engineering,
Hokkaido University,
Japan

This thesis is presented for the degree of
Doctor of Philosophy in Sustainable
Resources Engineering

August 2016

G.G. N.N. Amarakoon

HOKKAIDO
UNIVERSITY

Declaration

I declare that, except where specific reference is made in the text to the work conducted by other authors, this thesis is my own account of my research and contains as its main content work that has not previously been submitted for a degree at any university.

Name: G.G.N.N. Amarakoon Signature: _____

Date: 12-08-2016 Date: _____

Acknowledgement

Foremost, I would like to express my deepest gratitude to my supervisors: Prof. Satoru KAWASAKI, Prof. Yoshiaki FUJII, and Prof. Tatsuya ISHIKAWA, and Associate Prof. Kazunori NAKASHIMA for all of the valuable discussion, useful brainstorm, helpful advice and encouragement throughout the study. Their supervision and discussion brought me to have new insights and ideas in the field of not only bio-cementation but also science. Their overly enthusiasm on science has made a deep impression on me. Their expert supervision encouraged me to keep enthusiasm on innovation, and helped me to overcome my weakness of writing.

I would also like to gratefully acknowledge Assistant Prof. Masaji KATO for their generous cooperation. The experiments were explained and done together with Dr. T. Danjo, Mr. T. Koreeda and Mr. Watanabe. It was a pleasure to work with them and I would also like to thank and acknowledge them.

I would like to express special thanks to my lab partners at Hokkaido University who made it a convivial place to work. I would also like to give my special thanks to Mrs. Hitomi for her support during the years I have been working on this thesis.

LIST OF CONTENT

CHAPTER 04: Syringe solidification test using MICP method

CHAPTER 05: Model test for sand solidification using MICP method

CHAPTER 06: Conclusions and future research

LIST OF TABLES

LIST OF FIGURES

CHAPTER 1

INTRODUCTION

1.1 RESEARCH BACKGROUND

Human ingenuity has been said to be driven by need. The need to accommodate an ever-growing global population has taken center stage in many societies and has pushed human inventiveness to new levels. Population and consequently civil projects have increased significantly in different countries during recent years. One area of need that has relied on evolving resourcefulness is the development of civil infrastructure needed to accommodate expanding populations; in particular, civil infrastructure should be built on and within suitable ground that must reliably support it. The idea of suitable ground has taken new meaning as expanding populations move into previously undeveloped areas and into areas previously bypassed due to poor ground conditions. As a consequence of movement into these areas, engineers face new challenges in defining suitable ground. Areas where seismic activity, geologic hazards, rising sea levels and declining water tables affect ground conditions are of particular concern.

Soil liquefaction describes a phenomenon whereby a saturated soil substantially loses strength and stiffness in response to an applied stress, usually earthquake shaking, causing it to behave like a liquid. The effects of liquefaction have been long understood, it was more thoroughly brought to the attention of engineers after the 1964 Niigata earthquake and 1964 Alaska earthquake. In Japan, many areas are potential to liquefaction after the earthquake happens. During an earthquake, significant damage can result due to the instability of the soil in the area affected by internal seismic waves. The soil response depends on the mechanical characteristics of the soil layers, the depth of the water table and the intensities and duration of the ground shaking. If the soil consists of deposits of loose granular materials it may be

compacted by the ground vibrations induced by the earthquake, resulting in large settlement and differential settlements of the ground surface. This compaction of the soil may result in the development of excess hydrostatic pore water pressures of sufficient magnitude to cause liquefaction of the soil, resulting in settlement, tilting and rupture of structures.

Therefore, soil improvement is continuously in need due to the increase of civil infrastructure. According to the research in 2008, every year more than 40,000 soil improvement projects worth of more than 6 billion US dollars take place around the earth (DeJong et al., 2010). Available methods of soil improvement are often based on utilizing outside material (cement, chemical grout, geo-synthetics, strips and etc.) or mechanical energy (dynamic compaction, compaction piles, vibroflotation and etc.). Various techniques for ground improvement have been developed over the years to meet these challenges. Recently, efforts to develop new ground improvement techniques have focused on searching for sustainable, cost-effective methods to either supplement or replace traditional techniques.

Efforts to develop cost-effective ground improvement solutions to meet ground improvement challenges have become increasingly complex due to the varying nature and broad scope of problematic soils. These efforts are further complicated by sustainable considerations on local and global scales. Building materials, designs, and methods of previous generations often need to be either replaced or supplemented by innovative materials and sustainable practices to limit environmental impacts while simultaneously meeting design considerations. One prime example of a nearly indispensable building material that poses significant sustainability concerns is Portland cement and, by extension, its use in making concrete and mortars. Direct treatment with Portland cement is widely used in ground improvement applications where existing soils require strengthening through soil binding. Unfortunately, Portland cement production is extremely energy intensive and a major source of carbon dioxide (CO_2) pollution, as well as emissions of sulfur and nitrogen

oxides. Cement production, most commonly Portland cement, accounts for the second largest source of global greenhouse gas emissions (18%) within the industry sector (World Resources Institute 2005). It is estimated that the cement industry is one of the top two manufacturing industries responsible for global CO_2 emissions (van Oss & Padovani, 2003). Cement will mostly likely always be required for many construction projects. However, reductions in the widespread use of Portland cement through either substitution when possible or complementary use of environmentally friendly methods and materials would be a considerable contribution in meeting long-term sustainability goals.

As discussed above, sustainable construction practices rely on the use of environmentally friendly alternative building methods and materials where possible. This research investigates the sustainability and cost effective techniques for ground improvement. Biochemical methods are introduced in this thesis. It consists of two major sections.

1) Soil improvement with calcium phosphate compound (CPC)
2) Soil improvement with microbially induced calcite precipitation (MICP)

1.2 LITERATURE REVIEW

Novel grout materials have been developed to reinforce the ground and/or to control ground permeability with bacterially produced cement material (Dejong et al. 2006, Kawasaki et al. 2006, Whiffin et al. 2007, Ivanov et al. 2008, Terajima et al. 2009 and Van Paassen et al. 2010). These grout materials are called biogrouts. Three mechanisms of mineral formation have mainly been considered for biogrouts. The first mechanism is the precipitation of calcium carbonate by in situ microorganisms and/or added yeasts (Kawasaki et al. 2006). In this process, calcium carbonate is precipitated by the binding of carbonate ions released from microorganisms and calcium ions from the grout, which includes calcium

and glucose. The second mechanism was reported by Whiffin et al. (2007), who used urea instead of glucose and ureolytic *Sporosarcina pasteurii* instead of yeast and other in situ microorganisms; the decomposition of urea by *S. pasteurii* produced carbon dioxide, which supplied the carbonate ions. In both cases, additional pH buffers or ammonium ions play the role of pH adjusters for effective precipitation. The third mechanism is based on the pH dependence of the extension speed of the siloxane bond; this mechanism was reported by Terajima et al. (2009), who utilized the carbon dioxide produced by yeast to neutralize the alkaline active silica solution because the siloxane bond rapidly extends and gelates in the middle range of pH.

Soil and rock vary infinitely in their physical and chemical properties. This fact orients the development of biogrout along two main directions: one, to develop a highly general-purpose biogrout, and the other, to develop a specialized biogrout for a specific type of soil or rock. To apply biogrout to various soils and rocks, it is very important to increase the number of mechanisms available for the precipitation of cement materials.

1.2.1 Soil improvement with CPC method

In engineering as well as in science, it is essential to learn from nature. In nature, various minerals, such as calcium carbonate, calcium sulfate, calcium phosphate, calcium oxalate, silicate, and iron oxide are precipitated by living organisms. These biominerals are promising as engineering materials because they have considerable strength and low environmental impact. In this study, we carried out a fundamental examination of novel grout materials composed of calcium phosphate compounds (CPCs). CPCs exist as phosphate rocks (e.g., fluorapatite) in the natural environment and also as an important inorganic substance (e.g., hydroxyapatite, HA) in living organisms (Dorozhkin et al. 2002). As shown in Table 1.1, there are 11 known CPCs with various calcium-to-phosphate (Ca/P)

molar ratios in the ternary system $Ca(OH)_2$–H_3PO_4–H_2O. Research and development of materials composed of CPCs are currently in progress, especially in the fields of medicine and dentistry.

Medical CPC paste, however, is extremely expensive and has high viscosity, which makes it unfeasible for engineering applications. Therefore, we considered CPC use from an engineering viewpoint and aimed to develop a grout material that could be precipitated under normal temperature and pressure through microbial activity by using materials that can be easily handled. To the best of our knowledge, no existing grout material makes use of the self-setting mechanism of CPC alone or employs microbial pH adjustment activity for CPC precipitation. CPCs have unique physical and chemical properties. Their numerous advantages as a grout material include the following: (1) Gel-like or amorphous CPCs change into HA over time (Fig. 1.1 (Tung et al. 1998)). Therefore, CPC hardens after injection into soil and rock because of the self-setting mechanism.

Table 1.1: Properties of biologically relevant calcium orthophosphates. The table is adapted from Dorozhkin and Epple (2002).

Ca/P ratio	**Compound**	**Abbreviation**	**Formula**
0.5	Monocalcium phosphate monohydrate	MCPM (MCP)	$Ca(H_2PO_4)_2 \cdot H_2O$
0.5	Monocalcium phosphate anhydrate	MCPA (MCP)	Ca(H2PO4)2
1.0	Dicalcium phosphate dihydrate	DCPD (DCP)	$CaHPO_4 \cdot 2H_2O$
1.0	Dicalcium phosphate anhydrate	DCPA (DCP)	$CaHPO_4$
1.33	Octacalcium phosphate	OCP	$Ca_8(HPO_4)_2(PO_4)_4 \cdot 5H_2O$
1.5	α-tricalcium phosphate	α-TCP	$\alpha\text{-}Ca_3(PO_4)_2$
1.5	β-tricalcium phosphate	β-TCP	$\beta\text{-}Ca_3(PO_4)_2$
1.2-2.2	Amorphous calcium phosphate	ACP	$Ca_x(PO_4)_y \cdot nH_2O$
1.5-1.67	Calcium-deficient hydroxyapatite	CDHA	Ca10-x(HPO4)X(PO4)6-x $(OH)_{2-x}$ $(0 < x < 1)$
1.67	Hydroxyapatite	HA	$Ca_{10}(PO_4)_6(OH)_2$
2.0	Tetracalcium phosphate	TTCP	$Ca_4(PO_4)_2O$

1) The solubility of CPCs depends on the pH of the surrounding environment (Fig. 1.2 (Tung et al. 1998)). This makes it possible to utilize the mechanisms of pH adjustment by microorganisms, which are used in known biogrout methods to control CPC precipitation.
2) Phosphate and calcium stock solutions can be made from fertilizers, and calcium and phosphate can also be extracted from the bones of livestock and the shells of aquatic animals, respectively.
3) CPCs that precipitate after grout injection are non-toxic.
4) Unlike concrete, re-excavated muck that consists of soil, rock, and CPC grout is recyclable as agricultural fertilizer.

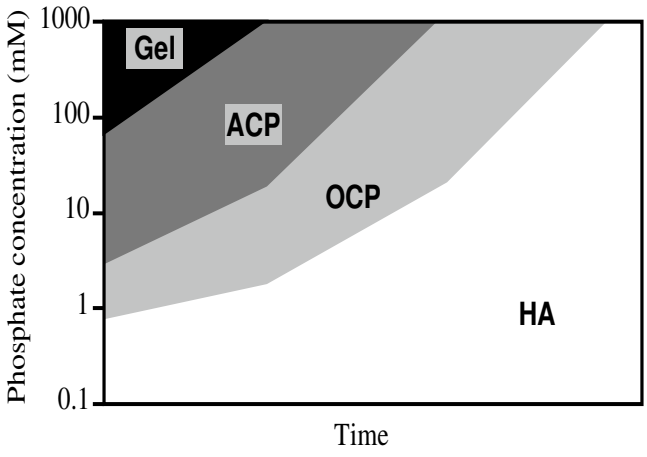

Fig. 1.1: Formation, stability, and hydrolysis of calcium phosphates as a function of phosphate concentration (log(P)) in solutions of amorphous calcium phosphate (ACP) at neutral pH. OCP, octacalcium phosphate; HA, hydroxyapatite. The figure is adapted from Tung (1998).

In recent years, a novel ground stabilizer to increase the number of options available among cementing mechanisms based on microorganisms (Akiyama and Kawasaki, 2012(a) and 2012(b)). Further, it is reported on a CPC chemical grout (CPC-Chem) that utilizes self-setting CPC mechanisms (Fig. 1.1), and on a CPC biogrout (CPC-Bio) whose solubility is dependent on its pH (Fig. 1.2), which can be increased by a microbial reaction. CPC-Chem is easy to obtain, safe to handle, non-toxic, and recyclable, advantages that make it suitable for the geotechnical application (Akiyama and Kawasaki, 2012(a)). The maximum UCS of sand test pieces cemented with CPC-Chem was found to be 63.5 kPa (Akiyama and Kawasaki, 2012(a)).

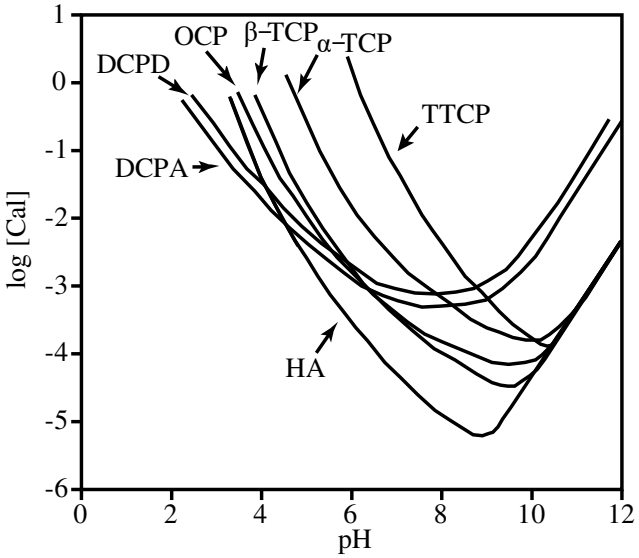

Fig. 1.2: Solubility phase diagrams for the ternary system, $Ca(OH)_2$–H_3PO_4–H_2O, at 25 °C, showing the solubility isotherms of $CaHPO_4$ (DCPA), $CaHPO_4 \cdot 2H_2O$ (DCPD), $Ca_8H_2(PO_4)_6 \cdot 5H_2O$ (OCP), α-$Ca_3(PO_4)_2$ (α-TCP), β-$Ca_3(PO_4)_2$ (β-TCP), $Ca_4(PO_4)_2O$ (TTCP), and $Ca_{10}(PO_4)_6 \cdot (OH)_2$ (HA). The figure is adapted from Tung (1998).

When CPC-Chem was converted to CPC-Bio by the addition of microorganisms and an ammonia source, the UCS increased from 42.9 kPa to 57.6 kPa (Akiyama and Kawasaki, 2012(b)). Our aim was to achieve a UCS value of 100 kPa, which is needed to avoid ground liquefaction during earthquakes (Yamazaki et al. 1998). This implies that the UCS of both CPC-Chem and CPC-Bio is not sufficient for use as a ground stabilizer, necessity of a preferable mechanism for further increase in UCS.

Research on CPC precipitation and solidification is also currently underway in the field of medical and dental science. A research on CPC paste has reported that the unconfined compressive strength (UCS) of CPC exceeds 10 MPa under normal temperature and pressure conditions (Fernandez et al. 1998). In addition, it has shown that the compressive strength of a mixture paste of di-calcium phosphate (DCP) and α-tricalcium phosphate (TCP) reached can be increase from 35 MPa to a maximum of 56 MPa by using calcium carbonate (CC) as the seed crystal (Fernandez et al. 1998).

A previous researcher said, the UCS of the test pieces with TCP and CC additives exceeded the targeted value of 100 kPa and increased to a maximum of 261.4 kPa and 209.7 kPa respectively (Kawasaki and Akiyama, 2013). This observation indicates that the existence of CC seed crystals can reinforce the strength of CPC grouts, such as the grout used in this study. CC is the main component of scallop shells, which are disposed of in large quantities as marine industrial waste (410,000tons/yearinJapan) (Guideline for recycling technology, Ports and Harbor Bureau). Moreover, it is non-toxic to handle and inexpensive to obtain. Thus, CC is a promising material in the geotechnical field from the viewpoint of waste utilization and cost effectiveness.

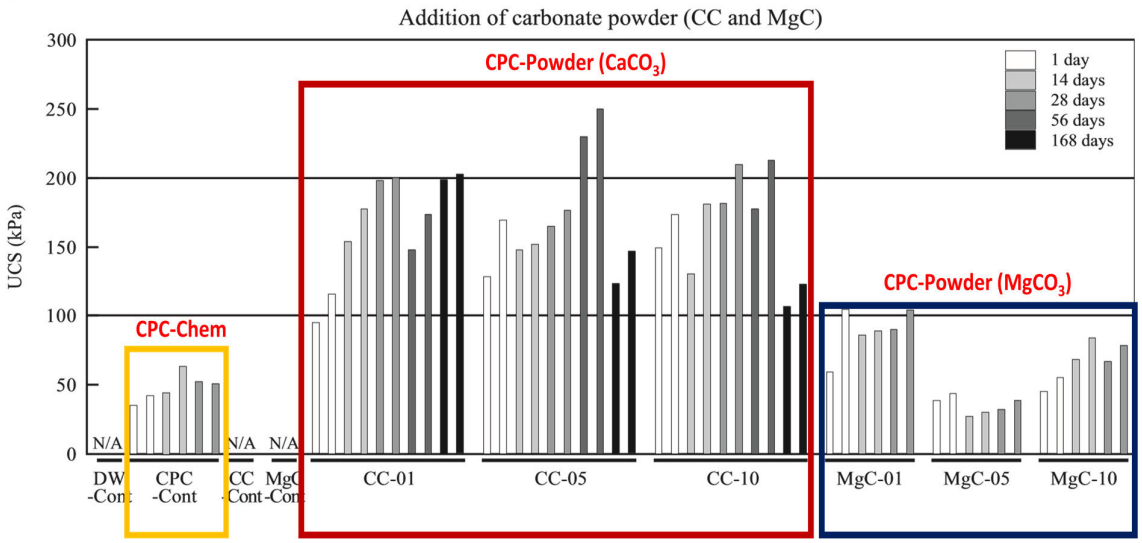

Fig. 1.3: UCS results for the samples prepared with CPC-powder methods.

In the present study, my aim was to improve strength by adding CPC with scallop shell powder. This study aims to exceed a maximum UCS of 100 kPa after 28 days of curing, which is the strength required to use the CPC and scallop shell powder combination as a countermeasure against soil liquefaction during an earthquake. We carried out UCS tests and scanning electron microscopy (SEM) observations on sand test pieces as a function of time. Based on the results, we discuss the effect of the kind and amount of added powders and crystal form on the UCS.

1.2.2 Soil improvement with microbially induced calcite precipitation (MICP)

One possible alternative method for ground improvement is microbially induced calcite precipitation (MICP), a biologically mediated subsurface process. Recent research has demonstrated the potential for soil improvement through biologically mediated subsurface processes. In particular, emerging research in the field of biogeotechnical engineering suggests soil cementation through MICP may be a promising method for mitigating a number

of geotechnical problems in granular soils. Successful development and implementation of microbial mineral precipitation for soil improvement would have wide application to a variety of important geotechnical problems including the stabilization of slopes; controlling soil erosion and scour; reducing under-seepage of levees and cut-off walls; increasing the bearing capacity of shallow foundations; facilitating excavation and tunneling in cohesionless soils; and remediating the potential for seismic settlement and liquefaction (Burbank et al. 2012; Chou et al. 2011; DeJong et al. 2006; Dejong et al. 2010; Harkes et al. 2010; Karatas 2008; Kavazanjian and Karatas 2008; van Paassen et al. 2008; van Paassen et al. 2010; Whiffin 2004). The utility of MICP extends beyond its use as a cementing agent, as it may be especially useful near or beneath existing structures, where the application of traditional soil improvement techniques is limited because of ground deformations and/or high cost associated with alternative techniques. Indeed, a directed cementation process making use of soil microbes through biostimulation or bioaugmentation could have a broad range of applications for ground improvement, and possibly groundwater remediation while simultaneously reducing the need for traditional energy intensive materials.

The biological basis for microbial mineral precipitation is well established. Microorganisms, bacteria, in particular, are associated with the formation of carbonate minerals and are thought to play a fundamental role in carbon cycling on the geologic timescale (Ehrlich 2002; Fredrickson and Fletcher 2001; Shock 2009; Warthmann et al. 2000). Estimates suggest that nearly half of the Earth's biomass is comprised of microorganisms found in the subsurface and oceanic subsurface (Whitman et al. 1998). The complex interactions between microorganisms and minerals have been well-documented through the efforts of researchers attempting to understand the formation, dissolution, and alteration of minerals by microorganisms on geologic and engineering timescales (Ehrlich 2002; Fredrickson and Fletcher 2001; Karatas 2008; Phoenix and Konhauser 2008; Shock

2009). Many microbial processes are capable of producing relatively strong soils through carbonate mineral precipitation. For example, a predominate calcium carbonate rock such as calcrete can have an average uniaxial compressive strength of 12 MPa with an associated modulus of elasticity between 29-65 MPa and an allowable bearing capacity between 1.5-2.0 MPa (Zorlu and Kasapoglu 2009). Although there are several pathways by which caliche can be formed, bio-mediated processes are one pathway that can explain the formation of calcrete (Dixon and Mclaren 2009).

Ground improvement via carbonate precipitation is one of the techniques for bioremediation subsurface processes. For example, microbes have long been the workhorses for many modern-day engineering processes such as wastewater treatment. Reclamation and treatment of wastewater have taken on a new sense of urgency in recent years as the ready availability of freshwater appears to be threatened in most parts of the world either due to increased demand, drought, climate change, contamination, or any combination thereof. In the face of such threats, many concerned authorities have recognized that any reasonable notion of sustainability must incorporate preservation of freshwater resources. A major source of water that has seen increased environmental and human-induced stress is groundwater. Groundwater has been and continues to be an important source of freshwater on earth, as well as an integral component of the hydrologic cycle. Recent estimates place approximately 22% (8,400,000 km^3) of Earth's freshwater in the subsurface where a large portion of this total figure can be readily accessed via aquifers (Christopherson 2009). Unfortunately, groundwater is susceptible to contamination through wells, unlined waste storage units, run-off, and surface waterways. The contamination of aquifers is a growing concern in many areas and, therefore, has been the focus of recent research efforts to develop novel and effective remediation methods.

One such novel approach is microbial calcite precipitation of radionuclides and metal contaminants through *in-situ* remediation of contaminated aquifers (Mitchell and Ferris 2005; Colwell et al. 2003; Fujita et al. 2000; Smith et al. 2004). The poor waste disposal practice has resulted in the release of low-level radioactive waste and metal contaminants (e.g., $^{90}Sr^{2+}$, $^{60}Co^{2+}$, Cd^{2+}) into the vadose zone and groundwater at many U.S. Department of Energy (DOE) weapons-production sites. These toxic waste products are a legacy of DOE chemical synthesis and nuclear waste facilities in locations such as Hanford, WA (100-N area) and the Idaho Nuclear Technology and Engineering Center (INTEC) at the Idaho National Engineering and Environmental Laboratory.

Microbial sequestration of metals is a microbially mediated mineral precipitation process that results in the formation of mineral deposits found in the natural environment, including calcium carbonate ($CaCO_3$) minerals such as calcite. In principle, the geochemical conditions conducive to carbonate precipitation are not unique to any specific microorganism; rather, carbonate precipitation can occur when carbonate (CO_3^{2-}) forms in the vicinity of suitable cations under alkaline conditions. Microbial sequestration of radionuclides and contaminant metals into calcite is essentially a co-precipitation reaction, governed by both thermodynamic and kinetic factors, in which suitable divalent cations are incorporated into the calcite lattice. Incorporation of divalent ions into the calcite structure appears to slow their transport and possibly immobilize them within the calcite structure (Mitchell and Ferris 2005; Colwell et al. 2003; Fujita et al. 2004; Fujita et al. 2000; Smith et al. 2004). If proven effective, immobilization of these contaminants through MICP may provide a sustainable and cost-effective *in-situ* remediation scheme for radionuclide and metal contaminated sites.

Ureolytic bacteria especially *Sporosarcina pasteurii* (formerly *Bacillus pasteurii*) and *Bacillus sphaericus* have generated a lot of interest in this area and have been studied

extensively (Fujita et al., 2000; Hammes et al., 2003; Dick et al., 2006; Muynck et al., 2007a,b; Ercole et al., 2007). These facultative bacteria are able to precipitate calcite through the enzymatic hydrolysis of urea. The microbial urease enzyme hydrolyzes urea to produce dissolved ammonium, dissolved inorganic carbon, and CO_2, and the ammonia released in the surroundings subsequently increases pH, leading to accumulation of insoluble $CaCO_3$ in a calcium rich environment. Quantitatively, 1 mol of urea is hydrolyzed intracellularly to 2 mol of ammonium (Eqs. (1) and (2)).

$$CO(NH_4)_2 + 2H_2O \longrightarrow CO_3^{2-} + 2NH_4^+ \qquad \text{Eq. (1)}$$

$$Ca^{2+} + CO_3^{2-} \longrightarrow CaCO_3 \qquad \text{Eq. (2)}$$

These reactions occur under the influence of natural environmental factors that control the activity of the urease enzyme. Factors such as the type of bacteria, bacteria cell concentration, temperature, urea concentration, calcium concentration, ionic strength, and the pH of the media may have a significant impact on MICP. The bacteria should possess high ureolytic efficiency, alkalophilic (optimum growth rate occurs at pH around 9, and no growth at all around pH 6.5), non-pathogenic, and posses the ability to deposit calcite homogeneously on the substratum. The bacteria should also have a high negative zeta-potential (Dick et al., 2006; Muynck et al., 2007a,b) to promote adhesion and surface colonization, and produce enormous amounts of urease enzyme in the presence of high concentrations of ammonium (Kaltwasser et al., 1972; Friedrich and Magasanik, 1977) to enhance both the rate of ureolysis and MICP (Nemati and Voordouw, 2003).

Urease-catalyzed ureolysis like any other enzymatic reaction is temperature dependent. However, the optimum temperature ranges from 20 to 37 ºC depending on environmental conditions and concentrations of other reactants in the system. Ferris et al. (2003), Nemati and Voordouw (2003), and Mitchell and Ferris (2005) reported that increasing the

temperature from 15 to 20 ºC increased rate of ureolysis, k_{urea} 5 times and 10 times greater than k_{urea} at 10 °C. It can, therefore, be emphasized that increasing temperature within the optimum range enhances the rate of ureolysis.

Nemati and Voordouw (2003) established that increasing urea and Ca^{2+} concentration beyond 36 and 90 g L^1 respectively do not increase the amount of $CaCO_3$ obtained by MICP. In addition, since Ca^{2+} is not likely utilized by microbial metabolic processes, it would accumulate outside the cell where it would be readily available for MICP (Silver et al., 1975).

Ionic charge influences enzymatic reactions like temperature and concentration. In bacteria transport in porous media, the total interaction energy needed by microbial particles to adhere and attach themselves to solid surfaces as explained by the classical Derjaguin–Landau–Verwey–Overbeek theory, is composed of the repulsive electrostatic forces and the attractive Van Der Waals forces. High ionic strength increases electrical double layer (EDL) compression by decreasing EDL repulsive forces leaving attractive Van Der Waals forces to dominate, and in the process promotes bacterial adhesion and attachment to the substratum (Faibish et al., 1998; Foppen and Schijven, 2006). Increase in ionic strength from 0.1 to 1.0 may increase the equilibrium constant for ammonia speciation from 9.3 to 9.4 (Martell and Smith, 1974).

A pH increase is an indication of urea hydrolysis and is an important property of alkalophiles (optimum growth at pH 9 and no growth below pH 6.5). At any media pH, NH_3 gas and dissolved NH_4^+ exist at different concentrations. Higher concentrations of NH_3 provide favorable conditions for MICP (Dick et al., 2006 and Muynck et al., 2007a,b).

In this study, it conducted a solidification test on silica sand using the ureolytic bacteria isolated from the soil near beachrock in Sumuide, Nago, Okinawa, Japan. The goal of this paper is to produce solidification of the specimen having an estimated unconfined compressive strength (UCS) of more than several MPa for soil improvement and preservation

of coastal erosion and/or healing of coastal concrete structures, and investigate the influence of varies factors on engineering properties of treated soil catalyzed by ureolytic bacteria. Moreover, in this study, I tried to perform uniformly solidified sand sample using MICP process.

A series of laboratory experiments was conducted for identifying parameters which were effected for solidification of the sample. Syringe solidification method was used for solidifying sample. Needle penetration test was conducted to obtain estimated UCS value and measured pH and Ca^{2+} concentration of the outlet solution.

1.3 SCOPE AND ORGANIZATION

The scope of this thesis is an investigation of different ground improvement techniques using biochemical methods. This thesis was consisted with two major sections as follows:

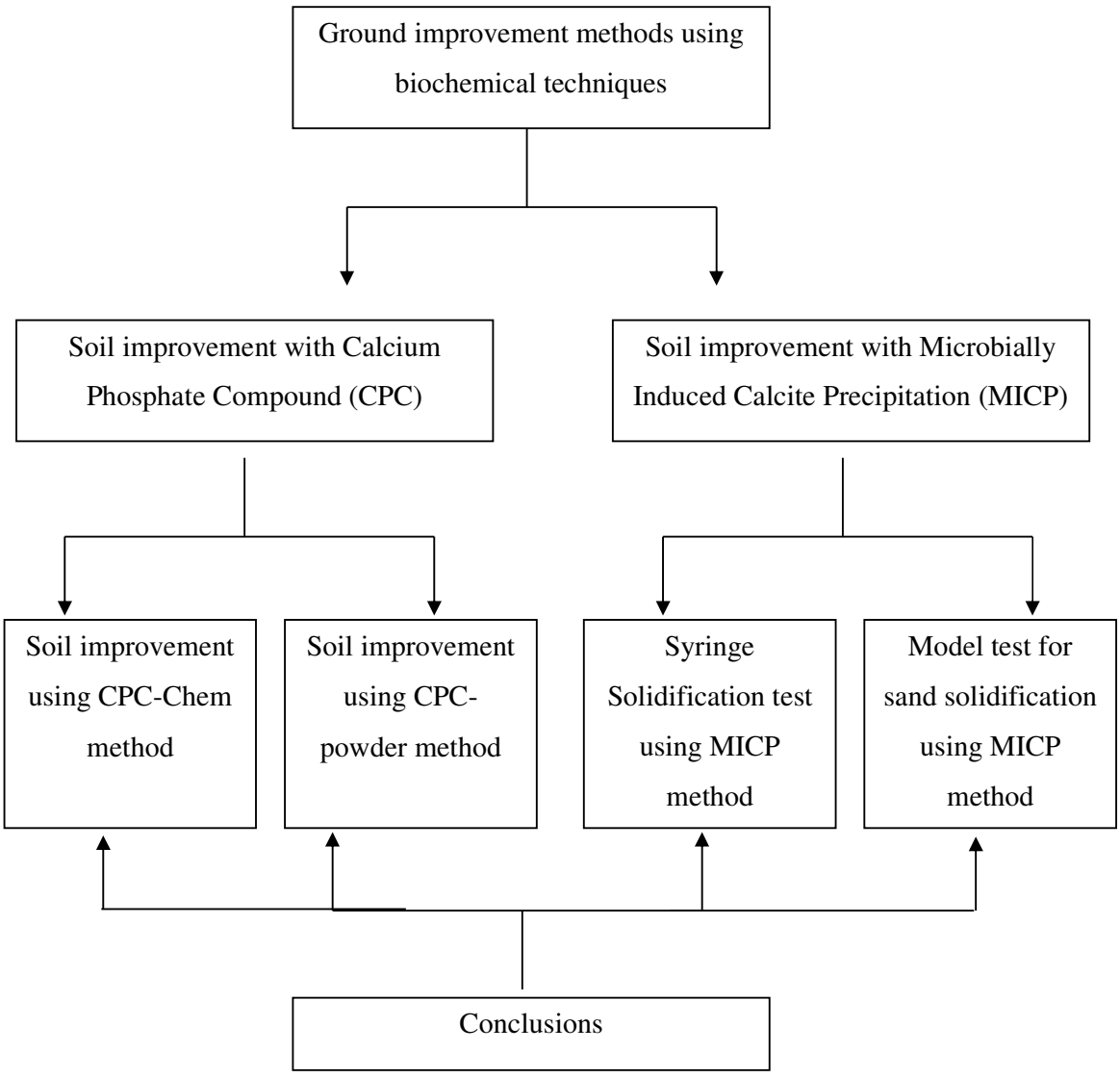

Fig. 1.4: Scope of the research.

Chapter 2 and Chapter 3 are described under the soil improvement with calcium phosphate compound (CPC). Chapter 4 and Chapter 5 are mentioned under the soil improvement with microbially induced calcite precipitation (MICP). Chapters of this thesis are as follows:

In Chapter 1, research background, objectives, and originality of thesis were described. Chapter 2 consisted with soil improvement using CPC-Chem method and Soil improvement using CPC-powder method was viewed in Chapter 3. In Chapter 4, under MICP process, Syringe solidification test using Ureolytic bacteria was detailed. Chapter 5 consisted with Model test for sand solidification using Ureolytic bacteria and finally, in Chapter 6 summarized and provided a conclusion that may guide future work.

1.4 ORIGINALITY OF THE THESIS

Few studies were done regarding cementation with CPC-Chem and CPC powder method. Therefore, in this study additional studies were done for identifying the best CPC mixture for sand solidification. Moreover, CPC-powder methods were conducted previous researchers and they used chemicals as a powder. But in this thesis bio-mineral was introduced as a powder instead of chemicals. In this research, CPC-powder method consisted of experiments using scallop cell powder.

Many types of research as mentioned in the section 1.2.2 were observed sand solidification with MICP method by using common ureolytic bacteria such as *Sporosarcina pasteurii* (formerly *Bacillus pasteurii*) and *Bacillus sphaericus*. From this research study, we introduced a new uearlytic bacteria for the MICP process. The bacterium was *Pararhodobacter* sp. which was found from Okinawa, Japan. It was originality of this research.

Moreover, previous researchers (Danjo, 2015 and Shimazaki, 2015) conducted solidification using *Pararhodobacter* sp. for marine purposes and they used artificial sea water for cultivation of bacteria and solidification process. However, in this research, solidification with *Pararhodobacter* sp. was used for land usage and distilled water was introduced instead of artificial sea water.

REFERENCES

Akiyama M, Kawasaki S, "Novel grout material using calcium phosphate compounds: in vitro evaluation of crystal precipitation and strength reinforcement," Journal of *Engineering Geology*, Vol. 125, 2012, pp. 119-128.

Akiyama M, Kawasaki S, "Microbially mediated sand solidification using calcium phosphate compounds," Journal of *Engineering Geology*, Vol. 137-138, 2012, pp. 29-39.

Antoniou P, Hamilton J, Koopman B, Jain R, Holloway B, Lyberatos G, Svoronos SA, "Effect of Temperature and pH on the Effective Maximum Specific Growth Rate of Nitrifying Bacteria," Journal of *Water Res.*, Vol.24 (1), 1990, pp. 97-101.

Beasley TM, Dixon PR, Mann LJ, "99Tc, 236U, and 237Np in the Snake River Plain Aquifer at the Idaho National Engineering and Environmental Laboratory, Idaho Falls, Idaho," Journal of *Environmental Science & Technology*, Vol. 32(24), 1998, pp. 3875-3881.

Christopherson RW, *Geosystems*. Pearson Education, Inc., Upper Saddle River, New Jersey, 2009.

Colwell FS, Smith RW, Ferris GF, Reysenbach AL, Fujita Y, Tyler TL, Taylor JL, Banta A, Delwiche ME, McLing TL, Watwood ME, "Microbially Mediated Subsurface Calcite Precipitation for Removal of Hazardous Divalent Cations." *Subsurface Contamination Remediation*, 2005, pp. 117-137.

Coplen TB, Hopple JA, Böhlke JK, Peiser HS, Rieder SE, Krouse HR, Rosman KJR, Ding T, Vocke, Jr RD, Révész KM, Lamberty A, Taylor P, De Bièvre P, "Compilation of Minimum and Maximum Isotope Ratios of Selected Elements in Naturally Occurring Terrestrial Materials and Reagents." U.S. Geological Survey Water- Resources Investigations, 2002, Report 01-4222.

Danjo T, Doctoral Thesis, Hokkaido University, Japan, 2015.

De Muynck W, Verbeken K, De Belie N, Verstraete W, "Influence of urea and calcium dosage on the effectiveness of bacterially induced carbonate precipitation on limestone," *Ecol. Eng*., Vol. 36, 2010, pp. 99-111.

DeJong JT, Fritzges MB, Nusslein K, "Microbial induced cementation to control sand response to undrained shear," Journal of *Geotechnical and Geoenvironmental Engineering*, Vol. 132, 2006, pp. 1381–1392.

DeJong JT, Mortensen BM, Martinez BC, Nelson DC, "Bio-mediated soil improvement," *Ecological Engineering,* Vol. 36, 2010, pp. 197-210.

Dekker, Fujita Y, Ferris FG, Lawson RD, Colwell FS, Smith RW, (2000). "Calcium Carbonate Precipitation by Ureolytic Subsurface Bacteria." Journal of *Geomicrobiology*, Vol. 17(4), 2000, pp. 305-318.

Dixon JC, McLaren SJ, Duricrusts, *Geomorphology of Desert Environments*. 2nd Ed. Netherlands, Springer Netherlands, 2009.

Dorozhkin SV, Epple M, "Biological and medical significance of calcium phosphates," Angewandte Chemie International Edition, Vol. 41, 2002, pp. 3130–3146.

Drever J, *The geochemistry of natural waters: surface and groundwater environments,* University of California, Prentice Hall, 1997.

Ehrlich HL, *Geomicrobiology*. New York, Marcel Dekker, 2002.

Fernández E, Gil FJ, Best SM, Ginebra MP, Driessens FCM, Planell JA, "Improvement of the mechanical properties of new calcium phosphate bone cements in the $CaHPO_4$-α-$Ca_2(PO_4)_2$ system: compressive strength and microstructural development," Journal of *Biomedical Materials Research*, Vol. 41, 1998, pp. 560–567.

Fredrickson J, Fletcher M, *Subsurface Microbiology and Biogeochemistry,* New York, Wiley-Liss, 2001.

Fujita Y, Ferris FG, Lawson RD, Colwell FS, Smith RW, "Calcium Carbonate Precipitation by Ureolytic Subsurface Bacteria," Journal of *Geomicrobiology*, Vol. 17(4), 2000, pp. 305-318.

Fujita Y, Redden GD, Ingram JC, Cortez MM, Ferris FG, Smith RW, "Strontium incorporation into calcite generated by bacterial ureolysis," *Geochimica et Cosmochimica Acta*, Vol. 68(15), 2004, pp. 3261–3270.

Ivanov V, Chu J, "Applications of microorganisms to geotechnical engineering for bioclogging and biocementation of soil in situ," Reviews in *Environmental Science and Biotechnology*, Vol. 7, 2008, pp. 139–153.

Karatas I, *Microbiological Improvement of the Physical Properties of Soils*. PhD. Dissertation, Department of Civil, Environmental, and Sustainable Engineering Arizona State University, Tempe, AZ, 2008.

Kawasaki S, Murao A, Hiroyoshi N, Tsunekawa M, Kaneko K, "Fundamental study on novel grout cementing due to microbial metabolism," Journal of the Japan Society of *Engineering Geology*, Vol. 47, 2006, pp. 2–12 (in Japanese with English abstract).

Kawasaki S, Akiyama M, "Enhancement of unconfined compressive strength of sand test pieces cemented with calcium phosphate compound by addition of various powders," Journal of *Soils and Foundations*, Vol. 53 (6), 2013, pp. 966-976.

Lee KC, Rittmann BE, "Applying a novel autohydrogenotrophic hollow-fiber membrane biofilm reactor for denitrification of drinking water," *Water Research,* Vol. 36, 2002, pp. 2040–2052.

Lee KC, Rittmann BE, "Effects of pH and precipitation on autohydrogenotrophic denitrification using the hollow-fiber membrane-biofilm reactor." *Water Research*, Vol. 37, 2003, pp. 1551–1556.

Meckenstock RU, Morasch B, Griebler C, Richnow HH, "Stable isotope fractionation analysis as a tool to monitor biodegradation in contaminated acquifers." Journal of *Contaminant Hydrology*, Vol. 75, 2004, pp. 215-255.

Mitchell AC, Ferris FG, "The coprecipitation of Sr into calcite precipitates induced by bacterial ureolysis in artificial groundwater: Temperature and kinetic dependence." Journal of *Geomicrobiology*, Vol. 69(17), 2005, pp. 4199-4210.

Mitchell AC, Ferris FG, "The Influence of *Bacillus pasteurii* on the Nucleation and Growth of Calcium Carbonate," Journal of *Geomicrobiology*, Vol. 23, 2006, pp. 213–226.

Nemati M, Voordouw G, "Modification of porous media permeability, using calcium carbonate produced enzymatically in situ," *Enzyme Microb. Technol.*, Vol. 33, 2003, pp. 635-642.

Nemati M, Greene EA, Voordouw G, "Permeability profile modification using bacterially formed calcium carbonate: comparison with enzymic option," *Process Biochem.*, Vol. 40, 2005, pp. 925-933.

Phoenix VR, Konhauser KO, "Benefits of bacterial biomineralization," *Geobiology,* Vol. 6, 2008, pp. 303–308.

Ports and Harbours Bureau, Recycling Technology Guidelines for Harbor and Airport Construction and Maintenance, edited in 2004. http://www.mlit.go. jp/kowan/recycle/.

Rittmann BE, Nerenberg R, Lee KC, Najm I, Gillogly TE, Lehman GE, Adham SS, "Hydrogen-based hollow-fiber membrane biofilm reactor (MBfR) for removing oxidized contaminants," *Water Supply*, Vol. 4, 2004, pp. 127-133.

Shock EL, "Minerals as Energy Sources for Microorganisms," *Economic Geology,* Vol. 104, 2009, pp. 1235–1248.

Shimazaki S, Master Thesis, Hokkaido University, Japan, 2015.

Smith RW, Fujita Y, Ferris GF, Cosgrove DM, Colwell RS, "Trace Metals in Groundwater & Vadose Zone Calcite: In Situ Containment & Stabilization of 90Strontium & Other Divalent Metals & Radionuclides at Arid West DOE Sites." USDOE Office of Science, Technical Report, OSTI ID: 839261, 2004.

Tandy S, Ammann A, Schulin R, Nowack B. "Biodegradation and speciation of residual SS-ethylenediaminedisuccinic acid (EDDS) in soil solution left after soil washing," *Environmental Pollution*, Vol. 142, 2006, pp. 191-199.

Tang Y, Zhou C, Ziv-El M, and Rittmann BE, "A pH-control model for heterotrophic and hydrogen-based autotrophic denitrification," *Water Resarch,* Vol. 45, 2011, pp. 232-240.

Terajima R, Shimada S, Oyama T, Kawasaki S, "Fundamental study of siliceous biogrout for eco-friendly soil improvement," JSCE Journal of *Geotechnical and Geoenvironmental Engineering*, Vol. 65, 2009, pp. 120–130 (in Japanese with English abstract).

Tung MS, "Calcium phosphates: structure, composition, solubility, and stability," in Zahid A (Ed), Calcium Phosphates in Biological and Industrial Systems, Kluwer Academic Publishers, Norwell, 1998, pp. 1–19.

Van Paassen LA, Ghose R, Van der Linden TJM, Van der Star WRL, Van Loosdrecht, MCM, "Quantifying biomediated ground improvement by ureolysis: Large-scale biogrout experiment," Journal of *Geotechnical and Geoenvironmental Engineering*, Vol. 136, 2010, pp. 1721–1728.

Van Paassen LA, Daza CM, Staal M, Sorokin DY, van der Zonb W, van Loosdrecht MC, "Potential soil reinforcement by biological denitrification," *Ecological Engineering,* Vol. 36(2), 2010, pp. 168-175.

Van Paassen LA, Daza CM, Staal M, Sorokin DY, van Loosdrecht MC, In situ soil reinforcement by microbial denitrification. 1st Int. Conf. on Bio-Geo-Civil Engineering, Netherlands: pp. 124-133, 2008, June 23-25.

Warthmann R, van Lith Y, Vasconcelos C, McKenzie JA, Karpoff AM, "Bacterially induced dolomite precipitation in anoxic culture experiments," *Geology,* Vol. 28(12), 2000, pp. 1091-1094.

Whiffin V, *Microbial CaCO3 precipitation for the production of biocement*, Ph.D. Dissertation, School of Biological Sciences and Biotechnology, Murdoch University, Australia, September, 2004.

Whiffin VS, Van Paassen LA, Harkes MP, "Microbial carbonate precipitation as a soil improvement technique," Journal of *Geomicrobiology*, Vol. 24, 2007, pp. 417–423.

Whitman WB, Coleman DC, Wiebe WJ, "Prokaryotes: The unseen majority," *Proc. Natl. Acad. Sci. USA,* Vol. 95, 1998, pp. 6578–6583.

Yamazaki H, Maeda K, Takahashi K, Zen K, Hayashi K, "Technical Note of Port and Harbour Research Institute," Vol. 905, 1998, pp. 1-29 (in Japanese).

Zorlu K, Kasapoglu KE, "Determination of geomechanical properties and collapse potential of a caliche by in situ and laboratory tests," *Environmental Geology*, Vol. 56, 2009, pp. 1449–1459.

CHAPTER 2

SOIL IMPROVEMENT USING CPC-CHEM METHOD

2.1 INTRODUCTION

The improved engineering behavior and performance of cemented soil over its un-cemented state contributed to the development of artificial cementation. However, cement grouting comprises several environmental problems such as high CO_2 emissions during cement production, the high energy cost for re-excavation and hard to recycling the improved ground.

In recent years, a new geotechnical method has been developed that involves the use of microorganisms for ground permeability control and/or reinforcement by Harkes et al (2010). The process of ground improvement by biological action is called “biogrouting” by Paassen et al (2009). Moreover, a novel ground stabilizer was developed to increase the number of options available among cementing mechanisms based on microorganisms by Akiyama and Kawasaki, (2012a) and Akiyama and Kawasaki (2012b).

As a grout material, calcium phosphate compounds (CPCs) have unique physical and chemical properties, such as:

1) The solubility of CPCs depends on the pH of the surrounding environment (Fig. 2.1) by Tung (1998).
2) Gel-like or amorphous CPCs change into HA over time (Fig. 2.2) by Tung (1998). Therefore, CPC hardens after injection into soil and rock because of the self-setting mechanism.
3) Phosphate and calcium stock solutions can be made from fertilizers, and calcium and phosphate can also be extracted from the bones of livestock and the shells of aquatic animals, respectively.

4) CPCs that precipitate after grout injection are non-toxic.
5) Unlike concrete, re-excavated muck that consists of soil, rock, and CPC grout is recyclable as agricultural fertilizer.

Novel grout using CPCs has been used for a countermeasure for liquefaction in geotechnical engineering applications and it is an economical and environmentally friendly technique that develops to form CPC precipitation throughout the soil, leading to an increase in soil strength.

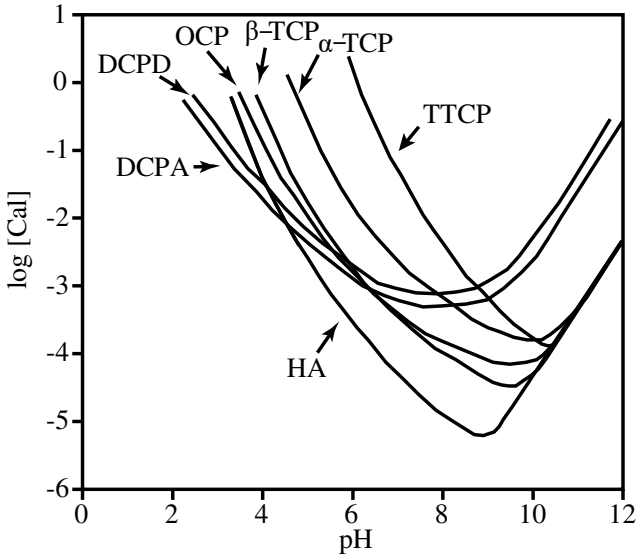

Fig. 2.1: Solubility phase diagrams for the ternary system, $Ca(OH)_2$–H_3PO_4–H_2O, at 25 °C, showing the solubility isotherms of $CaHPO_4$ (DCPA), $CaHPO_4 \cdot 2H_2O$ (DCPD), $Ca_8H_2(PO_4)_6 \cdot 5H_2O$ (OCP), α-$Ca_3(PO_4)_2$ (α-TCP), β-$Ca_3(PO_4)_2$ (β-TCP), $Ca_4(PO_4)_2O$ (TTCP), and $Ca_{10}(PO_4)_6 \cdot (OH)_2$, (HA). The figure is adapted from Tung (1998).

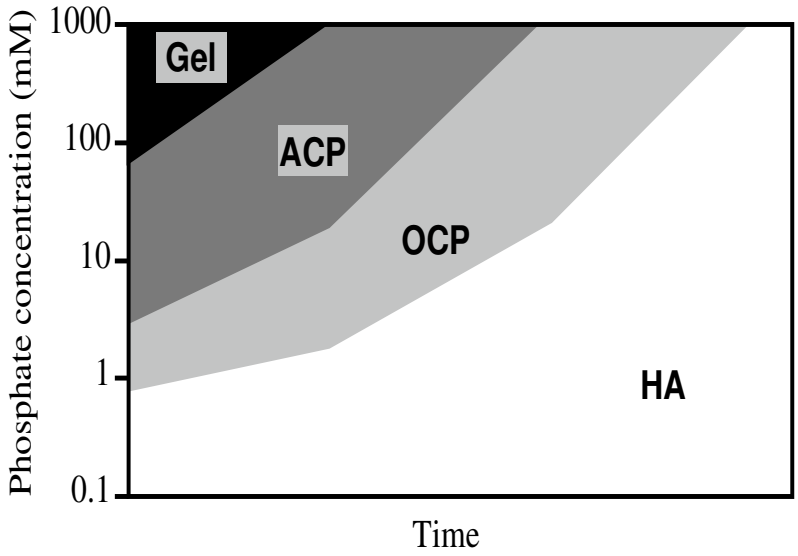

Fig. 2.2: Formation, stability, and hydrolysis of calcium phosphates as a function of phosphate concentration (log (P)) in solutions of amorphous calcium phosphate (ACP) at neutral pH. OCP, octacalcium phosphate; HA, hydroxyapatite. The figure is adapted from Tung (1998).

2.2 OBJECTIVE

In the present study's aim was examine the soil improvement by adding different CPC mixtures by using phosphate and calcium stock solutions. Although this study was used to evaluate the feasibility of using the unique and novel grout by exploiting the self-setting property of CPC and the microbial pH adjustment activity in CPC precipitation, respectively. Therefore, test pieces composed of sand cemented by CPC were subjected to unconfined compressive strength (UCS) tests and observed by scanning electron microscopy (SEM).

2.3 MATERIALS AND EQUIPMENT

2.3.1 Sand

Toyoura sand was used for the experiment. The physical properties of Toyoura sand is shown in Table 2.1.

Fig. 2.3: Toyoura sand sample.

Table 2.1: Physical characteristics of Toyoura sand.

Soil particle density, ρ_s (g/cm^3)	2.64
Minimum density, ρ_{dmin} (g/cm^3)	1.335±0.005
Maximum density, ρ_{dmax} (g/cm^3)	1.645±0.010
Maximum void ratio, e_{max}	0.973
Minimum void ratio, e_{min}	0.609
Mean grain size, D_{50} (mm)	0.17
10% diameter on grain size diagram, D_{10} (mm)	0.11
Fine fraction content, Fc (%)	0

2.3.2 Mold

A cylindrical plastic mold was used for the CPC solidification test. The diameter of the mold is 50 mm and the height is 100 mm. Mold remover was prepared for remove the plastic mold after samples solidified. Moreover, a collar was used when preparing the sample, because when performing compaction, the sand was slightly more than mold top surface. Therefore, the collar was put at the top of the surface and then compacted.

Fig. 2.4: Collar, cylindrical plastic model and remover.

2.3.3 Hand scoop and hand rammer

Hand scoop was used when weighed out the sand. Hand rammer was used for compacting the sand. Its weight is 758.91 g, total length 250 mm, and the face is a circular cross-section with a diameter of 30 mm.

Fig. 2.5: Hand scoop and hand rammer.

2.3.4 Magnetic stirrer

A magnetic stirrer was used when dissolving the reagent in water.

Fig. 2.6: magnetic stirrer.

2.3.5 pH meter

pH meter (manufactured OAKTON) was used for measure the pH value in the test .

Fig. 2.7: pH meter.

2.3.6 Uniaxial compression test equipment

Uniaxial compression test apparatus was used for measuring UCS value (unconfined compressive strength) of the CPC-Chem solidified samples. It consists of three devices: uniaxial compression testing machine (Makoto Research sha Co., Ltd., a desktop -type high-capacity compression testing machine, T266-31100), logger (Hamada Denki, HMD multi logger Jr) and PC software (Hamada Denki, HM1616Sx / Tx series).

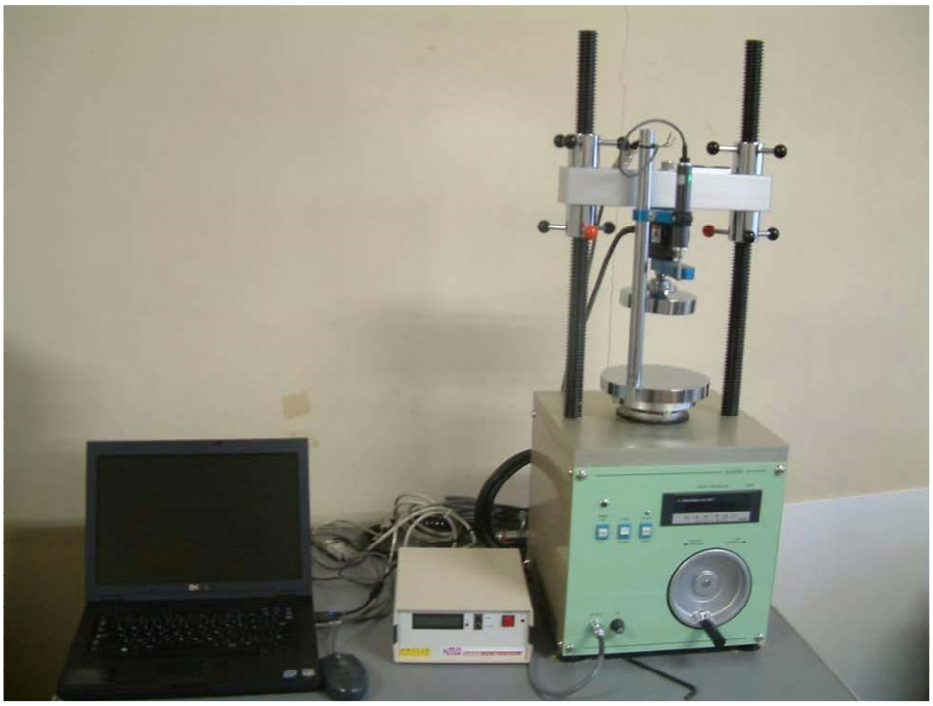

Fig. 2.8: Uniaxial compression test equipment.

2.3.7 Low vacuum and high vacuum SEM equipment

Segments of the UCS test pieces were observed by low vacuum and high vacuum SEM. Low vacuum SEM images were obtained just after open the sample and the machine for low vacuum SEM was shown in following figure (Fig. 2.9). The segments were naturally dried at 20°C for a few days and carbon-coated with a carbon coater. High vacuum SEM observations were carried out at an accelerating voltage of 15 kV and at x 2000 magnification.

Fig. 2.9: Low vacuum SEM instrument.

2.3.8 Choice of reagents

In this study, for the CPC-Chem, calcium acetate (CA) and calcium nitrate (CN) were used as a calcium solution, and diammonium phosphate (DAP) and dipotassium phosphate (DPP) were used as phosphate solutions.

Table 2.2: Chemical formula for the reagents.

Compound Name	Chemical Formula	Short form for this study
Calcium Acitate	$Ca(CH_3COO)_2$	CA
Calcium Nitrate	$Ca(NO_3)_2$	CN
Dipotassium Phosphate	K_2HPO_4	DPP
Diammonium Phosphate	$(NH_4)_2HPO_4$	DAP

The concentrations of CA and CN solutions were varied from 1.5 M to 0.5 M and the concentration of DAP and DPP was constant as 3.0 M for prepare the CPC-Chem solution mixture with two different Ca/P ratios (0.5 and 0.25). Eight CPC-chem mixtures were prepared.

Table 2.3: The concentration of the stock solutions.

Calcium Solution	Phosphate Solution	Ca/P Ratio
1.5 M CA	3.0 M DPP	0.5
0.75 M CA	3.0 M DPP	0.25
1.5 M CA	3.0 M DAP	0.5
0.75 M CA	3.0 M DAP	0.25
1.5 M CN	3.0 M DPP	0.5
0.75 M CN	3.0 M DPP	0.25
1.5 M CN	3.0 M DAP	0.5
0.75 M CN	3.0 M DAP	0.25

2.4 METHODOLOGY

2.4.1 Calculation for weight of Toyoura sand and volume of CPC grout

Here, I describe how to determine the Toyoura sand mass and volume of CPC grout used during the production of a single specimen. Mass of Toyoura sand necessary to fill the Toyoura sand to mold V_t (cm^3) was determined in the following manner. Before use Toyoura sand, it was dried for 24 hours in a constant-temperature drying oven at 110℃. Further, by molding a specimen is adhered, to minimize the damage of the specimen when removed from the mold and adhered to overhead projector (OHP) film having a thickness of 0.01 cm on the sides and bottom of the mold.

$V_t\ (cm^3) = 2.49\ (cm) \times 2.49\ (cm) \times \pi \times 9.99\ (cm)$

m_s (g) = ρ_{dmax} (g / cm³) × V_t (cm³) ≒ 320.1 (g)

Also, the grout injection rate into the interstitial space of Toyoura sand filled in the mold to 100%, was obtained the required grout volume of V_v (cm³) in the following manner.

V_v (cm³) = V_t (cm³) − m_s (g) / ρ_s (g / cm³) ≒ 73.3 (mL)

2.4.2 Experiment method

A standard sand test piece was made from 320.09 g of Toyoura sand (mean diameter D_{50} =170 μm, 15% diameter D_{15} =150 μm) and 73.3 mL of CPC-Chem according to the previous report (Akiyama and Kawasaki, 2012a). Considering the above values, 36.7 mL each of the phosphate and calcium stock solutions were mixed, making their final concentrations half of their initial concentrations. Immediately after the reaction mixture was prepared, it was uniformly mixed with weighted Toyoura sand in a stainless-steel ball for 2 min. This mixture was divided into quarters, each of which was placed into a mold with an overhead projector (OHP) sheet. The sand in the mold container was tamped down 30 times by a hand rammer after each of the four quarters was placed in the mold. Finally, the edge surface of the test piece was molded flat and covered with Parafilm to avoid desiccation.

The test pieces were cured in an airtight container at a high humidity for 1, 7, 14, and 28 days at 25 °C. The UCS of the test pieces removed from the mold container after curing was measured at an axial strain rate of 1 %/min by employing a UCS apparatus. For each curing time, two test pieces were used to perform the UCS test. To avoid the destruction of the test pieces during their removal from the mold, the inner wall of the mold container (φ = 5 cm, h = 10 cm) was covered with a 0.01-cm-thick overhead projector (OHP) sheet.

The pH of the test pieces was calculated as an average of three measurements (top,

bottom, and middle of each test pieces) using pH Spear (Eutech Instruments Pte., Ltd., Singapore). Segments of the UCS test pieces were observed by low vacuum and high vacuum SEM. The segments were naturally dried at 20 °C for a few days and carbon-coated with a carbon coater. High vacuum SEM observations were carried out at an accelerating voltage of 15 kV and at x 600 magnification.

In addition, X-Ray Computed Tomography (X-CT) was observed for the tested samples. X-CT is an indirect non-destructive imaging method. It allows to visualize the local absorption properties of a specimen.

Table 2.4: Testing conditions.

Ca	P	Ca (mol/L)	P (mol/L)	Ca/P	Curing date
$Ca(CH_3COO)_2$	K_2HPO_4	1.5	3	0.5	1
$Ca(CH_3COO)_2$	K_2HPO_4	1.5	3	0.5	7
$Ca(CH_3COO)_2$	K_2HPO_4	1.5	3	0.5	14
$Ca(CH_3COO)_2$	K_2HPO_4	1.5	3	0.5	28
$Ca(CH_3COO)_2$	K_2HPO_4	0.75	3	0.25	1
$Ca(CH_3COO)_2$	K_2HPO_4	0.75	3	0.25	7
$Ca(CH_3COO)_2$	K_2HPO_4	0.75	3	0.25	14
$Ca(CH_3COO)_2$	K_2HPO_4	0.75	3	0.25	28
$Ca(CH_3COO)_2$	$(NH_4)_2HPO_4$	1.5	3	0.5	1
$Ca(CH_3COO)_2$	$(NH_4)_2HPO_4$	1.5	3	0.5	7
$Ca(CH_3COO)_2$	$(NH_4)_2HPO_4$	1.5	3	0.5	14
$Ca(CH_3COO)_2$	$(NH_4)_2HPO_4$	1.5	3	0.5	28
$Ca(CH_3COO)_2$	$(NH_4)_2HPO_4$	0.75	3	0.25	1
$Ca(CH_3COO)_2$	$(NH_4)_2HPO_4$	0.75	3	0.25	7
$Ca(CH_3COO)_2$	$(NH_4)_2HPO_4$	0.75	3	0.25	14
$Ca(CH_3COO)_2$	$(NH_4)_2HPO_4$	0.75	3	0.25	28
$Ca(NO_3)_2$	K_2HPO_4	1.5	3	0.5	1
$Ca(NO_3)_2$	K_2HPO_4	1.5	3	0.5	7
$Ca(NO_3)_2$	K_2HPO_4	1.5	3	0.5	14
$Ca(NO_3)_2$	K_2HPO_4	1.5	3	0.5	28
$Ca(NO_3)_2$	K_2HPO_4	0.75	3	0.25	1
$Ca(NO_3)_2$	K_2HPO_4	0.75	3	0.25	7
$Ca(NO_3)_2$	K_2HPO_4	0.75	3	0.25	14
$Ca(NO_3)_2$	K_2HPO_4	0.75	3	0.25	28
$Ca(NO_3)_2$	$(NH_4)_2HPO_4$	1.5	3	0.5	1
$Ca(NO_3)_2$	$(NH_4)_2HPO_4$	1.5	3	0.5	7
$Ca(NO_3)_2$	$(NH_4)_2HPO_4$	1.5	3	0.5	14
$Ca(NO_3)_2$	$(NH_4)_2HPO_4$	1.5	3	0.5	28
$Ca(NO_3)_2$	$(NH_4)_2HPO_4$	0.75	3	0.25	1
$Ca(NO_3)_2$	$(NH_4)_2HPO_4$	0.75	3	0.25	7
$Ca(NO_3)_2$	$(NH_4)_2HPO_4$	0.75	3	0.25	14
$Ca(NO_3)_2$	$(NH_4)_2HPO_4$	0.75	3	0.25	28

2.5 RESULTS

Table 2.5: Results of the unconfined compressive strength for different calcium, phosphate stock solutions.

Ca	P	Ca (mol/L)	P (mol/L)	Ca/P	Curing date	Average UCS (kPa)
$Ca(CH_3COO)_2$	K_2HPO_4	1.5	3	0.5	1	75.00
$Ca(CH_3COO)_2$	K_2HPO_4	1.5	3	0.5	7	56.40
$Ca(CH_3COO)_2$	K_2HPO_4	1.5	3	0.5	14	119.00
$Ca(CH_3COO)_2$	K_2HPO_4	1.5	3	0.5	28	143.60
$Ca(CH_3COO)_2$	K_2HPO_4	0.75	3	0.25	1	26.25
$Ca(CH_3COO)_2$	K_2HPO_4	0.75	3	0.25	7	40.25
$Ca(CH_3COO)_2$	K_2HPO_4	0.75	3	0.25	14	18.90
$Ca(CH_3COO)_2$	K_2HPO_4	0.75	3	0.25	28	40.90
$Ca(CH_3COO)_2$	$(NH_4)_2HPO_4$	1.5	3	0.5	1	90.00
$Ca(CH_3COO)_2$	$(NH_4)_2HPO_4$	1.5	3	0.5	7	94.65
$Ca(CH_3COO)_2$	$(NH_4)_2HPO_4$	1.5	3	0.5	14	84.80
$Ca(CH_3COO)_2$	$(NH_4)_2HPO_4$	1.5	3	0.5	28	88.05
$Ca(CH_3COO)_2$	$(NH_4)_2HPO_4$	0.75	3	0.25	1	36.60
$Ca(CH_3COO)_2$	$(NH_4)_2HPO_4$	0.75	3	0.25	7	43.30
$Ca(CH_3COO)_2$	$(NH_4)_2HPO_4$	0.75	3	0.25	14	41.30
$Ca(CH_3COO)_2$	$(NH_4)_2HPO_4$	0.75	3	0.25	28	58.95
$Ca(NO_3)_2$	K_2HPO_4	1.5	3	0.5	1	69.90
$Ca(NO_3)_2$	K_2HPO_4	1.5	3	0.5	7	100.40
$Ca(NO_3)_2$	K_2HPO_4	1.5	3	0.5	14	120.80
$Ca(NO_3)_2$	K_2HPO_4	1.5	3	0.5	28	144.65
$Ca(NO_3)_2$	K_2HPO_4	0.75	3	0.25	1	34.80
$Ca(NO_3)_2$	K_2HPO_4	0.75	3	0.25	7	34.95
$Ca(NO_3)_2$	K_2HPO_4	0.75	3	0.25	14	33.35
$Ca(NO_3)_2$	K_2HPO_4	0.75	3	0.25	28	45.75
$Ca(NO_3)_2$	$(NH_4)_2HPO_4$	1.5	3	0.5	1	55.70
$Ca(NO_3)_2$	$(NH_4)_2HPO_4$	1.5	3	0.5	7	57.15
$Ca(NO_3)_2$	$(NH_4)_2HPO_4$	1.5	3	0.5	14	65.60
$Ca(NO_3)_2$	$(NH_4)_2HPO_4$	1.5	3	0.5	28	44.30
$Ca(NO_3)_2$	$(NH_4)_2HPO_4$	0.75	3	0.25	1	28.75
$Ca(NO_3)_2$	$(NH_4)_2HPO_4$	0.75	3	0.25	7	48.40
$Ca(NO_3)_2$	$(NH_4)_2HPO_4$	0.75	3	0.25	14	37.95
$Ca(NO_3)_2$	$(NH_4)_2HPO_4$	0.75	3	0.25	28	57.50

2.5.1 UCS test of sand test pieces cemented by CPC

Figs. 2.10 (a) and 2.10 (b) illustrate the effect of UCS on curing time for the test pieces cemented with eight CPC-Chem mixtures. According to Fig. 2.10 (b), the value of UCS is tended to increase for both CA: DPP=0.5 and CN: DPP=0.5. Also UCS is tended to constant for both CA: DAP=0.5 and CN: DAP=0.5.

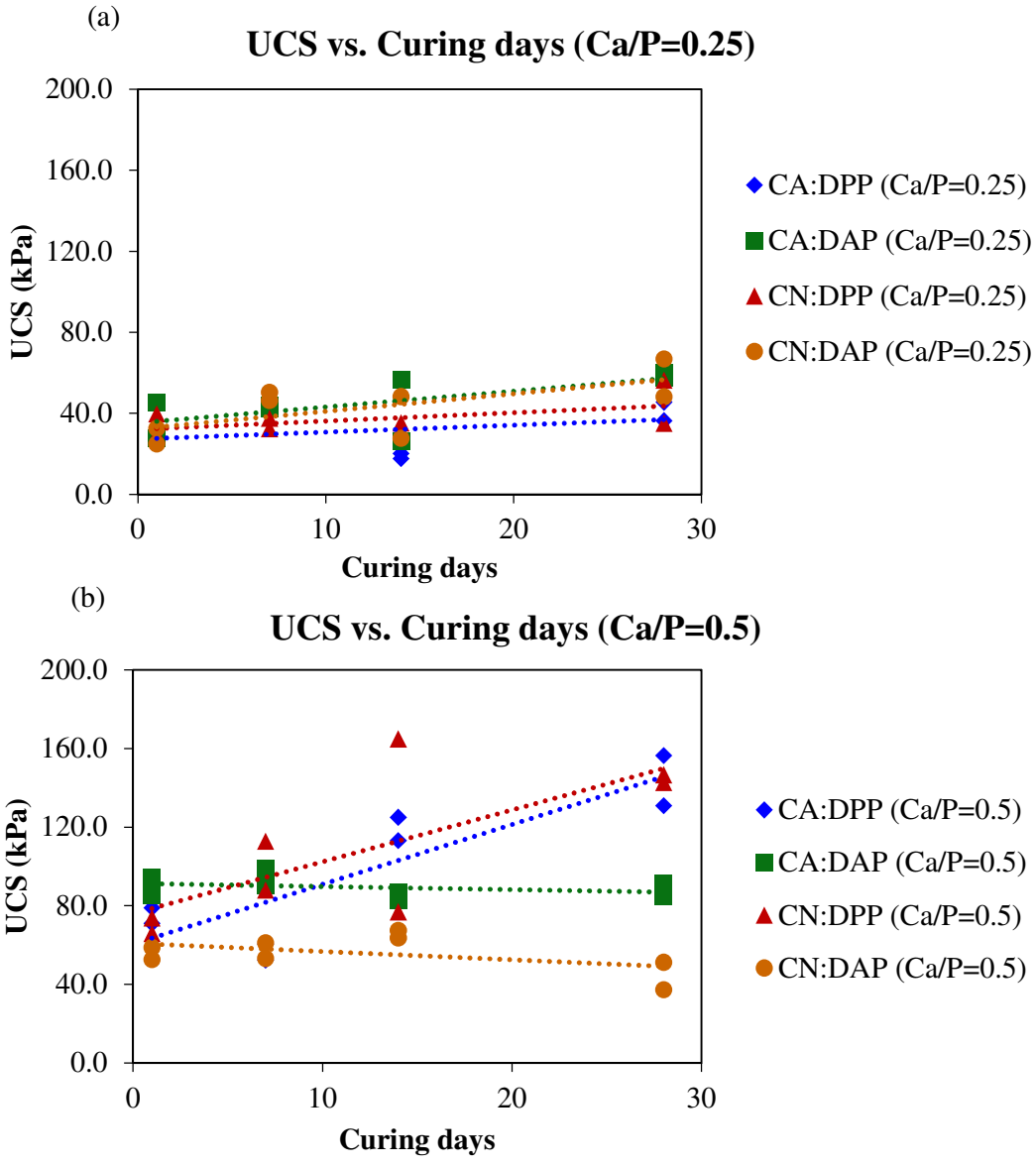

Fig. 2.10: Relationship between UCS and curing time of Toyoura sand test pieces cemented by (a) Ca/P = 0.25 and (b) Ca/P = 0.5.

Also, the UCS values of the test pieces cemented by adding DPP are larger than the UCS values of the test pieces cemented by adding DAP (Fig. 2.10 (b)). Moreover, from the Figs. 2.10 (a) and 2.10 (b), the UCS value of the test pieces with Ca/P=0.5 is larger than the UCS value of the test pieces with Ca/P=0.25.

2.5.2 pH of sand test pieces cemented by CPC

Figs. 2.11 (a) and 2.11 (b) illustrate the effect of pH for the test pieces cemented by CPC-Chem. The pH of the test pieces range from weakly acidic to alkaline (6.4-7.7) for Ca/P=0.5 and the pH range from weakly acidic to strong alkaline (6.7-8.5) for Ca/P=0.25. Moreover the pH is tended to increase with curing time for the samples prepared with CA: DPP = 0.5 and CA: DAP = 0.25 (Fig. 2.11 (a) and 2.11 (b)) and pH is decreased with the time for CN: DPP =0.5 while other samples remained the pH value was nearly constant.

(a)

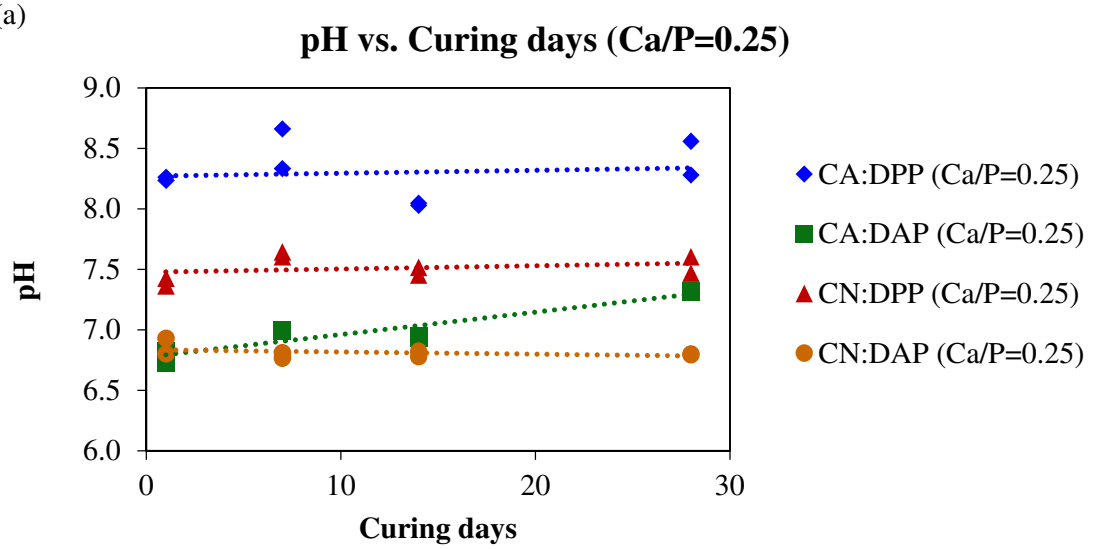

Fig. 2.11 (a): Relationship between pH and curing time of Toyoura sand test pieces cemented by Ca/P = 0.25.

(b)

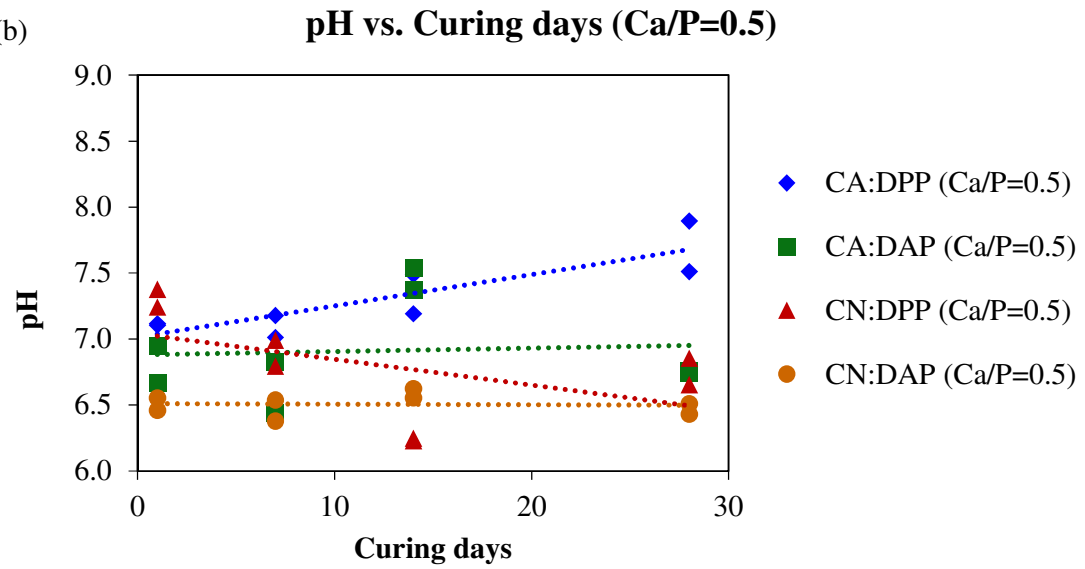

Fig. 2.11 (b): Relationship between pH and curing time of Toyoura sand test pieces cemented by Ca/P = 0.5.

2.5.3 Wet density of sand test pieces cemented by CPC

Figs. 2.12(a) and 2.12(b) illustrate the effect of wet density for the test pieces cemented by CPC-Chem. This density was measured just after preparation of the sample. Wet density of the samples prepared with CA: DPP, CA: DAP and CN: DPP with the concentration of Ca/P = 0.25 and CA: DPP, CA: DAP and CN: DPP with Ca/P = 0.5 were intended to increase with the time of cured. However, test pieces prepared with CN: DAP with Ca/P = 0.25 and 0.5 were not projected to increase with the curing time.

(a)

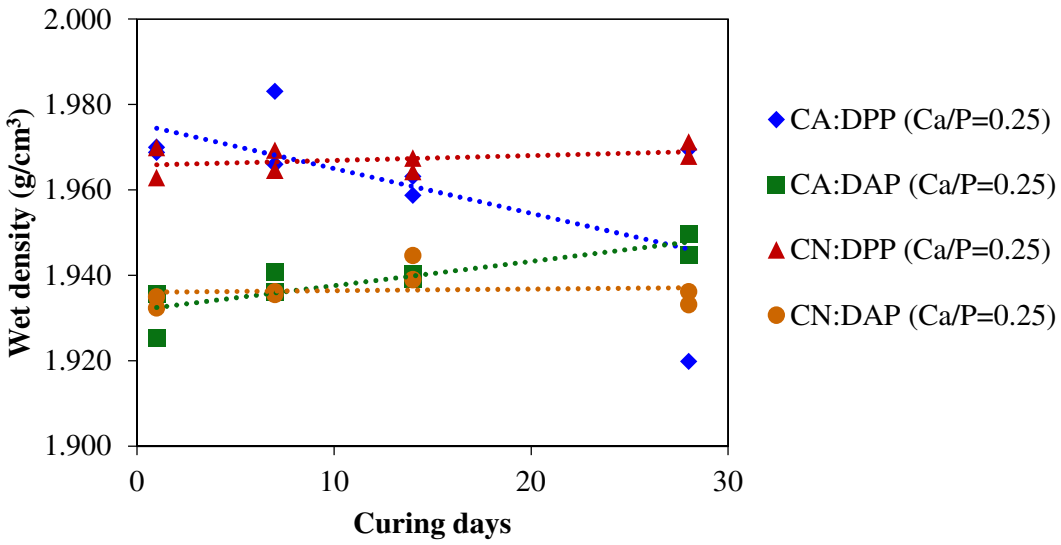

(b)

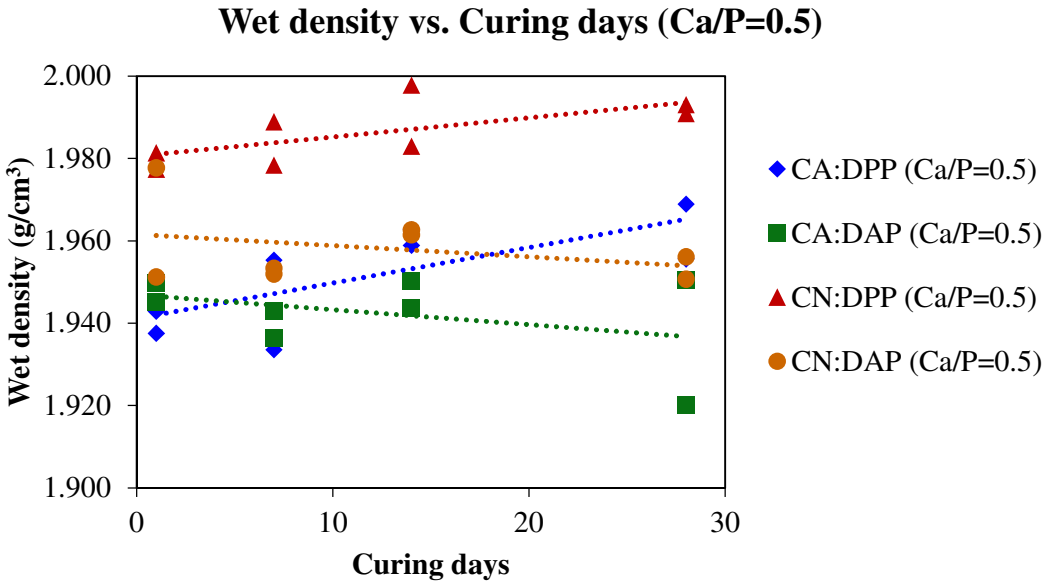

Fig. 2.12: Relationship between wet density and curing time of Toyoura sand test pieces cemented by (a) Ca/P = 0.25 and (b) Ca/P = 0.5.

2.5.4 SEM Observation

Figs. 2.13 to 2.16 show low vacuum SEM images of sand test pieces cemented with eight reaction mixture set of CPC-Chem and the curing time was 14 days.

(a)

(b)

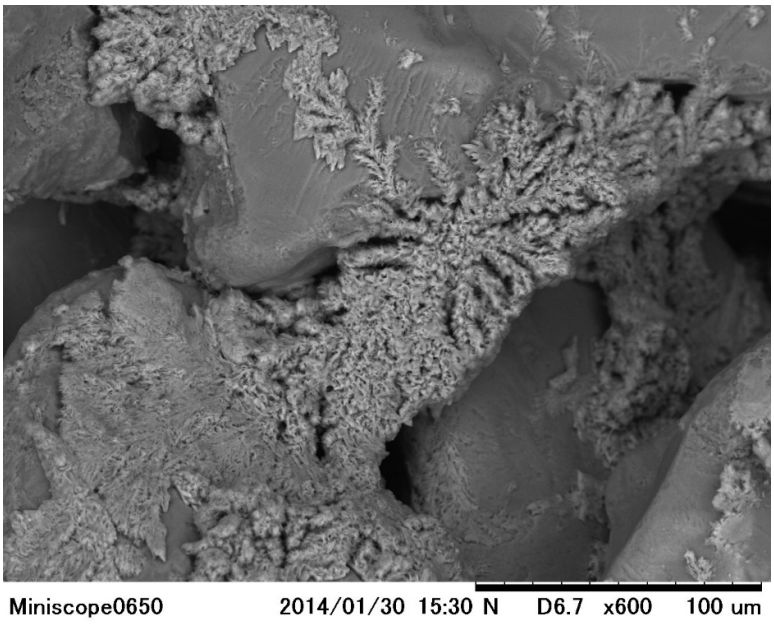

Fig. 2.13: SEM images for test samples after 14 days curing period (x 600). (a) CA: DPP=0.5, (b) CA: DAP=0.5.

Wisker-like crystal structure was observed in the sample prepared with CA: DPP=0.5 mixture and other samples were not clearly observed any crystal formation. The increase in UCS seemed to be because of the binding of the sand particles by the precipitated CPC that enveloped the CC particles.

(a)

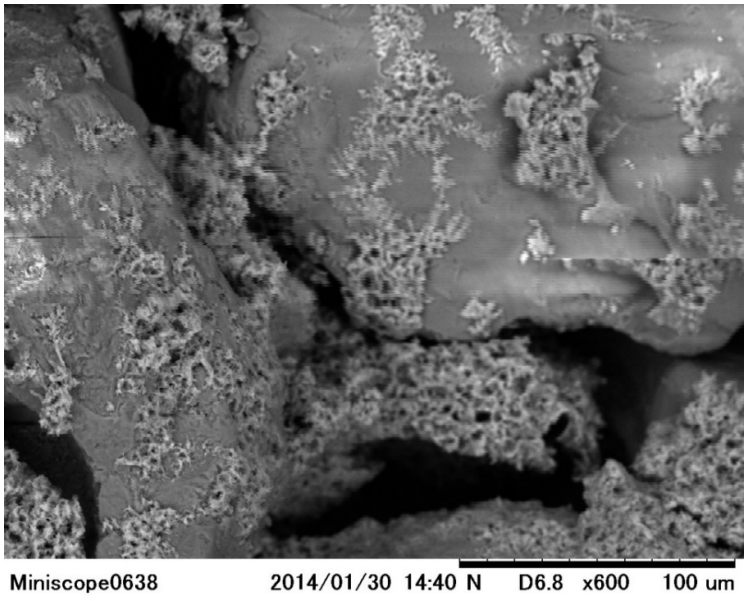

(b)

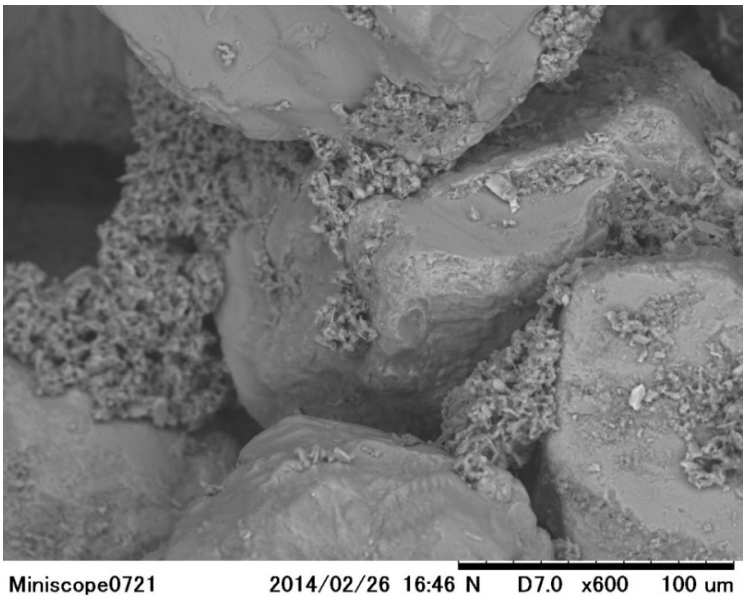

Fig. 2.14: SEM images for test samples after 14 days curing period (x 600). (a) CN: DPP=0.5 and (b) CN: DAP=0.5.

(a)

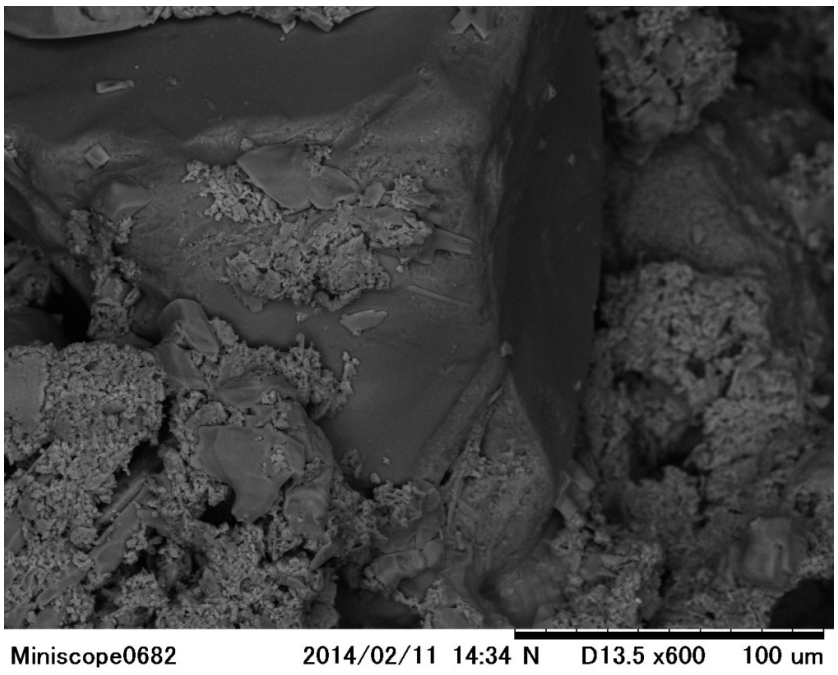

(b)

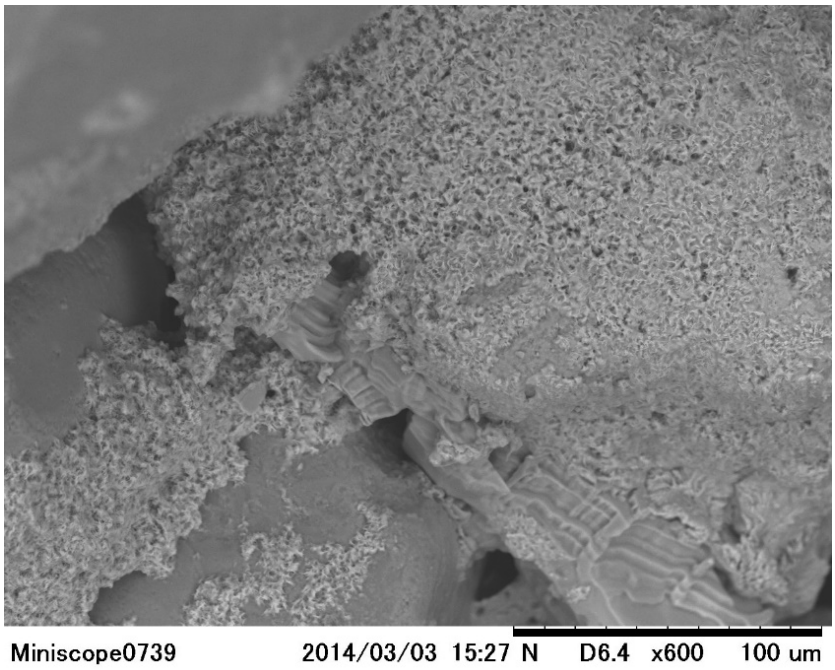

Fig. 2.15: SEM images for test samples after 14 days curing period (x 600). (a) CA: DPP=0.25, (b) CA: DAP=0.25.

(a)

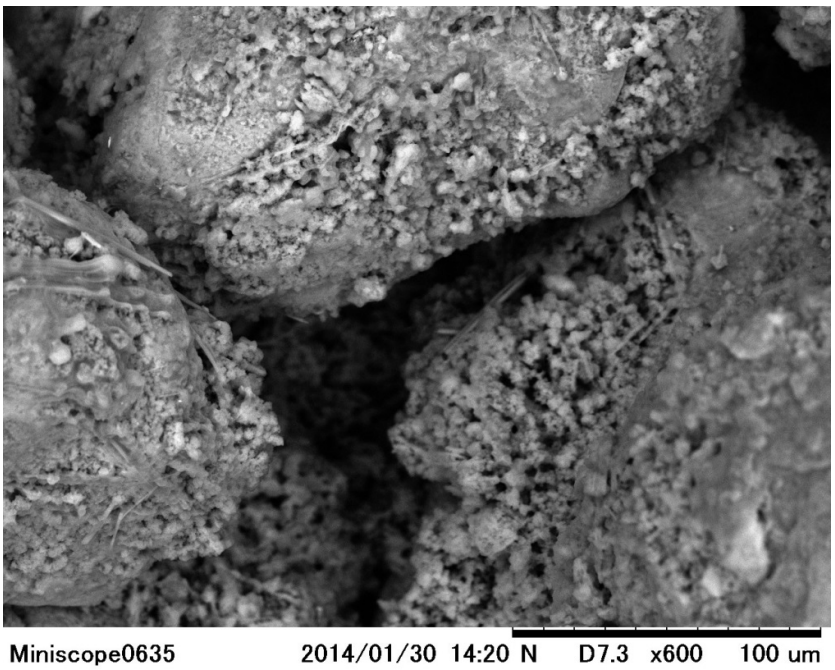

(b)

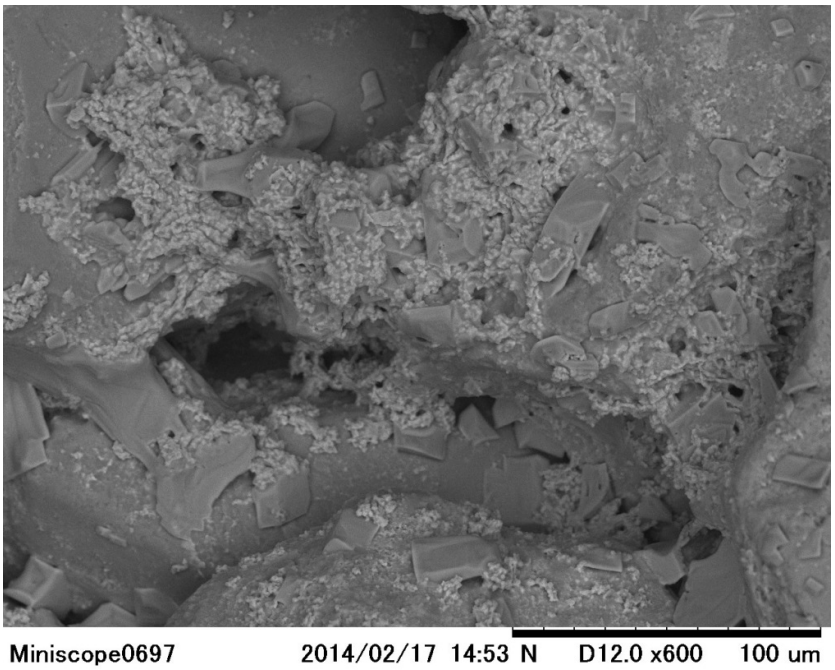

Fig. 2.16: SEM images for test samples after 14 days curing period (x 600). (a) CN: DPP=0.25 and (a) CN: DAP=0.25.

2.6 DISCUSSION

2.6.1 pH and UCS (Solubility and Strength)

Considering the solubility of CPC, it is dependent on its pH (Fig. 2.1) and results obtained, it is summarized that the solubility is minimum at pH is about 7 - 8. Considering the figures 2.17 (a) and 2.17 (b), relationship between pH and UCS value was more reliable for the mixtures of CA: DPP (Ca/P=0.25), CA: DAP (Ca/P=0.25) and CA: DPP (Ca/P=0.5).

Also, UCS value was increased with the increase of pH value. However, the UCS value of the test pieces prepared with CN: DPP with Ca/P = 0.5 was decreased with increase of pH value. For identify the reason for this matter, further investigation are required. In this experiment, the concentration of phosphate source was 3 mol/L and it was constant for all mixtures and calcium source was varied 0.75 mol/L for Ca/P = 0.25 and 1.5 mol/L for Ca/P = 0.5. Therefore, in the Fig. 2.17 (a), the UCS value was less due to less calcium source concentration.

The study`s aim was for the UCS value is more than 100 kPa for minimizing the liquefaction. Therefore, it is more difficult to get our objective value using Ca/P = 0.25 (Phosphate source: 3 mol/L and Calcium source: 0.75 mol/L).

From the results of Fig. 2.17 (b), the objective UCS value was satisfied by, CA: DPP and CN: DPP with the Ca/P ratio is 0.5. However, the test pieces prepared with CN: DPP (Ca/P = 0.5) was not shown relationship between UCS and pH value. Due to above reason, I could not select that mixture. Therefore, the best and more reliable mixture for satisfying our research objective was CA: DPP (Ca/P = 0.5).

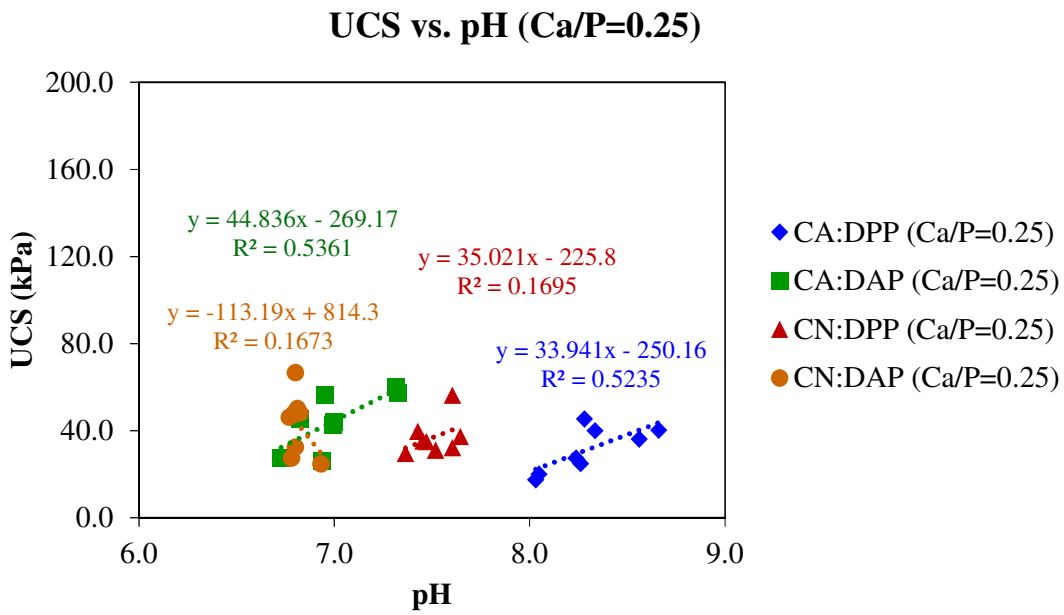

Fig. 2.17 (a): Relationship between UCS and pH for Ca/P = 0.25.

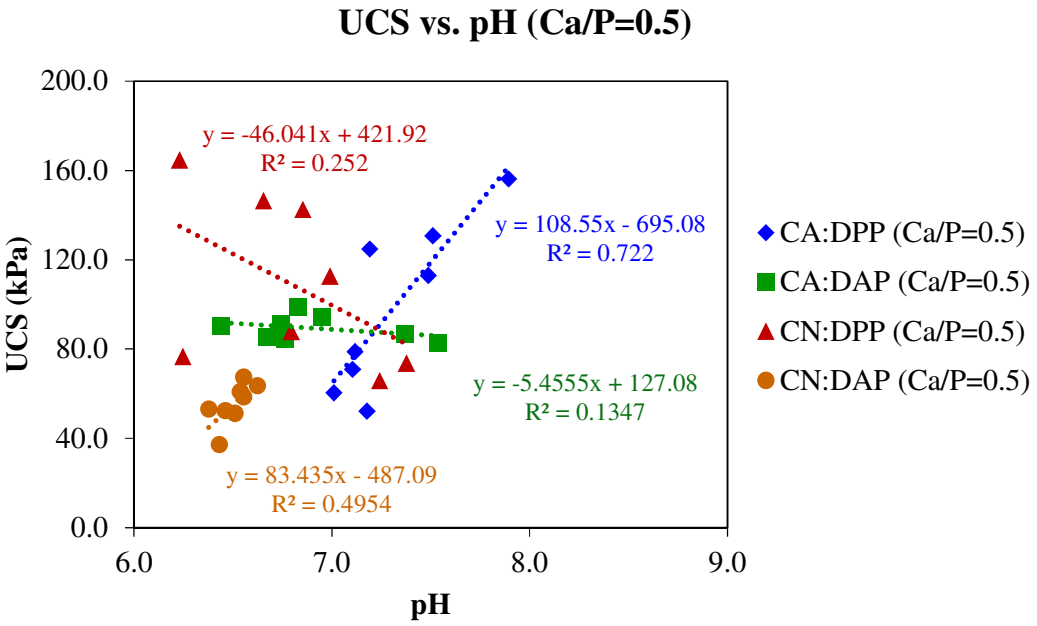

Fig. 2.17 (b): Relationship between UCS and pH for Ca/P = 0.5.

2.6.2 Wet density and UCS

The measured wet density of the test pieces vs. UCS value was provided in Figs. 2.18 (a) and 2.18 (b). Immediately after being produced and cured, the wet densities of two test pieces in each test case showed almost the same value. The mixtures of CN: DPP (Ca/P=0.5) and CA: DPP (Ca/P=0.5), shows a reliable mixture for the relationship between UCS and wet density.

As mentioned above, it is more difficult to get the objective value (UCS > 100 kPa) using Ca/P = 0.25 (Phosphate source: 3 mol/L and Calcium source: 0.75 mol/L). The wet density increase mean the voids between sand particles filled with CPC precipitation and it caused to increase the UCS of the sample.

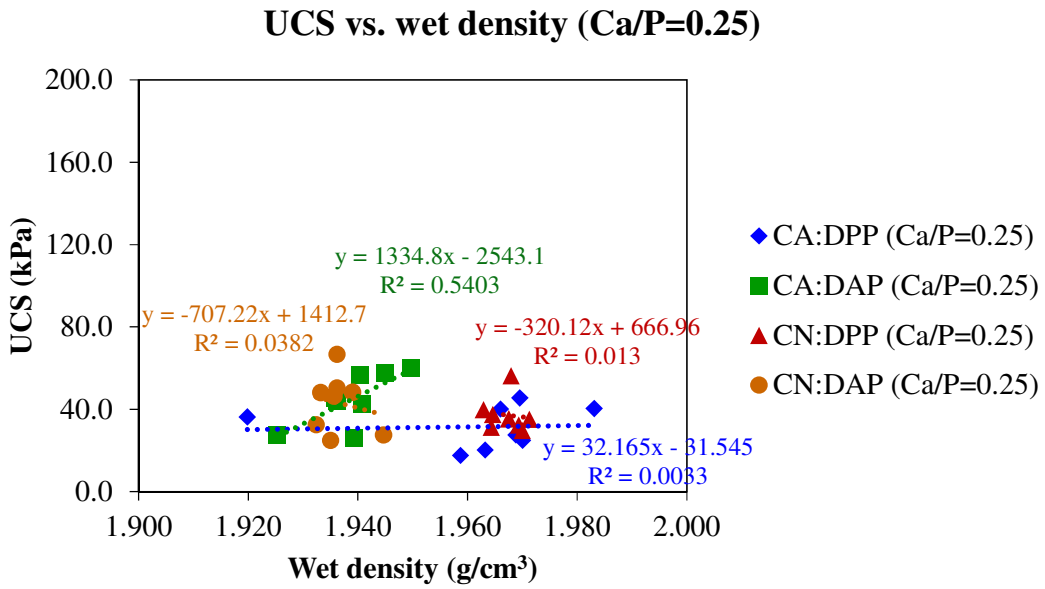

Fig. 2.18 (a): Relationship between UCS and pH for Ca/P = 0.25.

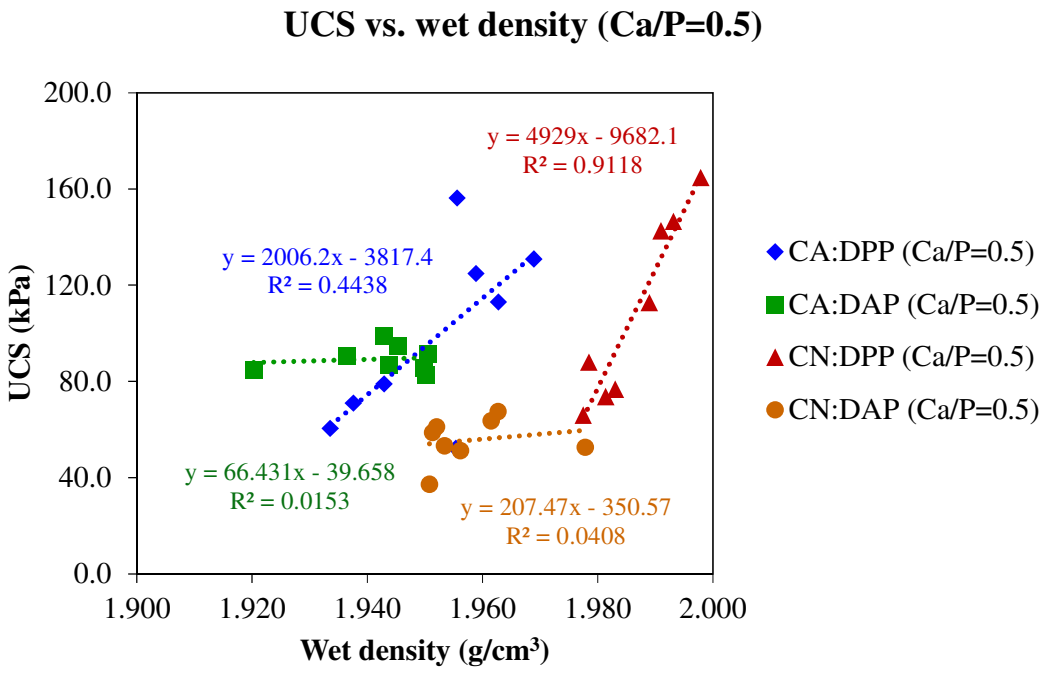

Fig. 2.18 (b): Relationship between UCS and pH for Ca/P = 0.5.

2.6.3 UCS and Ca/P ratio

The UCS value was increased with the increase of Ca/P ratio. Moreover, the increase of increasing UCS was lower in CN: DAP comparing other mixtures. The object value of UCS > 100 kPa was reached CA: DPP and CN: DPP samples.

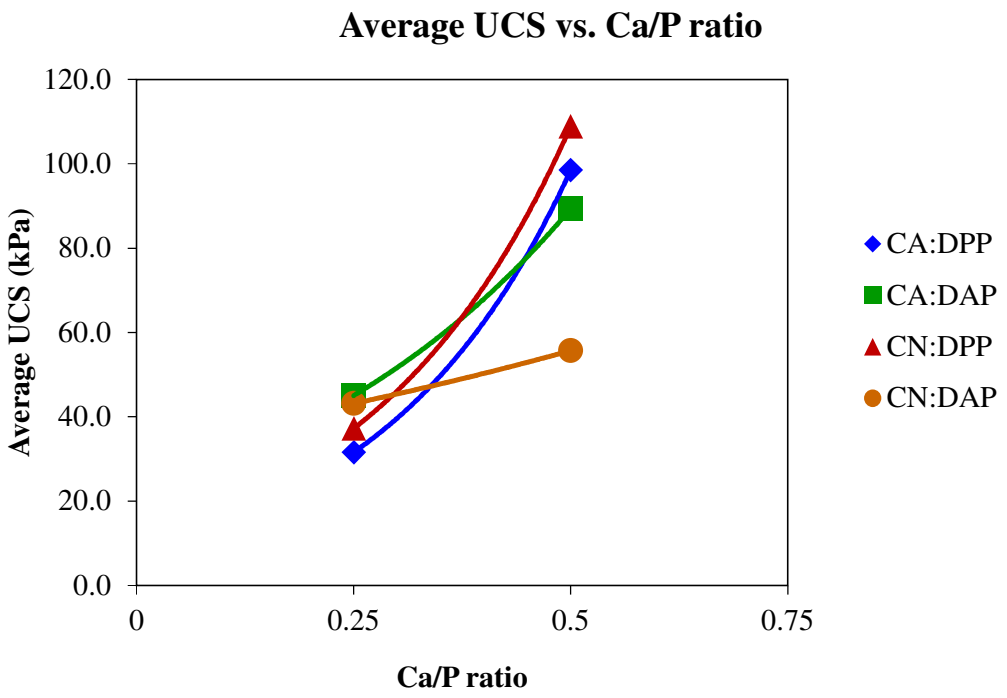

Fig.2.19: Relationship between Average UCS value and Ca/P ratio of the test pieces.

Wisker-like crystal structure was observed in the sample prepared with CA: DPP=0.5 mixture and other samples were not clearly observed any crystal formation. It has been reported that HA whiskers are formed by adding an acetic acid solution to amorphous calcium phosphate (Toyama et al, 2001). In Portland cement, the formation of ettringite, which shows whisker-like crystals, promotes solidification and increases strength (Sakai E. at al, 2004).

From the results of the experiment, CA: DPP with Ca/P = 0.5 is the best stock solution for reach my aim to mitigate the liquefaction. The governing factors for this mixture was, pH value, wet density and SEM observation.

For the mixture of CA: DPP with Ca/P = 0.5, the testing was conducted with changing packing ratio. I selected $Ca(CH_3COO)_2$ and K_2HPO_4 solutions for CPCs with $Ca(CH_3COO)_2$-

1.5 mol/L and K_2HPO_4 - 3.0 mol/L. Then same volume of $Ca(CH_3COO)_2$ and K_2HPO_4 solutions was taken for different packing ratio of Toyoura sand (70%, 85% and 100%). Two cases of specimens were prepared for each packing ratio by different curing periods (1 day and 14 days).

For the specimens, I conducted the tests such as: UCS test, Low vacuum SEM, High vacuum SEM observation with Energy-dispersive X-ray spectroscopy (EDX) and micro-focus X-ray CT.

Table 2.6: Quantity of solutions for difference packing ratio.

Packing Ratio	**Quantity of Solutions**
100%	36.65 mL
85%	31.15 mL
70%	25.66 mL

2.6.4 Results of UCS, pH and wet density with curing time

Figure 2.20 is shown the relationship with UCS and curing time, pH and curing time and wet density and curing time. From the results, it is concluded that the USC, pH and wet density with the time of curing were large for the sample prepared with 100% packing ratio.

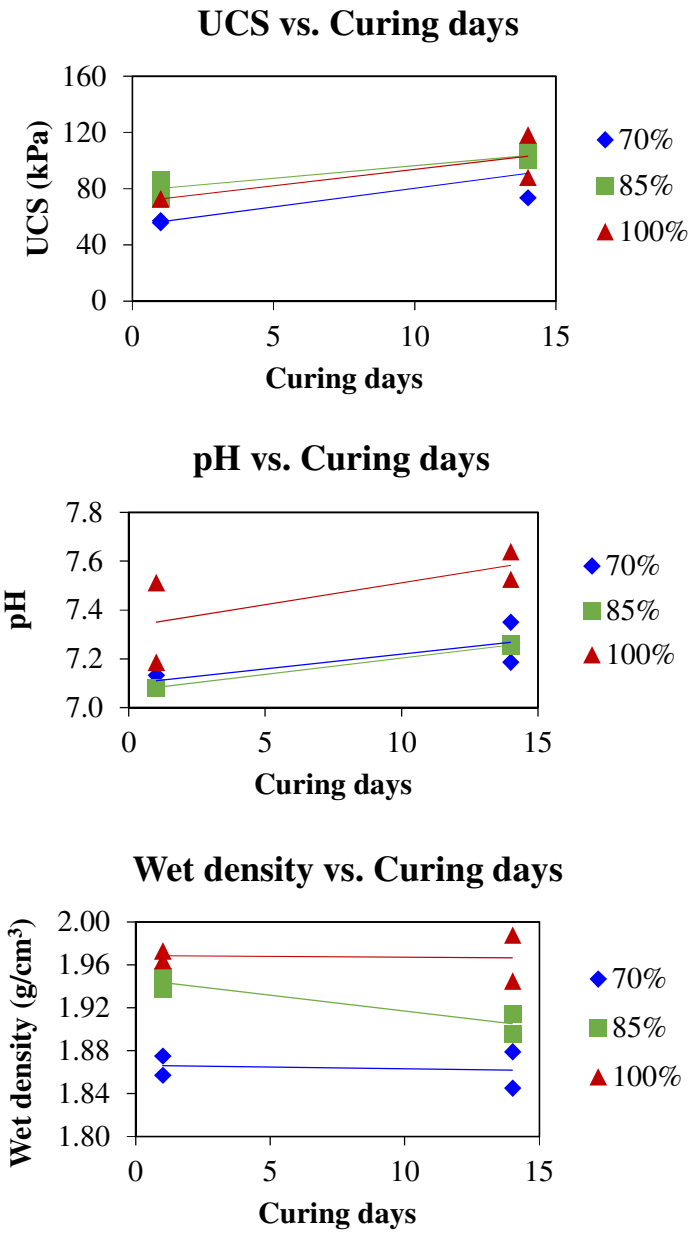

Fig. 2.20: Average UCS value, pH and wet density with the time.

2.6.5 Relationship between UCS and pH, wet density and packing ratio

The results shows that the UCS was intended to increase with the increase of pH value of the sample. Moreover, the UCS value was increased when increased the packing ratio from 70% to 100% and the strength was larger at the sample curing with 14 days than 1 day.

(a)

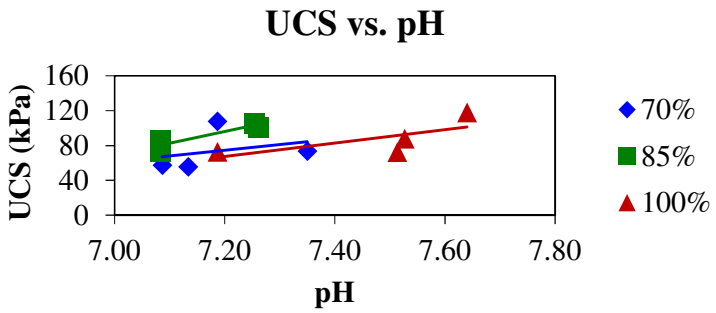

(b)

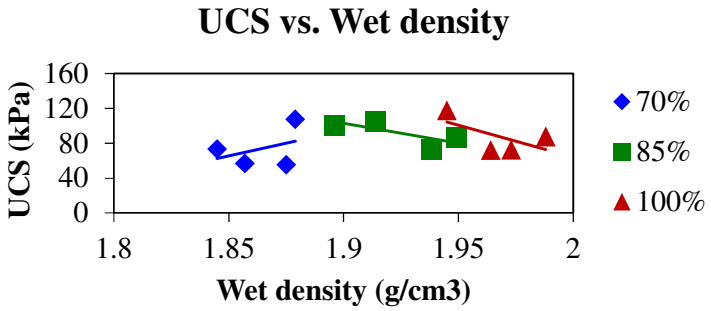

(c)

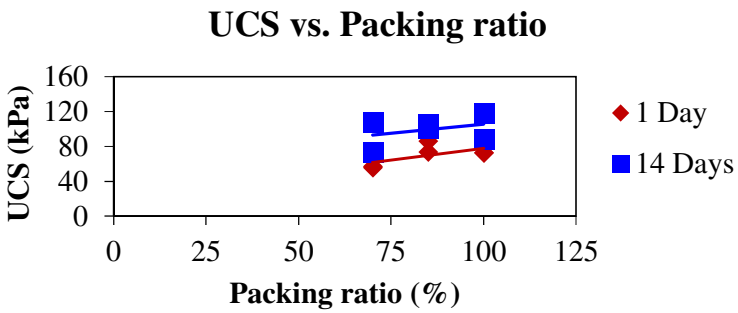

Fig. 2.21: Relationship between (a) UCS vs pH, (b) UCS vs wet density, and (c) UCS vs packing ration for the test pieces prepared with different packing ratios.

2.6.6 Low vacuum SEM observation

Low vacuum SEM images for the sample prepared with different packing ratios with 1 day and 14 days curing period was shown in following figures (Figs. 2.22 and 2.23). However, any crystal formation were not identified.

(a)

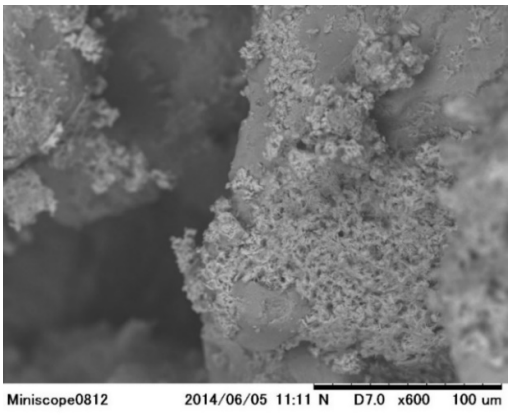

(b)

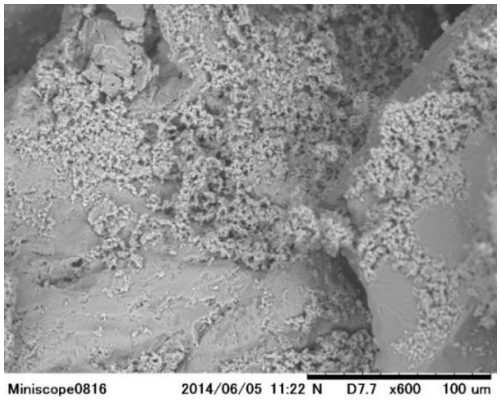

(c)

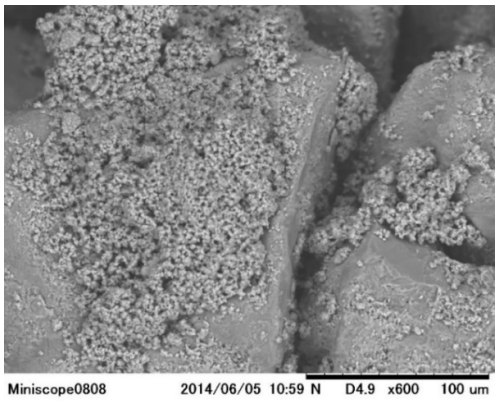

Fig. 2.22: SEM images for packing ratio (a) 70%, (b) 85% and (c) 100 % after 1 day curing period.

(a)

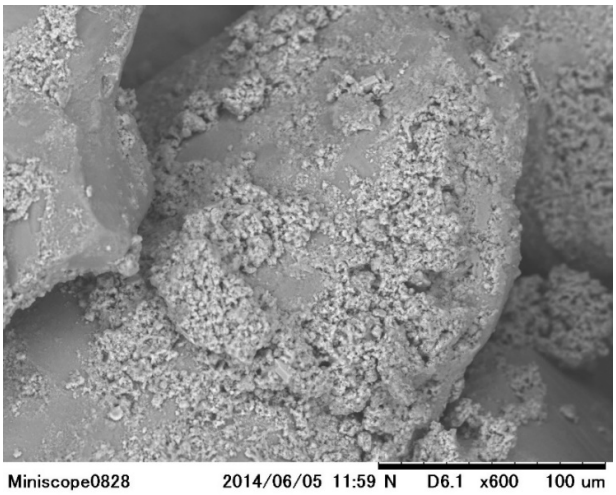

(b)

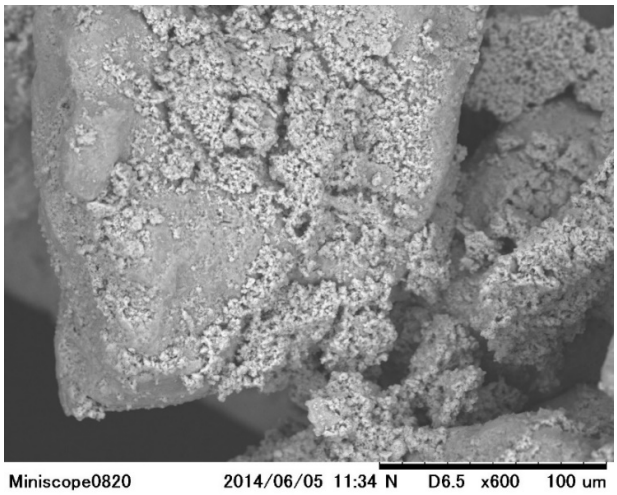

(c)

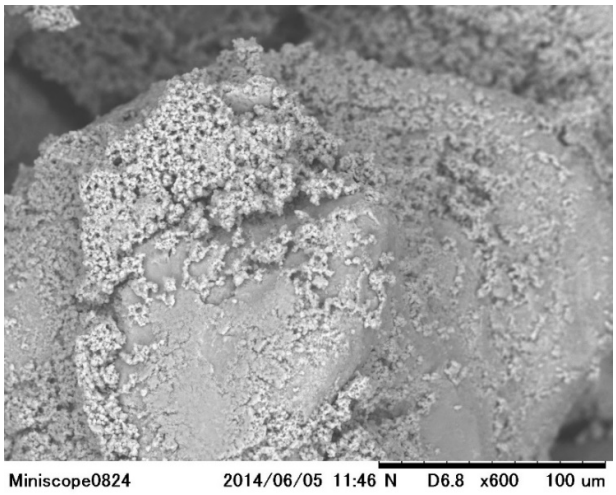

Fig. 2.23: SEM images for packing ratio (a) 70%, (b) 85% and (c) 100 % after 14 day curing period.

2.6.7 EDX and high vacuum SEM results

According to the EDX results, calcium and phosphate concentration was higher in the sample prepared with 100% packing ration than 70% packing ratio. This phenomenon was similar both 1 day and 14 day curing period as shown in Fig. 2.24 and Fig. 2.25.

(a)

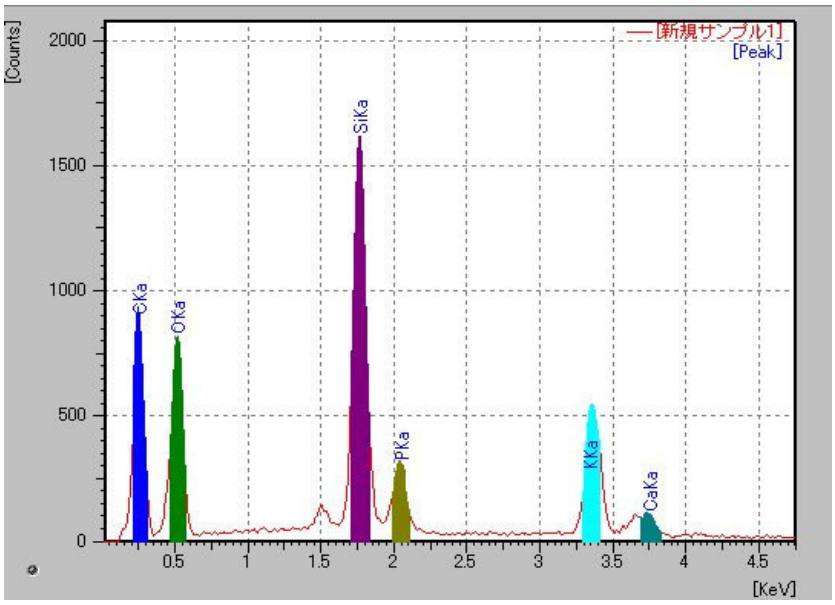

70%

(b)

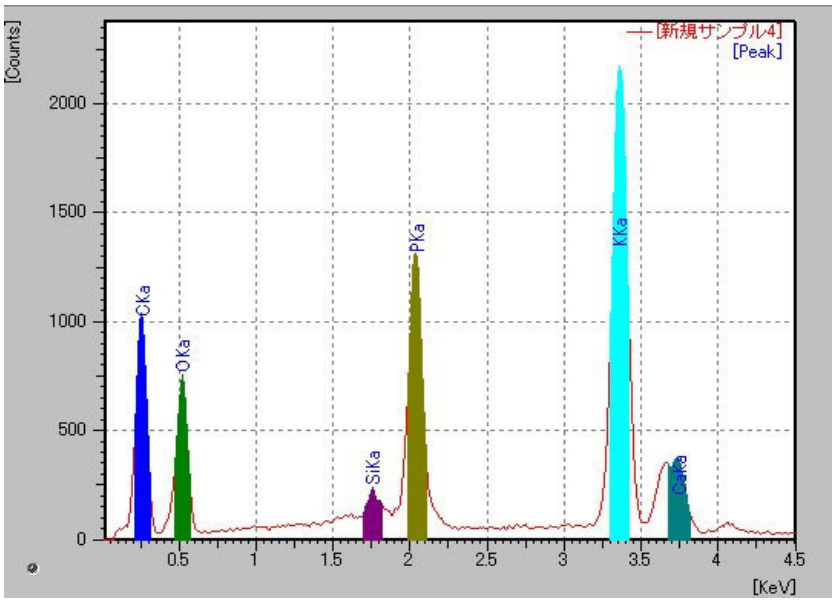

100%

Fig. 2.24: EDX results for packing ratio (a) 70% and (b) 100 % after 1 day curing period.

(a)

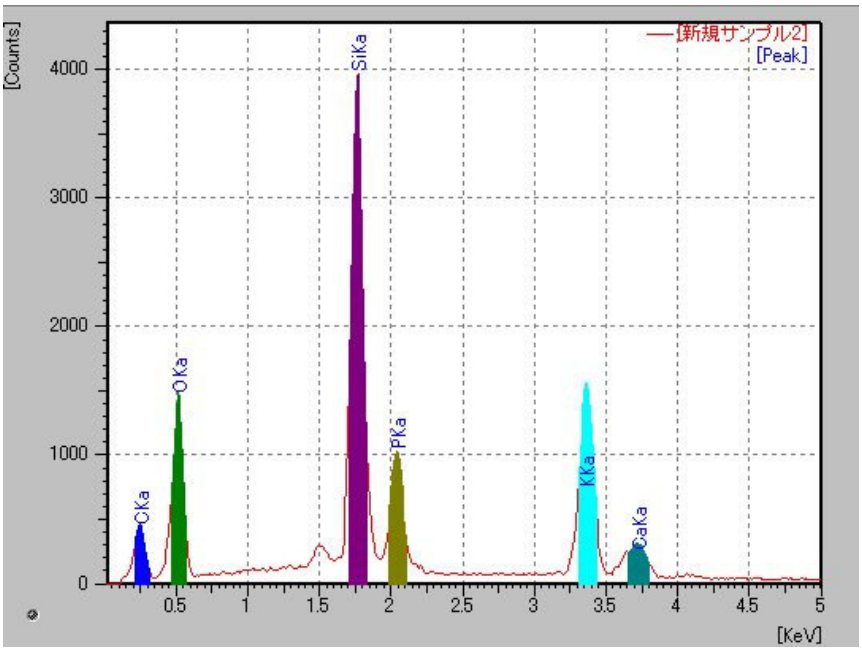

70%

(b)

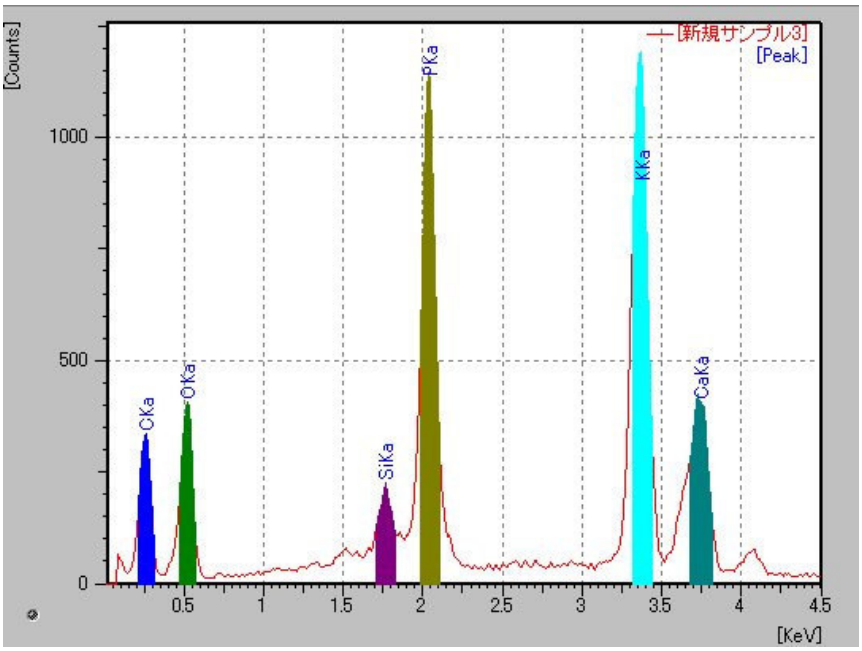

100%

Fig. 2.25: EDX results for packing ratio (a) 70% and (b) 100 % after 14 day curing period.

The following figures (Figs. 2.26 and 2.27) show the clear SEM images of the sample which were in dry condition. In addition, images shows that the CPC precipitation on the sand sample very evidently.

(a)

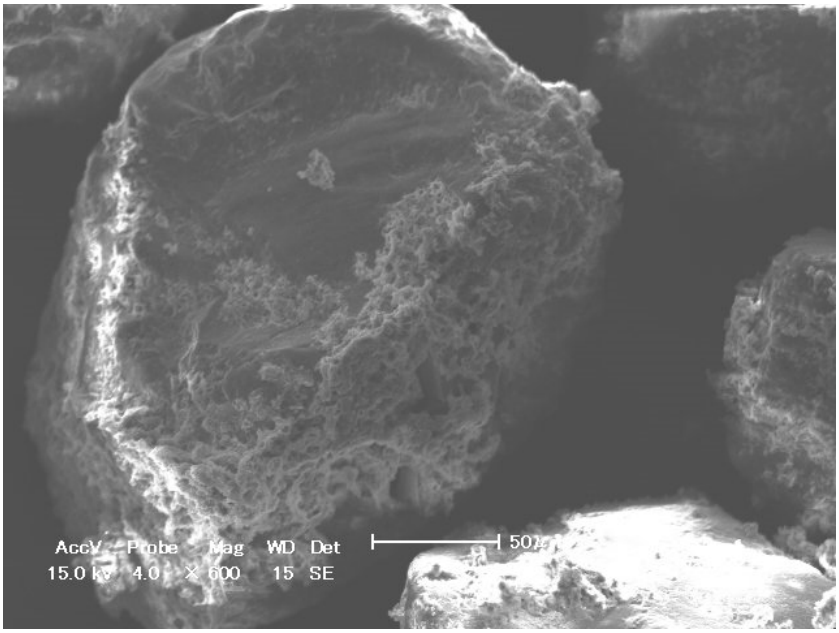

(b)

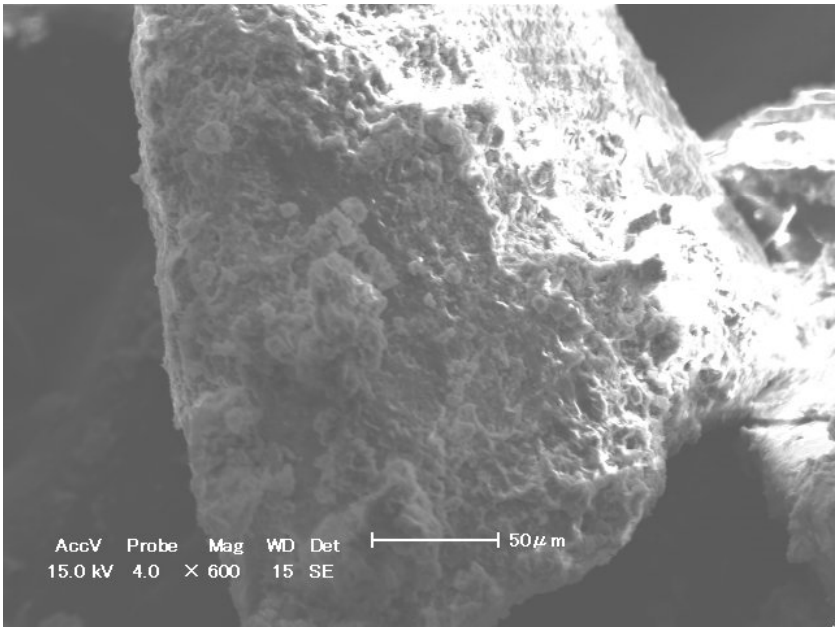

Fig. 2.26: SEM images for packing ratio (a) 70% and (b) 100 % after 1 day curing period.

(a)

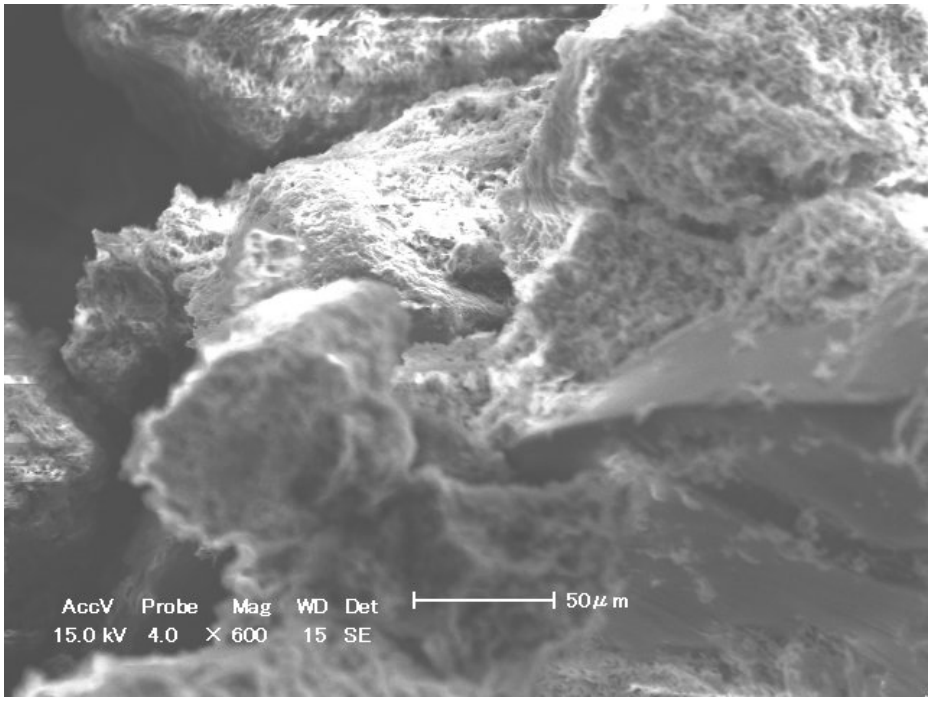

(b)

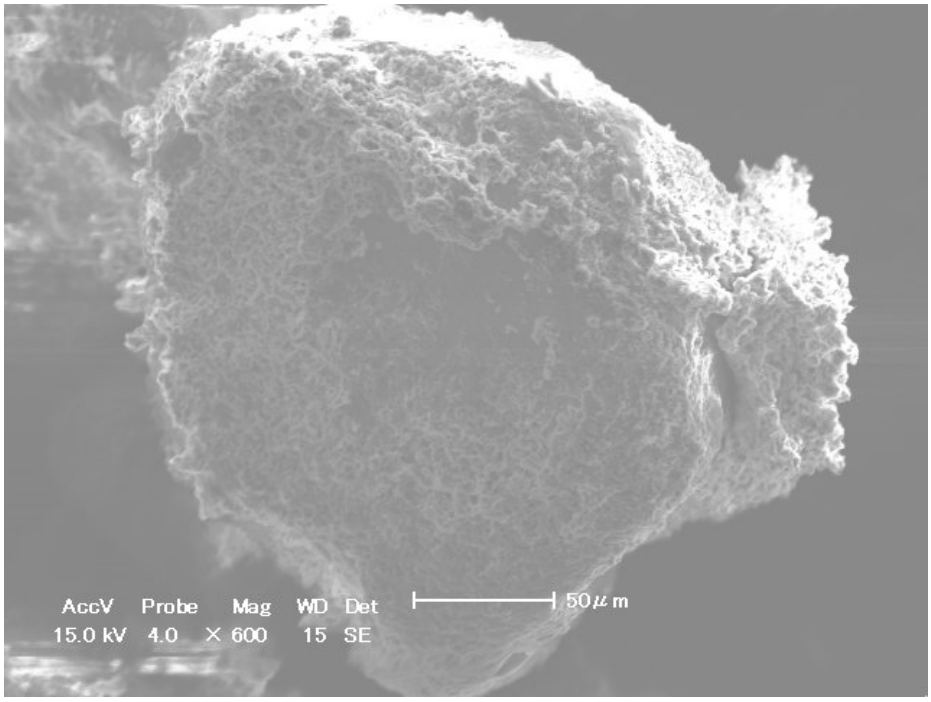

Fig. 2.27: SEM images for packing ratio (a) 70% and (b) 100 % after 14 days curing period.

2.6.8 Relationship with porosity and UCS

Porosity of the samples was increased with the increase of packing ratio of the solution. With the time porosity was decreased, because of filling CPC between sand particles. Therefore, the strength of the sample was increased when the porosity is reduced. The following figure (Fig. 2.29) shows that the X-CT images for the samples prepared with different packing ratios. In that figure, it is clearly notified that the voids of the sample decreased when the packing ratio increased.

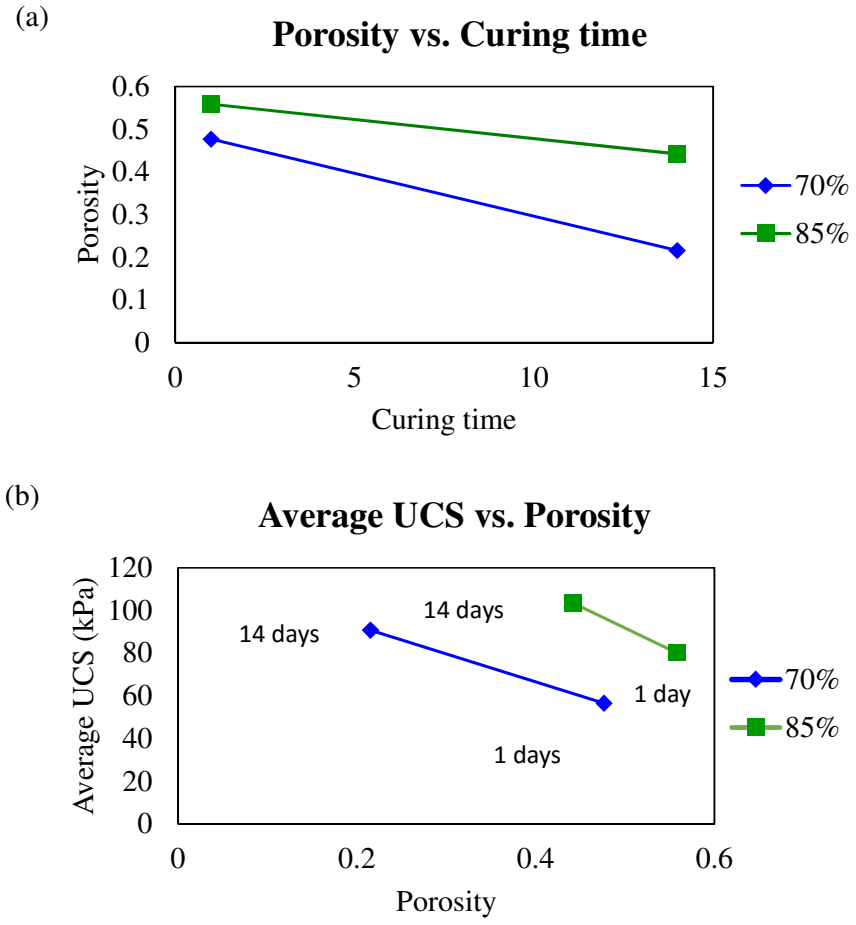

Fig. 2.28: (a) Relationship between porosity and curing time for the different packing ratios. (b) Relationship between average UCS and porosity of the samples.

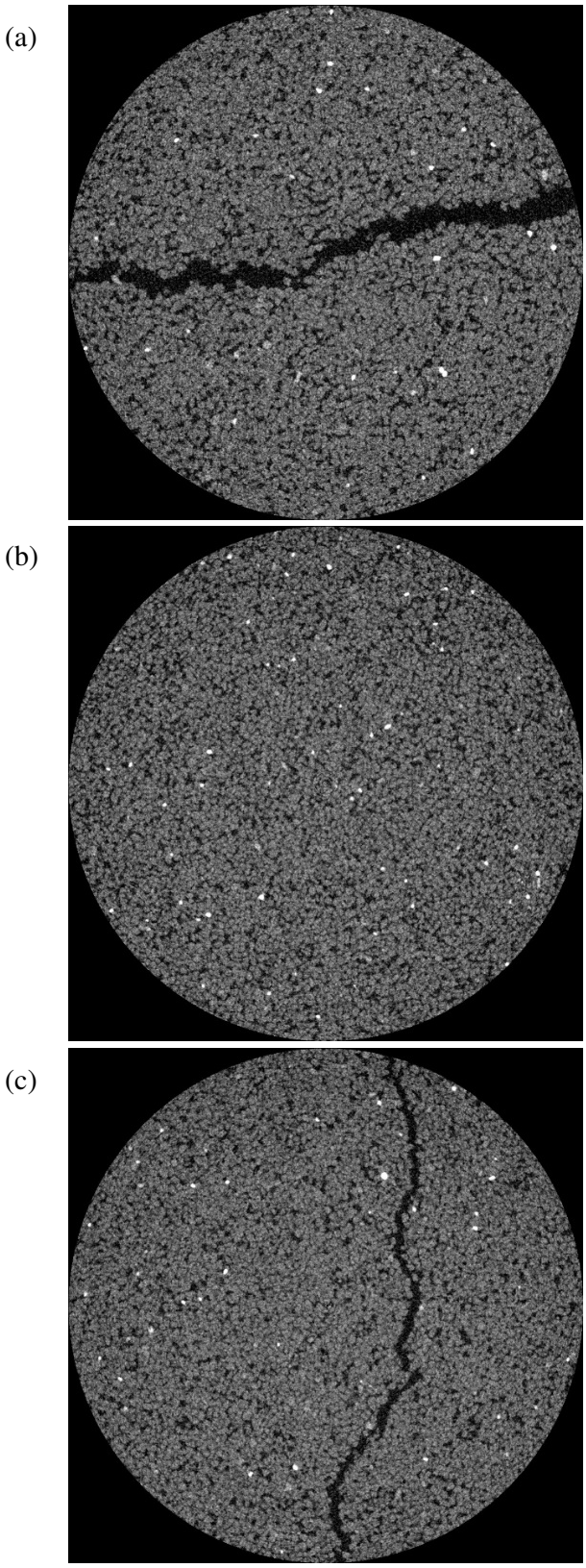

Fig. 2.29: X-CT images for the packing ratio (a) 70%, (b) 85% and (c) 100%.

2.7 CONCLUSION

In this study, the condition for CPC precipitation using different mixtures of calcium and phosphate stock solutions was investigated and analyzed. For that, Toyoura sand test pieces were cemented by CPC solutions and cured up to 28 days and carried out unconfined compressive strength (UCS) test. The strength of the samples was large for 1.5 M CA: 3.0 M DPP and 1.5 M CN: 3.0 M DPP mixtures with the concentration of Ca/P ratio is 0.5. The UCS values of Toyoura sand test piece cemented with CA: DPP and CN: DPP were 144.65 kPa and 143.60 kPa respectively. Furthermore, pH measurement and scanning electron microscope (SEM) were observed. The results indicate that the pH value was increased with the curing time for the calcium to phosphate molar ratio was 0.5. Wisker-like crystal formation showed the only sample prepared with CA: DPP=0.5 mixtures. It has been reported that HA whiskers are formed by adding an acetic acid solution to amorphous calcium phosphate (Toyama et al, 2001). In Portland cement, the formation of ettringite, which shows whisker-like crystals, promotes solidification and increases strength (Sakai E. at al, 2004). Therefore, it is concluded that the CPC mixture of 1.5 M CA: 3.0 M DPP with the concentration of Ca/P ratio = 0.5 is better than other mixtures tested in this study.

Changes in the concentration of the reaction mixture were not reflected proportionally in the strength of the sand test pieces. In the future, additional tests aimed at determining the improvement in the strength by CPC are needed to understand more clearly the underlying mechanical processes and to facilitate practical application. The relationship between the strength and the various CPC precipitation parameters (concentration and pH of the reaction mixture, curing time, etc.) should be examined in further detail, as continued research is needed to identify the process or processes that link crystal precipitation to the increase in strength. Furthermore, shearing and permeability tests using pieces cemented by CPC should be conducted to evaluate the applicability of CPCs for purposes such as permeability control

and reinforcement of soil and rock.

REFERENCES

Akiyama M, Kawasaki S, "Novel grout material using calcium phosphate compounds: in vitro evaluation of crystal precipitation and strength reinforcement," Journal of the Japan Society of *Engineering Geology*, Vol. 125, 2012a, pp. 119-128.

Akiyama M, Kawasaki S, "Microbially mediated sand solidification using calcium phosphate compounds, " Journal of the Japan Society of *Engineering Geology*, Vol. 137-138, 2012b, pp. 29-39.

Harkes MP, Van Paassen LA, Booster J.L, Whiffin VS, Van Loosdrecht MCM, *Ecological Engineering*, Vol. 36, 2010, pp. 112-117.

Tung MS, Calcium phosphates: structure, composition, solubility, and stability, in: A. Zahid (Ed.), Calcium phosphates in biological and industrial systems, Kluwer Academic Publishers, Norwell, 1998, pp. 1-19.

Van Paassen LA, Harkes MP, Van Zwieten GA, Van der Zon WH, Van der Star WRL, Van Loosdrecht MCM, Conference Proceedings, in Proc. 17th Int. Conf. on Soil Mechanics and Geotechnical Engineering, 2009, pp 2328-2333.

CHAPTER 3

SOIL IMPROVEMENT USING CPC-CHEM POWDER METHOD

3.1 INTRODUCTION

Soil liquefaction describes a phenomenon whereby a saturated soil substantially loses strength and stiffness in response to an applied stress, usually earthquake shaking, causing it to behave like a liquid. The effects of liquefaction have been long understood, it was more thoroughly brought to the attention of engineers after the 1964 Niigata earthquake and 1964 Alaska earthquake (Geologist arrive to study liquefaction, 2011). In Japan, many areas are potential to liquefaction after the earthquake happens. Therefore, there is an urgent need for countermeasures for soil liquefaction (Japanese geotechnical society, 2011).

Cement grouting is commonly used for as a ground improvement method and it plays an important role as countermeasures against disasters, including ground liquefaction during an earthquake (Karol, 2003). However, cement grouting comprises quite a lot of environmental problems. Therefore, in recent years, grout materials that use mechanisms of cement material production by microorganisms have been developed for ground permeability control and reinforcement (Whiffin et al. 2007, De Muynck et al. 2010, Dejong et al. 2010, Harkes et al. 2010, and Kawasaki et al. 2010). The process of ground improvement by biological action is called “biogrouting” (Van Paassen et al. 2009). For biogrouting, there are three mechanisms of mineral formation have to be considered: precipitation of calcium carbonate by in situ microorganisms and/or added yeasts,(Kawasaki et al. 2006) precipitation using urea and ureolytic bacteria, (Harkes et al. 2010) and siloxane bond formation using glucose and yeast (Terajima et al. 2009).

In recent years, a novel ground stabilizer to increase the number of options available among cementing mechanisms based on microorganisms (Akiyama and Kawasaki, 2012a and

2012b). Further, it is reported on a CPC chemical grout (CPC-Chem) that utilizes self-setting CPC mechanisms (Fig. 2.2 in Chapter 02), and on a CPC biogrout (CPC-Bio) whose solubility is dependent on its pH (Fig. 2.1 in Chapter 02), which can be increased by a microbial reaction. Since CPC-Chem is easy to obtain, safe to handle, non-toxic, and recyclable, advantages that make it suitable for the geotechnical application (Akiyama and Kawasaki, 2012a). The maximum UCS of sand test pieces cemented with CPC-Chem was found to be 63.5 kPa (Akiyama and Kawasaki, 2012a). When CPC-Chem was converted to CPC-Bio by the addition of microorganisms and an ammonia source, the UCS increased from 42.9 kPa to 57.6 kPa (Akiyama and Kawasaki, 2012b). This study`s aim was to achieve a UCS value of 100 kPa, which is needed to avoid ground liquefaction during earthquakes (Yamazaki et al. 1998). This implies that the UCS of both CPC-Chem and CPC-Bio is not sufficient for use as a ground stabilizer, necessity of a preferable mechanism for the further increase in UCS. Research on CPC precipitation and solidification is also currently underway in the field of medical and dental science. A research on CPC paste has reported that the unconfined compressive strength (UCS) of CPC exceeds 10 MPa under normal temperature and pressure conditions (Fernandez et al. 1998). In addition, it has shown that the compressive strength of a mixture paste of dicalcium phosphate(DCP) and α-tri calcium phosphate (TCP) reached can be increased from 35 MPa to a maximum of 56 MPa by using calcium carbonate (CC)as the seed crystal (Fernandez et al. 1998).

A previous research said, the UCS of the test pieces with TCP and CC additives exceeded the targeted value of 100 kPa and increased to a maximum of 261.4 kPa and 209.7 kPa respectively (Kawasaki and Akiyama, 2013). This observation indicates that the existence of CC seed crystals can reinforce the strength of CPC grouts, such as the grout used in this study. CC is the main component of scallop shells, which are disposed of in large quantities as marine industrial waste (410,000 tons/year in Japan) (Ports and Harbor bureau). Moreover, it

is non-toxic to handle and inexpensive to obtain. Thus, CC is a promising material in the geotechnical field from the viewpoint of waste utilization and cost effectiveness.

3.2 OBJECTIVE

In the present study, the aim was to improve strength by adding CPC with scallop shell powder. This study aim was to exceed a maximum UCS of 100 kPa after 28 days of curing, which is the strength required to use the CPC and scallop shell powder combination as a countermeasure against soil liquefaction during an earthquake. I carried out UCS tests and scanning electron microscopy (SEM) observations on sand test pieces as a function of time. Based on the results, I discussed the effect of the kind and amount of added powders and crystal form on the UCS.

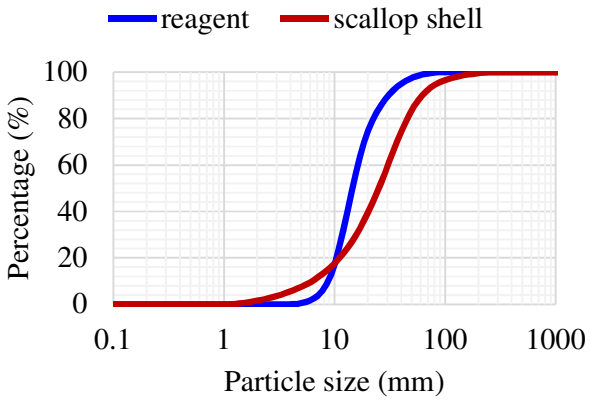

Fig. 3.1: Particle size distribution of scallop shell powder and the regent ($CaCO_3$ powder).

3.3 METHODOLOGY

The CPC-Chem used in this study were 0.75 M: 1.5 M mixture of calcium acetate (CA) and diammonium phosphate (DAP). This mixture was used because it has previously been reported that this mixture yields the highest UCS among all combination ratios of DAP with calcium nitrate or CA, (Akiyama and Kawasaki, 2012a) and 0.6 M: 1.2 M mixture of calcium acetate (CA) and dipotassium phosphate (DPP). Toyoura sand test pieces were cemented by

CPCs with $CaCO_3$ (CC) powder which was taken by commercially and CPCs with scallop shell (SS) powder and cured and these specimens also analyzed with UCS tests. Hereafter, $CaCO_3$ powder is referred to as CC method and scallop shell powder is referred to as SS method. A standard sand test piece was made from 320.09 g of Toyoura sand (mean diameter D_{50} =170 µm, 15% diameter D_{15} =150 µm) and 73.3 mL of CPC-Chem according to the previous report, and the examined test pieces were made with the combination ratio and wet density shown in Fig. 2. 1% (3.2 g) (Case SS-01 and CC-01), 5% (16.0 g) (Case SS-05 and CC-05), and 10% (32.0 g) (Case SS-10 and CC-10) of CC (mean diameter D_{50} =14.52 µm) and SS (mean diameter D_{50} =25.12 µm) were mixed with 72.21 mL, 67.84 mL, and 62.38 mL of CPC-Chem respectively and added to weight of a standard sand test piece of 320.09 g. It was uniformly mixed in a stainless-steel ball for 2 min and the mixture was divided into quarters, each of which was placed into a plastic mold container (ϕ=5 cm, h =10 cm). The sand in the mold contained was tamped down 30 times by a hand hammer after each of the four quarters was placed in the mold. The molded test pieces were subsequently cured in an airtight container at a high humidity for 56 days at 20 °C. The control samples were test pieces cemented with only CPC-Chem (Case CPC-Cont). Hereafter, the method of improving ground strength by adding CC powder to CPC-Chem is referred to as the CPC-CC method and SS powder to CPC-Chem is referred to as the CPC-SS method. The UCS of the test pieces removed from the mold container after curing was measured at an axial strain rate of 1%/m in with the UCS apparatus T266-31100 (Seikensha Co., Ltd., Japan). In all cases, two test pieces were tested.The pH of the test pieces was calculated as an average of three measurements (top, bottom, and middle of each test pieces) using pH Spear (Eutech Instruments Pte., Ltd., Singapore). Segments of the UCS test pieces were observed by low vacuum SEM. The segments were naturally dried at 20 °C for a few days and carbon-coated with a carbon coater and low vacuum SEM observations were carried out.

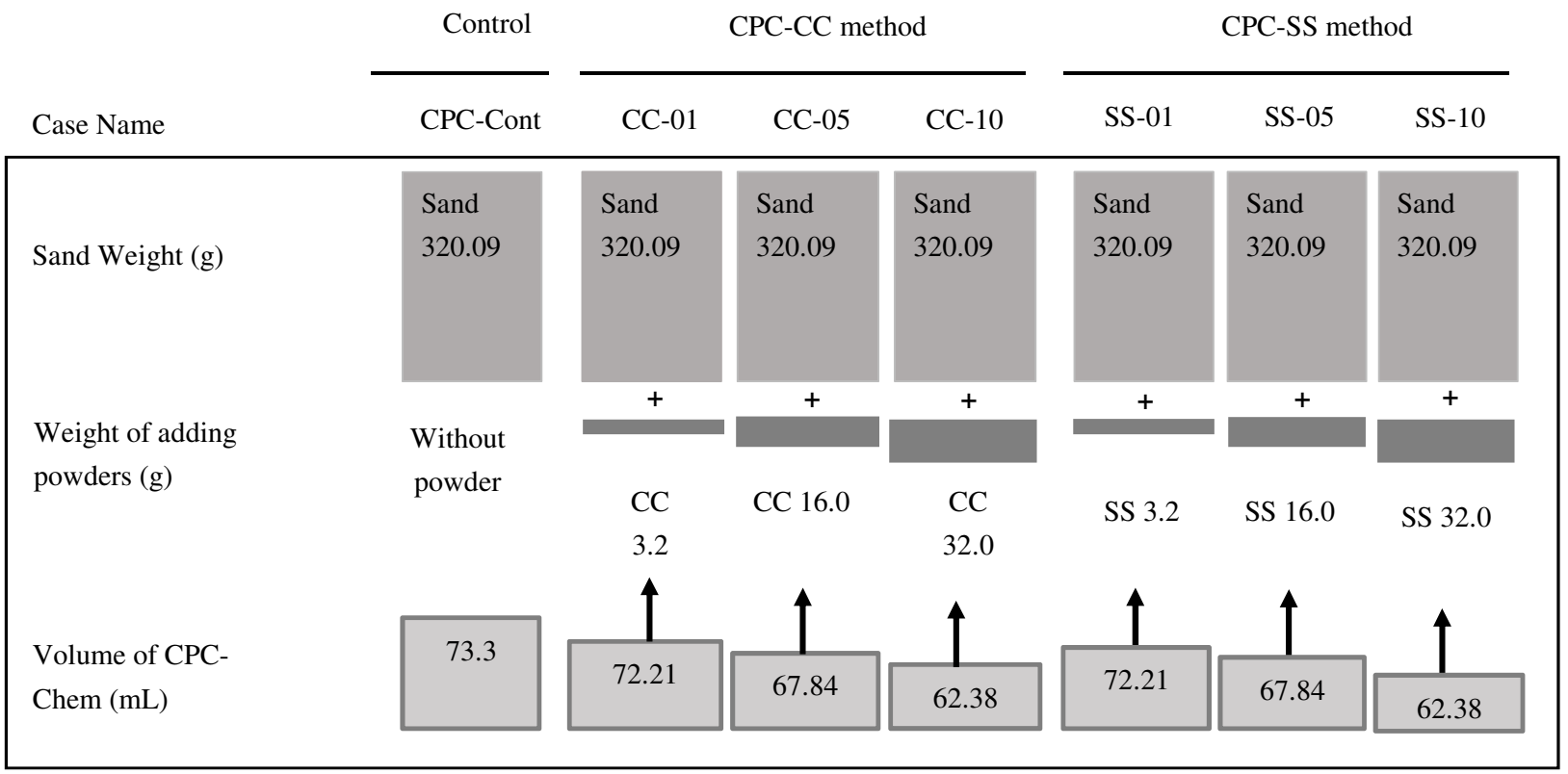

Fig. 3.2: Conceptual image of the contents.

3.4 RESULTS

3.4.1 UCS of sand test pieces

In this study, Toyoura sand test pieces cemented by seven reaction mixture sets were chosen (adding CA: DPP = 0.6 M: 1.2 M mixture with no adding powders and adding CC and SS powders; the percentage of powders varied to 1%, 5%, and 10%). The measured UCS in this study ranged from 49.9 to 176.3 kPa. The maximum value was measured when the DPP/CA ratio was 1.2 M: 0.6 M with adding CC reagent 10% (Fig. 3.3 (b)). The UCS tended to increase with the curing time for 14 days but after that, the UCS value is decreased with the curing time for the samples with adding CC powder. In Fig. 3.3(a), the test pieces with SS-10% showed the value of UCS neither increasing nor decreasing after 14 days. In both figures, it says that the UCS tended to increase with the curing time for control samples (CPC-Cont). The test pieces with SS -10% showed that the UCS tended to decrease at 14 days curing period, it is assumed that some error could occur when preparing a sample. To clarify this result, further examination of the test pieces is needed in the future. Also, the UCS value of the test pieces with SS-1% is higher than the UCS value of the test pieces with SS-5% but the UCS value of the test pieces with SS-10% is higher than SS-1% and 5% (Fig. 3.3(a)). Regarding the value of UCS, the difference between SS-1% and SS-5% is small. This is because the pH value is higher in SS-10% and then pH is high in SS-1% and pH is low in SS-5% (Fig. 3.4(a)). To clarify the reason for the decrease in pH in SS-5% test pieces, further examination of the test pieces in the CPC-SS method is needed in the future.

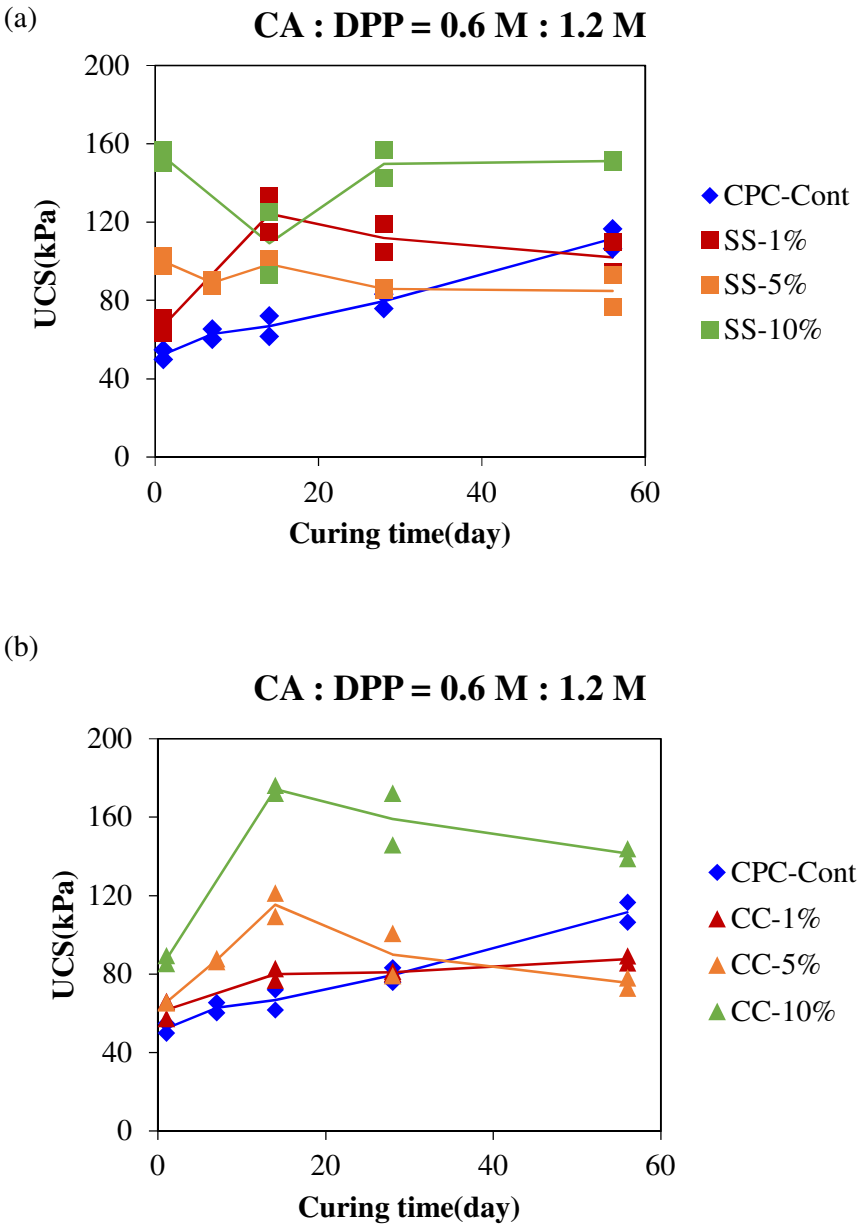

Fig. 3.3: (a) Unconfined compressive strength (UCS) of Toyoura sand test pieces cemented by CPC with SS. (b) Unconfined compressive strength (UCS) of Toyoura sand test pieces cemented by CPC with CC.

3.4.2 pH of sand test piece

For the CPC-Cont samples, the pH of the test pieces ranged from an acidic to weakly alkaline (6.5-7.6), while the addition of SS-Powder and CC-Powder resulted in a strong alkaline (7.6–9.0) pH (Fig. 3.4(a) and 3.4(b)). The pH tended to increase with the time. Moreover, the pH value of CPC-SS Samples is higher than pH values of CPC-CC samples (Fig.3.5). Not only that, Fig. 3.5 comprises that the concentration of SS and CC powder increased, pH value is intended to increase. The results showed in Fig. 3.6(a) comprises when curing time is increased, UCS is tended to increase and although, that the UCS tended to increase as the pH increase. Apparently, the reason for this phenomenon is the solubility of CPC become low when increasing the pH and the solubility of CPC is low means the $CaCO_3$ precipitation is high.

When considering CPC-Cont and CC-1% samples, it is utilized the following (Fig. 3.6(b)):

pH (CPC-Cont, 1 Day) < pH (CC-1%, 1 Day), UCS (CPC-Cont, 1 Day) = UCS (CC-1%, 1 Day)

pH (CPC-Cont, 56 Day) = pH (CC-1%, 1 Day), UCS (CPC-Cont, 1 Day) > UCS (CC-1%, 56 Day)

pH (CPC-Cont, 56 Day) < pH (CC-1%, 56 Day), UCS (CPC-Cont, 56 Day) > UCS (CC-1%, 56 Day)

Considering that the solubility of CPC is dependent on its pH (Fig. 2.1) and results in I taken it is summarized that the solubility is minimum at pH is about 8.

(a)

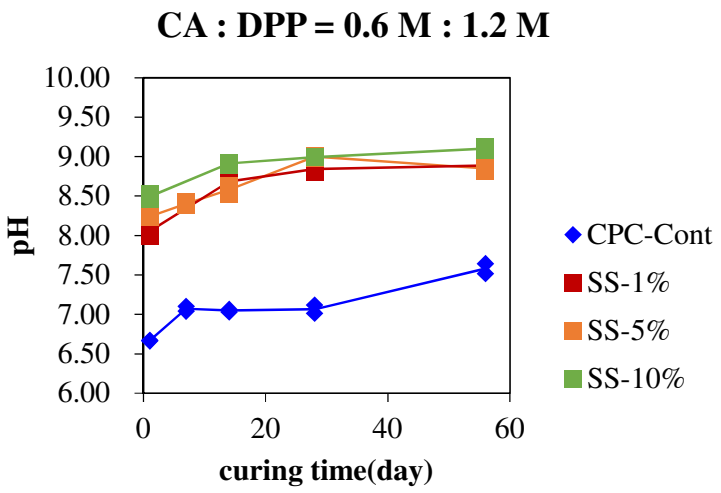

(b)

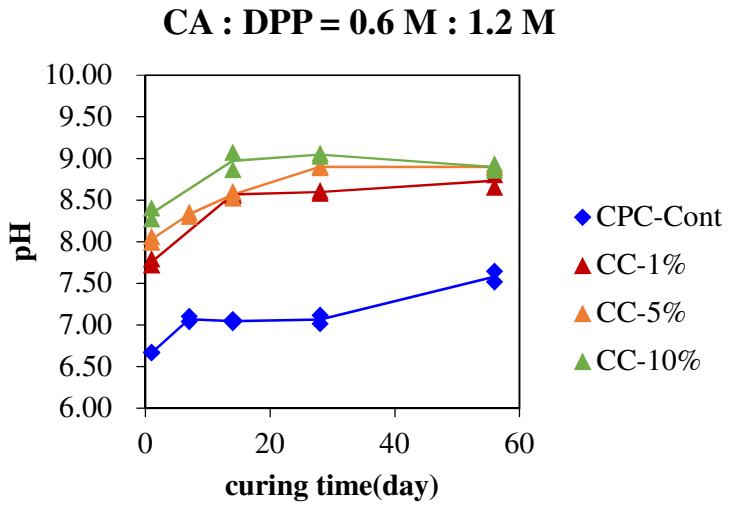

Fig. 3.4: (a) pH of Toyoura sand test pieces cemented by CPC with SS. (b) pH of Toyoura sand test pieces cemented by CPC with CC.

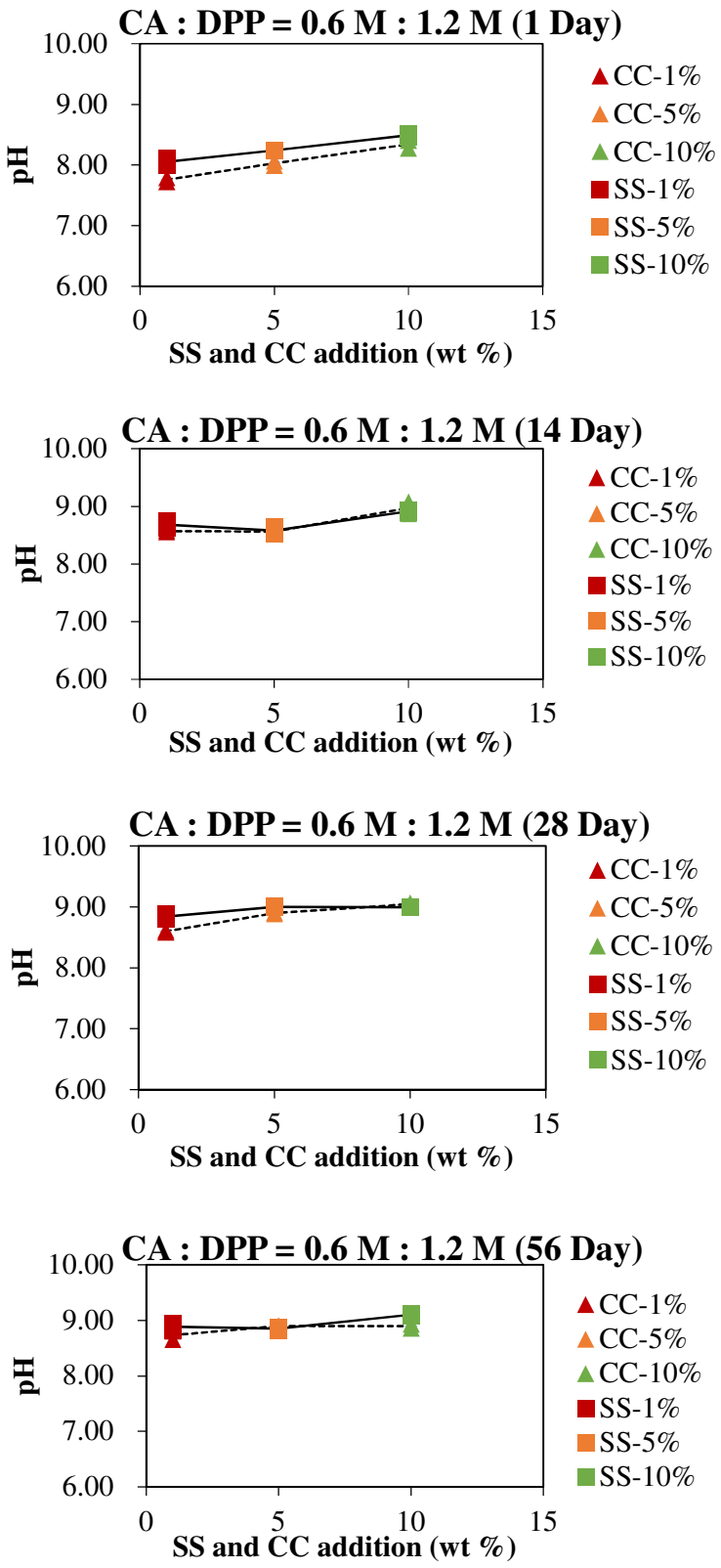

Fig. 3.5: Relationship between pH and SS, CC addition (wt%) with time.

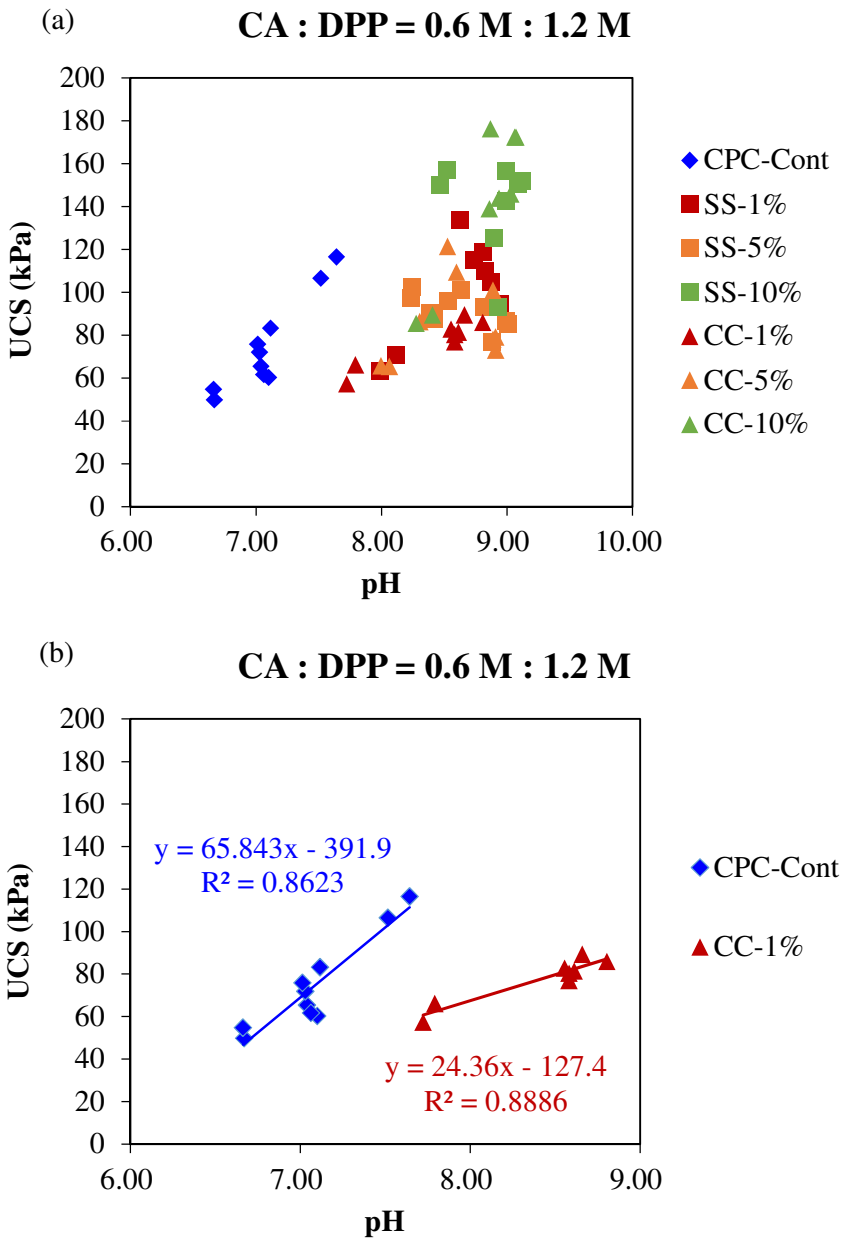

Fig.3.6: (a) Relationship between pH and UCS for CPC-Cont, CPC-CC and CPC-SS test pieces.

(b) Comparison between CPC-Cont and CC-1% test samples using pH vs UCS.

3.4.3 Effect of wet density on UCS

The measured wet density of the test pieces is provided in Figs. 3.7 (a) and 3.7 (b). The results show, UCS value is increased with the increase of density. Moreover, when curing time is increased the UCS is tended to increase. In addition, when the percentage (%) of SS and CC powders increased the wet density intended to increase. Since the density of CC powder (2.93 g/cm^3) was greater than that of Toyoura sand (1.65 g/cm^3), the density of the test pieces would increase with the mass % of CC powder and SS powder in the test pieces; it is expected that the increase in density would result in an improvement in UCS. In the case of the test pieces treated by the CPC-CC and CPC-SS method, the increase in CC content increased the filling of voids between sand particles because of the increase in wet density.

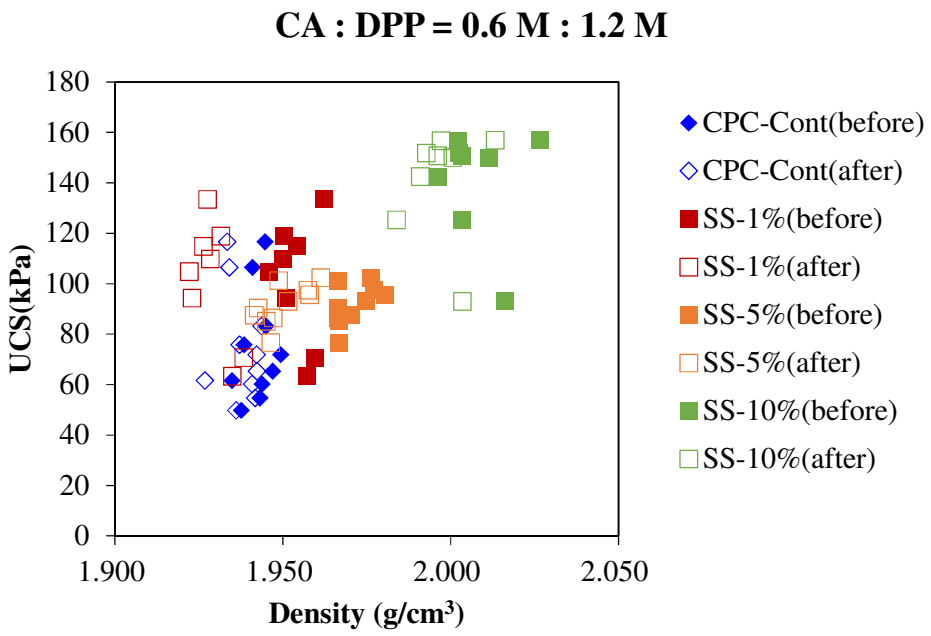

Fig. 3.7 (a): Wet density of Toyoura sand test pieces cemented by CPC with SS.

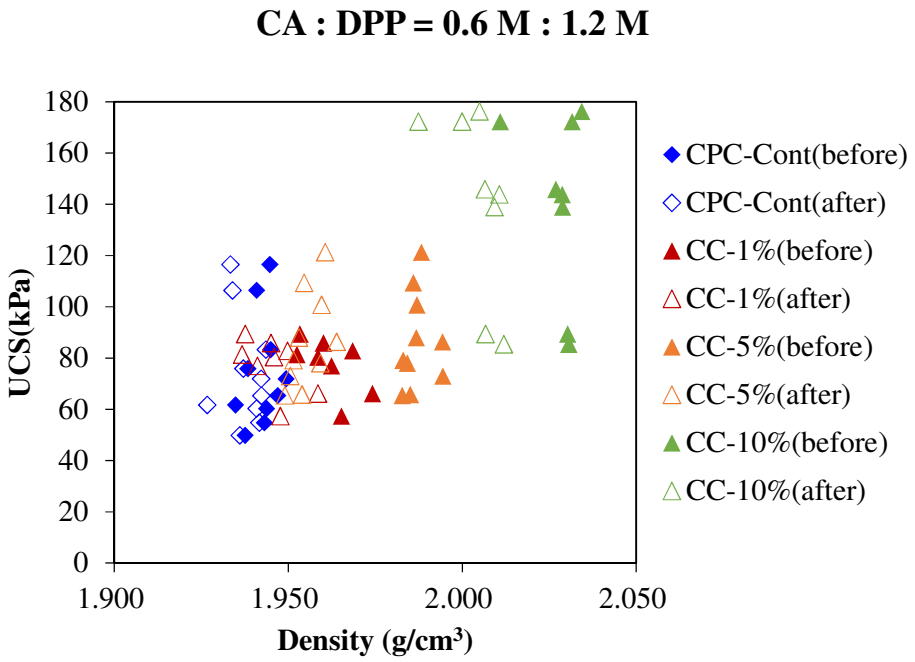

Fig. 3.7 (b): Wet density of Toyoura sand test pieces cemented by CPC with CC.

3.4.4 SEM observation of sand test pieces

Fig. 3.8 shows SEM images of seven sets of test samples. The crystal structures were not clearly observed in CPC-Cont, CPC-SS, and CPC-CC samples. The samples which the precipitated CPC that enveloped the CC particles bonded with the surface of the sand particles; such binding was also observed in sand test pieces, but without the formation of any crystal structure. The increase in UCS seemed to be because of the binding of the sand particles by the precipitated CPC that enveloped the CC particles. The analysis revealed that the improvement in UCS afforded by the CPC-CC and CPC-SS methods were because of the filling of the voids between sand particles and the uniting of the particles of cement material comprising Ca and P are stronger than CPC-Cont samples.

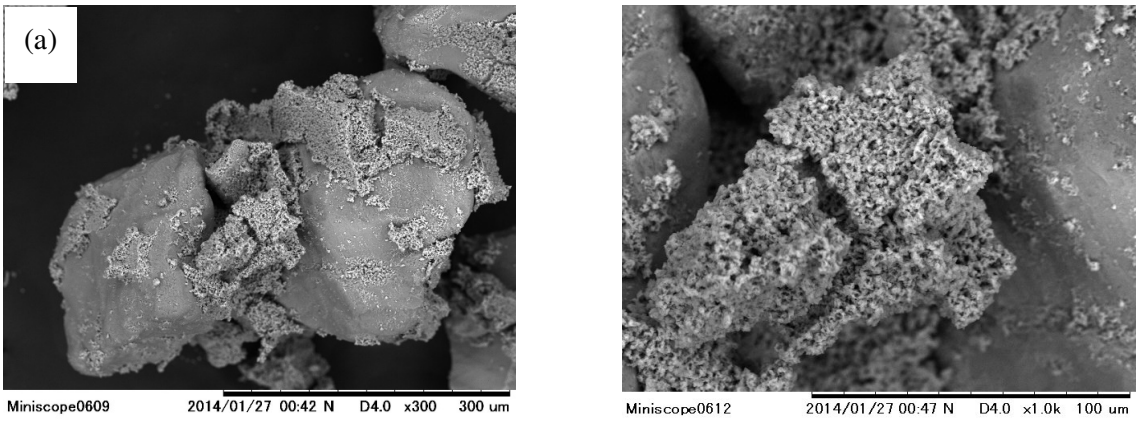
(a)
Miniscope0609 2014/01/27 00:42 N D4.0 x300 300 um
Miniscope0612 2014/01/27 00:47 N D4.0 x1.0k 100 um

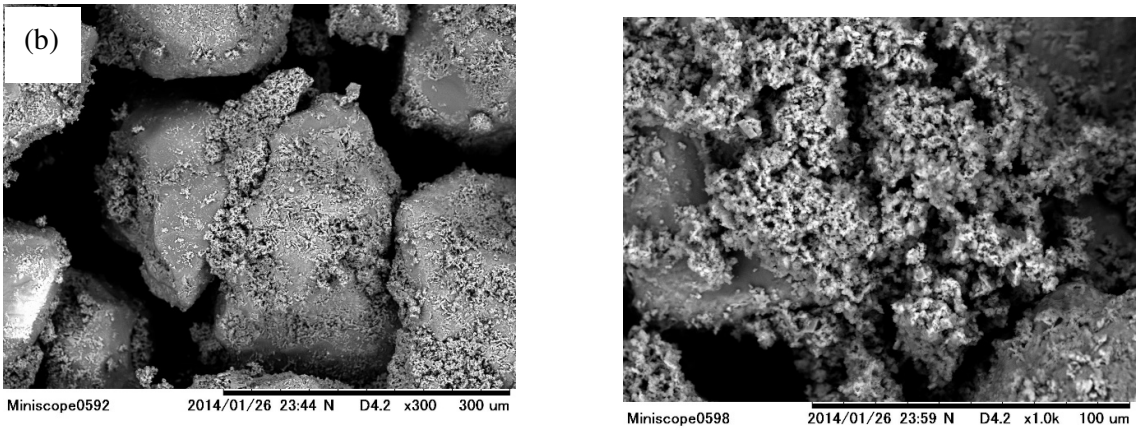
(b)
Miniscope0592 2014/01/26 23:44 N D4.2 x300 300 um
Miniscope0598 2014/01/26 23:59 N D4.2 x1.0k 100 um

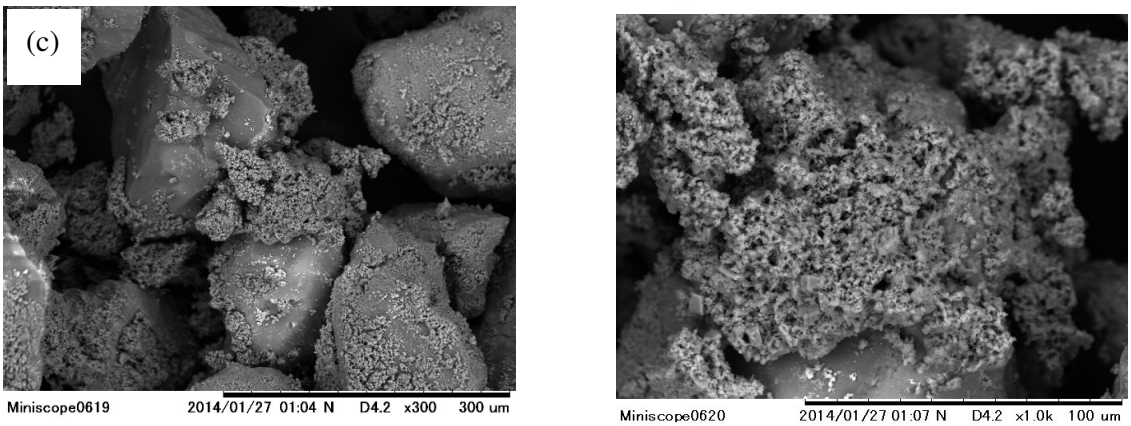
(c)
Miniscope0619 2014/01/27 01:04 N D4.2 x300 300 um
Miniscope0620 2014/01/27 01:07 N D4.2 x1.0k 100 um

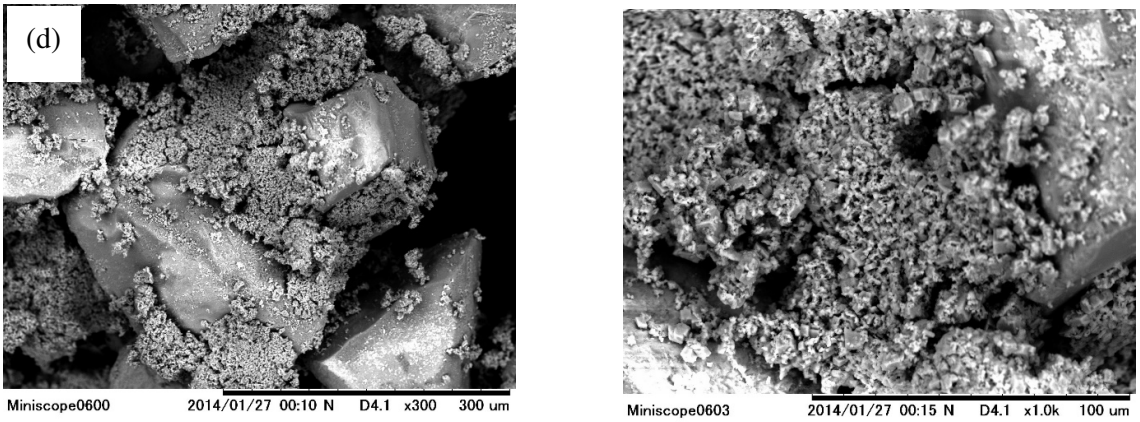
(d)
Miniscope0600 2014/01/27 00:10 N D4.1 x300 300 um
Miniscope0603 2014/01/27 00:15 N D4.1 x1.0k 100 um

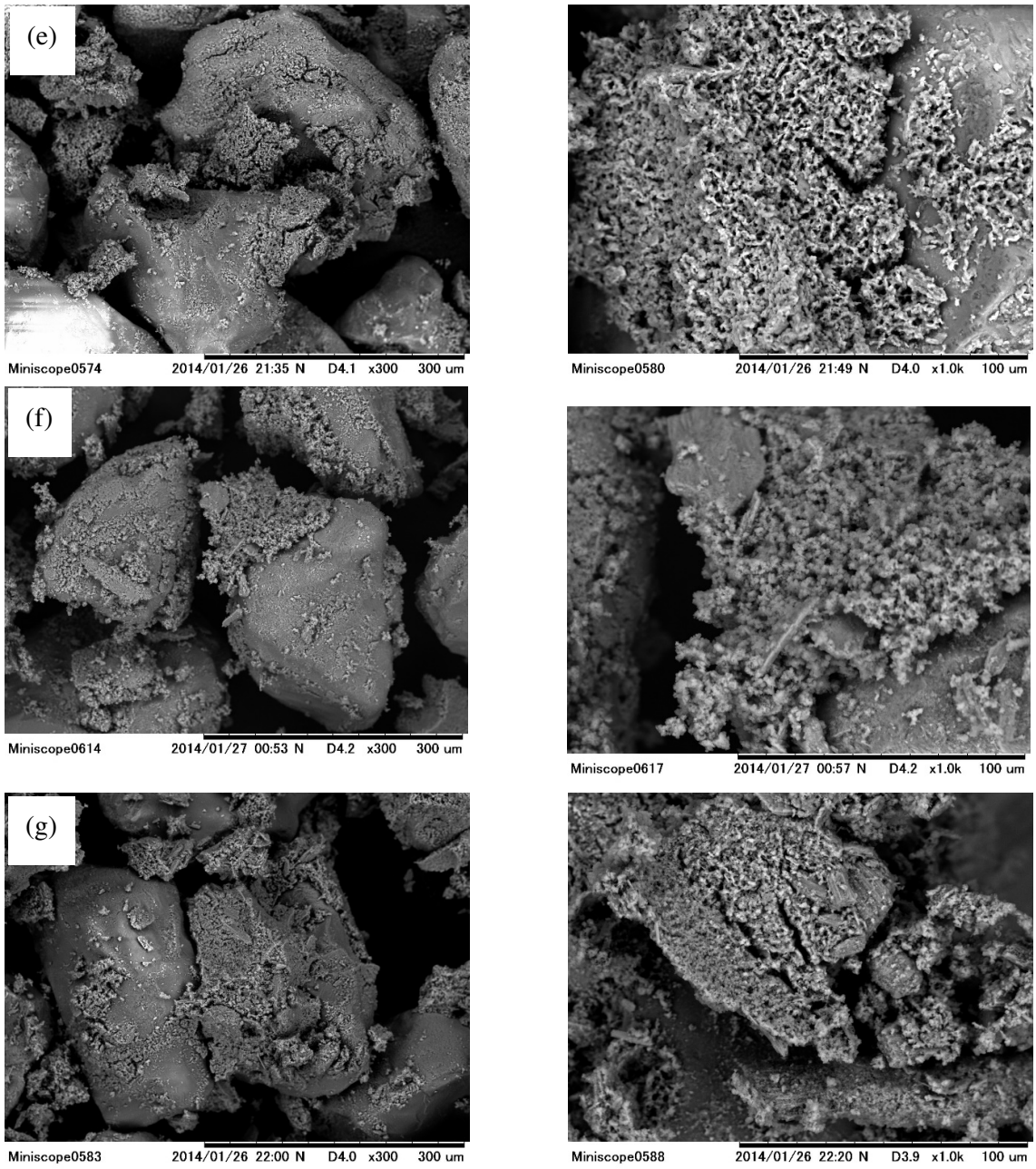

Fig. 3.8: SEM images for test samples CA: DPP=0.6 M: 1.2M after 1 day (300x and 1000x). (a) CPC-Cont, (b) CPC-CC-1%, (c) CPC-CC-5%, (d) CPC-CC-10%, (e) CPC-SS-1%, (f) CPC-SS-5%, (g) CPC-SS-10%.

3.5 DISCUSSION

3.5.1 Effect on addition of SS and CC on the UCS of test pieces

Fig. 3.3 shows the UCS test results. The UCS of test pieces cemented with CPC-SS and CPC-CC was larger than that for CPC-Chem alone, and it increased with time (Fig. 3.3).

For the SS-10 samples, in particular, the UCS was around 150 kPa after 1 day; it was nearly constant with the time except UCS after 14 days. It is assumed that some error could occur when preparing a sample. To clarify this result, further examination of the test pieces is needed in the future.

The UCS of the CC-10 sample also increased from about 80 kPa to 180 kPa and it remained at that level. Although the UCS of the CC-01 and CC-05 samples showed an increasing trend over 14 days, the UCS thereafter decreased. To clarify the reason for the decrease in UCS over time for some test pieces, further examination of the long-term strength of test pieces in the CPC-Powder method is needed in the future.

Practically the test pieces to which the SS and CC powder with 10% was added showed a UCS larger than 100 kPa. This statement recommends that through control of the CC content, the CPC-SS and CPC-CC method would allow for adjustment of strength according to the required strength properties of the ground while maintaining a UCS of over 100 kPa. In addition, the improvement in UCS afforded by the CPC-CC and CPC-SS methods were because of the filling of the voids between sand particles and the uniting of the particles of cement material comprising Ca and P are stronger than CPC-Cont samples.

Considering the results of UCS, pH, wet density and SEM images as discussed earlier, the governing factors for increase the strength of the sample are pH and wet density.

3.5.2 Merits of adding CC and SS powders

When considering up to 28 days curing period in Fig. 3.3, it seems that the UCS value for CPC-CC and CPC-SS method is higher than CPC-Cont. This happened because of enhancement of strength of the samples by the addition of CC or SS powders. Therefore, it is one of the merits for ground improvement by addition of CC and SS powders. However, after 56 days curing period the UCS value of adding powders is lower than no adding powders. To clarify the reason for the decrease, further examination is needed in the future.

Finally, I consider about cost effectiveness of preparing samples. CPC solutions are very expensive. This study`s aim is getting the strength more than 100 kPa. When the samples are prepared with only adding CPC-Chem, it needs to increase the concentration of calcium and phosphate solutions. From this research, using 0.6 M CA: 1.2 M DPP is not reached appropriate strength. If it is increased the concentration of the solutions, the cost is also increased. However it can get the same strength by using a smaller amount (0.6 M CA: 1.2 M DPP) of CPC by adding CC or SS powders and the cost will be reduced. Hence, CPC-CC and CPC-SS method are more cost effective techniques than adding CPC-Chem only.

3.5.3 Differences between CC and SS powders

When comparing the differences between CC and SS powders, here I consider UCS, pH and wet density parameters. In Fig. 3.3, the UCS value of SS-10% sample is nearly constant with the time. However, the UCS value of CC-10% sample increased until 14 days curing period and then decreased with the time. Moreover, the UCS values of SS-1% and SS-5% are greater than the UCS values of CC-1% and CC-5% samples.

Regarding pH measurements, the results are not much different between CPC-SS and CPC-CC method (Fig. 3.4 (a) and 3.4 (b)). Initially, the pH value of CPC-SS method is slightly high when comparing CPC-CC method. However, later the pH value is reached to nearly same

value (nearly 9).

Next, the wet density is increased; CPC-Cont< SS and CC-1% < SS and CC-5% < SS and CC-10% (Figs. 3.7 (a) and 3.7 (b)). Although when density increased, UCS value is intended to increase. However, the wet density of CPC-SS samples is less than CPC-CC samples.

Comparing above results, the CPC-SS method is more effective than CPC-CC method. However, it is difficult to get accurate conclusions using CPC-Chem solutions, because the structure of the solution varied with time (Fig. 2.2 in chapter 2).

3.5.4 Effect on addition of various CPC solutions (CA with DPP and DAP) on the UCS of test pieces

In this study, two reaction mixtures were selected; CA: DPP and CA: DAP with Ca/P ratio is 0.5. The test pieces were prepared by adding CPC-Chem only, adding CPC-Chem with 5% CC and adding CPC-Chem with 5% SS. For this study, we reported from now on that powder percentage is 5%.

The measured UCS in this study is higher in the test pieces cemented by the addition of DAP than the addition of DPP for CPC-Cont, CPC-SS and CPC-CC method (Fig. 3.9). However after 56 days curing period, the UCS of CPC-Cont sample cemented with DAP decreased with the sample cemented with DAP (Fig. 3.9 (a)). It is assumed that some error could occur when preparing the sample. To clarify this result, further examination of the test pieces is needed in the future.

However, the pH value of test pieces cemented with DAP is less than the pH value of test pieces cemented with DPP (Fig. 3.10). In addition, the pH value of test pieces increased with the time (Fig. 3.11).

SEM images of test pieces subjected to DAP and DPP treatment with no adding

powders were not clearly identified any crystal structures (Figs. 3.12 (a) and 3.12 (b)). SEM images of test pieces subjected to DAP treatment with CC powders showed cuboid crystal formation and SS powders showed whisker-like crystal formation among particles of Toyoura sand (Figs. 3.13 (a), 3.13 (b), 3.14 (a) and 3.14(b)). It has been reported that HA whiskers are formed by adding an acetic acid solution to amorphous calcium phosphate (Toyama at al. 2001). In Portland cement, the formation of ettringite, which shows whisker-like crystals, promotes solidification and increases strength (Park, 2000 and Sakai at al. 2004).These results suggest that the strength of the test pieces subjected to DAP treatment in this study might increase if whisker-like HA crystals are formed within them.

Considering results of UCS, pH and SEM images as discussed earlier, the governing factor for increasing the strength of the sample is crystal formation. The most suitable combination of CA and phosphate stock solution concentrations for improving the strength of the UCS test piece was a DAP/CA ratio of 1.5 M: 0.75 M, for which the UCS reached a maximum of 137 kPa. Moreover, this research shown, it is difficult to get accurate results using CPC-Chem solutions, because the structure of the solution varied with time.

In this study, it is focusing on the development of novel grout material intended for sand and assume that the phosphate solution and calcium solution are mixed just before injection or that they are mixed in the ground after being sequentially injected. It is also necessary to conduct a detailed evaluation of the relationship between the UCS and the rate of stiffening because temporal variation in the UCS over the long term may prove to be one of the most important parameters in determining the applicability of CPC.

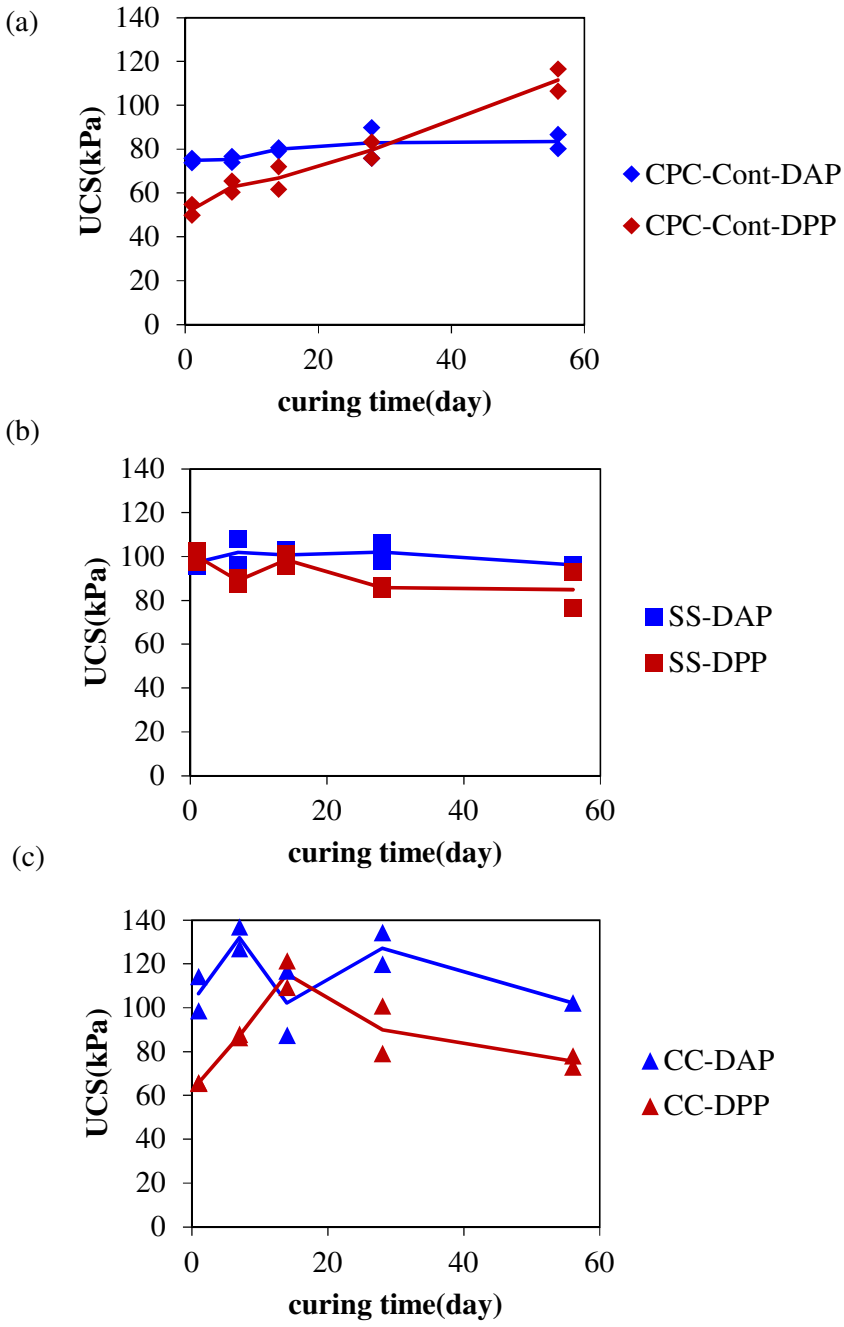

Fig. 3.9: Relationship between UCS and curing time for DAP and DPP. (a) CPC-Cont samples (b) CPC-SS samples (c) CPC-CC samples.

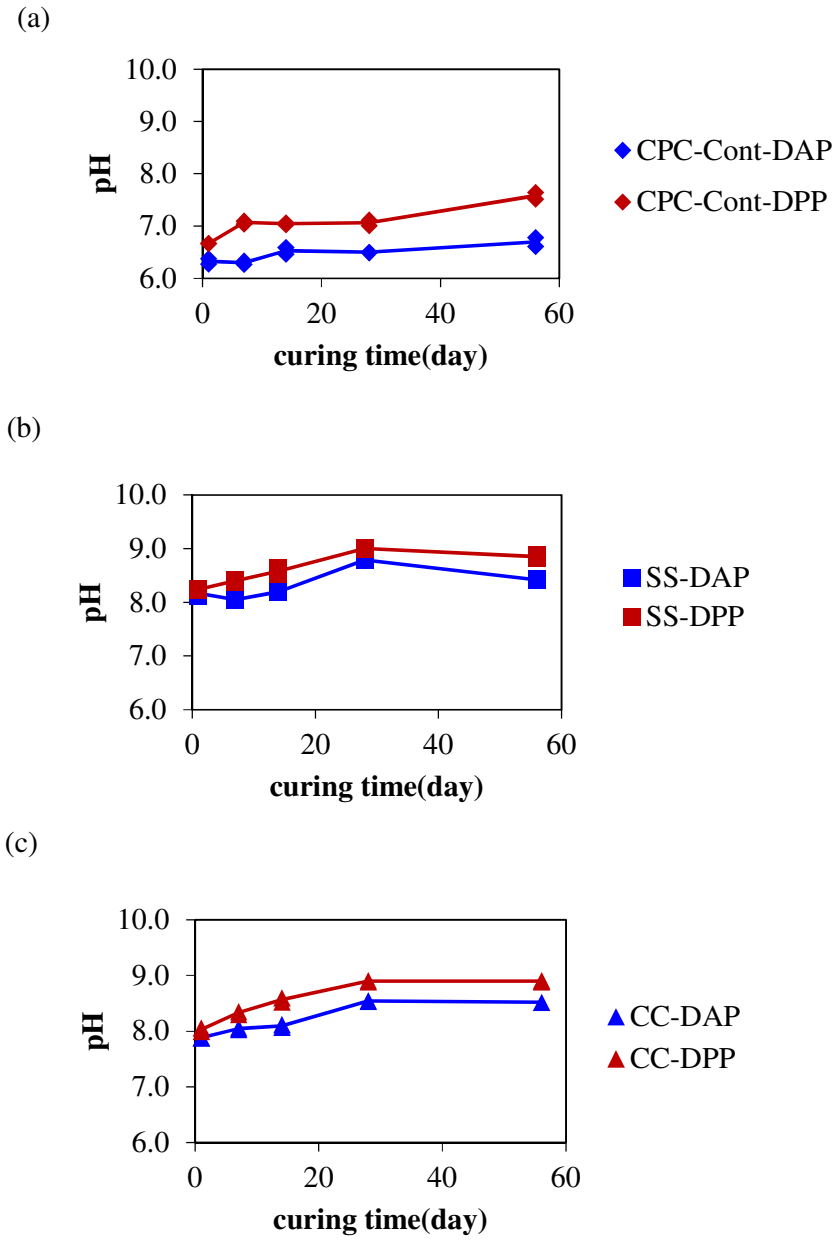

Fig. 3.10: Relationship between pH and curing time for DAP and DPP. (a) CPC-Cont samples (b) CPC-SS samples (c) CPC-CC samples.

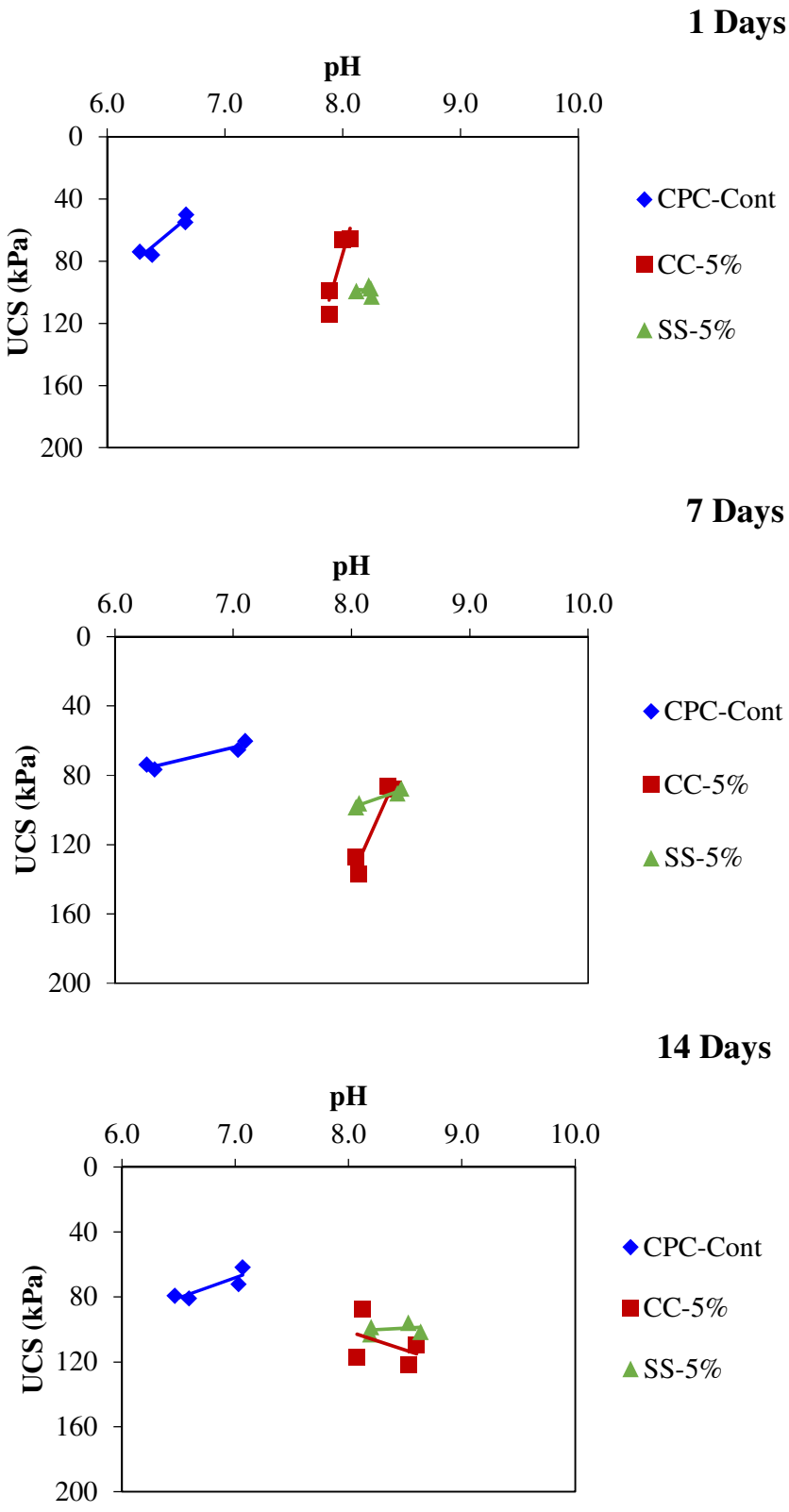
1 Days
pH
6.0
7.0
8.0
9.0
10.0
0
40
80
120
160
200
UCS (kPa)
CPC-Cont
CC-5%
SS-5%
7 Days
pH
6.0
7.0
8.0
9.0
10.0
0
40
80
120
160
200
UCS (kPa)
CPC-Cont
CC-5%
SS-5%
14 Days
pH
6.0
7.0
8.0
9.0
10.0
0
40
80
120
160
200
UCS (kPa)
CPC-Cont
CC-5%
SS-5%

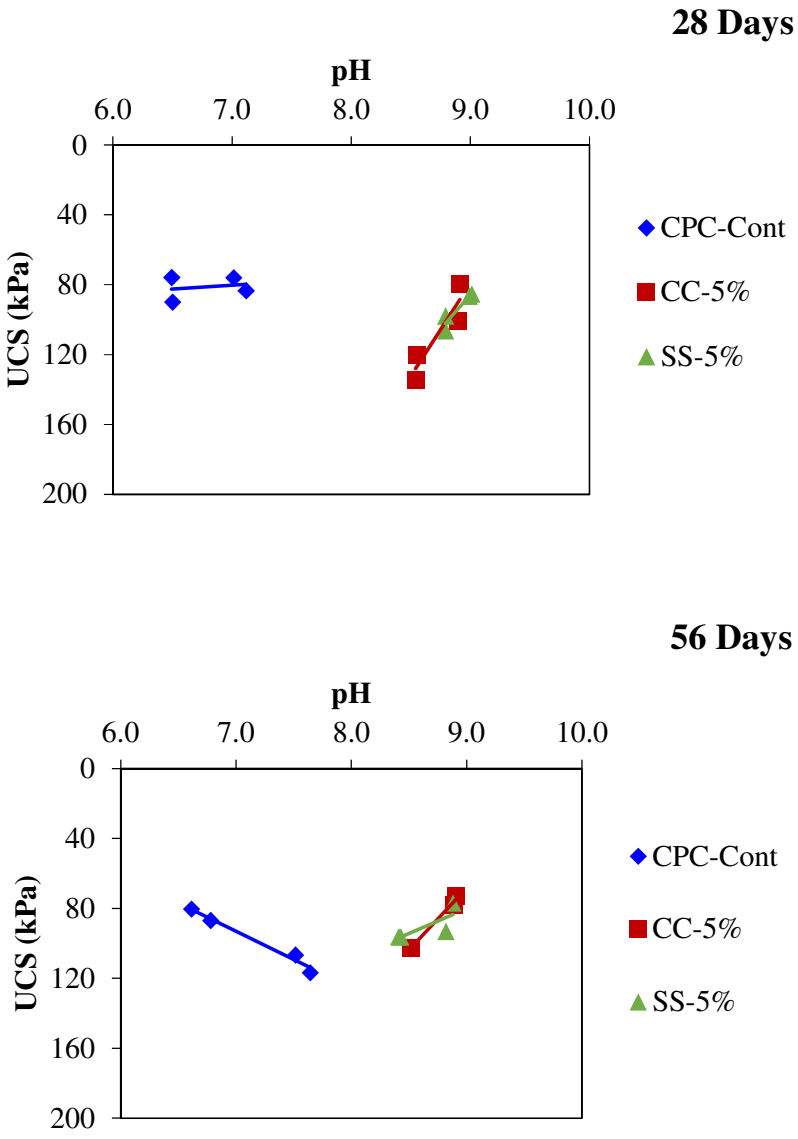

Fig. 3.11: Relationship between UCS and pH for test pieces with CPC-Cont, CC-5% and SS-5% for different curing days.

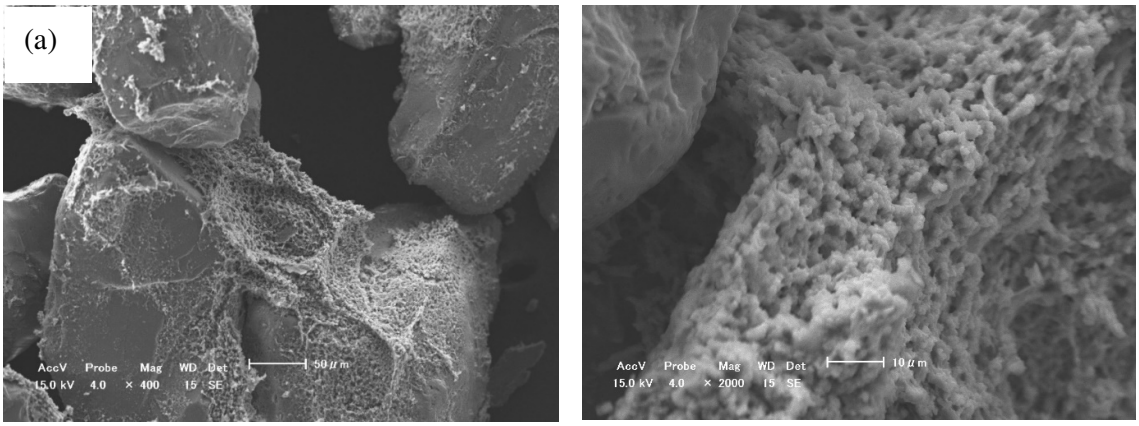

400x 2000x

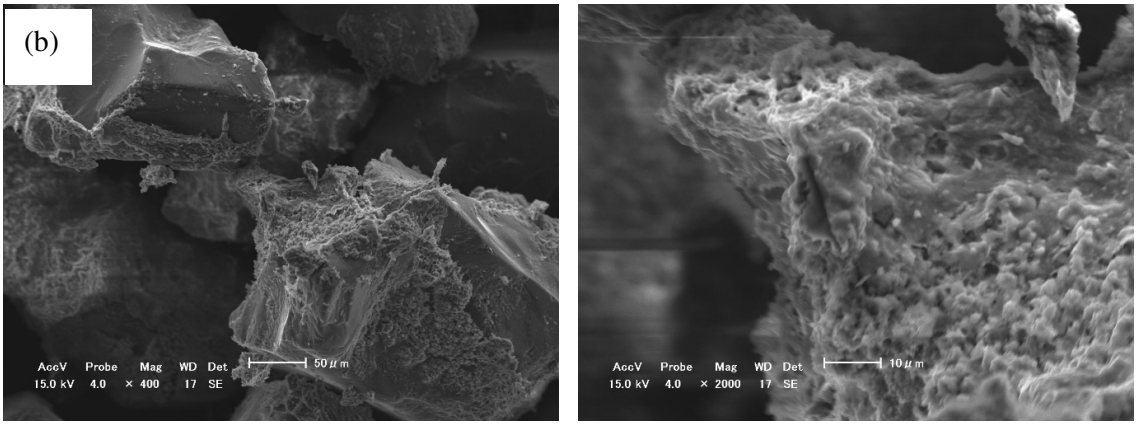

400x 2000x

Fig.3.12: SEM images for test samples not adding powders, after 14 days (400x and 2000x). (a) CA: DAP=0.75 M: 1.5 M and (b) CA: DPP=0.6 M: 1.2 M.

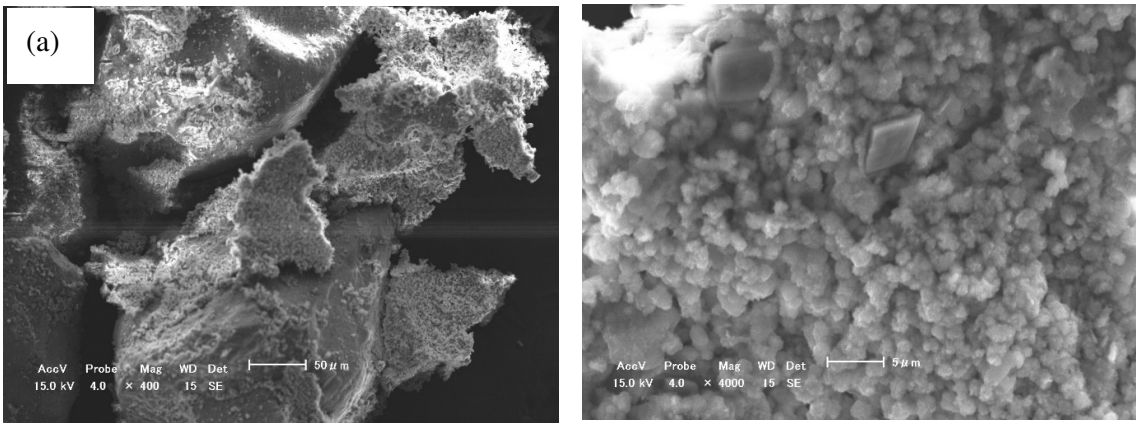

400x 2000x

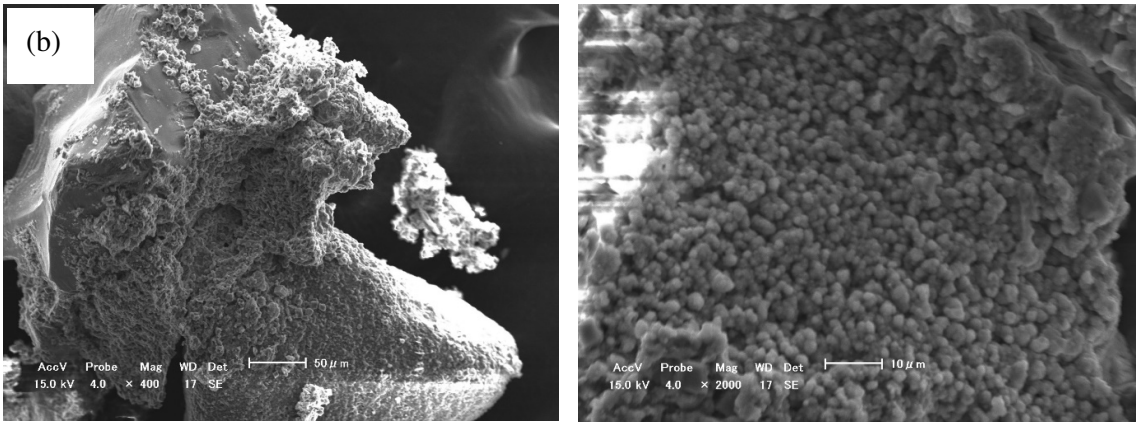

400x 2000x

Fig. 3.13: SEM images for test samples adding 5% of CC powders, after 14 days (400x and 2000x). (a) CA: DAP=0.75 M: 1.5 M and (b) CA: DPP=0.6 M: 1.2 M**.**

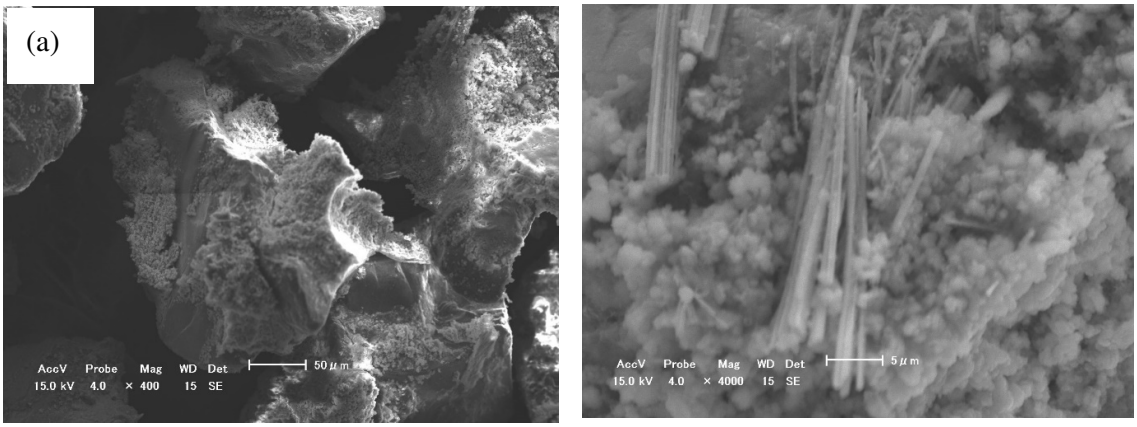

400x 2000x

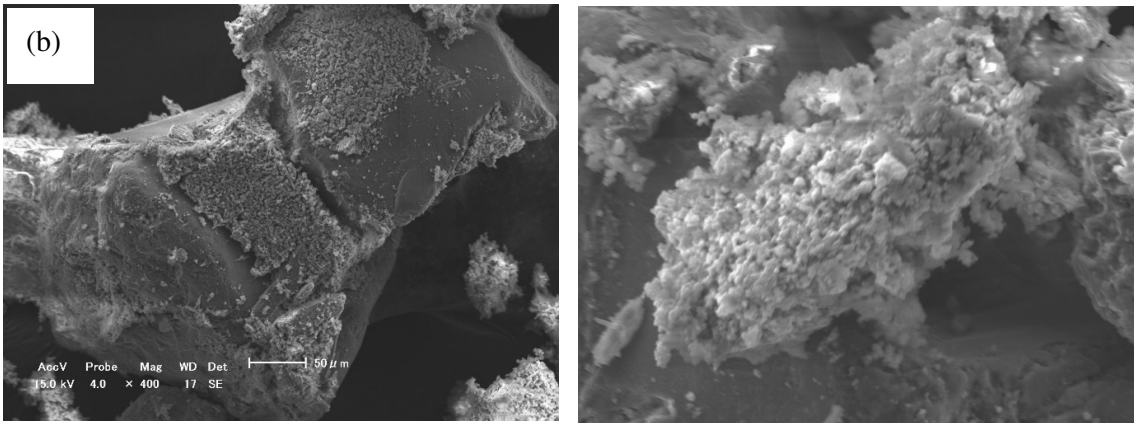

400x 2000x

Fig. 3.14: SEM images for test samples adding 5% of SS powders, after 14 days (400x and 2000x). (a) CA: DAP=0.75 M: 1.5 M and (b) CA: DPP=0.6 M: 1.2 M.

3.5.5 Applicability of CPC-powder method

In this study, it showed that CPC-powder has significant potential as a geotechnical material. The UCS of a sand test piece cemented with the CPC-powder method increased to a maximum of 156.9 kPa. The aim of the present study was to use CPC-Chem to achieve a maximum UCS of over 100 kPa, which is the strength required to prevent ground liquefaction. Using the CPC-powder method, it far exceeded this objective by achieving a UCS of over 150 kPa. When considering many advantages and mechanical properties of CPC-powder method, it is a good method for ground improvement technique.

Here, I discuss the applicability of CPC-powder method. The CPC-powder method can be applied to underpin existing foundations, create excavation support walls, create water cutoff walls and stabilize soils for tunneling. For underpinning applications, it offers the advantages of being easily performed where access and space are limited, and of not requiring a structural connection to the foundation being underpinned.

Moreover, CPC-powder method can use for deep soil mixing and for jet grouting which is an erosion replacement technology that can be used very effectively to create various geometries of stabilized soil, in-situ, for a wide range of applications. Other than that, for aggregate piers can use this CPC-powder method. Aggregate piers are columns of compacted stone placed in situ which can be designed to reduce settlement, improve bearing capacity, mitigate liquefaction potential and increase shear resistance.

Also, this mixture can use as an injection for expansive soils which is a method used for pre-swelling and/or stabilizing expansive clay soils. The addition of these reagents can be extremely beneficial to improve bearing capacity, increase shear strength and expedite the workability of muddy construction sites and also it is useful for soil fertilization.

3.6 CONCLUSION

This study`s aim was to improve strength by adding CPC with scallop shell powder and exceed a maximum UCS of 100 kPa after 28 days of curing, but the expectation is achieved after 14 days of the curing period. The results defined that the addition of powder increases the UCS of the test pieces. The UCS of test pieces cemented with CPC-Chem and calcium compound powders (SS and CC) significantly increased compared to cases where no powder was added to CPC-Chem. In particular, SS-01, SS-05, and SS-10 maintained a stable UCS of around 150 kPa for 56 days.

After analyzing the results obtained from this study, the CPC-SS method can be used as instead of CPC-CC method. In addition, it is cheaper to find scallop shell powder. Therefore, CPC-SS method is cost effective method when comparing CPC-CC method.

The CPC-powder method has the potential to be a non-contaminating and recyclable method for ground reinforcement that can satisfy the strength requirements for the actual ground while avoiding the problems of existing cement-based hardeners, and it may provide very interesting and unique properties for geotechnical and geoenvironmental engineering.

In addition, from this study it comprises, the governing factor for rising strength of samples can be pH, wet density, crystal formation or combination of these factors.

REFERENCES

"Geologists arrive to study liquefaction". *One News*. 10 September 2010. Retrieved 12 November 2011.

Akiyama M, Kawasaki S, "Microbially mediated sand solidification using calcium phosphate compounds," Engineering Geology, Vol. 137-138, 2012, pp. 29-39.

Akiyama M, Kawasaki S, "Novel grout material using calcium phosphate compounds: in vitro evaluation of crystal precipitation and strength reinforcement," Engineering Geology, Vol. 125, 2012, pp. 119-128.

Chemical Book Web site, 2012. http://www.chemicalbook.com/.

De Muynck W, De Belie N, Verstraete W, Ecological Engineering, Vol. 36, 2010, pp. 118-136.

DeJong JT, Mortensen BM, Martinez BS, Nelson DC, Ecological Engineering, Vol. 36, 2010, pp. 197-210.

Fernández E, Gil FJ, Best SM, Ginebra MP, Driessens FCM, Planell JA, "Improvement of the mechanical properties of new calcium phosphate bone cements in the $CaHPO_4$-α-$Ca_2(PO_4)_2$ system: compressive strength and microstructural development," Journal of *Biomedical Materials Research*, Vol. 41, 1998, pp. 560–567.

Harkes MP, Van Paassen LA, Booster JL, Whiffin VS, Van Loosdrecht MCM, Ecological Engineering, Vol. 36, 2010, pp. 112-117.

Japanese Geotechnical Society: Geo-hazards during earthquakes and mitigation measures, Japanese Geotechnical Society, Tokyo, 2011.

Karol RH, Chemical grouting and soil stabilization, 3rd Ed, CRC Press, Boca Raton, FL, 2003.

Kawasaki S, Akiyama M, "Enhancement of unconfined compressive strength of sand test pieces cemented with calcium phosphate compound by addition of various powders," Journal of *Soils and Foundations*, Vol. 53 (6), 2013, pp. 966-976.

Kawasaki S, Murao A, Hiroyoshi N, Tsunekawa M, Kaneko K, "Fundamental study on novel grout cementing due to microbial metabolism," Journal of the Japan Society of *Engineering Geology*, Vol. 47, 2006, pp. 2–12 (in Japanese with English abstract).

Kawasaki S, Ogata S, Hiroyoshi N, Tsunekawa M, Kaneko K, Terajima R, "Effect of temperature on precipitation of calcium carbonate using soil microorganisms," Journal of the Japan Society of *Engineering Geology*, Vol. 51, 2010, pp. 10–18 (in Japanese with English abstract).

Park CK, Hydration and solidification of hazardous wastes containing heavy metals using modified cementitious materials. Cement and Concrete Research, Vol.30, 2000, pp. 429–435.

Ports and Harbours Bureau. Recycling Technology Guidelines for Harbor and Airport Construction and Maintenance, edited in 2004. http://www.mlit.go. jp/kowan/recycle/.

Sakai E, Nikaido Y, Itoh T, Daimon M, Ettringite formation and microstructureof rapid hardening cement. Cement and Concrete Research, Vol. 34, 2004, pp. 1669–1673.

Terajima R, Shimada S, Oyama T, Kawasaki S, "Fundamental study of siliceous biogrout for eco-friendly soil improvement," Journal of Geotechnical and *Geoenvironmental Engineering* JSCE, Vol. 65, 2009, pp. 120–130 (in Japanese, with English abstract).

Toyama T, Ohshima A, Yasue T, "Hydrothermal synthesis of hydroxyapatite whisker from amorphous calcium phosphate and effect of carboxylic acid," Journal of the *Ceramic Society of Japan*, Vol. 109, 2001, pp. 232–237 (in Japanese, with English abstract).

Tung MS, Calcium phosphates: structure, composition, solubility, and stability, in: A. Zahid (Ed.), Calcium phosphates in biological and industrial systems, Kluwer Academic Publishers, Norwell, 1998, pp. 1-19.

Van Paassen LA, Harkes MP, Van Zwieten GA, Van der Zon WH, Van der Star WRL, Van Loosdrecht MCM, Proceedings of the 17th International Conference on Soil Mechanics and Geotechnical Engineering , 2009, pp. 2328-2333.

Whiffin VS, Van Paassen LA, Harkes MP, Journal of *Geomicrobiology*, Vol. 24, 2007, pp. 417-423.

Yamazaki H, Maeda K, Takahashi K, Zen K, Hayashi K, Technical Note of Port and Harbour Research Institute, Vol. 905, 1998, pp. 1-29 (in Japanese).

CHAPTER 4

SYRINGE SOLIDIFICATION TEST USING MICP METHOD

4.1 INTRODUCTION

Present soil improvement applications comprise soil replacement, preloading for consolidation, chemical admixture, and grouting stabilization. These techniques are time-consuming, expensive, and environmentally harmful (DeJong et al. 2010). In addition, coastal erosion is a significant problem throughout the world.

Breakwater construction is used for preventing coastal erosion. Production of cement, which is a major construction material for breakwater construction, is energy consuming and environmentally un-friendly. During the process of cement production, it releases a large amount of CO_2. In addition, the process is time consuming. Therefore, additional studies into discovery alternative techniques for soil improvement are vital to achieving optimum performance, economic viability, and environmental sustainability.

Biomineralization is a promising and environmentally innocuous technology to improve soil engineering properties. It naturally happens and is induced by nonpathogenic organisms that are native to the soil environment (DeJong et al. 2006). One common biomineralization process is microbially induced calcite precipitation (MICP), which can bind sand grains together and improve the engineering properties of sand.

Improvement of soil mechanical properties by MICP is currently of particular interest to engineers and microbiologists and has been demonstrated by several researchers at varying scales (DeJong et al. 2006; Whiffin et al. 2007; Van Paassen et al. 2010). The technique can alter soil characteristics to increase shear strength and stiffness while maintaining adequate permeability (Burbank et al. 2011). The technique involves introducing aerobically cultivated bacteria with highly active urease enzyme into soil, harnessing the urease enzyme to catalyze the hydrolysis of urea to produce ammonium and carbonate ions. The chemical reaction involved in

this process is shown as follows (Eq. (4.1)):

$$CO(NH_2)_2 + 2H_2O \rightarrow 2NH_4^+ + CO_3^{2-} \quad \text{Eq. (4.1)}$$

In the presence of an introduced calcium source, often calcium chloride ($CaCl_2$), the calcium carbonate ($CaCO_3$, calcite) forms throughout the soil matrix based on the following chemical reaction (Eq. (4.2)):

$$Ca^{2+} + CO_3^{2-} \rightarrow CaCO_3 \downarrow \quad \text{Eq. (4.2)}$$

The produced microbially induced $CaCO_3$ precipitates bridge adjacent soil particles by cementing the soil grains together to form cemented sand illustrative of calcareous rock (DeJong et al. 2006).

The engineering properties of MICP-treated soil may vary because MICP is a complex biochemical process, which can be affected by many factors. The MICP contains two key steps, as above equations. The urea hydrolysis is mainly dependent on the concentration of ureolytic bacteria and the available substrate (e.g., urea), whereas calcite precipitation relates to available Ca^{2+} (Mortensen et al. 2011). In accordance with the growth of nutrient concentration and incubation time, the $CaCO_3$ content increases. The particle size also has an effect on MICP bonded soil. The efficiency of MICP is related to the permeability of the soil being sufficient to allow chemicals to flow to the bacteria and also the cement effect of $CaCO_3$ precipitation away particles (Mitchell and Santamarina 2005; Rebata-Landa 2007). Rebata-Landa (2007) showed a relation between grain size and $CaCO_3$ content, and maximum carbonate deposition observed on grains was approximately 100 μm in size. Qabany et al. (2012) also found well-graded and coarser sands had a higher rate of precipitation than finer and poorly graded soils.

4.2 OBJECTIVE

In this paper, I conducted a solidification test on silica sand using the ureolytic bacteria isolated from the soil near beach rock in Sumuide, Nago, Okinawa, Japan. The goal of this paper is to perform solidification of the specimen having an estimated

unconfined compressive strength (UCS) of more than several MPa for soil improvement and preservation of coastal erosion and/or healing of coastal concrete structures, and investigate the influence of varies factors on engineering properties of treated soil catalyzed by ureolytic bacteria.

A series of laboratory experiments conducted for identifying parameters which were affected for solidification of the sample. Syringe solidification method was used for the solidifying sample. Needle penetration test was conducted to obtain estimated UCS value and measured pH and Ca^{2+} concentration of the outlet solution.

4.3 MATERIALS AND METHODS

4.3.1 Sands

Physical properties of Mikawa sand, Mizunami sand Toyoura sand which was used in the experiments are shown in Table 4.1.

Table 4.1: Physical properties of Mikawa sand, Mizunami sand, and Toyoura sand.

Sand Type	**Mizunami Sand**	**Mikawa Sand**	**Toyoura Sand**
Soil particle density (ρ_s) (g/cm^3)	2.67	2.66	2.64
Minimum density (ρ_{min}) (g/cm^3)	1.348	1.256	1.335
Maximum density (ρ_{max}) (g/cm^3)	1.491	1.476	1.645
Mean diameter (D_{50}) (μm)	1200	600	200

4.3.2 Bacteria

The microorganism used was *Pararhodobacter* sp., an ureolytic bacterium isolated from the soil near beachrock in Okinawa, Japan (Danjo and Kawasaki 2013) (Fig.4.1). The bacteria were cultivated in ammonium-yeast extract media (NH_4-YE) (growth media; ATCC 1376), which contained the following per liter of deionized

water: (1) 0.13 M tris buffer (pH = 9.0), (2) 10 g $(NH_4)_2SO_4$, and (3) 20 g yeast extract. After incubating aerobically at 30°C in a shaker at 160 rpm (revolutions/ min) for 72 hours, the bacteria and growth media were centrifuged at 5000 rpm for 10 min.

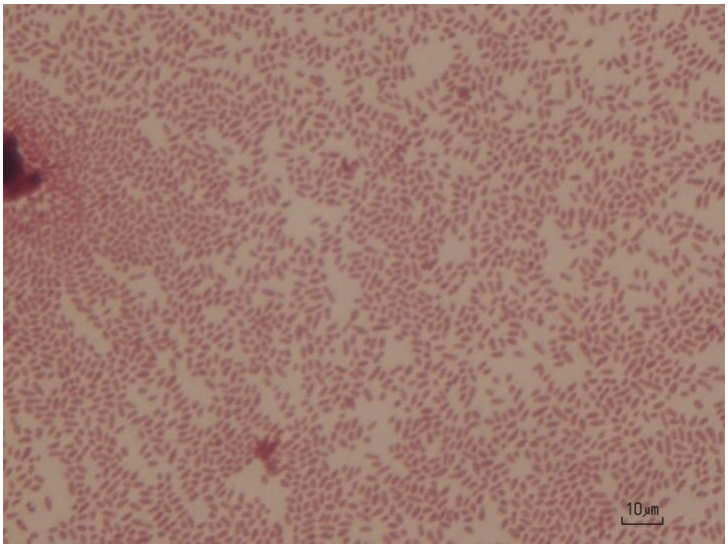

Fig. 4.1: Grain stain of *Pararhodobactor* sp.

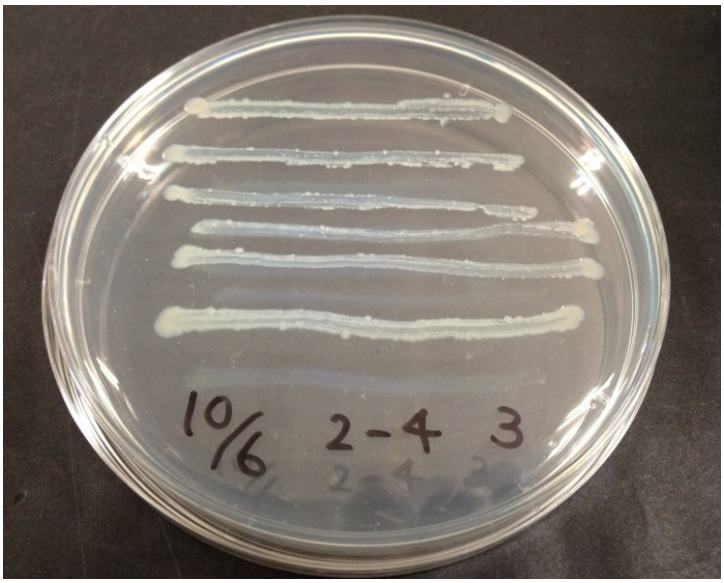

Fig. 4.2: Cultivation of *Pararhodobactor* sp.

Urease activity test

Preparation of urease activity measurement solution

Cresol red solution, the composition of the urease activity measurement solution are shown in Table 4.2 and Table 4.3.

Table 4.2: The composition of the cresol red solution (per 100 mL, solvent: distilled water).

Cresol red (powder)	0.1 g
Ethanol (concentration 95%)	20 mL

Table 4.3: The composition of the urease activity measurement solution (per 100 mL, solvent: distilled water).

urea	2.5 g
Cresol red solution	2 mL

1) A cresol red was added to the beaker containing 95% ethanol, and dissolved by stirring.
2) It was transferred to the volumetric flask, and filled up to a predetermined amount of distilled water to prepare a cresol red solution.
3) Distilled water to a beaker and stirred by adding urea, cresol red solution in this order.
4) Transferred to a volumetric flask, and filled up to a predetermined amount of distilled water to produce a urease activity measurement solution.
5) Cresol red, discolored area is a pH indicator of 7.2 to 8.8, color and pH is raised to neutral to alkaline is discolored from yellow to purple.

Method for Urease activity test

1) The state of the discoloration of the urease activity measurement solution is shown in Figure 4.3.
2) By the number of sample number +1 (control) providing a styrene screw bottle for 20 mL, it was dispensed the urease activity measurement solution by about 20 mL to each minute.
3) After isolation of the bacteria, taken out microorganisms were cultured for 24 hours from the incubator, it was added to each urease activity measured solution in a clean bench.
4) After stirring vertically about sealed to 20 times, allowed to stand in an incubator set at 45 °C, as compared to control the color change of after 2 hours, was measured the pH.

Since the urease activity measurement solution contains urea, when examined samples were ureolytic bacteria, progress in the hydrolysis of the urea in solution, pH of the solution is increased. Along with this, because cresol red may change color to purple from yellow, differences in the color of the control, and the difference between the measured values of pH, it is possible to determine the presence and magnitude of urea resolution. The temperature of the incubator (45 °C) is to facilitate the action of microorganisms.

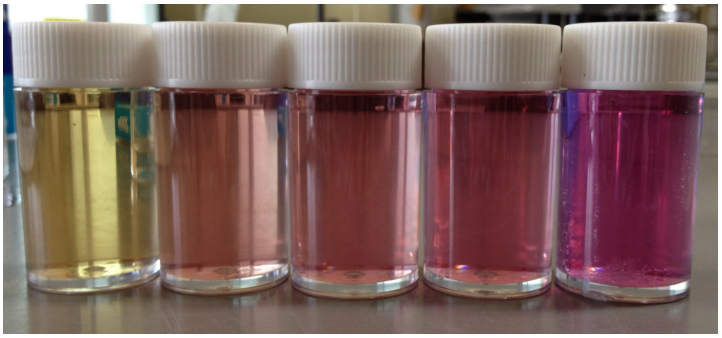

Fig. 4.3: Appearance of discoloration of the urease activity measurement solution (yellow is neutral, purple is alkaline).

Genetic analysis of microorganisms

For strains, discoloration was seen of the indicator in the urease activity test. The genetic analysis of microorganism is shown in Table 4.4 (Danjo, 2015).

Table 4.4: Genetic analysis of microorganisms.

DNA extraction	Achromopeptidase (Wako Pure Chemical Industries, Ltd., Osaka, Japan)
PCR amplification	PrimeSTAR HS DNA Polymerase (Takara Bio, Shiga)
Cycle sequencing	BigDye Terminator v3.1 Cycle Sequencing Kit (Applied Biosystems, CA, USA)
Use primer	PCR amplification : 9F, 1510R Sequence : 9F, 785F, 802R, 1510R
Sequence	ABI PRISM 3130 xl Genetic Analyzer System (Applied Biosystems, CA, USA)
Sequencing	ChromasPro 1.7 (Technelysium Pty Ltd., Tewantin, AUS)
BLAST homology search, and simple molecular phylogenetic analysis	software Apollon 2.0 (Techno Suruga Lab , Shizuoka) Database Apollon DB-BA9.0 (Techno Suruga Lab , Shizuoka) International Nucleotide Sequence Database (GenBank / DDBJ / EMBL)

Results of Urease activity test

The results of urease activity test against the isolated strain from the soil near beach rock in Sumuide, Nago, Okinawa, Japan are shown in Table 4.5. Discoloration of the urease activity measurement solution was observed in five of the strains. From

the Table 4.5, it is found that the pH after 2 h is 9.0 or more. The color difference between the control sample and testing samples was evident for the value of pH.

Table 4.5: Urease activity test results.

Strain No	pH value after 2 hours
1	9.0
2	9.1
3	9.0
4	9.1
5	9.0

The urease activity results and color of the samples were similar in five strains which summarized in Table 4.5.Therefore, partial nucleotide sequence analysis of 16S rDNA (about 1500 bp) was carried out for one strain instead of five strains. From the results of homology using Apollon DB-BA9.0 database (September 13, 2013), *Rhodobacteraceae* family such as *Roseicitreum* genus and species *Haematobacter* shows a high homology. In addition, *R. antarcticum* showed the highest homology of homology 95.6% (Table 4.6).

Moreover, according to the homology results using GenBank / DDBJ / EMBL database (September 13, 2013), *Rhodobacteraceae* family shows high homology and the reference strain for *R. antarcticum* showed 95.6% homology (Table 4.7).

In addition, the strain obtained in the simplified molecular phylogenetic tree forms a P. aggregans and the cluster. This cluster has been supported by the high bootstrap value of 96% (Fig.4. 4).

From the above results, the strains are considered as a new species of the *Pararhodobacter* genus. However, on the other hand, the strain is different as a species than the P. aggregan (September 13, 2013).

Table 4.6: BLAST homology search results for Apollon DB-BA9.0 (9 May 13, 2013).

Registered name	Ltd. name	Accession No.	Homology	BSL
Roseicitreumantarcticum	ZS2-28	FJ196006	1330/1391 (95.6%)	
Haematobactermassiliensis	Framboise	AF452106	1318/1391 (94.8%)	
Haematobactermissouriensis	H1892	DQ342315	1315/1388 (94.7%)	
Rhodobacterjohrii	JA192	AM398152	1316/1390 (94.7%)	
Rhodobactersphaeroides	ATCC17023	DQ342321	1313/1387 (94.7%)	
Pseudorhodobacteraquimaris	HDW-19	GU086365	1314/1389 (94.6%)	
Roseinatronobactermonicus	ROS35	DQ659236	1322/1397 (94.6%)	
Rhodobacterazotoformans	JCM9340	AB607332	1314/1390 (94.5%)	
Rhodobacterveldkampii	ATCC35703	D16421	1314/1390 (94.5%)	
Paracoccusmarinus	KKL-A5	AB185957	1316/1394 (94.4%)	
Rhodobactermegalophilus	JA194	AM421024	1311/1388 (94.5%)	
Roseibacaekhonensis	EL-50	AJ605746	1309/1385 (94.5%)	
Rhodobacabogoriensis	LBB1	AF248638	1312/1393 (94.2%)	
Rhodobacabarguzinensis	VKM_B-2406	EF554833	1299/1371 (94.7%)	
Paracoccuskoreensis	Ch05	AB187584	1303/1387 (93.9%)	
Rhodobacterovatus	JA234	AM690348	1298/1374 (94.5%)	
Rhodobactercapsulatus	ATCC11166	DQ342320	1302/1389 (93.7%)	
Paracoccusniistensis	NII-0918	FJ842690	1299/1386 (93.7%)	
Paracoccusisoporae	sw-3	FJ593906	1305/1394 (93.6%)	
Rhodobactervinaykumarii	JA123	AM408117	1284/1365 (94.1%)	
Tropicimonasaquimaris	DPG-21	HQ340608	1298/1392 (93.2%)	
Tropicimonassediminicola	M97	JF748735	1297/1391 (93.2%)	
Paracoccusfistulariae	22-5	GQ260189	1297/1392 (93.2%)	
Rhodobacterblasticus	ATCC33485	DQ342322	1298/1392 (93.2%)	
Rhodobacteraestuarii	JA296	AM748926	1278/1369 (93.4%)	
Roseovariuspacificus	81-2	DQ120726	1295/1393 (93.0%)	
Paracoccuschinensis	KS-11	EU660389	1268/1352 (93.8%)	
Rhodobactermaris	JA276	AM745438	1278/1366 (93.6%)	
Pseudorhodobacterantarcticus	ZS3-33	FJ196030	1297/1405 (92.3%)	
Profundibacteriummesophilum	KAUST-100406-0324	JF776971	1303/1400 (93.1%)	

Blank of BSL means the level 1.

Table 4.7: BLAST homology search results for the GenBank / DDBJ / EMBL (9 May 13, 2013).

Registered name	Ltd. name	Accession No.	Homology
*Rhodobacter*sp.	SS12.40	KC160928	1378/1392 (99.0%)
Rhodobacter sp.	SS12.28	KC160919	1375/1392 (98.8%)
Rhodobacteraceae bacterium	SK1	JF951963	1353/1390 (97.3%)
Rhodobacter sp.	Bo10-19	EU839358	1332/1388 (96.0%)
uncultured bacterium	-	DQ813946	1333/1390 (95.9%)
Rhodobacter sp.	R18	AB607872	1332/1390 (95.8%)
uncultured *Rhodobacter* sp.	-	HM003638	1333/1388 (96.0%)
uncultured *Rhodobacter* sp.	-	JQ624272	1336/1394 (95.8%)
uncultured *Rhodobacteraceae* bacterium	-	JQ624307	1332/1392 (95.7%)
uncultured bacterium	-	JN684001	1332/1393 (95.6%)
uncultured bacterium	-	JN683961	1332/1393 (95.6%)
uncultured bacterium	-	JN683954	1332/1393 (95.6%)
uncultured bacterium	-	JN245810	1331/1393 (95.5%)
uncultured bacterium	-	JN245772	1331/1393 (95.5%)
Roseicitreumantarcticum	ZS2-28	FJ196006	1330/1391 (95.6%)
bacterium enrichment culture	clone AOM-SR-B5	HQ405622	1328/1391 (95.5%)
uncultured bacterium	-	JN683991	1330/1393 (95.5%)
uncultured bacterium	-	JF935177	1327/1390 (95.5%)
uncultured bacterium	-	FJ623306	1327/1390 (95.5%)
bacterium enrichment culture	clone R1492-6	JF449939	1326/1392 (95.3%)
bacterium enrichment culture	clone R1492-7	JF449940	1324/1392 (95.1%)
uncultured bacterium	-	DQ521542	1322/1389 (95.2%)
*Rhodobacter*sp.	2002-65602	AY244771	1325/1393 (95.1%)
uncultured *Rhodobacter* sp.	-	FJ542844	1326/1393 (95.2%)
*Rhodobacter*sp.	CR07-5	EU979473	1326/1394 (95.1%)
uncultured bacterium	-	EF632943	1323/1389 (95.2%)
uncultured bacterium	-	KC211848	1322/1389 (95.2%)
uncultured *Rhodobacter* sp.	-	FJ542904	1325/1393 (95.1%)
uncultured alpha proteobacterium	-	DQ432231	1320/1390 (95.0%)
uncultured bacterium	-	KC211849	1322/1389 (95.2%)

Table 4.8: Homology with the reference strains of the resulting strain and *Pararhodobacter* aggregans: BLAST search.

Registered name	Ltd. name	Accession No.	Homology
Pararhodobacteraggregans	D1-19	AM403160	1161/1195 (97.2%)

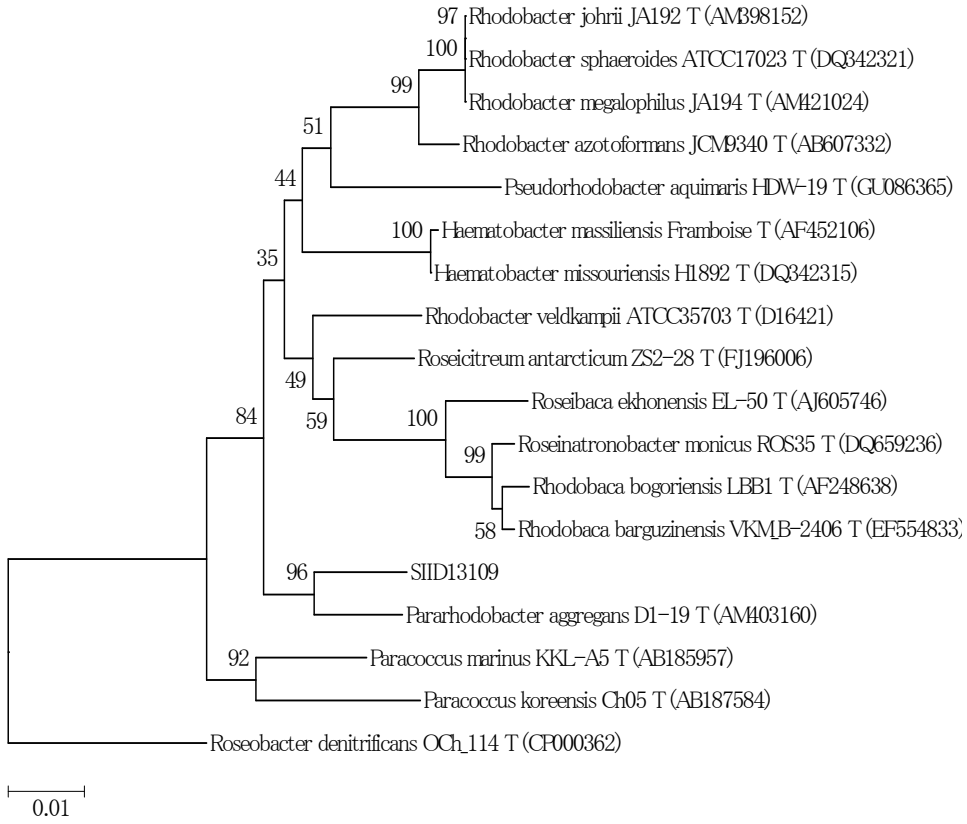

Fig. 4.4: Resulting strain (SIID13109) simple molecular phylogenetic tree based on 16S rDNA partial nucleotide sequence. The bottom left line shows a scale bar and the numbers bootstrap values located in the branch of the branch system. The end of the T of the stock name is the species of the type strain.

4.3.3 Growth characteristics of *Pararhodobacter* sp. in various culture conditions

In this research, NH_4-YE medium was used for cultivation of bacteria. Previous studies: Danjo (2013) and Shimazaki (2015) were conducted *Pararhodobacter* sp. using ZoBell2216E medium. Also, they used artificial sea water for their experiments. In this research, distilled water was used for preparing culture medium (NH_4-YE medium) and other entire experiments.

Preparation of NH_4-YE medium

Table 4.9: Chemical concentration for NH_4-YE medium.

Chemical	**Chemical Concentration (g/L)**
Yeast extract (g)	20
$(NH_4)_2SO_4$ (g)	10
0.13 M Tris buffer (pH 9.0) (g)	15.75
Agar (g)	20

1) 15.75 g of 0.13 M Tris buffer (pH 9.0) was added to the 1000 mL of distilled water and mixed using magnetic stirrer.
2) After solved completely, the solution was divided into three beakers. (100 mL, 100 mL and 800 mL)
3) For two beakers which contained 100 mL solutions, 20.0 g of Yeast extract and 10.0 g of $(NH_4)_2SO_4$ added separately and mixed using magnetic stirrer.
4) The remaining beaker with 800 mL solutions was mixed with 20.0 g of agar.
5) After completion of mixing chemicals in the solutions, three beakers were wrapped with aluminum foil and autoclave separately (No growth occurs when ingredients are sterilized together) 15minutes at 121 ℃ and kept about one hour.

6) After that, the solutions remove from the autoclave and mixed together to the Erlenmeyer flask in the clean bench.
7) Then, the solution was added to the disposed plates and each plates contained around 10 mL of solution.
8) Then kept few minutes for cool the solution became jell and closed by a cap and kept upside down and the plated were wrapped with wrapping foil and wait for cultivate the bacteria.

Cultivation of bacteria

1) The *pararhodobacter* sp. was cultivated by sterilized toothpick. The bacteria was taken from the previous bacterial plate and draw lines in the NH_4-YE medium plates.
2) Then after drawn several plates, plates were inserted into the sealed bag and kept at 30 ℃ incubated by 7 days.

Adding bacteria to the culture medium

1) NH_4-YE liquid culture medium was prepared same as NH_4-YE medium, the changing step is not adding agar. Other steps are same as the previous method.
2) After autoclave, the solutions was moved into the clean bench and mixed together in an Erlenmeyer flask.
3) For this experiment, sterilization treatment with 70% ethanol was used for clean the electronic balance and moved into the clean bench.
4) Then 0.1 g of bacteria was measured using sterilized medicine spoon and added to the liquid medium in the Erlenmeyer flask.
5) After the addition, Erlenmeyer flask was capped with a cap and set at a constant temperature (25℃) (Tokyo Rika instrument, FMC-100) in a shaker (Tokyo Rika instrument, MMS-310) by 160 rpm.
6) They were cultured in 72 hours.

Testing conditions

Changes of the amount of bacteria, the volume of culture medium and shaking speed were used for identifying the relationship with bacterial population with the time. Testing cases are shown in the following table.

Table 4.10: Testing conditions for different culture solution.

Testing case	**Amount of bacteria (g)**	**Volume of culture solution**	**Speed of shaker (Rpm)**
01	0.1	100	160
02	0.3		
03	1.0		
04		200	
05		100	80

- Testing case 01 to 03: Amount of bacteria was changed 0.1 g, 0.3 g, and 1.0 g and the bacteria were added to the 100 mL volume culture medium and capped with the cap. After that put in the shaker and shaking 160 rpm.
- Testing case 03 and 04: The bacterial amount is 1.0 g and the volume of the culture solution was changed 100 mL and 200 mL with 160 rpm.
- Testing case 04 and 05: The bacterial amount is 1.0 g and added to the 100 mL volume of culture solution and the shaking speed was changed 160 rpm and 80 rpm.

OD_{600} and viable count measurement

Bacterial cell concentration was quantified by measuring absorbance (optical density) of the suspension using a spectrophotometer [ultraviolet (UV)-1700 UV-visible spectrophotometer, Shimadzu) at the 600-nm wavelength (OD_{600}; Ehrlich 2002; Fredrickson and Fletcher 2001).

Total Viable Count (TVC) gives a quantitative idea about the presence of microorganisms such as bacteria, yeast, and mold in a sample. To be specific, the count actually represents the number of colony forming units; CFU per mL of the sample.

After started the shaking of the culture solution, $OD_{600,}$ and the viable count was measured at the time interval: 1 hour, 3 hours, 6 hours, 9 hours, 24 hours, 48 hours, 72 hours etc. The results of this experiment mentioned in the section of results (section 4.5.1) in this chapter.

Fig.4.5: Culture solutions on the shaking table.

4.3.4 Cementation Media

Cementation media was used to provide chemical compositions for ureolysis, including urea, $CaCl_2 \cdot 2H_2O$, NH_4Cl, $NaHCO_3$, and nutrient broth (Mortensen et al. 2011). Table 4.11 shows the chemical compositions of cementation media for bacteria experiments.

Table 4.11: Chemical compositions for cementation media.

Chemical	**Chemical Concentration (g/L) – 0.5M Ca**
Nutrient Broth (g)	3
NH_4Cl (g)	10
$NaHCO_3$ (g)	2.12
$(NH_2)_2CO$ (g)	30.03
$CaCl_2$ (g)	55.49

4.4EXPERIMENTAL METHOD

4.4.1 Syringe Solidification Test

1) First, 0.1 g of bacterium *Pararhodobacter* sp. was shaken in with 100 mL NH_4-YE medium for 3 days at 30° C.
2) The bacteria and growth media were centrifuged at 5000 rpm for 10 min.
3) Then, 45 g of Mikawa sand dried at 110ºC for more than 2 days, was placed in a 30 mL syringe.
4) Subsequently, 16 mL of a culture medium solution (NH_4-YE solution) and 20 mL of the cementation media for consolidation (the compositions are shown in Table 4.11) were injected into the syringe and drained off leaving about 2 mL of solution above the top surface of the sand.
5) This solution for consolidation was then injected and drained once a day or once every two days and the curing period was 14 days.
6) Ca^{2+} concentration and pH value of outlet solution were measured.
7) The syringe solidification test is shown in Figure 4.6.

Fig. 4.6: Syringe solidification test.

4.4.2 Needle Penetration Test

After 14 days of curing, the needle penetration inclination (N_p) values of each sample were measured using needle penetration device (SH-70, Maruto Testing Machine Company, Tokyo, Japan) and the UCS was estimated from N_p value. The N_P device consists of eight parts as shown and described in Fig. 4.7. Before testing, the surface, on which the test would be carried out, should be clean and smooth. The test doesn't require a specially prepared specimen. The N_P can be used in any direction both in the field and laboratory. Then by holding rather tightly the removable cap and the main body, the load is perpendicularly and slowly applied to the rock surface. If the test is carried out in the laboratory, the specimen should be fixed to prevent its movement during penetration. For weak and saturated rocks, the needle may be penetrated to a maximum depth of 10 mm. When this depth is reached, no more penetration could be applied and the needle is slowly pulled out. Where the rock is hard and the penetration force has come up to 100 N before the needle penetrates for 10 mm, the needle is withdrawn. After the test is completed, the needle is slowly pulled out and the penetration load and penetration depth are read from the load scale (Fig. 4.7, part 4) and the position of the presser on the penetration scale (Fig.4.7, part 3), respectively. The strength of the sample (N_p value) was calculated from the following equation (Eq. (4.3)).

$$N_P = F/D \qquad \text{Eq. (4.3)}$$

Where, *F* is the penetration load (N) and *D* is the depth of penetration (mm). The unit of N_p is N/mm. From the chart of UCS-N_p correlation, estimated UCS value was observed.

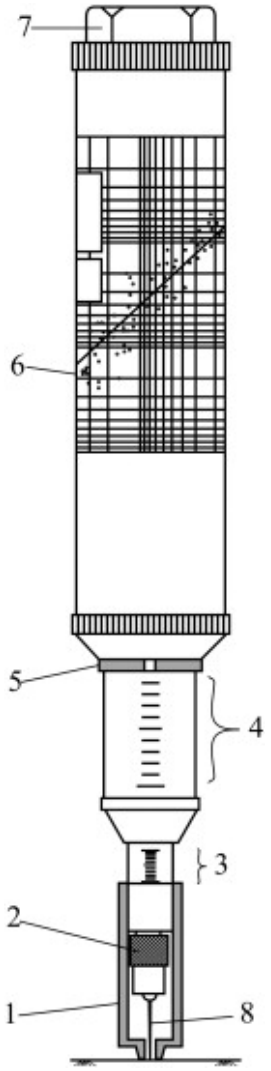

Fig. 4.7: Needle Penetrometer manufactured by Maruto Co. Ltd. (2006) and its parts: 1. presser, 2. chuck, 3. penetration scale, 4. load scale, 5. load indicating ring, 6. UCS–N_p correlation chart, 7. removable cap, and 8. penetration needle.

4.4.3 Experimental Conditions

To consider the effect of conditions on the UCS of a specimen, the bacterial population, reinjection of bacteria, curing time, curing temperature, injection interval, concentration of cementation media, and particle size of the sand were changed (as shown in Tables 4.12 and 4.13). The testing cases were summarized according to the investigation purpose.

In Case 1 to 3, it is investigated the effect of bacterial population, Case 4 and 5 for identifying the effect of re-injection of bacteria, Cases 3, 6 and 7 investigated the effect of curing time. For investigating the temperature effect, it was conducted Case 3, 8 and 9. Moreover, Cases 10 and 11 were conducted for identifying the effect of injection interval of cementation media and for investigating the effect of concentration of cementation media, Cases 10, 12 and 13 were used. Cases 3, 14 and 15 were used for investigating the effect of particle size for the solidification.

Table 4.12: Purpose of conduction testing cases.

Case No.	Purpose – How to effect for the solidification
1, 2, 3	Effect of bacterial population
1, 3, 4, 5	Effect of re-injection of bacteria after 7 days of curing period
6, 7, 10	Effect of curing time
8, 9, 10	Effect of curing temperature
10, 11	Effect of injection interval of cementation media
10, 12, 13	Effect of concentration of cementation media
3, 14, 15	Effect of particle size and different sand samples

Table 4.13: Experimental conditions.

Case No.	Temp. (°C)	Population of Bacteria (g)	Injection interval	Re-injection of Bacteria (After 7 days)	Curing Days	Concentration of cementation media	Sand material with Particle Size (mm)
1	30	0.1 with centrifuge	1		14	0.5 M	Mikawa-0.6
2		0.3 with centrifuge					
3		1.0 with centrifuge					
4		0.1 with centrifuge		x			
5		1.0 with centrifuge		x			
6					7		
7					21		
8	25				14		
9	35						
10	30						
11			2				
12			1			0.3 M	
13						0.7 M	
14						0.5 M	Misunami-1.2
15							Toyoura-0.2

4.5 RESULTS

4.5.1 Growth characteristics of *Pararhodobacter* sp. in various culture conditions

The results show that how to affect the bacterial growth for different conditions for bacterial cultivation. The testing conditions were mentioned in the methodology part. From the results of three figures (Fig. 4.8 to Fig. 4.10), the best testing condition is 1.0 g of bacteria adding with 100 mL culture solution with shaking 160 rpm rate. Also, after 72 hour time period, the increase of OD_{600} value was getting low. Therefore, for the experiments from the present, I used bacterial solution for adding to the soil after shaking 72 hours with the speed of 160 rpm.

At this moment, the best bacterial growth method is adding 1.0 g of *Pararhodobacter* sp. bacteria to the 100 mL of NH_4-YE culture solution and shaking 72 hours with the rate of 160 rpm.

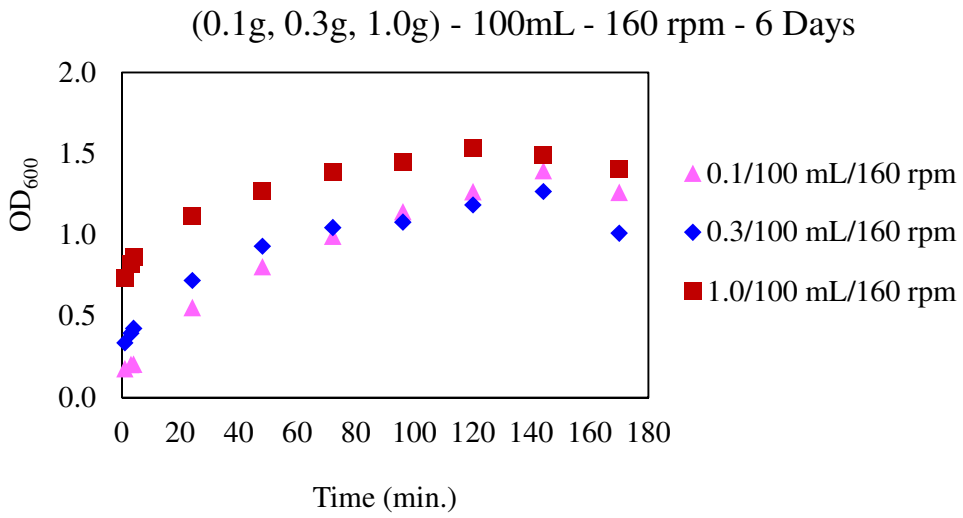

Fig. 4.8: Results of the the bacterial population in the culture solution when changing the bacterial population.

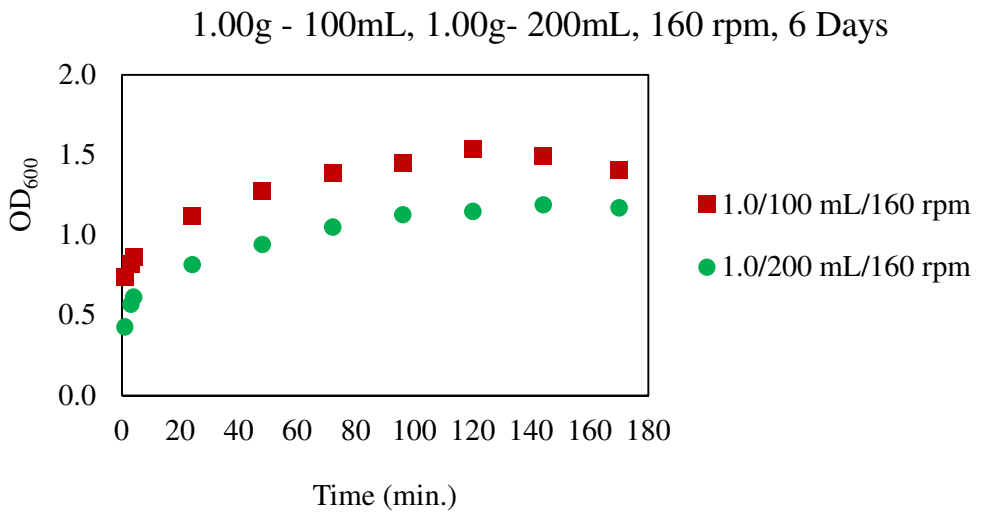

Fig. 4.9: Results of the the bacterial population in the culture solution when changing the volume of culture solution.

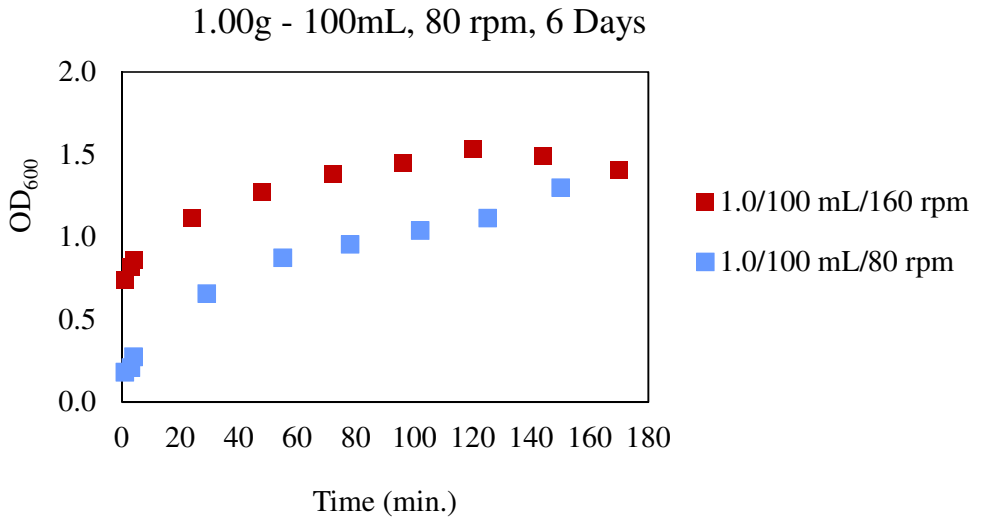

Fig. 4.10: Results of the the bacterial population in the culture solution when changing the speed of shaking.

Fig. 4.11 shows the relationship between OD_{600} and viable count (CFU/mL) for the *Pararhodobacter* sp. cultivated with NH_4-YE medium.

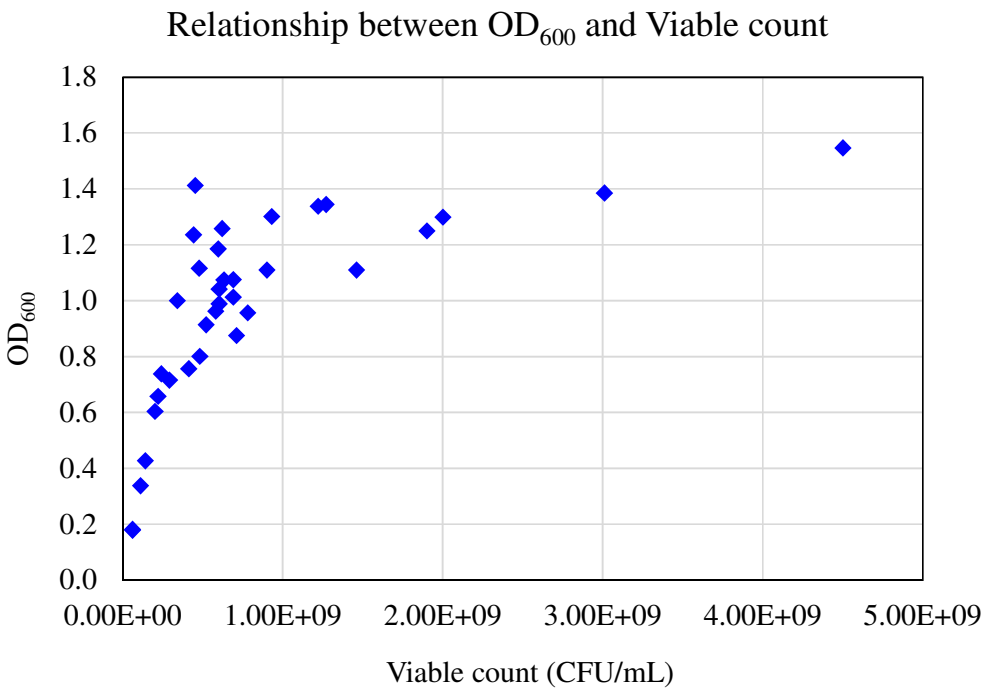

Fig. 4.11: Relationship between OD_{600} and viable count measurement.

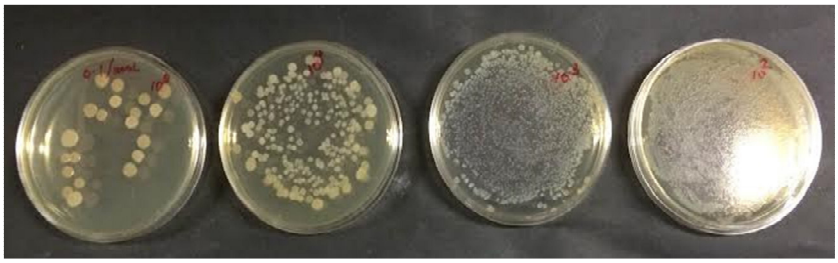

Fig. 4.12: Viable count measurement of *pararhodobacter* sp.

4.5.2 Effect of bacterial population

Fig.4.13 (a) shows that the estimated UCS of the sample increased with the increase of bacterial population. This finding indicates that bacteria plays a key role on MICP, i.e., (1) producing an enzyme to hydrolyze urea, and (2) acting as nucleation sites for the formation of calcium carbonate crystals (mainly calcite; Fujita et al. 2000).

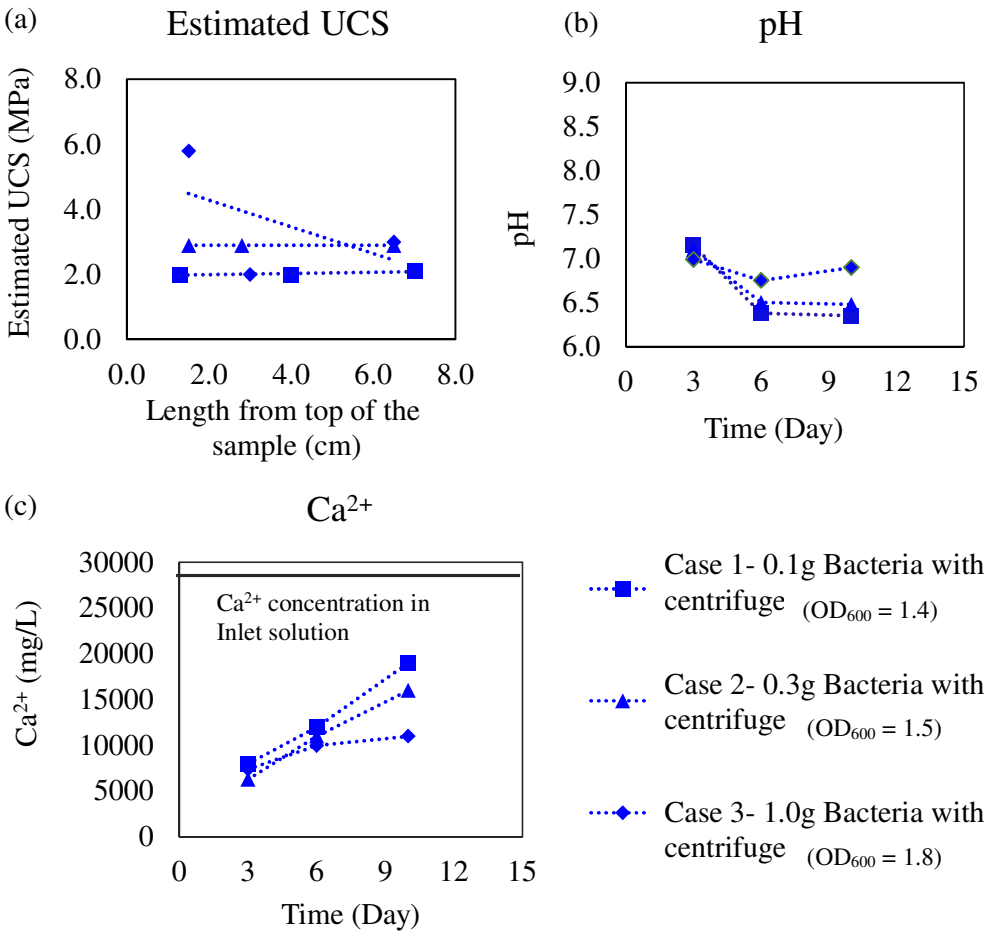

Fig. 4.13: Results of MICP-treated sample catalyzed by *Pararhodobactor* sp. under different bacteria concentrations: (a) Estimated UCS value with the depth of the sample, (b) pH with time and (c) Ca^{2+} concentration with time.

More bacteria in the solution can promote more enzymes and provides more nucleation sites for the MICP.

The pH value in outlet solution was larger in high bacterial concentration sample than low bacterial concentration sample. Although pH value decreased with the time for all testing cases. The results of Ca^{2+} concentration in outlet solution were opposite to the results of pH value (Fig.4.13 (b) and 4.13 (c)).

4.5.3 Effect of re-injection of bacteria

Fig. 4.14 shows the results of Case 1, Case 3, Case 4 and Case 5. Here, I considered about re-injection of the bacterial solution after 7 days and without re-injection. From the Fig. 4.14 (a) shows that the USC value was larger when bacteria re-injected after 7 days than without re-injection of bacterial solution.

According to Fig. 4.14 (b), pH value decreased with the time without re-injection method (Case 1 and 3). In Case 4 and 5, the pH value decreased until 7 days and after re-injection, pH value intended to increase and it fluctuated around 7. The bacterial effect can optimize when the pH value is maintained around 7. Because the optimal growth for *Pararhadobacter* sp. is at 30-40 ºC and pH 7.0-8.5 (Foesel et al. 2011). Ca^{2+} concentration was intended to increase with the time in the case of without adding bacteria after 7 days. Moreover, Ca^{2+} concentration decreased when re-injection of bacteria and again it increases with the time.

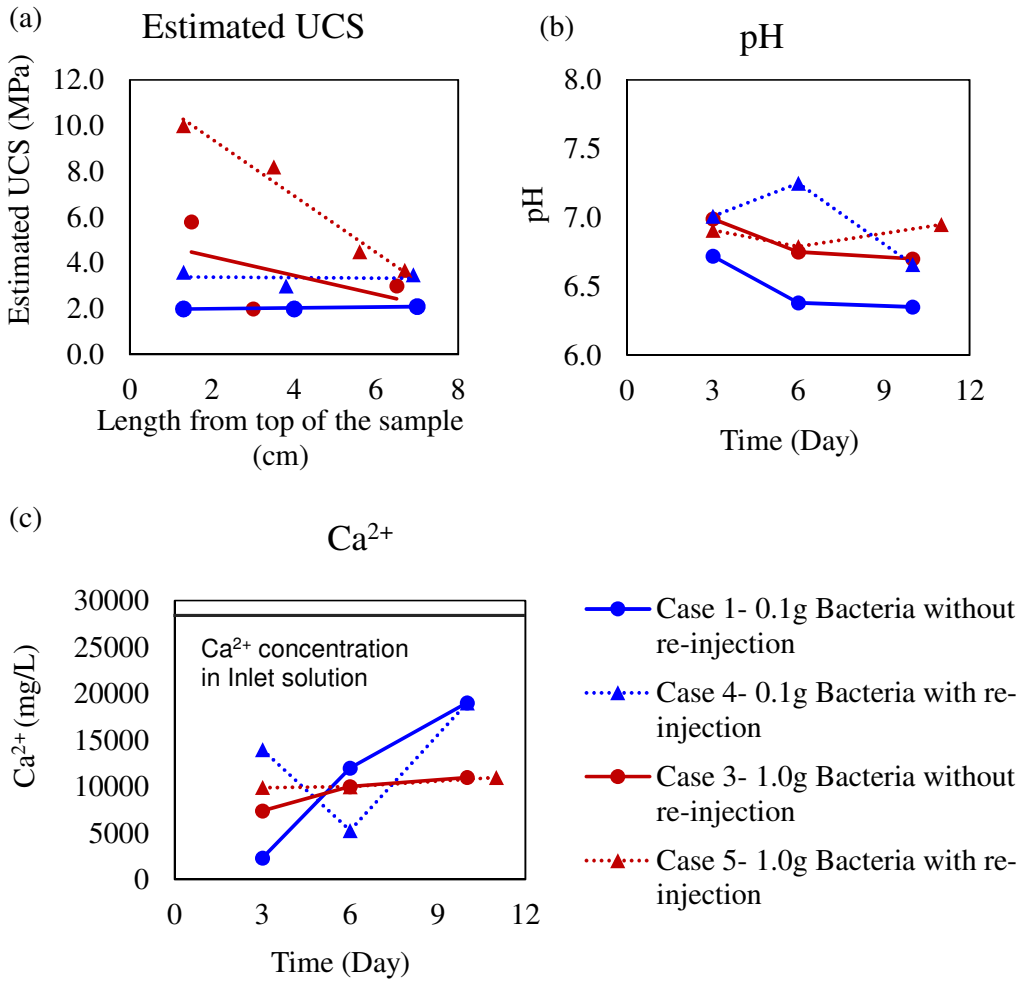

Fig. 4.14: Results of MICP-treated sample catalyzed by *Pararhodobactor* sp. under different injection method of bacteria: (a) Estimated UCS value with the depth of the sample, (b) pH with time and (c) Ca^{2+} concentration with time.

4.5.4 Effect of curing time

Figure 4.15 shows the results of the experiments conducted for different curing periods: 7 days, 14 days and 21 days. The UCS of the sample after 7 days curing period was less than curing time 14 days and 21 days. However, the UCS values of the sample tested for 14 days and 21 days were nearly same. The reason for this matter is, after 14 days the outlet solution rate was getting decrease with the time.

It could happen due to the clogging. The clogging of soil restricts the water flow through the soil, and hence reduces its permeability. pH decreased with the time of curing and the concentration of Ca^{2+} increased with the time.

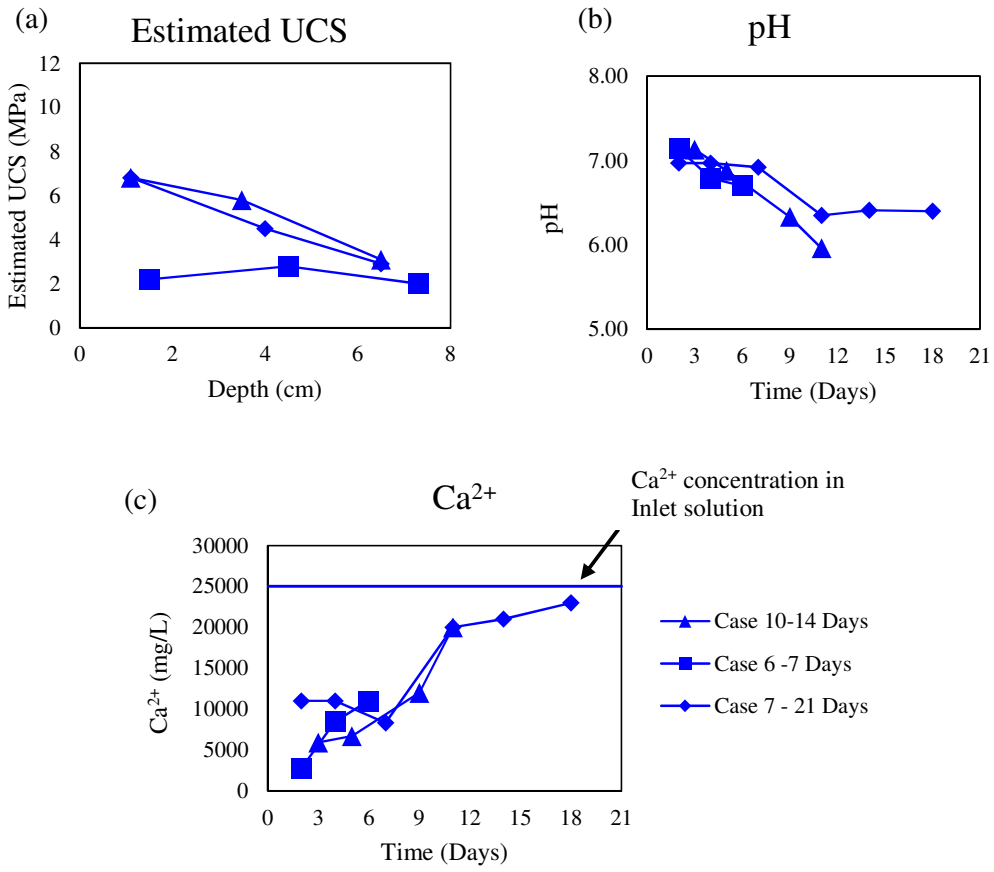

Fig. 4.15: Results of MICP-treated sample catalyzed by *Pararhodobactor* sp. under different curing time: (a) Estimated UCS value with the depth of the sample, (b) pH with time and (c) Ca^{2+} concentration with time.

4.5.5 Effect of curing temperature

Following figure (Fig. 4.16) shows that the investigation results of the effect of temperature. In this investigation, 3 testing cases were used: 25°C, 30°C and 35°C.

The UCS value was higher at 30°C than 25°C and 35°C. In this method, the samples tested at 35°C, when adding the cementation media every day, the penetration through the soil reduced due to clogging happened in between the sand particles. Here, 2 samples were tested and both samples faced same matter. Further investigation is needed for clarifying the reason for getting low UCS value at 30 ºC.

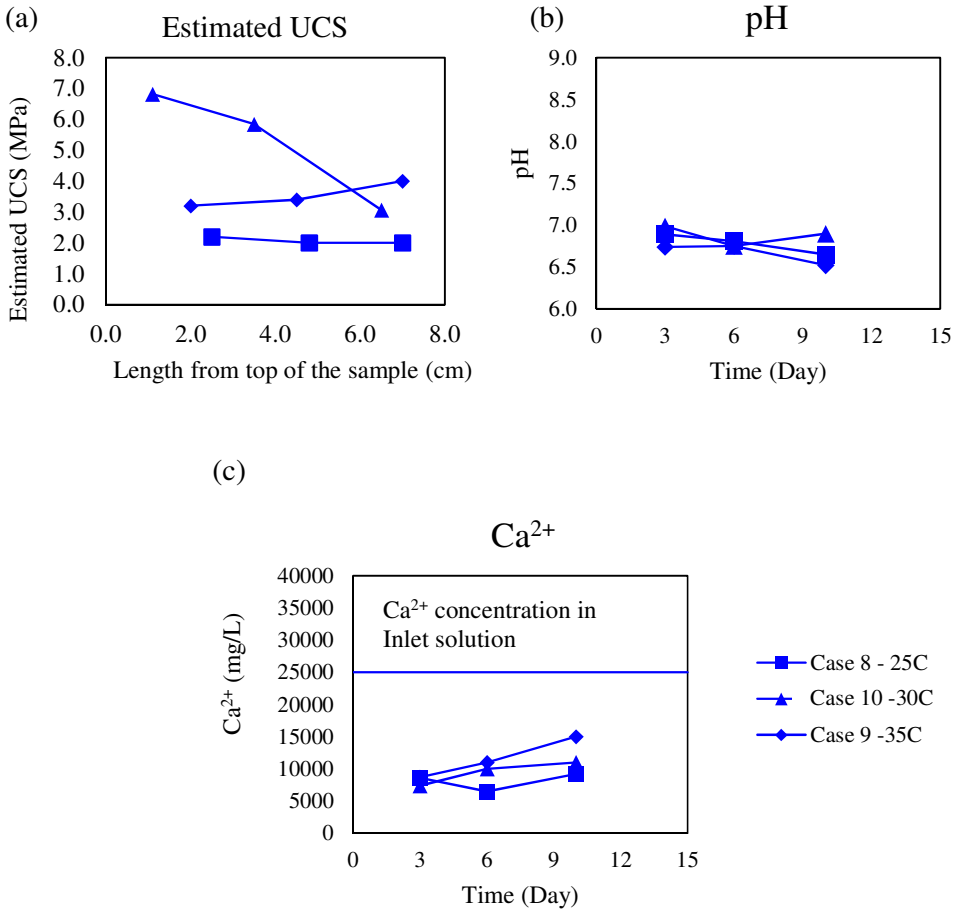

Fig. 4.16: Results of MICP-treated sample catalyzed by *Pararhodobactor* sp. under different temperature: (a) Estimated UCS value with the depth of the sample, (b) pH with time and (c) Ca^{2+} concentration with time.

4.5.6 Effect of injection interval of cementation media

In this part, two testing cases were accompanied with adding cementation

media to the syringe every day or after every 2 days (Case 10 and Case 11 respectively). In this study, the strength of the sample prepared with adding cementation media in every day was larger than the sample prepared with adding cementation media in 2 days interval until 14 days of the curing period. The reason for this observation is the adding Ca^{2+} concentration of the cementation media ($CaCl_2$) was large in the Case 10 than Case 11. However, with the depth of the syringe sample (top to bottom), the strength reduced.

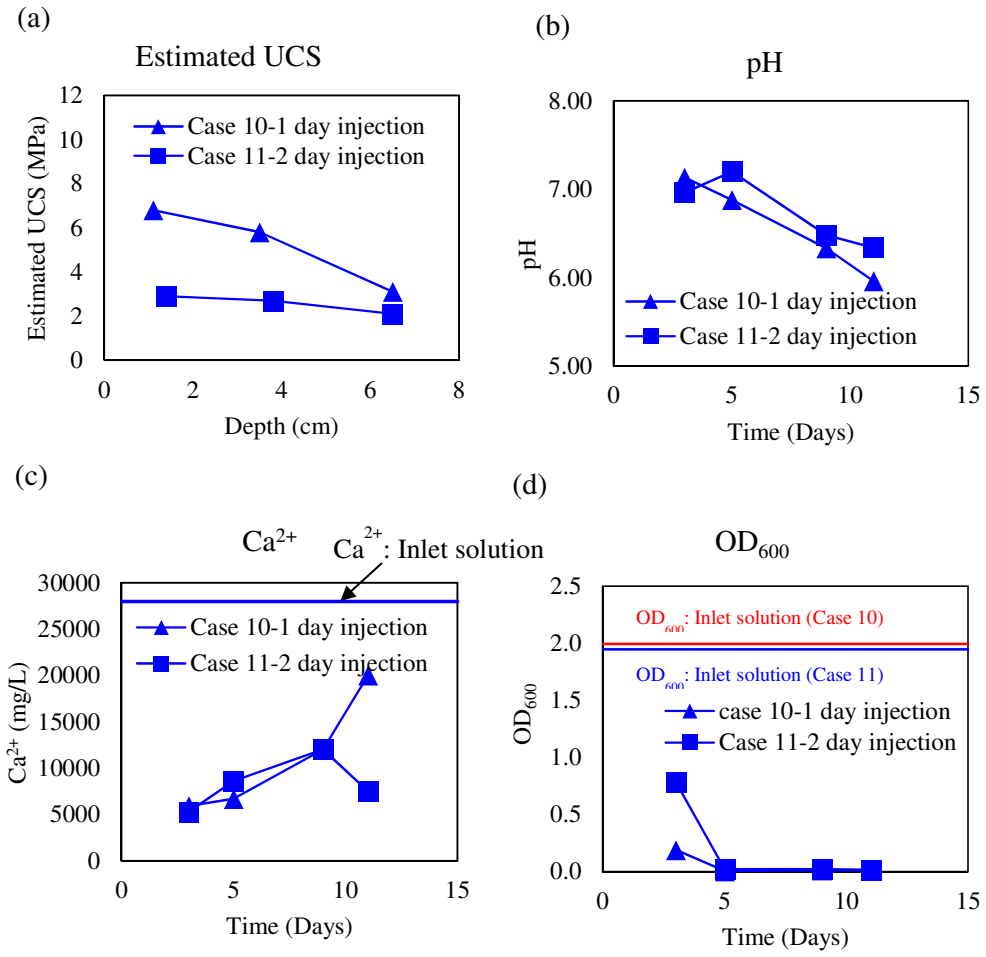

Fig. 4.17: Results of MICP-treated sample catalyzed by *Pararhodobactor* sp. under different injection interval: (a) Estimated UCS value with the depth of the sample, (b) pH with time, (c) Ca^{2+} concentration with time and (d) OD_{600} with time.

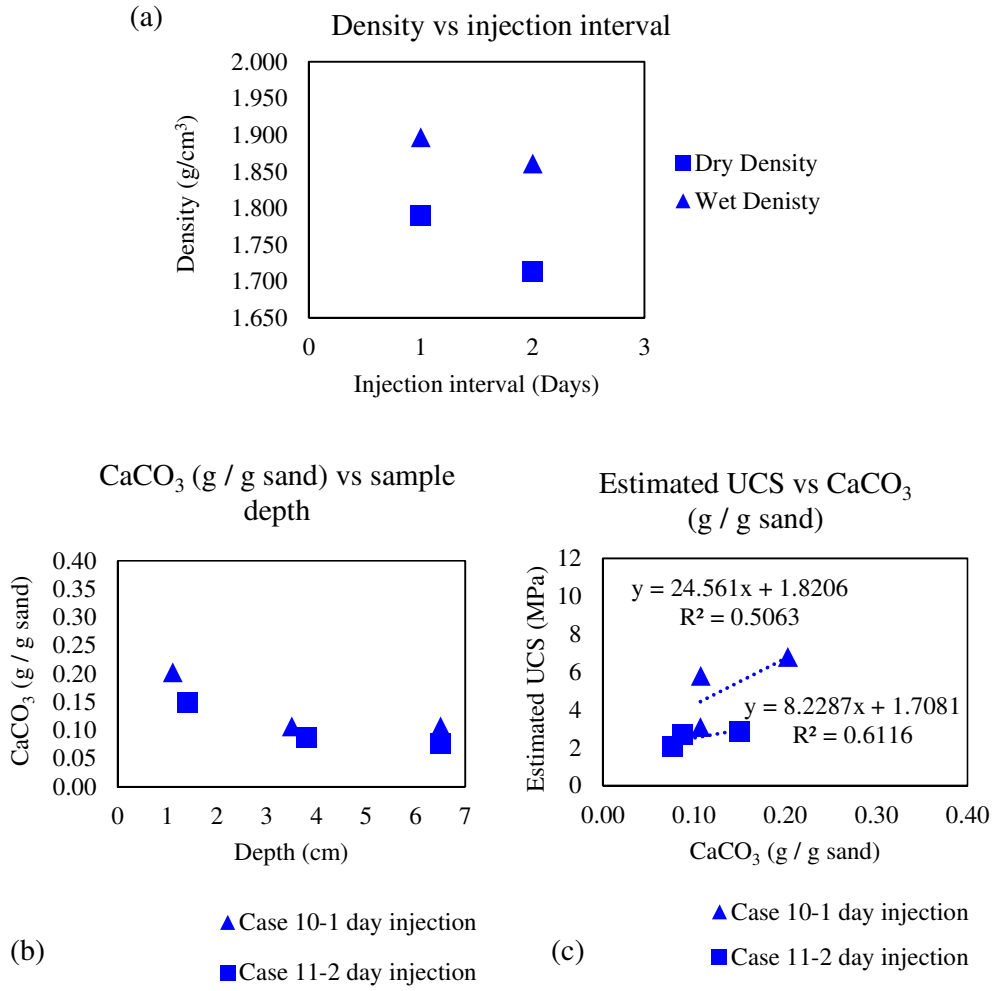

Fig. 4.18: Results of MICP-treated sample catalyzed by *Pararhodobactor* sp. under different temperature: (a) density of the sample with injection interval, (b) weight of $CaCO_3$ with sample depth and (c) Estimated UCS with $CaCO_3$ weight.

Moreover, here the wet density of the sample for two cases was measured and measure the $CaCO_3$ (g/ g sand) at three phases of the sample: top, middle and bottom. From these results, the density increased in the sample with the injection interval of 24 hours than the 48 hours injection interval. That means, if the wet density was high

means, the strength of the sample was high. Although, $CaCO_3$ content increased with the increase of estimated UCS in the samples. Meanwhile, $CaCO_3$ content decreased with the depth of the sample from top to bottom. This observation revealed that the strength of the sample decreased with the depth of the sample, due to that it was couldn't obtain a uniformed syringe sample. Therefore, the advance examination is required for solve this problem.

4.5.7 Effect of concentration of cementation media

Figure 4.19 shows that the results using different concentrations of cementation media for the solidification of syringe samples. The strength of the sample increased with the increased of the concentration of cementation media solution. Here, 0.3 M, 0.5 M, and 0.7 M concentrations were used. If the concentration of cementation media is increased, the rate of $CaCO_3$ precipitation is increased due to that the strength is getting increased.

Refer to Eq. (4.1) and Eq. (4.2) equations; the products from 1 mole of urea and 1 mole of calcium chloride would react to form 1 mole of calcite. A solution contains equimolar of both reactants would provide better conversion to calcite (Nemati et al. 2005). In terms of weight, the stoichiometric ratio of 2.5 for urea and calcium chloride is critical in order to achieve complete production of calcite, considering the molecular weights of urea ($CO(NH_2)_2$) and calcium chloride ($CaCl_2 \cdot 2H_2O$) are approximately 60 g/mole and 147 g/mole, respectively.

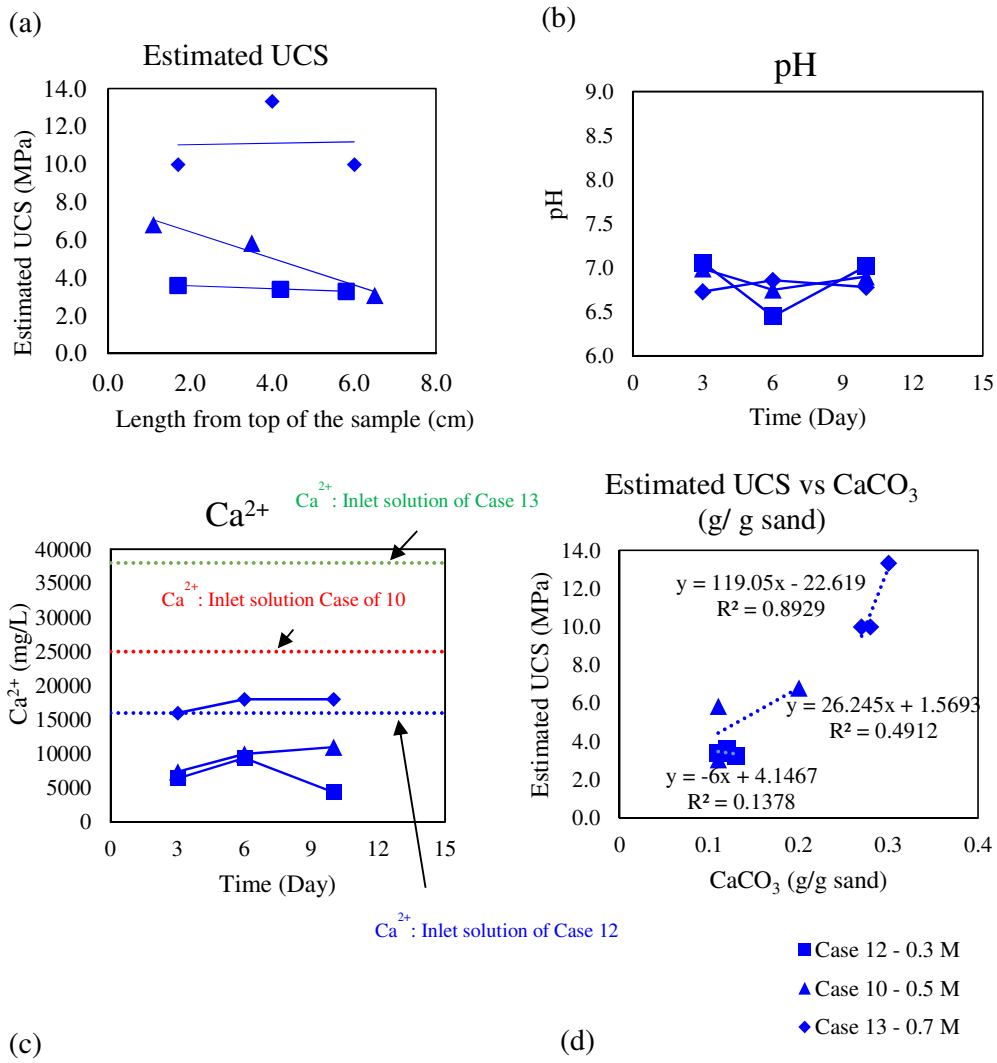

Fig. 4.19: Results of MICP-treated sample catalyzed by *Pararhodobactor* sp. under different concentration of cementation media: (a) Estimated UCS value, (b) pH with time, (c) Ca^{2+} concentration with time and (d) Estimated UCS with $CaCO_3$ weight.

4.5.8 Effect of particle size and different sand samples

Three different types of silica sand with three types of particle size were used for MICP-treated soil. Fig.4.20 (a), 4.20 (b) and 4.20 (c) show that the solidified samples after catalyzed by *Pararhodobactor* sp. for Toyoura sand, Mikawa sand, and Mizunami sand, respectively.

(a)

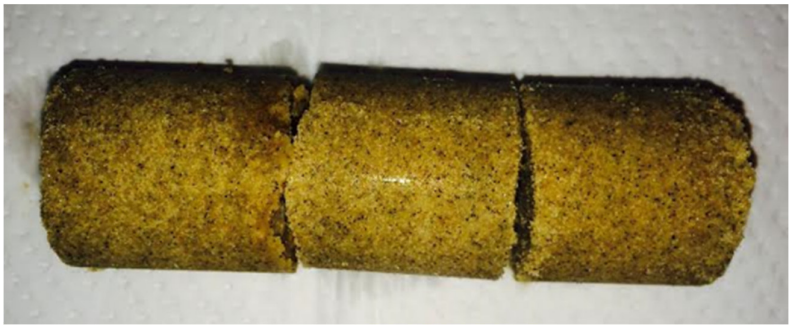

(b)

(c)

Fig. 4.20: (a) Solidified sample with Mikawa sand, (b) solidified sample with Toyoura sand and (c) solidified sample with Mizunami sand.

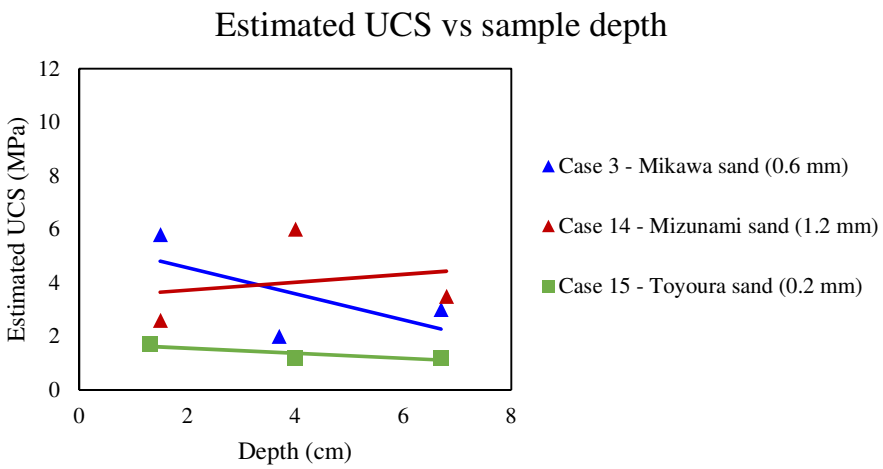

Fig. 4.21: Estimated UCS value of MICP-treated sample catalyzed by *Pararhodobactor* sp. under different particle size of sand samples.

Fig. 4.21 shows the estimated UCS value at the top, middle and bottom of the sample. From the results, estimated UCS value was larger in Mizunami sand with 1.2 mm mean diameter than Mikawa sand sample which has mean diameter 0.6 mm and estimated UCS value in Toyoura sand sample with mean diameter 0.2 mm. However, the estimated UCS value at the top of the sample in the Mizunami sand (1.2 mm) sample was less than the Mikawa sand sample (0.6 mm). To identifying the reason, future investigation is recommended.

The particle size of Toyoura sand is small than other two sand samples. Due to the very small particle size, the penetration rate of cementation media can be low when to compare with Mikawa and Mizunami sand samples. This reason may cause for decreasing the bacterial process. Then the hydrolysis process also getting slow. As a result of this, $CaCO_3$ precipitation decreasing and UCS value getting lower in Toyoura sand sample than Mikawa or Mizunami sand sample. Therefore, the particle size of the sample was mainly effect for solidification of the sample.

Therefore, the applicable range of sand particle size is 0.6 mm to 1.2 mm (mean diameter) according to this study results.

4.5.9 Effect of Color of Test Samples

Fig. 4.22 shows that the color changes of the samples with time. With time, the sample color was getting whitish color. It concluded that the $CaCO_3$ precipitation happened with time. Therefore, measurement of the color of the sample was a significant factor for solidification. The color was measured by using a colorimeter. But, it did not get successful values for the syringe samples due to not enough surfaces for a set with a colorimeter. Because each of the syringe test samples has a circular surface and is very small. Although, I tried to measure the color for the samples with a flat surface and the results of color measurement was described in next chapter.

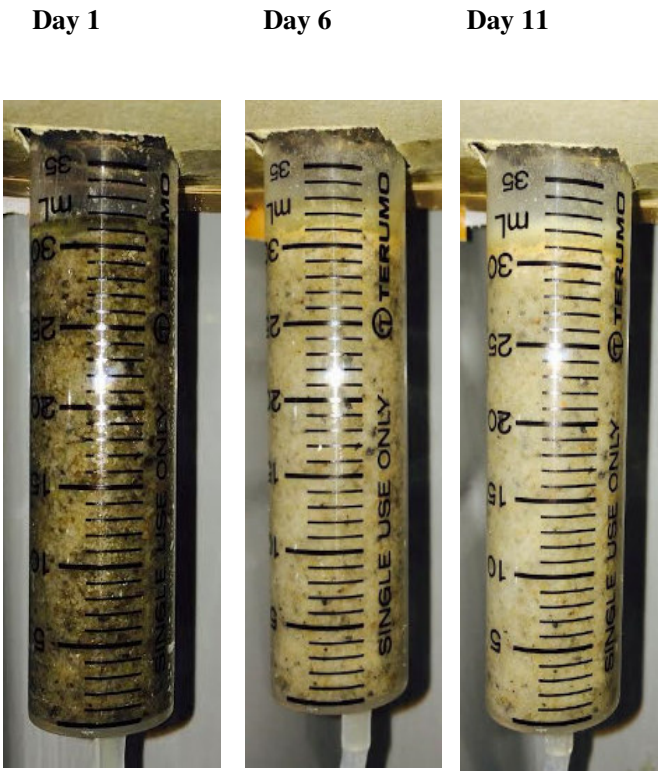

Fig 4.22: Changes of color with time for MICP-treated soil.

4.6 DISCUSSION

4.6.1 Temperature for the MICP process

The microbial activity and growth are less sensitive to the temperature within the range of 20 to 30°C. The rate of urea hydrolysis is marginally higher at 30°C, as compared to 20°C. The increment in temperature after 30°C does not promote the decomposition rate any further (Nemati et al. 2005). It is, however, impractical to alter or control the soil temperature while the MICP treatment is performed on soil specimen or in situ.

It is suggested to select a calcite forming bacteria that live in optimum soil temperature. The soil temperature varies with latitude, altitude, incident solar radiation, moisture content, conduction, type of soil, depth of soil and etc. (Seliness, (2005), Jacobson, (2005), Doty et al. (2009)). As an example, Nik et al. performed a study on soil temperature in Malaysia at the open area and forest (Nik et al. 1986). They found that the average soil temperature for the open area (from depth 0 to 30 cm) is approximately 30 °C throughout the year.

In terms of urease enzyme, Sahrawat (1984) indicated that the optimum temperature for urease activity is at approximately 60 °C. Urease activity increased with increasing temperature from 10 °C and reached a peak at 60 °C, the activity was inhibited at 100 °C when the temperature was raised further. The optimum temperature reported by Sahrawat (1984) is consistent with the findings from Liang et al. (2005) and Chen et al. (1996). This optimum temperature for urease activity, however, is impractical to be applied for soil treatment either on site or in the laboratory.

4.6.2 Concentration of cementation media

The concentration of reagents and the salinity have their influences on the MICP process (Riyadeneyra et al. 2004). The effects of reagents (e.g. urea and calcium chloride) concentration on calcite precipitation were studied by Nemati et al. (2005). Higher concentration of urea and calcium chloride extends the amount of

composited calcite (Nemati et al. (2005) and Okwadha et al. (2010). This phenomenon is further supported by Muynck et al. (2010), where the weight gain of soil sample due to carbonate precipitation was higher with a higher concentration of reagents.

This statement, however, is only valid for a certain concentration of reagents. High salinity has an inhibitory effect on microbial activity and calcite precipitation (Riyadeneyra et al. 1998). The salinity of cementation fluid is mainly contributed by calcium salt. Urea and calcium chloride with lower concentration contribute to a satisfied level of urea decomposition into ammonia. The microbial activity might be retarded by high salinity, thus limiting or eliminating the urease production from ureolytic bacteria (Nemati et al. (2005) and Riyadeneyra et al. (2000)). In the other case, urease is still available for MICP process at high salinity but the ratio of calcite precipitated and theoretically calcite composition decreased with increasing reactants' concentrations (Nemati et al. 2003, Muynck et al. 2010 and Ferrer et al. 1988).

The variation of calcite precipitation in high salinity can be explained by the halophilic characteristic of bacteria, where salinity has a less inhibitory effect on moderately halophilic bacteria compare to those with non-halophilic. Moderately halophilic bacteria has a capable of growing at a wide range of salinity, and should be used in the soil treatment if environment with high salinity is expected (Riyadeneyra et al. 2004). Several moderately halophilic bacteria were studied for their calcite precipitation capability in salinity environment, and they showed different response towards increasing concentration (Ferrer et al. 1988, Riyadeneyra et al. 1993 and Riyadeneyra et al. 1994).

4.6.3 Comparison of bacterial sand cementation techniques of this study and previous studies

For comparing bacterial sand cementation technique of this study with those of previous studies, I compared the relationship between the total $CaCO_3$ precipitation and the UCS of sand specimens cemented by each bacterium.

The results for other bacteria are shown in Fig. 4.23 (Van Paassen et al. 2010 and Cheng et al. 2013). *Sporosarcina pasteuriiis* the bacterium that has been most widely applied for investigation of sand improvement using bacteria. *Bacillus sphaericus*was isolated by Al-Thawadi and Cord-Ruwisch (2012).

Danjo (2015) found that the UCS of the specimen prepared using *Pararhodobacter* sp. was higher than that of the specimen generated using *Sporosarcina pasteurii*, even though these specimens contained the same amount of total $CaCO_3$ precipitation (Fig. 4.23). However, because these specimens contained different kinds of sand and were cured under different conditions, it is unclear which bacteria is better for sand cementation. Conversely, the different amounts of total precipitation could explain the different UCS of the specimens produced using *Bacillus sphaericus* or the other two bacteria. In addition, these findings are similar to those for sand cemented by enzymatically induced calcite precipitation (Yasuhara et al. 2012).

From this study, using Fig. 4.24 it is found that the relationship between estimated UCS and total $CaCO_3$ precipitation as follows:

$$\boldsymbol{q_{eu} = 44.06\, x^2 + 21.973\, x} \qquad \text{Eq. (4.5)}$$

Where, q_{eu} = Estimated UCS

x = $CaCO_3$ content (g / g sand)

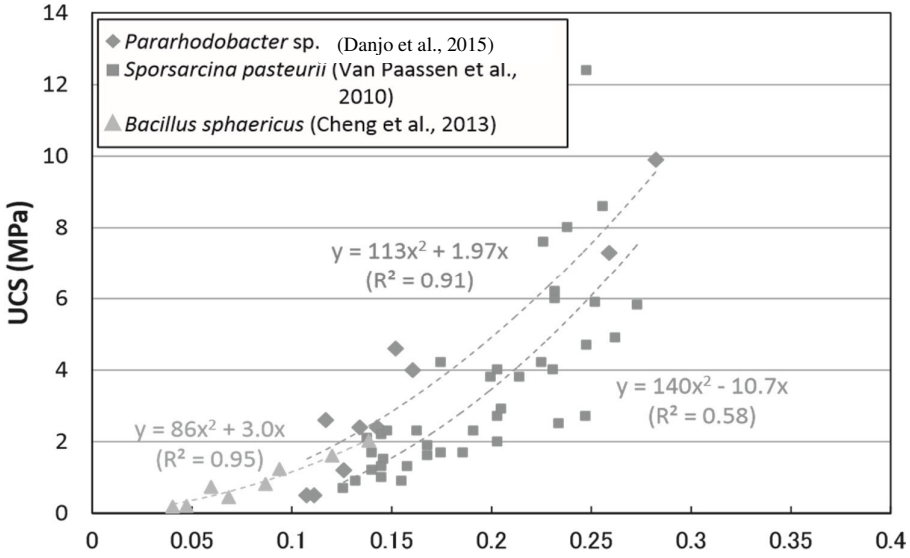

Fig. 4.23: Relationship between UCS and total $CaCO_3$ precipitation content for previous studies.

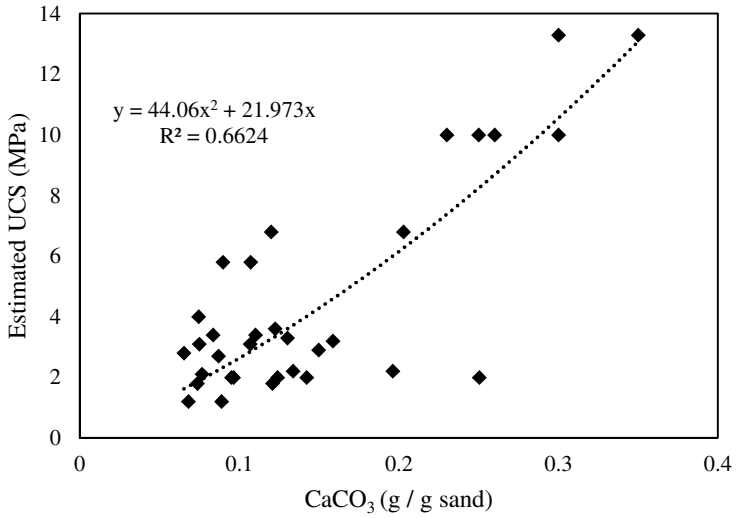

Fig. 4.24: Relationship between estimated UCS and total $CaCO_3$ precipitation content for this studies.

4.6.4 Suggested formula for prediction of estimated UCS

Multiple regression analysis was conducted in this study to analyze the relative importance of each test condition to the estimated UCS, and to determine experimentally a formula that can predict estimated UCS as a useful reference for future cementation tests and field tests.

In this study, multiple regression analysis was conducted using the results of the syringe solidification. In this analysis, the syringe test conditions were set as explanatory variables and the measured UCS was the objective variable. The following relational expression (Eq. (4.6)) and Table 4.14 were generated by this analysis.

Table 4.14: Results of the multiple regression analysis of data from the syringe solidification test.

	Coefficients	***Standard Error***	***t Stat***	***P-value***
Intercept	2.259	1.198	1.8857	0.0887
Bacterial Population (g) $\boldsymbol{B_p}$	3.370	2.519	1.3381	0.2105
Concentration of Cementation media (M) $\boldsymbol{C_{Ca}}$	9.749	3.164	3.0807	0.0116
Curing time (Days) $\boldsymbol{D}$	0.231	0.109	2.1251	0.0595
Injection Interval (Days) $\boldsymbol{I_i}$	1.165	1.184	0.9839	0.3484
Particle size (mm) $\boldsymbol{M}$	1.175	1.888	0.6224	0.5476
Temperature (°C) $\boldsymbol{T}$	0.061	0.056	1.0873	0.3024

Equation for estimated UCS value are as follows:

$$\boldsymbol{q_{eu} = 3.37\ B_p + 9.75\ C_{Ca} + 0.23\ D + 1.16\ I_i + 1.17\ M + 0.06\ T + 2.26} \quad \text{Eq. (4.6)}$$

Where; q_{eu} = Estimated UCS (MPa)

B_p = Bacterial population (g)

C_{Ca} = Concentration of cementation media (M)

D = Curing time (Days)

I_i = Injection interval (Days)

M = Particle size (mm)

T = Temperature (°C)

In Table 4.14, the partial regression coefficient indicated the coefficient of each multiple regression equations, which is set so that the theoretical value is close to the measured value. Additionally, the standard error was determined as follows: only one set of all intended experiments was conducted, but it was assumed that several sets were conducted. The frequency distributions of the partial regression coefficients and the constant term were then obtained by multiple regression analyses against each set of all intended experiments. The standard deviation of the normally distributed histogram obtained by calculating the frequency distributions is the standard error. The t value was obtained by dividing the partial regression coefficient by the standard error. From the t values, the degree of importance of each explanatory variable to the objective variable can be judged. The P-value was twice as much as the upper probability of the t value on the t distribution. In this study, a $P \leq 0.01$ and $0.01 < P \leq 0.05$ was considered to indicate that both explanatory variables are important, because the significance levels were 1% and 5%, respectively, while a $P > 0.05$ indicated that the explanatory variable was not important.

As shown in Table 4.14, the concentration of cementation media, curing time, injection interval were significant. Based on each t value, the concentration of cementation media had the highest degree of importance followed by curing time, injection interval, bacterial population, curing temperature and particle size.

To suggest a more reliable formula for prediction of the UCS than Eq. (4.6), the more important explanatory variables against the objective variable were selected. Because the P values of the concentration of cementation media, curing time, injection interval were less than 0.05. These conditions were selected as explanatory variables, and the UCS of specimens generated at a curing temperature of 30°C, 1.0g of bacterial population, and 0.6mm particle size diameter (Mikawa sand) were used as objective variables. The results of this multiple regression re-analysis are shown in

Eq. (4.7) and Table 4.15.

Table 4.15: Results of the multiple regression re-analysis of data from the syringe solidification test.

	Coefficients	*Standard Error*	*t Stat*	*P-value*
Intercept	-0.09	1.38	-0.0617	0.9547
Concentration of Cementation media (M) C_{Ca}	13.99	2.81	4.9696	0.0157
Curing time (Days) D	0.37	0.10	3.9071	0.0298

$$q_{eu} = 13.99\, C_{Ca} + 0.37\, D - 0.09 \qquad \text{Eq. (4.7)}$$

The P-values of three explanatory variables (Table 4.15) were lower than 0.05. Therefore, Eq. (4.7) can be considered a reliable formula for prediction of UCS. However, it should be noted that this formula is only reliable for samples generated using the curing temperature, bacterial population, and particle size of the sand material, described above. In addition, the conditions of the explanatory variables can change within the range of syringe tests. Hence, further cementation tests need to be performed to develop a reliable formula for prediction of UCS under more varied conditions. Nevertheless, Eq. (4.7) will be useful for further cementation tests and field tests.

4.7 CONCLUSIONS

MICP has many applications in civil engineering and in particular in the geotechnical area. It can be used for reinforcement of soil and to prevent internal erosion in earth dams (piping) and the destruction of dikes in the occurrence of natural disasters as floods and storms at sea (Paassen, 2011). It also can be a good solution to treat soils with a high potential for liquefaction. There are also other applications such as the replacement of asphalt in roads (Wang, 2010), the ability to dig tunnels in the sand and solidify the ocean floor to facilitate the work of extracting oil and natural gas (Latil et al.,2008).

Microbial induced calcite precipitation utilizing urea hydrolysis is a complex biochemical process, especially when it takes place between sand particles for improvement of soil engineering properties. There are many factors that may affect this process. Some of these factors reported in this paper included bacteria concentration, re-injection of bacteria, sand type and particle size of the sample, injection interval of the cementation media, concentration of the cementation media, curing time, temperature, and viscosity of the bacterial solution.

The results of estimated UCS value show that all the studied factors have an obvious effect on the MICP treated sand. Case 3, Case 4 and Case 5 obtained the estimated UCS value more than 3 MPa: (1) Case 3-1.0g of bacteria with centrifuge but without re-injection of bacteria after 7 days, (2) Case 4- 0.1g of bacteria with centrifuge and with re-injection of bacteria after 7 days, and (3) Case 5- 1.0g of bacteria with centrifuge and with re-injection of bacteria. The estimated UCS value at the top of the sample in Case 5 was 10 MPa. Also, the estimated UCS value was more than 10 MPa at the top of the sample in the case of changing concentration of 0.7 M.

In this study, two equations were derived.

01) Relationship between estimated UCS and $CaCO_3$ precipitation

$$q_{eu} = 44.06\, x^2 + 21.973\, x$$

Where, q_{eu} = Estimated UCS (MPa)

x = $CaCO_3$ weight (g/g sand)

02) Formula for estimated UCS according to the different parameters

$$q_{eu} = 13.99\, C_{Ca} + 0.37\, D - 0.09$$

Where; q_{eu} = Estimated UCS (MPa)

C_{Ca} = Concentration of cementation media (M)

D = Curing time (Days)

Most studies on MICP soil improvement used cylindrical columns or syringes for sample preparation by pumping or injections methods. Although pumping or injections promoted cementation media penetration into soil pores under pressure to some extent, the effluent also reduces the number of bacteria as well as a portion of urease produced by bacteria, and the samples may not be uniform along the flow.

REFERENCES

Burbank MB, Weaver TJ, Green TL, Williams BC, Crawford RL, “Precipitation of calcite by indigenous microorganisms to strengthen liquefiable soils,” Journal of *Geomicrobiology*, Vol. 28(4), 2011, pp. 301–312.

Chen YY, Clancy KA, Burne RA, "Streptococcus salivarius urease: genetic and biochemical characterization and expression in a dental plaque streptococcus," *Infect. Immun.,* Vol. 64, 1996, pp. 585-92.

Danjo T, Kawasaki S, “A study of the Formation mechanism of beach rock in Okinawa, Japan: Toward making Artificial Rock.” Int. Journal of *GEOMATE*, Vol. 5 (1), 2013, pp. 633-638.

Danjo T, Kawasaki S, “Microbially induced sand cementation method using Pararhodobacter sp. strain S01, inspired by beachrock formation mechanism, ” Journal of *Materials Transactions*, Vol. 57 (3), 2016, pp. 428-437.

Danjo T, Kawasaki S, “Formation mechanisms of beachrocks in Okinawa and Ishikawa, Japan, with a focus on cements, ” Journal of *Materials Transactions*, Vol. 55 (3), 2014, pp. 493-500.

Danjo T, Doctoral Thesis, Hokkaido University, Japan, 2015.

De Muynck W, Verbeken K, De Belie N, Verstraete W, "Influence of urea and calcium dosage on the effectiveness of bacterially induced carbonate precipitation on limestone," *Ecol. Eng.,* Vol. 36, 2010, pp. 99-111.

DeJong JT, Fritzges MB, Nusslein K, “Microbially induced cementation to control sand response to undrained shear,” Journal of *Geotech. Geoenviron. Eng*., Vol.11 (1381), 2006, pp. 1381–1392.

DeJong JT, Mortensen BM, Martinez BC, Nelson DC, (2010). “Biomediated soil

improvement." *Ecological Engineering*, Vol. 36(2), 2010, pp. 197–210.

Doty S, Turner WC, Energy management handbook, 7th ed. Lilburn, Ga.: Fairmont Press ; London : Taylor & Francis, 2009, pp. 734.

Ehrlich HL, Geomicrobiology, Marcel Dekker, New York, 2002.

Ferrer MR, QuevedoSarmiento J, Bejar V, Delgado R, RamosCormenzana A, Rivadeneyra MA, "Calcium carbonate formation by Deleyahalophila: Effect of salt concentration and incubation temperature," Journal of *Geomicrobiol.,* Vol. 6, 1988, pp. 49-57.

Ferrer MR, Quevedo-Sarmiento J, Rivadeneyra MA, Bejar V, Delgado R, Ramos-Cormenzana A, "Calcium carbonate precipitation by two groups of moderately halophilic microorganisms at different temperatures and salt concentrations," *Curr. Microbiol.,* Vol. 17, 1988, pp. 221-227.

Foesel BU, Darke HL, Schramm A, "Defluviimonasdenitrificans gen. nov., sp. nov., and Pararhodobactoraggregans gen. nov., sp. nov., non-phototropic Rhodobacteraceae from the biofiter of a marine aguaculture," Journal of *Systematic and applied microbiology*, Vol. 34, 2011, pp. 498-502.

Fredrickson JK, Fletcher M, "Subsurface microbiology and biogeochemistry." Wiley-Liss, Hoboken, NJ, 2001.

Fujita Y, Ferris EG, Lawson RD, Colwell FS, Smith RW, "Calcium carbonate precipitation by ureolytic subsurface bacteria," Journal of *Geomicrobiol,* Vol. 17(4), 2000, pp. 305–318.

Jacobson MZ, Fundamentals of atmospheric modeling, 2nd ed. Cambridge: Cambridge University Press, 2005, pp. 254-255.

Liang ZP, FengYQ, Meng SX, Liang ZY, "Preparation and Properties of Urease Immobilized onto Glutaraldehyde Cross-linked Chitosan Beads," *Chin. Chem. Letters,* Vol. 16, 2005, pp. 135-138.

Mitchell JK, Santamarina CJ, “Biological considerations in geotechnical engineering,” Journal of *Geotech. Geoenviron. Eng*., Vol. 131(10), 2005, pp. 1222–1233.

Mortensen BM, Haber MJ, DeJong JT, Caslake LF, Nelson DC, “Effects of environmental factors on microbial induced calcium carbonate precipitation,” Journal of *Appl. Microbiol*., Vol. 111(2), 2011, pp. 338–349.

Nemati M, Greene EA, Voordouw G, "Permeability profile modification using bacterially formed calcium carbonate: comparison with enzymic option," *Process Biochem.,* Vol. 40, 2005, pp. 925-933

Nemati M, Voordouw G, "Modification of porous media permeability, using calcium carbonate produced enzymatically in situ," *Enzyme Microb. Technol.,* Vol. 33, 2003, pp. 635-642.

Nik AR, Kasran B, Hassan A, "Soil temperature regimes under mixed dipterocarp forests of Peninsular Malaysia " *Pertanika J. Sci. Technol.,* Vol. 9 1986, pp. 277-284.

Okwadha GD, and Li J, "Optimum conditions for microbial carbonate precipitation," *Chemosphere,* Vol. 81, 2010, pp. 1143-8.

Qabany AA, Soga K, Santamarina C, “Factors affecting the efficiency of microbially induced calcite precipitation,” Journal of *Geotech. Geoenviron. Eng*., Vol. 138(8), 2012, pp. 992–1001.

Ramachandran SK, Ramakrishnan V, Bang SS, “Remediation of concrete using microorganisms,” Journal of *ACI Mater*, Vol. 98(1), 2011, pp. 3–9.

Rebata-Landa V, “Microbial activity in sediments: Effects on soil behavior.” Ph.D. thesis, Georgia Institute of Technology, Atlanta, GA, 2007.

Rivadeneyra MA, Párraga J, Delgado R, Ramos-Cormenzana A, Delgado G, "Biomineralization of carbonates by Halobacillustrueperi in solid and liquid media with different salinities," *FEMS Microbiol. Ecol.,* Vol. 48, 2004, pp. 39-46.

Rivadeneyra MA, Delgado G, Ramos-Cormenzana A, Delgado R, "Biomineralization of carbonates by Halomonaseurihalina in solid and liquid media with different salinities: crystal formation sequence," *Res. Microbiol.,* Vol. 149, 1998, pp. 277-87.

Rivadeneyra MA, Delgado G, Soriano M, Ramos-Cormenzana A, Delgado R, "Precipitation of carbonates by Nesterenkoniahalobia in liquid media," *Chemosphere,* Vol. 41, 2000, pp. 617-24.

Rivadeneyra MA, Delgado R, Delgado G, Moral AD, Ferrer MR, RamosCormenzana A, "Precipitation of carbonates by Bacillus sp. isolated from saline soils," Journal of *Geomicrobiol.,* Vol. 11, 1993, pp. 175-184.

Rivadeneyra MA, Delgado R, Moral AD, Ferrer MR, Ramos-Cormenzana A, "Precipatation of calcium carbonate by Vibrio spp. from an inland saltern," *FEMS Microbiol. Ecol.,* Vol. 13, 1994, pp. 197204.

Sahrawat K, "Effects of temperature and moisture on urease activity in semi-arid tropical soils," *Plant and Soil, V*ol. 78, 1984, pp. 401-408.

Selinus O, "*Essentials of medical geology: impacts of the natural environment on public health*."Amsterdam; London: Elsevier Academic Press, 483, 2005.

Shimazaki S, Master Thesis, Hokkaido University, Japan, 2015.

Van Paassen LA, Ghose R, van der Linden TJM, van der Star WRL, van Loosdrecht MCM, "Quantifying biomediated ground improvement by ureolysis: large-scale bio grout experiment" Journal of *Geotech.Geoenviron. Eng*., Vol 136(12), 2010, pp. 1721–1728.

Whiffin VS, van Paasse, LA, Harkes MP, "Microbial carbonate precipitation as a soil improvement technique," Journal of *Geomicrobiol*, Vol. 24(5), 2007, pp. 417–423.

CHAPTER 5

MODEL TEST FOR SAND SOLIDIFICATION USING MICP METHOD

5.1 INTRODUCTION

The engineering properties of MICP-treated soil may vary because MICP is a complex biochemical process, which can be effected by many factors. The MICP contains two key steps, as follows: (1) urea hydrolysis, and (2) calcite precipitation. The urea hydrolysis is mainly dependent on the concentration of urease enzymes (i.e., bacteria or urease concentration) and the available substrate (e.g., urea), whereas calcite precipitation relates to available Ca^{2+} (Mortensen et al. 2011). Chou et al. (2011) conducted direct shear tests to compare sand samples treatment by bacteria. The friction angles of the growing-cell treatment samples inoculated at 10^7 colony-forming units (CFU)/mL are greater than those at 10^3 CFU/mL. Rebata-Landa (2007) prepared samples in 60-mL plastic syringes with nutrient circulation for 64 days and found a strong correlation between nutrient concentration (urea and $CaCl_2$), incubation time, and apparent cementation of sand. In accordance with the growth of nutrient concentration and incubation time, the $CaCO_3$ content increases. The particle size also has effect on MICP bonded soil. The efficiency of MICP is related to the permeability of the soil being sufficient to allow chemicals to flow to the bacteria and also the cement effect of $CaCO_3$ precipitation away particles (Mitchell and Santamarina 2005; Rebata-Landa 2007). Rebata-Landa (2007) showed a relation between grain size and $CaCO_3$ content, and maximum carbonate deposition observed on grains was approximately 100 μm in size. Qabany et al. (2012) also found well-graded and coarser sands had a higher rate of precipitation than finer and poorly graded soils.

Most studies on MICP soil improvement used cylindrical columns or syringes for sample preparation by pumping or injections methods. In the previous chapter, it described syringe solidification test. However, it was faced many practical issues. In the syringe test, there can be a possibility of block the bacterial solution and the

consolidation solution. This happened, the syringe size was very small and there may be a possibility to happening bio-clogging easily. To avoid this problem, the large size of sample preparation was used. In this chapter, the small size of lab model test was described. The methodology was same as syringe solidification test and here, materials are needed more than compare to the syringe test. In addition, unconfined compressive strength (UCS), X-ray diffraction (XRD), X-CT, primary and secondary wave velocity of the sample (Vp and Vs) and color measurement tests were conducted, which could not be conducted for syringe samples, because the sample size is not matched with the required size for conducting previously mention testing. To mitigate the above mentioned inconveniences, a small size of the rectangular plastic container box (20 cm x 12.5 cm x 15 cm) was used for sand solidification.

5.2 OBJECTIVE

Laboratory model tests were conducted for obtained uniformly strengthen soil sample. Moreover, the strength characteristics were observed. In addition, unconfined compressive strength (UCS), X-ray diffraction (XRD), X-CT, Primary and secondary wave velocity of the sample (Vp and Vs) and color measurement tests were conducted for solidified samples.

5.3 METHODOLOGY

Materials and the concept of methodology were same as syringe solidification test (Chapter 4). In this experiment series, two types of sand material were used: Mikawa sand and Mizunami sand. In this method, Toyoura sand was not used. The particle size of Toyoura sand was too small (0.2 mm), therefore clogging can happen easily. The weight of sand, weight of bacterial population, volume of culture solution and cementation media was too large when compare to the amount of syringe test.

The physical properties of sand materials and the figure of the concept were shown in the following Table 5.1 and Fig. 5.1 respectively.

Table 5.1: Physical properties of Mikawa sand and Mizunami sand.

Sand Type	**Mizunami Sand**	**Mikawa Sand**
soil particle density (ρ_s) (g/cm^3)	2.67	2.66
minimum density (ρ_{min}) (g/cm^3)	1.348	1.256
maximum density (ρ_{max}) (g/cm^3)	1.491	1.476
mean diameter (D_{50}) (μm)	1200	600

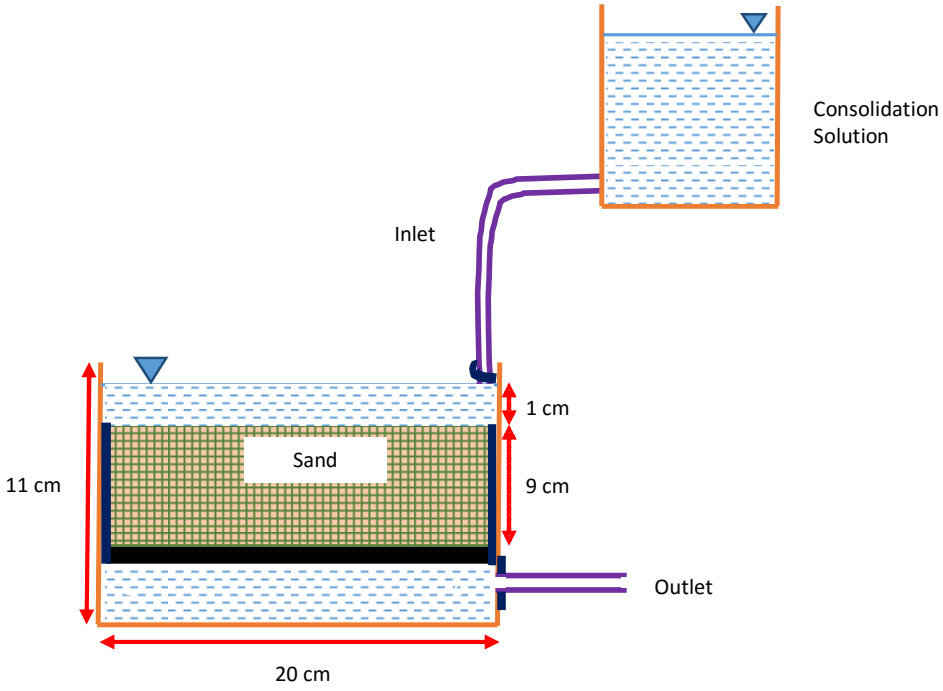

Fig. 5.1: Concept of the lab-model experiment for sand solidification using ureolytic bacteria.

5.3.1 Calculation for sand weight, bacterial population and volume of cementation media

The height of the sample was 9 cm, the width of the plastic container box was 12.5 cm and the length of the model box was 20 cm.

For Mikawa Sand

Volume of the box	= 20 x 9 x 12.5
	= 2250 cm^3
Weight of Mikawa sand	= Volume x maximum density
	= 2250 x 1.476
	= 3321 g
Volume of culture solution	= 2250 – (3321/2.66) + 250
	= 1250 mL
Bacterial population	= 13.0 g
Volume of cementation media	= 1250 + 250
	= 1500 mL

For Mizunami Sand

Volume of the box	= 20 x 9 x 12.5
	= 2250 cm^3
Weight of Mizunami sand	= Volume x maximum density
	= 2250 x 1.491
	= 3355 g
Volume of culture solution	= 2250 – (3355/2.67) + 250
	= 1250 mL
Bacterial population	= 13.0 g
Volume of cementation media	= 1250 + 250
	= 1500 mL

Table 5.2: Culture solution for 1300 mL.

Chemical	**Chemical Concentration (g)**
Tris buffer	20.475
Yeast extract	26
$(NH_4)_2SO_4$	13

Table 5.3: Cementation media for 1500 mL.

Chemical	**Chemical Concentration (g)**
Nutrient Broth	4.5
NH_4Cl	15
$NaHCO_3$	3.18
Urea	45.06
$CaCl_2$	83.25

5.3.2 Experiment Conditions

In this study, four testing cases were carried out as shown in Table 5.4. In addition, all testing cases conducted at room temperature (25 °C) and cementation media added every day. The height of sample, curing time and sand type were changed.

Table 5.4: Experiment conditions.

<table>
<tr><th rowspan="2">Case No.</th><th rowspan="2">Temperature (°C)</th><th>Injection Interval</th><th rowspan="2">Curing time</th><th rowspan="2">Population of bacteria (g)</th><th rowspan="2">Adding bacteria (After 7 days)</th><th rowspan="2">Height of sample (cm)</th><th rowspan="2">Sand material (Particle Size mm)</th></tr>
<tr><th>1 Day</th></tr>
<tr><td>1</td><td rowspan="4">25</td><td rowspan="4">x</td><td rowspan="3">14</td><td>3</td><td rowspan="3"></td><td>2 cm</td><td rowspan="2">Mikawa (0.6 mm)</td></tr>
<tr><td>2</td><td rowspan="3">13</td><td rowspan="3">9 cm</td></tr>
<tr><td>3</td><td>Mizunami (1.3 mm)</td></tr>
<tr><td>4</td><td>21</td><td>x</td><td>Mikawa (0.6 mm)</td></tr>
</table>

5.3.3 Experiment method

1) An oven dried the weight of about 3500 g of Mikawa or Mizunami sand two days before the experiment started at 110 ℃ in constant temperature.
2) Cooled down the sand from oven over 30 min.
3) The model box was covered with unwoven cloth and after cooled the sand, add 3321 g of sand to the box with three layers.
4) The outlet of the box was set with a tube and the tube was locked with a pinch lock.
5) Then added bacterial solution (Bacterial solution was prepared 3 days before the experiment as same as syringe test, and shake 72 hours) to the model box for saturating the sand with bacterial solution.
6) Then prepare 1500 mL of cementation media, and added the cementation media to the sample box as shown in the figure.
7) The solution level adjusted and maintain 2 cm above the sand layer. Also, every 24 hours interval, cementation media was added.
8) pH, Ca^{2+} concentration, and OD_{600} were measured by collection the samples in the outlet solution.
9) This procedure was conducted until the curing period was completed.
10) After solidification was finished, the sample was opened and coring cylindrical samples with the diameter of 3 cm and the height was 6 cm.
11) UCS test, Needle penetration test, Vs and Vp measurement, color of the sample, XRD (X-Ray deflection), SEM-EDX observation and $CaCO_3$ content was conducted for the cored samples.

The method of needle penetration test was described in the previous chapter. (Chapter 4).

Measurement of Color

For identifying the color quantitatively, a colorimeter is used. The

colorimeter is equipped with a pulsed lighting system for stable and uniform illumination of the subject, photocells with filters to match the CIE standard observer spectral response and electronic circuitry to determine accurate tri-stimulus values. Using this equipment, it is easily and instantly describe colors in terms of the values of standard color systems such as L*a*b* color space.

Initially for familiar with the equipment, color paper was used and get the readings.

The color of the rock samples was measured by the colorimeter and described based on L*a*b* color space. L* represents psychometric lightness, and a* and b* represent psychometric chromaticness.

For one sample, 4 readings take and get the average value. Then calculate the Standard Deviation for L*, a* and b* for all samples.

The standard deviation is found by taking the square root of the average of the squared differences of the values from their average value.

$$S = \sqrt{\frac{1}{N-1}\sum_{i=1}^{N}(xi - \bar{x})2}$$

Where, S – Standard Deviation, N – No of Samples and $\bar{x}$-Mean value (Average)

Fig. 5.2: Colorimeter.

Sample Coring after solidification

After solidified the sample, rock coring machine was used for core the 3 cm diameter and 6 cm height cylindrical samples. The following figures show the steps of coring samples.

Fig. 5.3: Procedure for sample coring using rock coring machine.

Measurement of Vp and Vs

Primary velocity (Vp) and secondary velocity (Vs) was measured for cored samples by using the following machine. Primary waves (P-waves) are compressional waves that are longitudinal in nature. P waves are pressure waves that travel faster than other waves through the earth to arrive at seismograph stations firstly, hence the name "Primary". These waves can travel through any type of material, including fluids, and can travel at nearly twice the speed of S waves. In the air, they take the form of sound waves, hence, they travel at the speed of sound. Typical speeds are 330 m/s in air, 1450 m/s in water and about 5000 m/s in granite.

Secondary waves (S-waves) are shear waves that are transverse in nature. Following an earthquake event, S-waves arrive at seismograph stations after the faster-moving P-waves and displace the ground perpendicular to the direction of propagation. Depending on the propagational direction, the wave can take on

different surface characteristics; for example, in the case of horizontally polarized S waves, the ground moves alternately to one side and then the other. S-waves can travel only through solids, as fluids (liquids and gasses) do not support shear stresses. S-waves are slower than P-waves, and speeds are typically around 60% of that of P-waves in any given material.

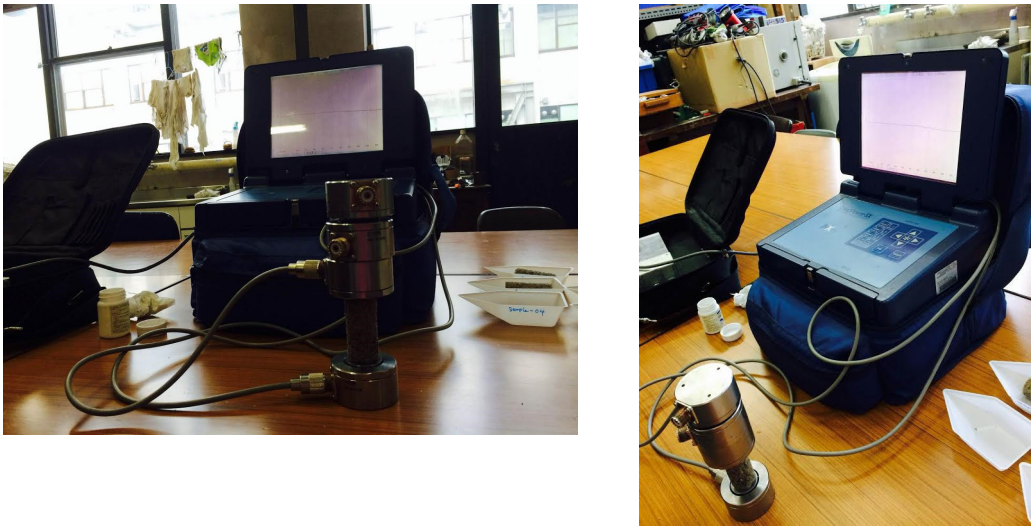

Fig. 5.4: The equipment for measure the Vp and Vs values.

Measurement of UCS test

UCS was measured directly by using unconfined compressive strength machine. Cored samples were trimmed up sharply with 3 cm in diameter and 6 cm in height. Then the samples were wrapped with two load cells as shown in the figure (Fig. 5.5) and set the strain gauges to the sample. Then segment was set into the UCS machine and the operation was started (Fig. 5.6). The stress-strain curve can be obtained from a personal computer and the test was stopped when the sample was broken or the stress was reduced with the increase of strain (%).

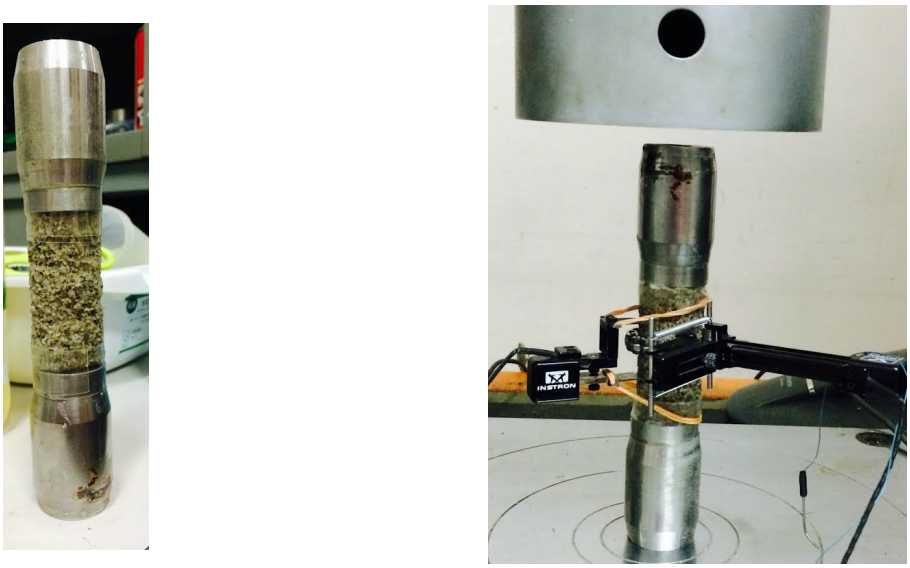

Fig. 5.5: Sample preparation before conducting UCS test.

Fig. 5.6: Controlling unit and the computer which related to the UCS test machine.

5.4 RESULTS AND DISCUSSION

5.4.1 TESTING CASE 01

Small lab model for solidification of Mikawa sand with 2 cm height using ureolytic bacteria

The weight of 750 g of Mikawa sand used for the model test. The height of the sample is 2 cm. 1.0 g x 3 of bacteria were used for each 100 mL x 3 culture solution. Every 24 hours interval, 0.5 M consolidation solution were injected. After 14 days of the curing period, completed solidified samples were obtained. pH value and Ca^{2+} concentration of the outlet solution were measured after every three days.

Needle penetration test (NPT) was conducted at several areas marked as in Figs. 5.7 (b) and 5.7 (c), every points with 2 cm in width and 2 cm in length. NPT was conducted in the top and bottom of the sample for obtained strength of the solidified sample. From the results of NPT test, the box sample seems to be solidified almost uniformly.

(a)

(b)

(c)

Fig. 5.7: (a) Solidified sample of with 2 cm height (Mikawa sand), (b) selected areas which conducted NPT at the top of the sample and (c) selected area which conducted NPT at the bottom of the sample.

Estimated UCS value of the sample

The estimated UCS value of each area was shown in Figure 5.8. The average strengths are 3.6 MPa, 2.2 MPa, 2.9 MPa, 3.3MPa and 3.4 MPa at the areas of 1, 2, 3, 4 and 5 respectively. Moreover, it is identified that the estimated UCS value was larger at the locations which were near to the outlet point. The reason for that may be the bacterial population and Ca^{2+} concentration can be larger than other area.

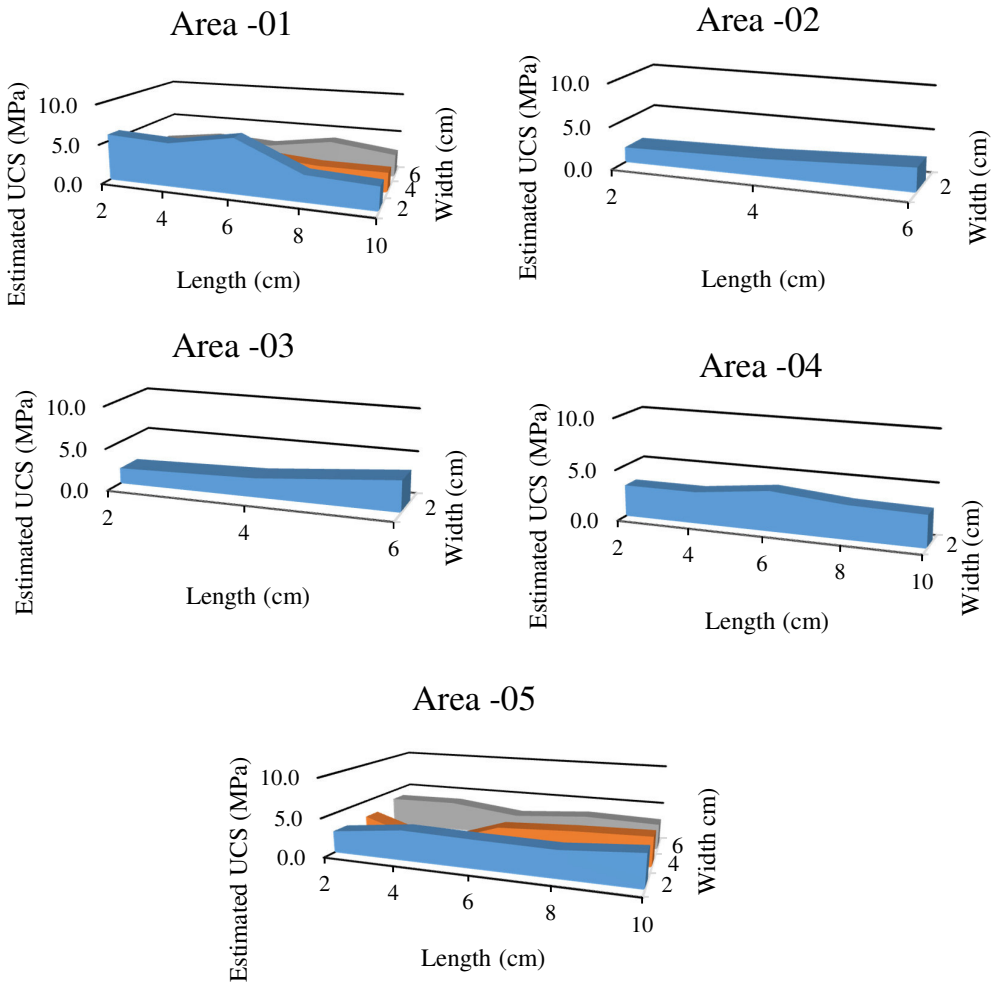

Fig. 5.8: Estimated UCS of the solidified sample at selected areas in top and bottom of the sample.

pH and Ca^{2+} concentration with the time

Figure 5.9 shows the pH value and Ca^{2+} concentration of outlet solution. pH value was between 7.0 and 8.0. Ca^{2+} concentration was lower than 1000 mg/L. The pH value and Ca^{2+} concentration in the inlet solution was 6.85 and 25000 mg/L respectively. When comparing pH value and Ca^{2+} concentration in inlet and outlet solutions, it is clearly identified that the hydrolysis process may be highly activated

due to the presence of bacteria and it means the pH value getting increase. In addition, the $CaCO_3$ precipitation also accelerated which can notified that the Ca^{2+} concentration was very low in the outlet solution when compare with inlet solution.

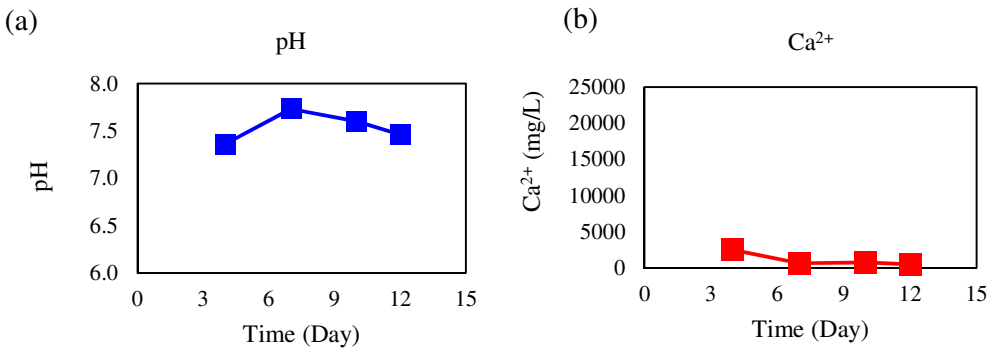

Fig. 5.9: (a) Changing pH value with time and (b) Ca^{2+} concentration of the outlet solution of the Testing Case 01.

5.4.2 TESTING CASE 02

Lab model for solidification of Mikawa sand with 9 cm height using ureolytic bacteria

In this testing case, the sample height was 9 cm. Therefore, bacterial solution was increased compare to the testing case 01. Sample photo was taken every day for observation of the color changes of the sample, and it was clearly identified that the sample color changed to whitish color compared to the 1st day of the sample and with time the color changed to whitish color. It was an evidence for the precipitation of $CaCO_3$. However, there were 20 points that were marked in the box and measure the color by using a colorimeter with time. And also, the pH value and Ca^{2+} concentration in the outlet solution were measured.

pH and Ca^{2+} concentration with the time

In this experiment, bacterial solution was added at the initial stage of the test. The test was conducted for 14 days of curing period. With time, pH value was decreased. The reason for this matter is bacterial population was decreased with time and it caused to reduce the hydrolysis process. Therefore, $CaCO_3$ precipitation also become low with time. Due to low precipitation of $CaCO_3$, the Ca^{2+} concentration in the outlet solution was getting increased.

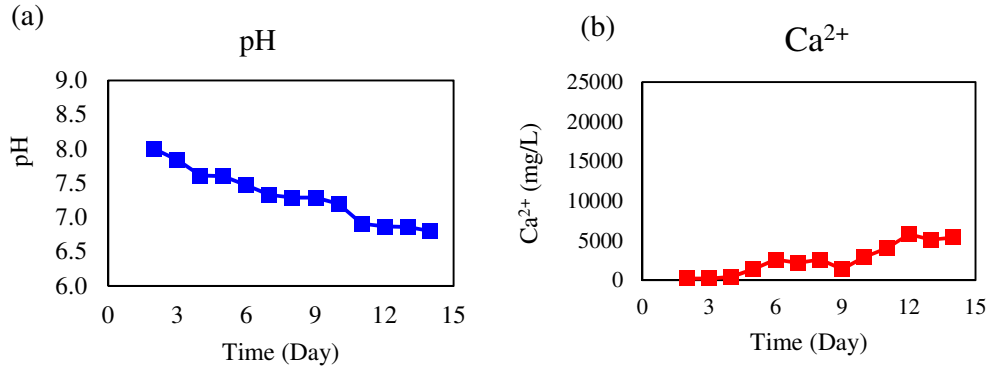

Fig. 5.10: (a) Changing pH value with the time and (b) Ca^{2+} concentration of the outlet solution of the Testing Case 02.

Color observation with the time

Color measured by visually through the experiment conducted. The color changed to whitish color than the first day of the test started. The following Figs. 5.11 (a) to 5.11 (c) show the change of color of the sample very clearly. Not only that, the color was measured at 20 points of the sample with time by using a colorimeter. The results of color were shown, the color of each point was getting whitish color with time. However, the value of color was obtained with the plastic container box. It is assumed that there is no restriction for measuring the color of the sample.

(a)

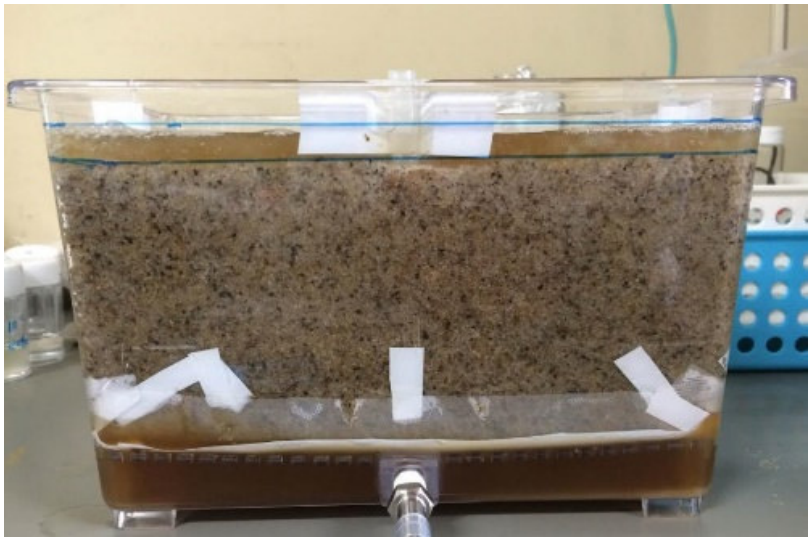

Day 01

(b)

Day 07

(c)

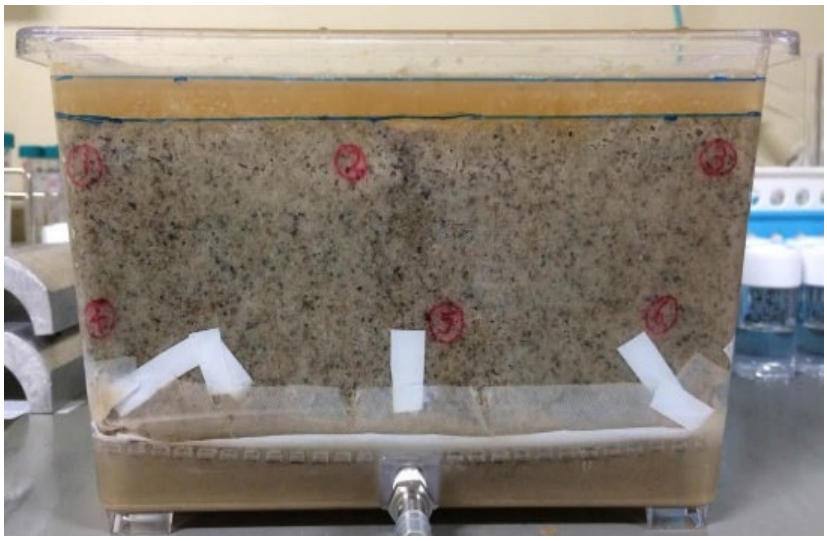

Day 14

Fig. 5.11: Lab model sample photos with different curing period when the testing was conducted; (a) after 01 days, (b) after 07 days and (c) after 14 days.

Using a colorimeter, color measurement was obtained at 4 phases of the sample box as shown in Figure 5.12. The measurement was taken, 2 cm from the top level of the sand layer and 2 cm from the bottom level of the sample. Four measurements were taken at each point and got the average value for the results of color. With time, mostly at each point, the color (ΔL^*) was increased.

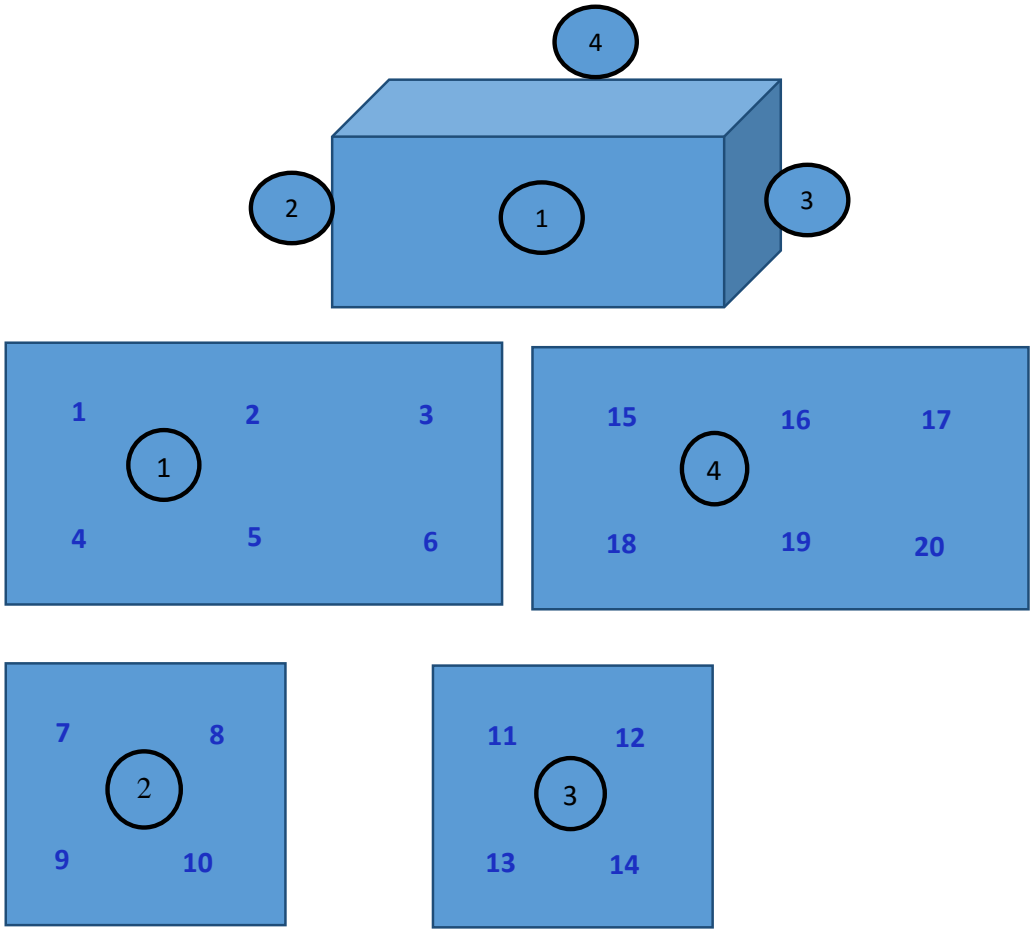

Fig. 5.12: Measurement point of the color using a colorimeter.

Figs. 13 (a) and 13 (b) show the results of color at each point (20 points as marked in Fig. 5.12). The color measurement of the Day 01 was the reference value and the color was measured at every day with respect to the first day value. Then calculate the ΔL* value with respect to the first day value. X-axis has marked the measuring points of the sample (1-20). And Y-axis has indicated the value of color with respect to the value of color in starting day of the experiment (ΔL*). Fig. 5.13 (a) shows the measurements of color at day 01, 06, 08, 09, 11, 12 and 14. In addition, to get a clear idea about the measurements of color, it was summarized for 3 days of testing (Day 01, 06 and 14) in Fig. 5.13 (b).

(a)

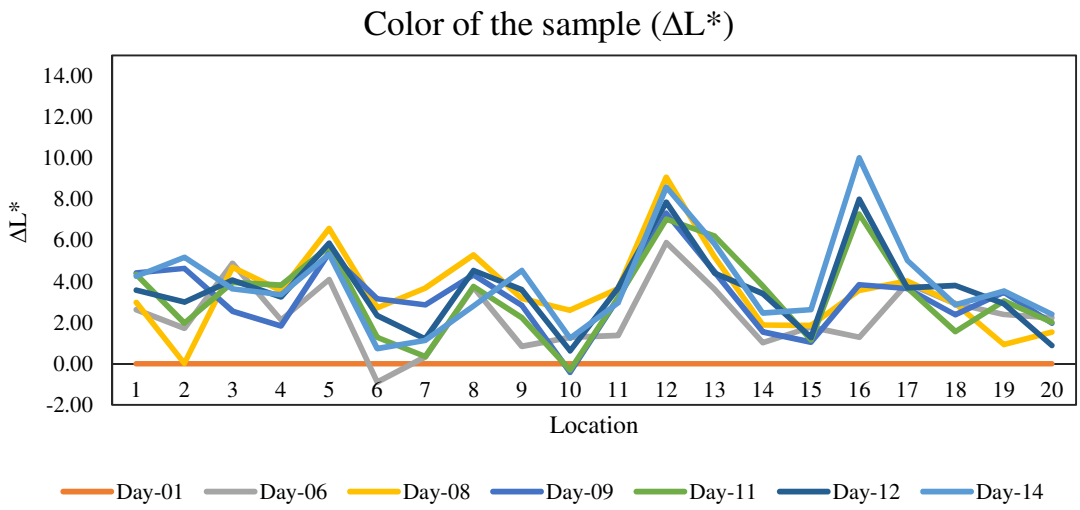

(b)

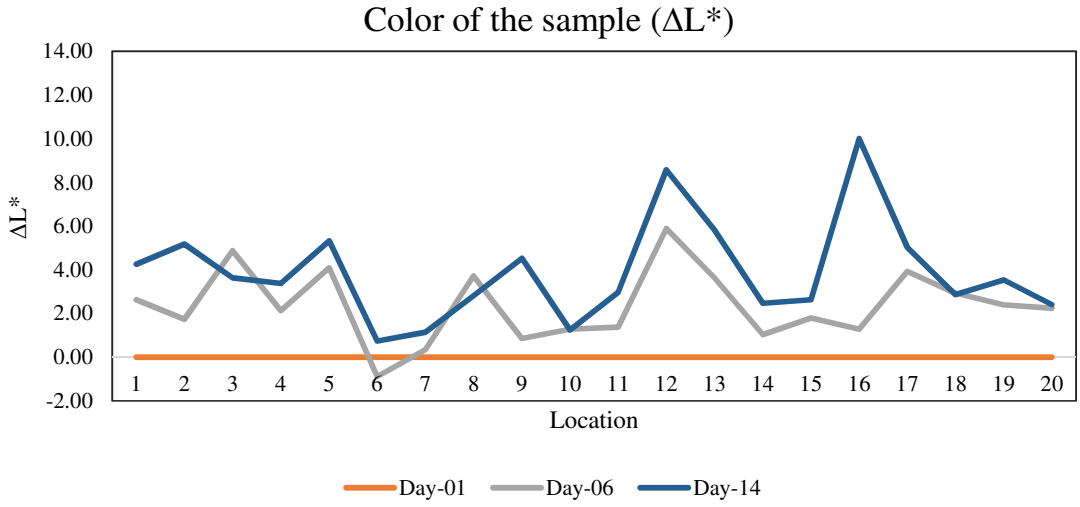

Fig. 5.13: Results of color of the 20 points of the samples; (a) The results of color for 7 days of testing period and (b) Summarized results of color for 3 days of testing period.

Nevertheless, the average value of the points in the top and bottom for each sides were calculated (For example: If considering phase (1) in the Fig. 5.12, the average value of color (ΔL*) at the top was calculated by using the results of 1, 2 and 3 points and the average value of color at the bottom was measured by averaging the results of 4, 5 and 6. The results are shown in Fig. 5.14. For getting a clear observation of color measurement, further investigation is needed.

After 14 days of the curing period, the sample box was opened and fully solidified sample was obtained (Fig. 5.16). Then the sample was cored for obtaining cylindrical samples. Four horizontally cored samples and seven vertically cored samples were obtained after coring the box sample (Fig. 5.15). From the cored samples, 6 samples (2 horizontally cored and 4 vertically cored samples) were used for conducting UCS test to get the direct value for UCS, primary and secondary wave velocities (Vp and Vs), color and density of the sample. In addition, remained 5 samples were used to conduct needle penetration test for obtaining the estimated UCS values of the sample. To identify the strength of the samples at different depth, NPT was conducted at 3 points of the sample. (Top, middle and bottom). It could not be obtained this observation by using UCS test because it gives an average value of the sample.

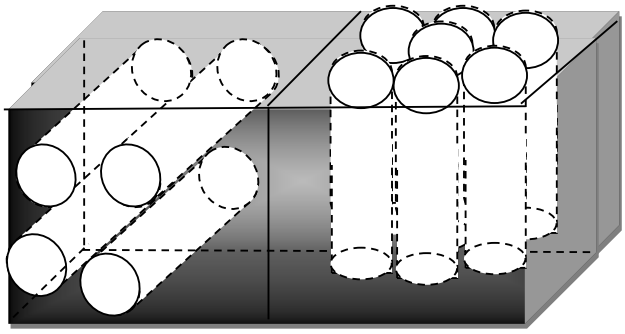

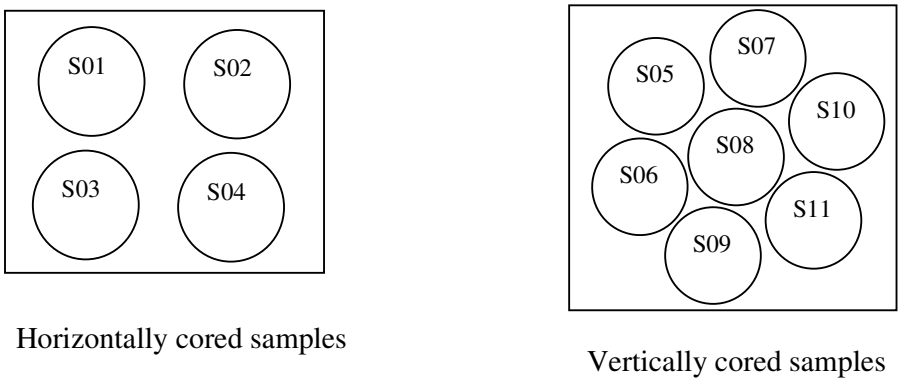

Horizontally cored samples

Vertically cored samples

5.15: Locations of vertically and horizontally cored samples.

Fig. 5.16: Completely solidified sample photos after open the sample box.

Results of Vp and Vs

Primary waves (P-waves) are compressional waves that are longitudinal in nature. P waves are pressure waves that travel faster than other waves through the earth to arrive at seismograph stations firstly, hence the name "Primary". These waves can travel through any type of material, including fluids, and can travel at nearly twice the speed of S waves. In the air, they take the form of sound waves, hence, they travel at the speed of sound. Typical speeds are 330 m/s in air, 1450 m/s in water and about 5000 m/s in granite.

Secondary waves (S-waves) are shear waves that are transverse in nature. Following an earthquake event, S-waves arrive at seismograph stations after the faster-moving P-waves and displace the ground perpendicular to the direction of propagation. Depending on the preoperational direction, the wave can take on different surface characteristics; for example, in the case of horizontally polarized S-waves, the ground moves alternately to one side and then the other. S-waves can travel only through solids as fluids (liquids and gasses) do not support shear stresses. S-waves are slower than P-waves, and their speeds are typically around 60% of that of P-waves in any given material.

From this results of Fig. 5.17, Vs varied within 1000 – 1500 m/S and Vp values varied within 1500-2600 m/S. Further examination is needed for getting a worthy relationship with UCS and Vp or Vs.

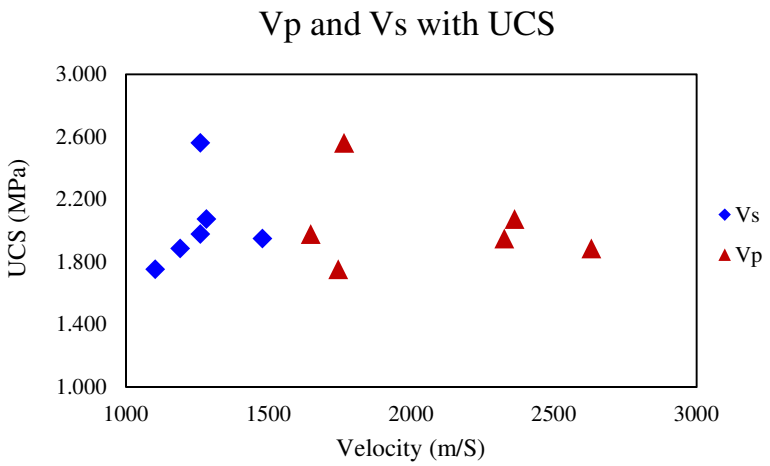

Fig. 5.17: Relationship between Vp, Vs, and UCS of the core samples.

Color with UCS

The color was measured at three points of the cored sample: top, middle and bottom. Then for obtaining the relationship with UCS value, the average value of color of the sample was calculated. The UCS value was increased with the increase of color (L*). However, for this cored samples, the initial color (L_i*) value could not able to measure. Therefore, here only L* value was measured, not ΔL^* ($L_i^* - L^*$) value.

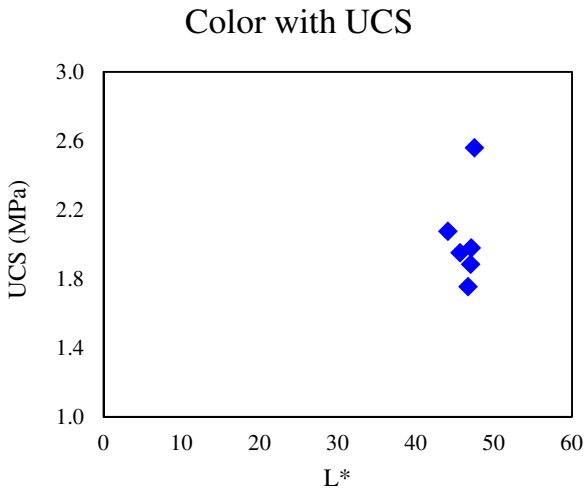

Fig. 5.18: Relationship between UCS and color of the sample.

Density with UCS

This Fig. 5.19 indicates that the UCS value increases when the density of the sample increases. It was obviously imagined, when $CaCO_3$ precipitation occurs, the voids of the sample decreased with time. Therefore the density of the sample increased. If the wet density of the sample shows high means, the $CaCO_3$ precipitation was high. That means the strength of the sample was large. Therefore, UCS value was increased with the increase of density of the sample.

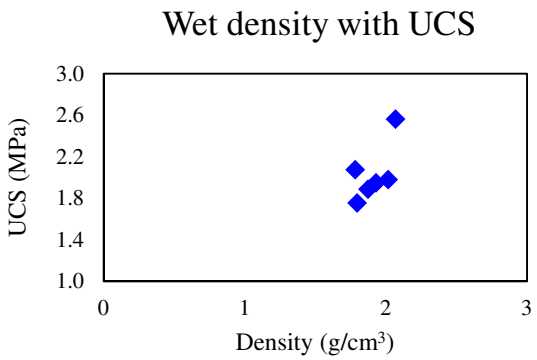

Fig. 5.19: relationship with UCS and wet density of the sample.

Estimated UCS results

Five cored samples (S01, S05, S06, S10, and S11 as shown in Fig.5.15) were used for conducted NPT. For all samples, the strength decreased with the depth of the sample as shown in Fig. 5.20. The estimated UCS value at the top of the sample was larger than the estimated UCS value at the bottom of the sample with except to the Sample 10. Moreover, the estimated UCS value of the samples was vary from 10 MPa to 3 MPa. Therefore, I could not obtain uniformly solidified sample. The aim of this study was obtained uniformly solidified sample.

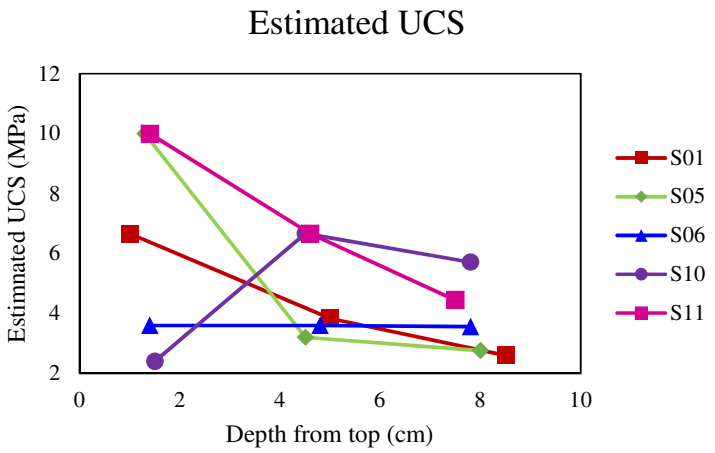

Fig. 5.20: Relationship between estimated UCS value and depth of the sample.

High vacuum SEM images of cored samples

Formation of MICP was examined by high vacuum scanning electron microscopy (SEM). SEM observation was conducted for 2 samples, which was obtained from the top and bottom of the sample. The SEM images show that the calcite crystals were mainly irregular bulk, similar to the observation made by Qabany et al. (2012).

(a)

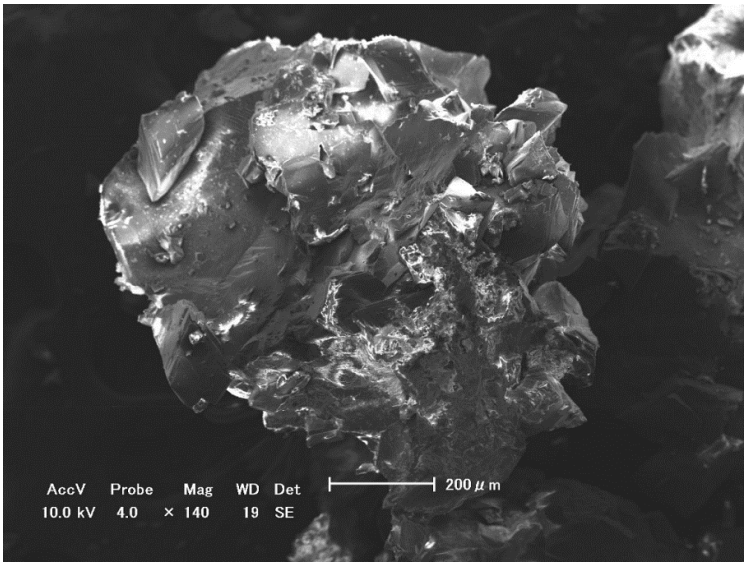

(b)

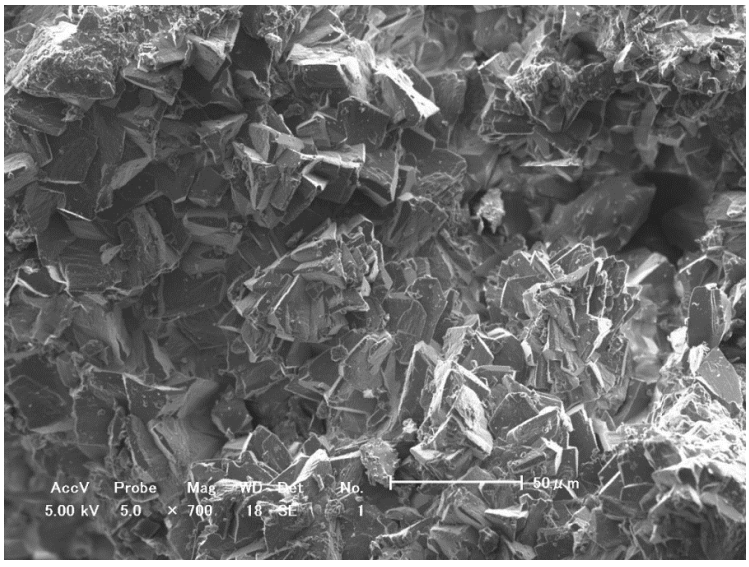

Fig. 2.21: SEM images for solidified model sample: (a) low magnification (x 140) and (b) high magnification (x 700).

EDX results

Two samples were conducted for EDX analysis using an X-ray analyzer for identifying the chemical composition of the sample. The results of EDX analysis demonstrated that the dominant minerals were SiO_2 and $CaCO_3$, and Ca, O and C were the main elements in the mineral precipitations (Fig. 5.22 and Fig. 5.23). Previous studies by Passan (2009) and Qabany et al. (2012) reported that the crystals observed were actually calcite precipitated in the silica sand.

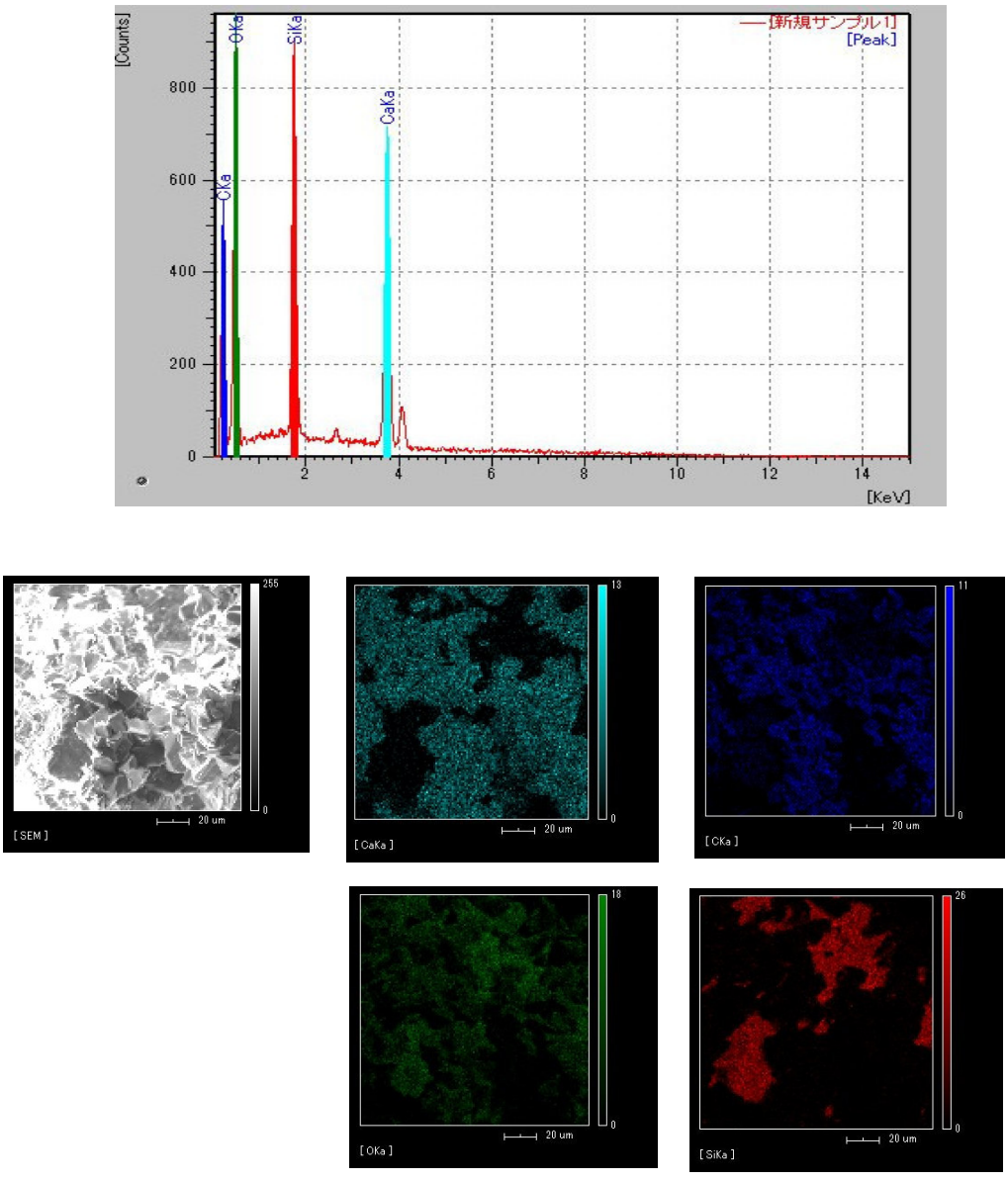

Fig. 5.22: EDX analysis for sample S06.

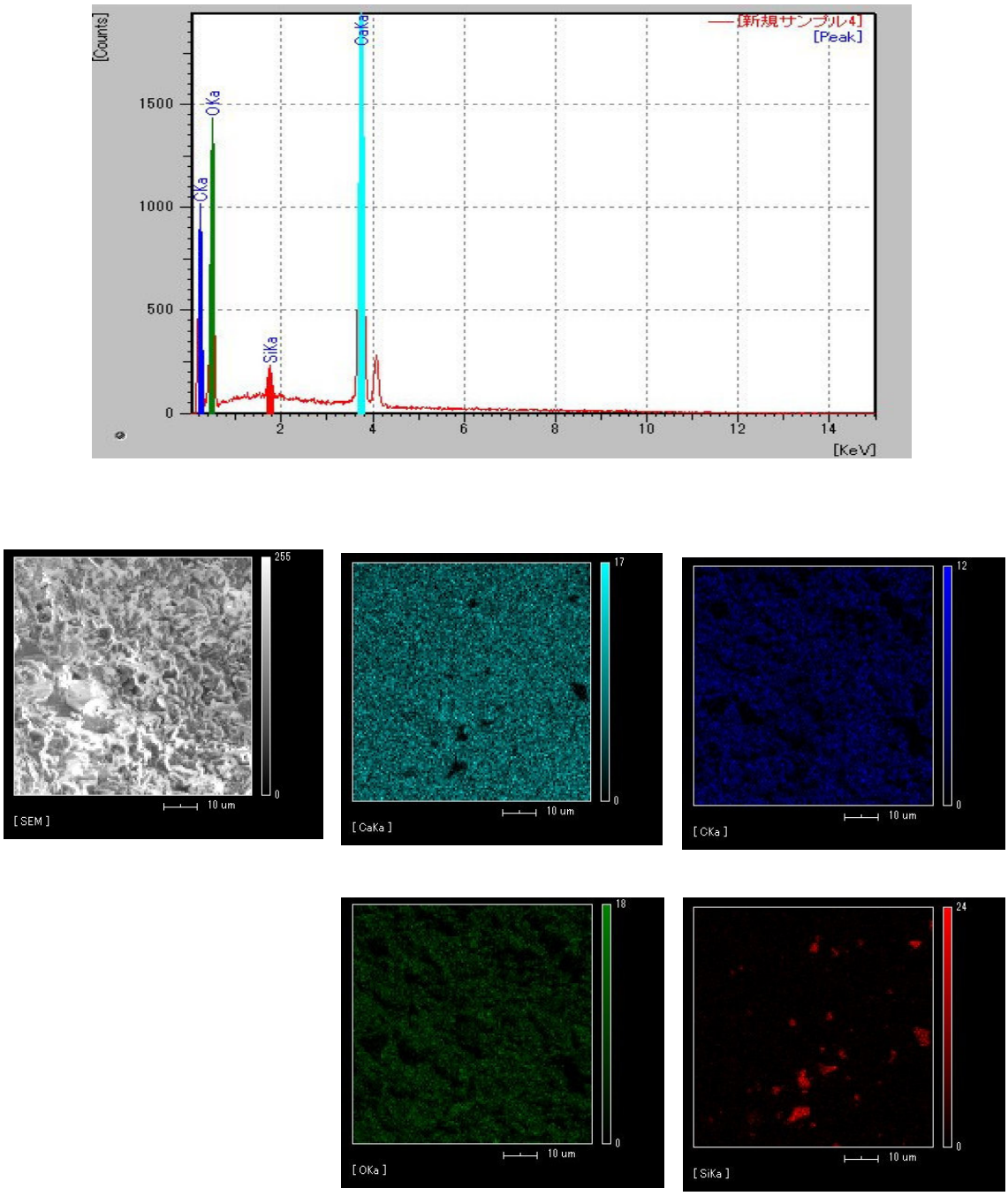

Fig. 5.23: EDX analysis for sample S11.

Results of XRD observation

Cylindrical cored samples were grinded by using ball mill machine and powder samples were obtained after ball milling. That sample was used for the XRD observation. Powder samples were obtained at the top and bottom of the cylindrical cored sample for getting a quantitatively value for the calcite precipitation. After XRD experiment, the results were analyzed by using "Match!" software. The results of XRD observation are shown in Figs. 5.24 (a) and 5.24 (b). The results indicate that the calcite precipitation was larger at the top of the sample than bottom of the sample. From the Fig. 5.24 (a), the sample contained with 86.3% of SiO_2 and 13.7% of $CaCO_3$. Furthermore, 90.3% of SiO2 and 9.7% of CaCO3 consisted with bottom sample (Fig. 5.24 (b)).

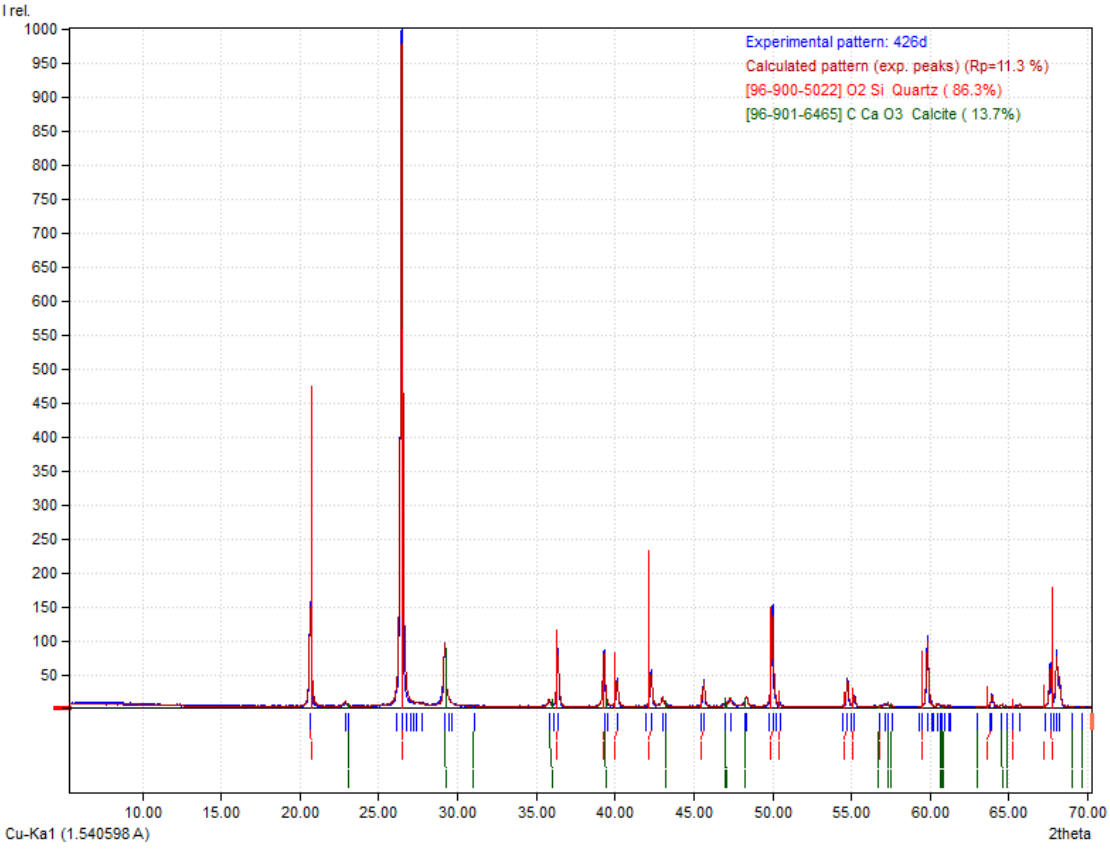

Fig. 5.24 (a): XRD results for the top of the sample.

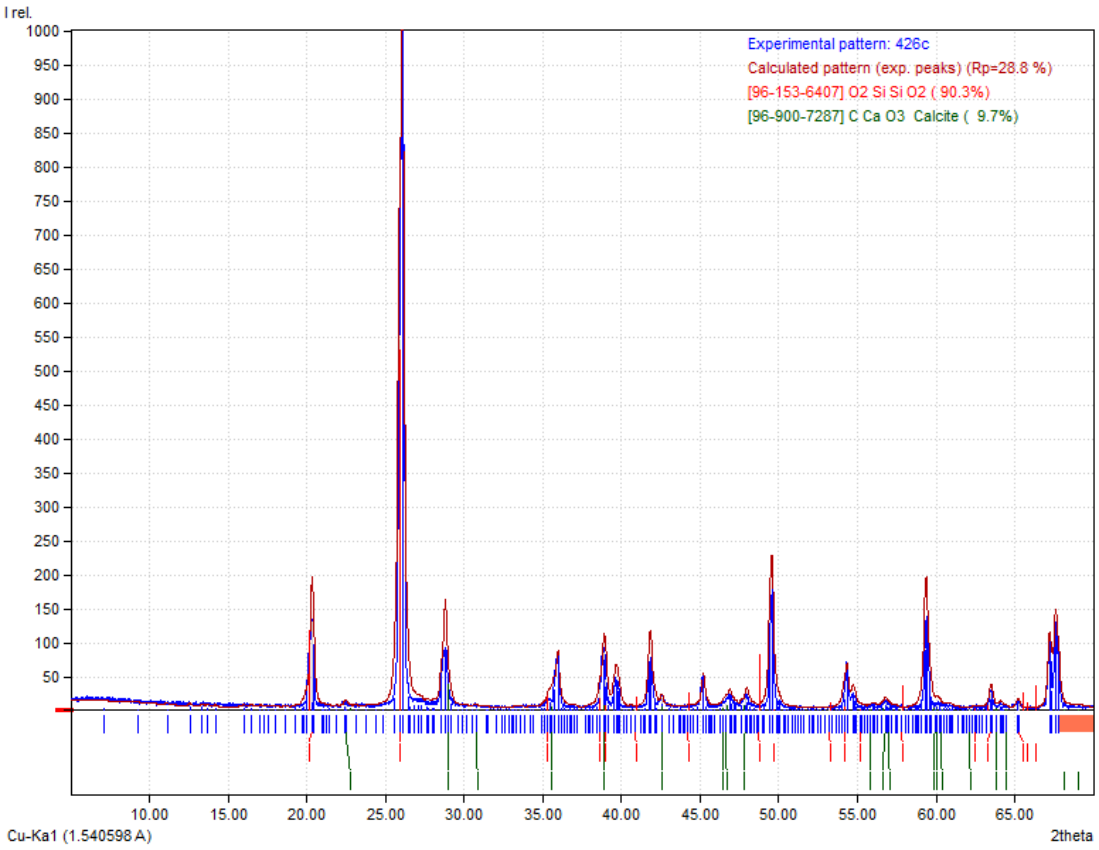

Fig. 5.24 (a): XRD results for the bottom of the sample.

5.4.3 TESTING CASE 03

Lab model for solidification of Mizunami sand with 9 cm height using ureolytic bacteria

In this experiment, the sand material was changed. In previous, Mikawa sand with 0.6 mm diameter sand was used. Here the particle size of the sand material was increased. Therefore, Mizunami sand with 1.3 mm diameter was used for this experiment. The testing method was similar to the previous methods and the testing was conducted for 14 days of the curing period. After finished the experiment, tried to core the sample using a rock coring machine. However, the coring was failed with this sample. Due to the particle size of this sample, it very difficult to obtaining cylindrical samples. Namely, the core sampler was rotating at the same place but it did not go through the sample.

Therefore, UCS could not conduct for this sample and needle penetration test was

conducted for obtaining the estimated UCS value. Color, pH and Ca^{2+} concentration were measured as same as the previous methods. pH value decreased with time, on the other hand, Ca^{2+} concentration of the outlet solution increased with the time as same as the previous testing cases.

Color of the sample

The color change of the sample was clearly observed by visually for Mizunami sand sample. The sample color changed from gray to whitish color with time (Fig. 5. 25).

(a)

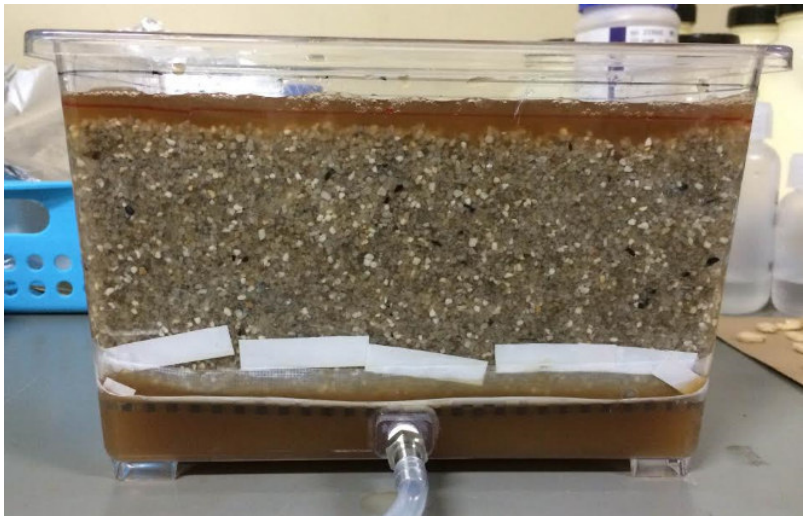

Day 01

(b)

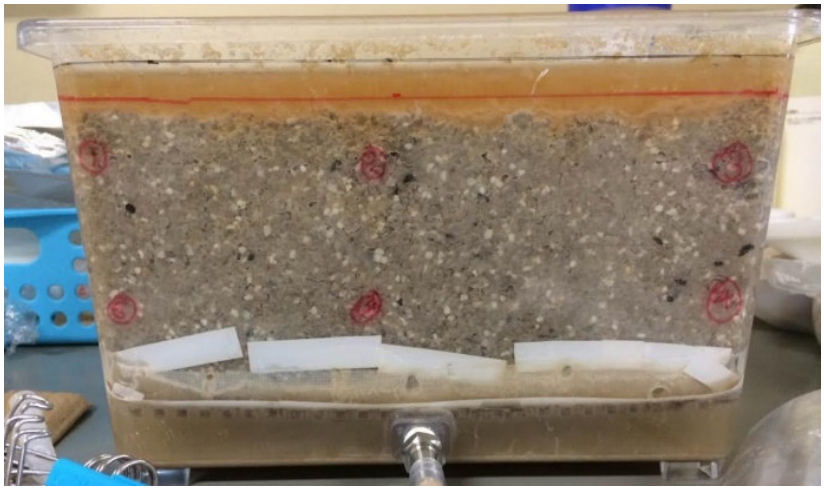

Day 07

(c)

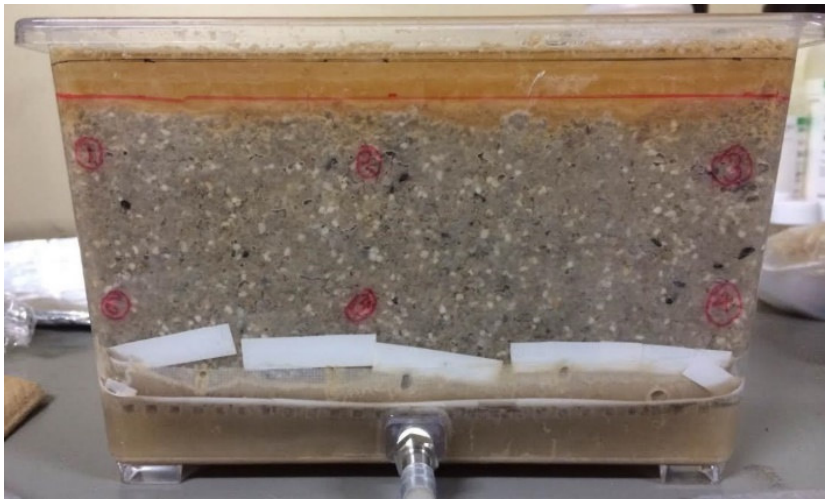

Day 14

Fig. 5.25: Mizunami sand lab model sample photos with different curing period when the testing was conducted; (a) after 01 days, (b) after 07 days and (c) after 14 days.

Figs. 5.26 (a) and 5.26 (b) show the results of color at each point (20 points as marked in Fig. 5.12). The color measurement of the Day 01 was the reference value and the color was measured at every day with respect to the first day value. Then the ΔL* value with respect to the first day value was calculated. In the graph, X-axis has marked the measuring points of the sample (1-20). And Y-axis has indicated the value of color with respect to the value of color in starting day of the experiment (ΔL*) at each points. Fig. 5.26 (a) shows the measurement of color at day 01, 06, 08, 09, 11, 12 and 14. In addition, to get a clear indication about the measurement of color, it was summarized for 3 days of testing (day 01, 06 and 14). When considering Fig. 5.26 (b), The color was increased at each and every point with the time.

(a)

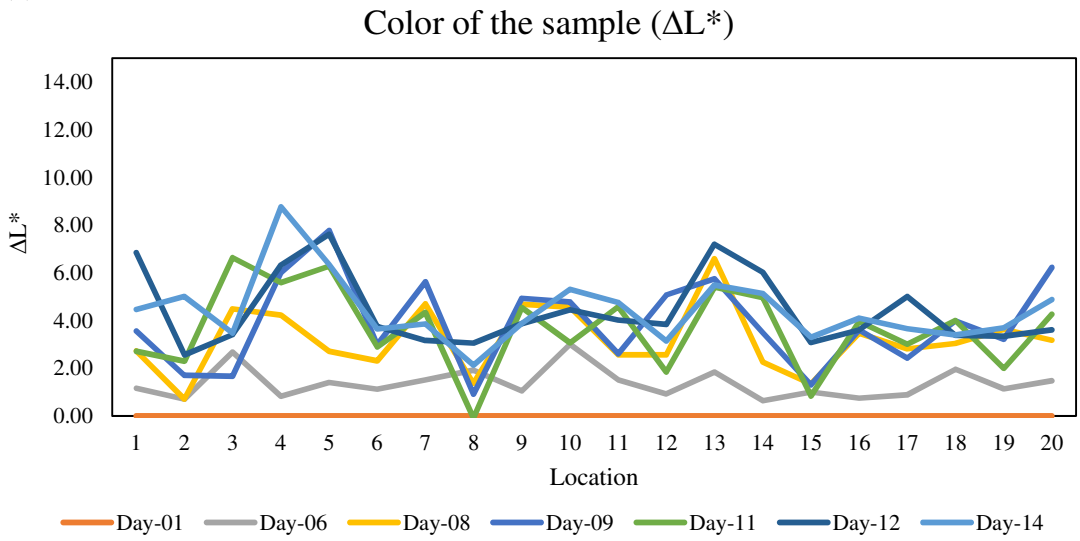

(b)

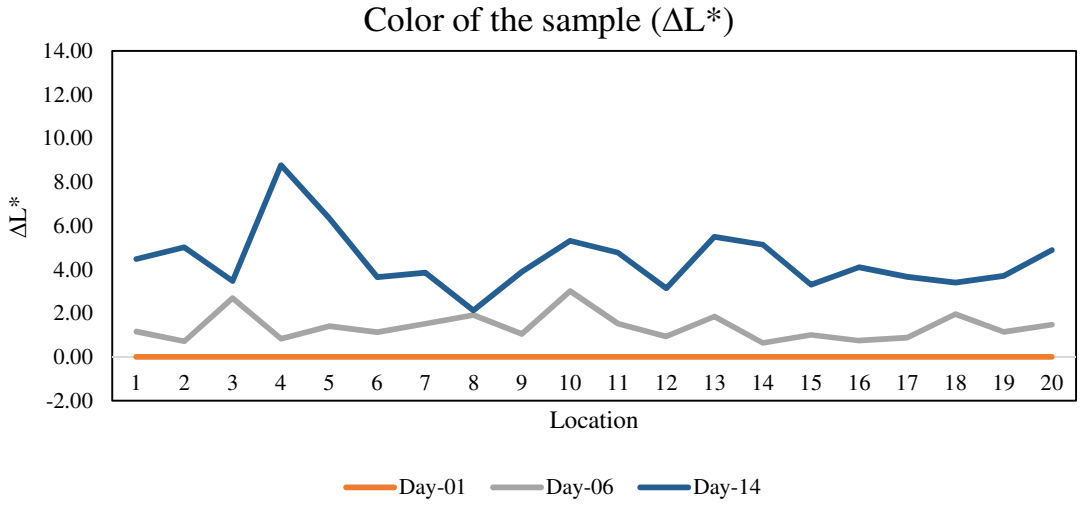

Fig. 5.26: Results of color of the 20 points of the samples; (a) the results of color for 7 days of testing period and (b) summarized results of color for 3 days of testing period.

In addition, the average value of the points in the top and bottom for each sides were calculated (For example: If considering phase (1) in the Fig. 5.12, the average value of color (ΔL*) at the top was calculated by using the results of 1, 2 and 3 points and the average value of color at the bottom was measured by averaging the results of 4, 5 and 6. The results are shown in Fig. 5.27. For getting a clear observation of color measurement, further investigation is needed.

Estimated UCS value

As mentioned above, coring was failed for this sample. It may happen due to the particle size of this sand was larger than Mikawa sand. Therefore, the core sampler was rotated at the same location and not penetrated into the solidified sample. Therefore, NPT was conducted for measure the estimated UCS value. The results show that the average estimated UCS of the sample was 4.4 MPa. According to the Fig. 5.28, the estimated UCS value at the top of the sample was unevenly distributed. The reason for this problem may be that calcite precipitation at some area was high due to poor penetration through the sand and it may cause high precipitation of calcite in the top.

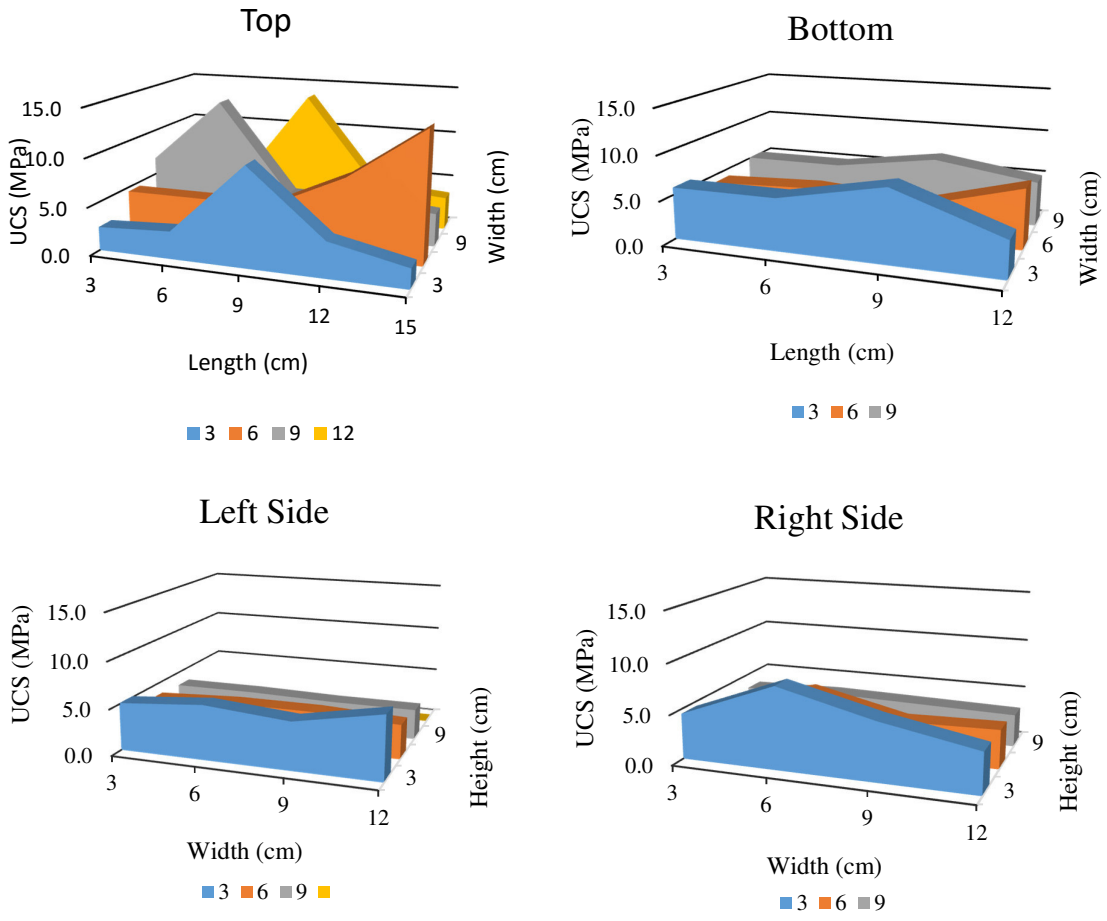

Fig. 5.28: Estimated UCS of the solidified sample at the top, bottom and two other sides of the sample.

Color with Estimated UCS

The color was measured by colorimeter at each point where the NPT were conducted. Figure 5.29 shows the results of estimated UCS and color of the sample. The color of the sample increased with increase of estimated UCS. Therefore, there was a close relationship between color and estimated UCS value. From the results, following equation can be derived. Eq. (5.1). This equation only valid for Mizunami sand sample.

$$q_{eu} = 0.7669\, L^* - 33.921 \qquad \text{Eq. (5.1)}$$

Where; q_{eu}= Estimated UCS (MPa)

L^* = Color (L*)

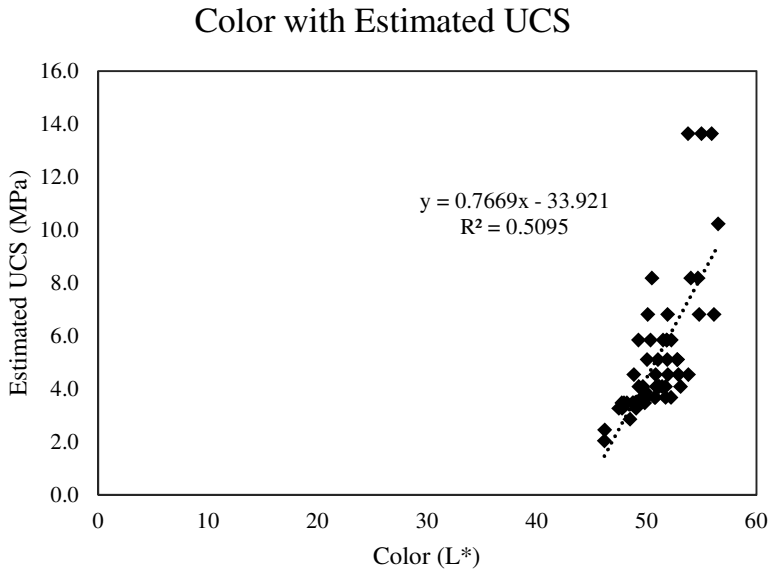

Fig. 5.29: Relationship between estimated UCS and color of the Mizunami sand sample.

Results of XRD observation

Fig. 5.30 shows the results of XRD analysis of the powder sample which was selected at the top of the solidified sample. From the results, the sample consisted with SiO_2 79.2 % and $CaCO_3$ 20.8%.

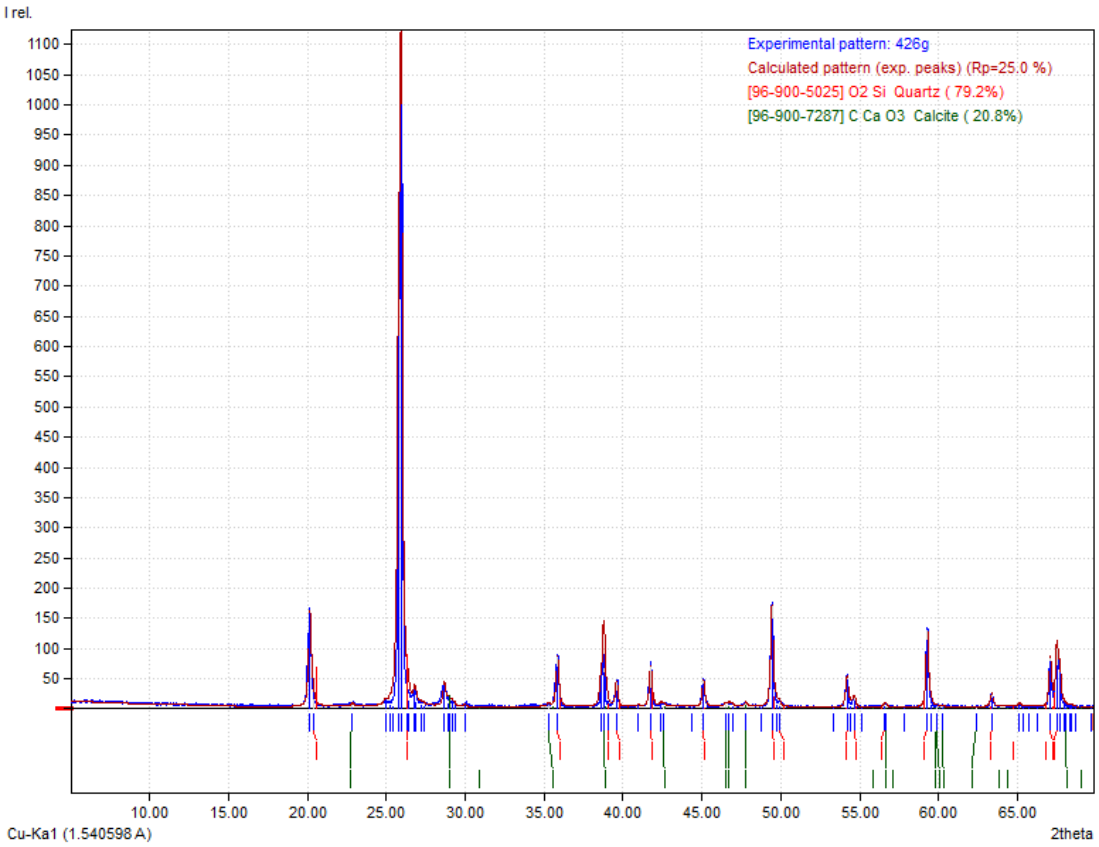

Fig. 5.30: XRD results for the top of the sample.

5.4.4 Testing case 04

Lab model for solidification of Mikawa sand with 9 cm height using ureolytic bacteria and re-injection of bacteria after 7 days

The results of the previous methods, it is failed to obtain uniformly solidified samples. In all cases, the strength of the sample was high at the top of the sample and the strength decreased with the depth of the sample. To get uniformly solidify sample, this case was modified. In this experiment, Mikawa sand sample with the same diameter (0.6 mm) was

used. The bacterial solution was re-injected after 7 days and the curing period was maintained until 21 days.

(a)

Day 01

(b)

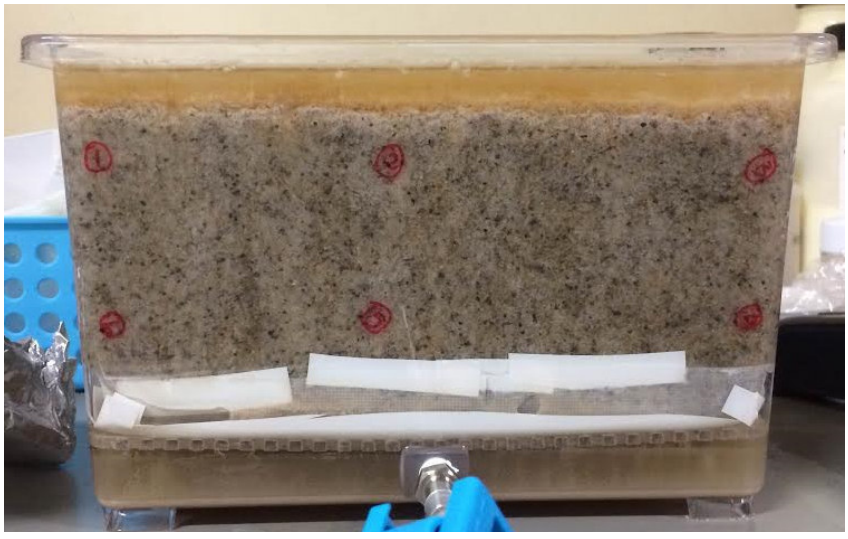

Day 07

(c)

Day 14

(d)

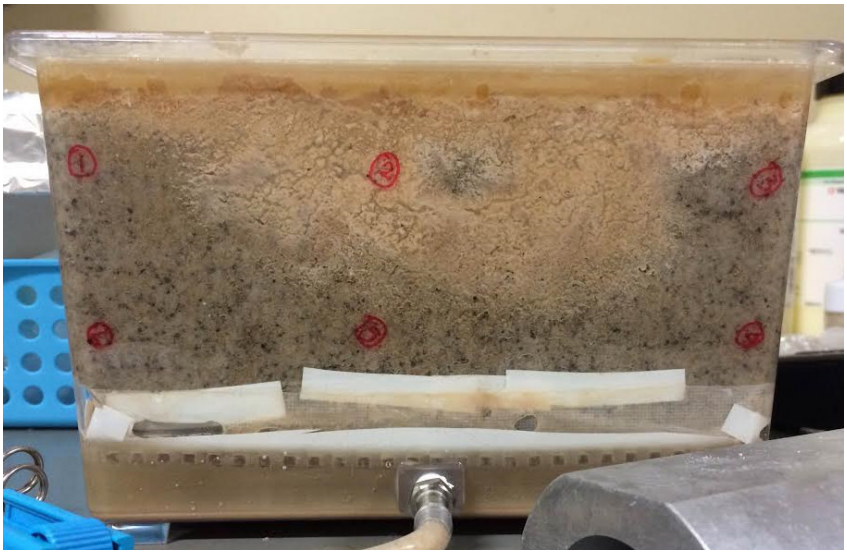

Day 21

Fig. 5.31: Mikawa sand lab model sample photos with different curing period when the testing was conducted; (a) after 01 days, (b) after 07 days and (c) after 14 days and (d) after 21 days.

pH and Ca^{2+} concentration

pH value decreased with time as same as previous results, but after 7 days of the curing period, bacteria solution was re-injected. Then, pH value was again increased and maintained the value of 7. It was very important to maintain because the optimal pH value for *Pararhodobacter* sp. is 7 to 8. If the pH value maintains the value between 7 and 8, the activity of bacteria keeps high and it causes to the increase the rate of hydrolysis process and this gives finally the high $CaCO_3$ precipitation. The results of the Ca^{2+} concentration of the outlet solution s chowed the evidence for high precipitation of $CaCO_3$. In the previous results, Ca^{2+} concentration increased with time when no adding bacterial solution after 7 days (Fig. 5.32). However, in this time, the concentration of Ca^{2+} in outlet solution was small during the curing period.

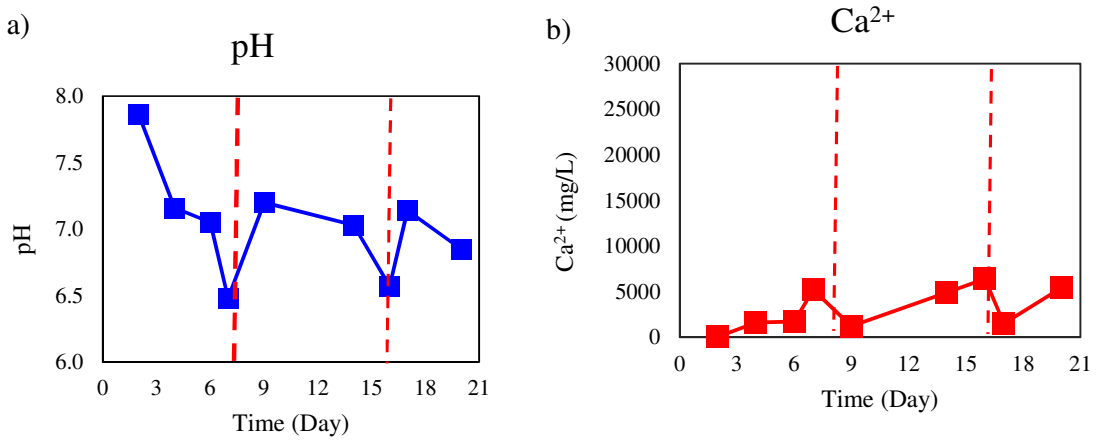

Fig. 5.32: (a) Changing pH value with the time and (b) Ca^{2+} concentration of the outlet solution of the Testing case 04.

Color of the sample

The color was measured at 20 points of the sample box. The results indicated that the sample color changed to whitish color with time at each point.

(a)

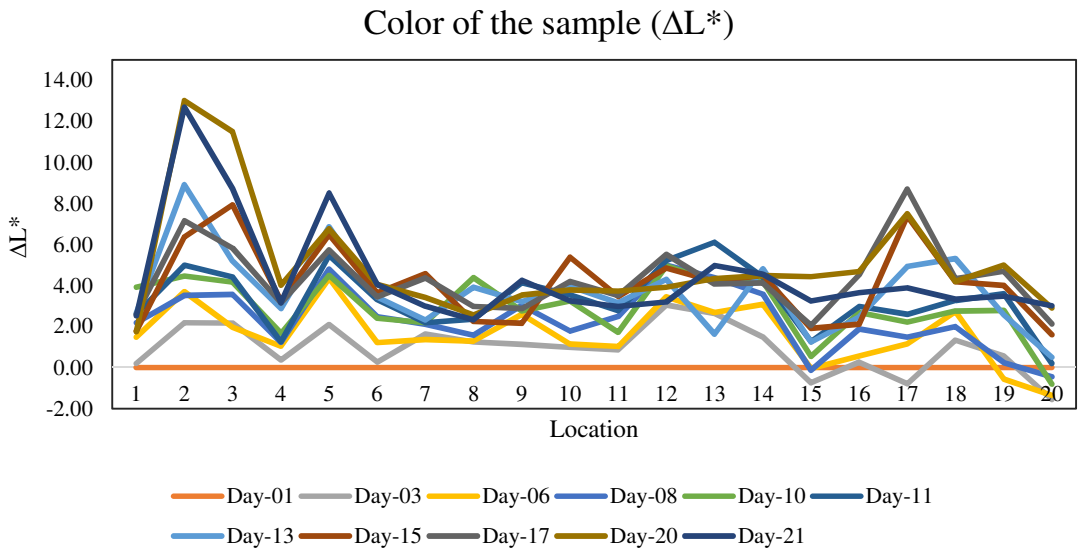

(b)

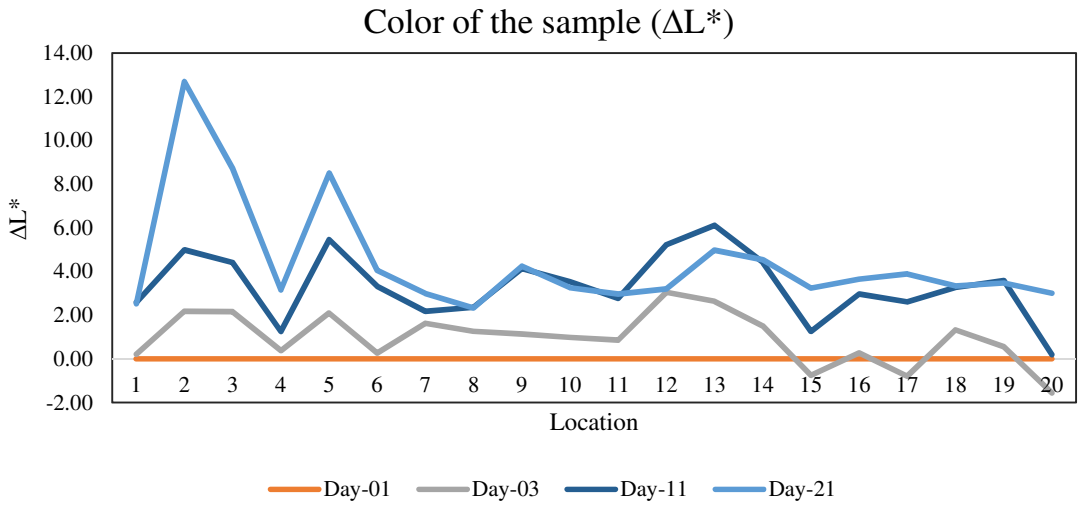

Fig. 5.33: Results of color of the 20 points of the samples; (a) The results of color for 11 days of testing period and (b) Summarized results of color for 4 days of testing period.

In addition, the average value of the points in the top and bottom for each sides were calculated (For example: If considering phase (1) in the Fig. 5.12, the average value of color (ΔL*) at the top was calculated by using the results of 1, 2 and 3 points and the average value of color at the bottom was measured by averaging the results of 4, 5 and 6. The results are shown in Fig. 5.34. Further investigation is needed in the future.

The sample was cored and vertical and horizontal cylindrical samples with the diameter of 3 cm and the height of 6 cm were obtained (as shown in Fig. 5.35). For using selected samples, UCS test, Vp and Vs measurements and wet density were observed. Other remaining samples were used for conducting NPT for obtained estimated UCS value and wet density.

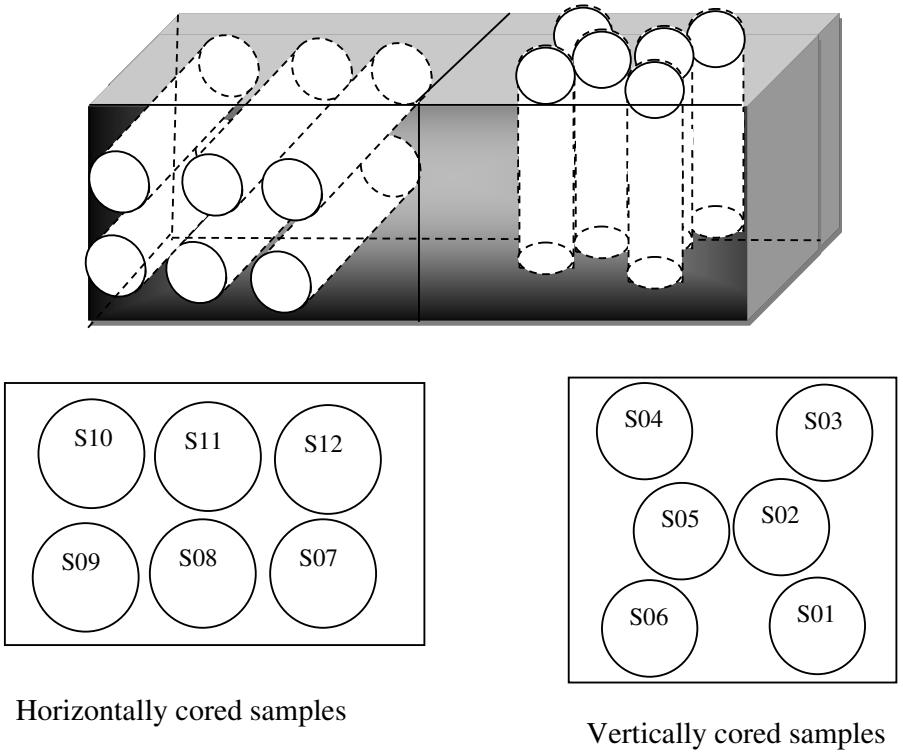

5.35: Locations of vertically and horizontally cored samples with sample numbering.

Vp and Vs with UCS

Fig. 5.36 shows that the UCS was intended to increase with the increased of Vp and Vs. In addition, Vp and Vs were measured at the solidified box sample itself before coring. It is obtained 3 measurements from the box sample by measuring 3 directions of the sample (Fig. 5.37).

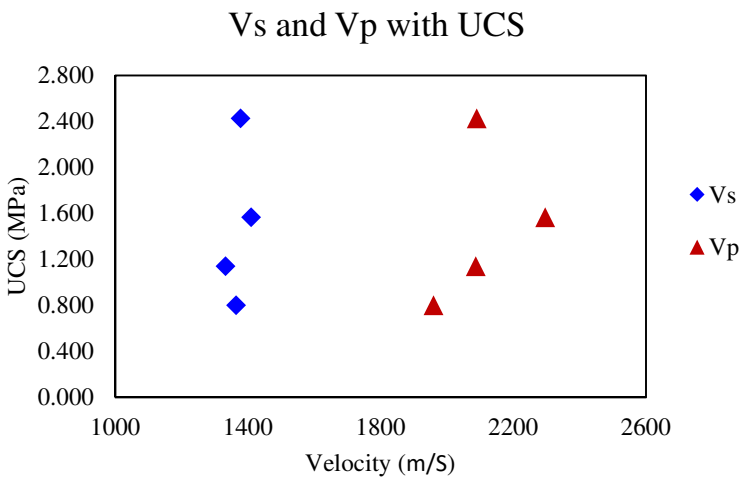

Fig. 5.36: Relationship between Vp, Vs and UCS of the solidified samples with Mizunami sand.

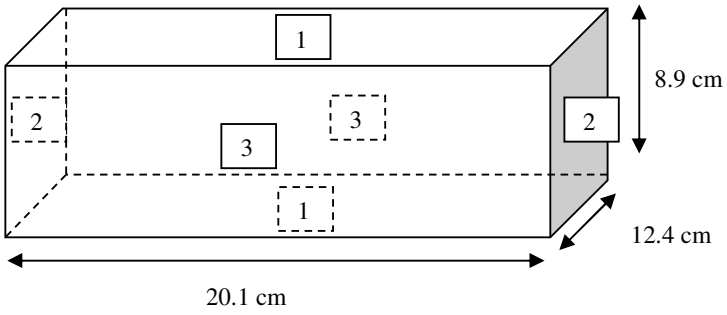

Fig. 5.37: The directions of Vp and Vs measurements obtained from the box sample.

Table 5.5: Results of Vp and Vs for box sample.

Direction	Vp (m/S)	Vs (m/S)
1 - 1	2020	1190
2 - 2	2480	1820
3 -3	2510	2050

Wet density with UCS and estimated UCS

The Fig. 5.38 shows that both UCS and estimated UCS was intended to increase with the increase of wet density.

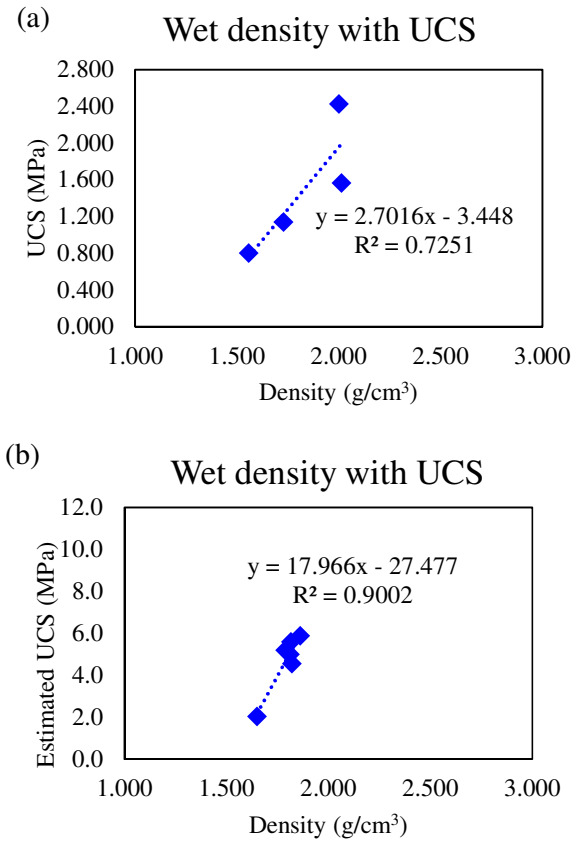

Fig. 5.38: (a) Results of UCS with wet density for UCS test samples and (b) results of estimated UCS with wet density for NPT samples.

Estimated UCS for vertically and horizontally cored samples

From the result of Fig. 5.39 (a), it described that the estimated UCS value decreased with the depth of the sample. In addition, the cored samples in Fig. 5.39 (b) were horizontally drilled samples that mean the sample was in the same depth. Therefore, the strength of the sample did not depend on the depth of those samples. The UCS values were varied because of unequally solidification. Further investigation is needed for getting a homogeneously solidified sample.

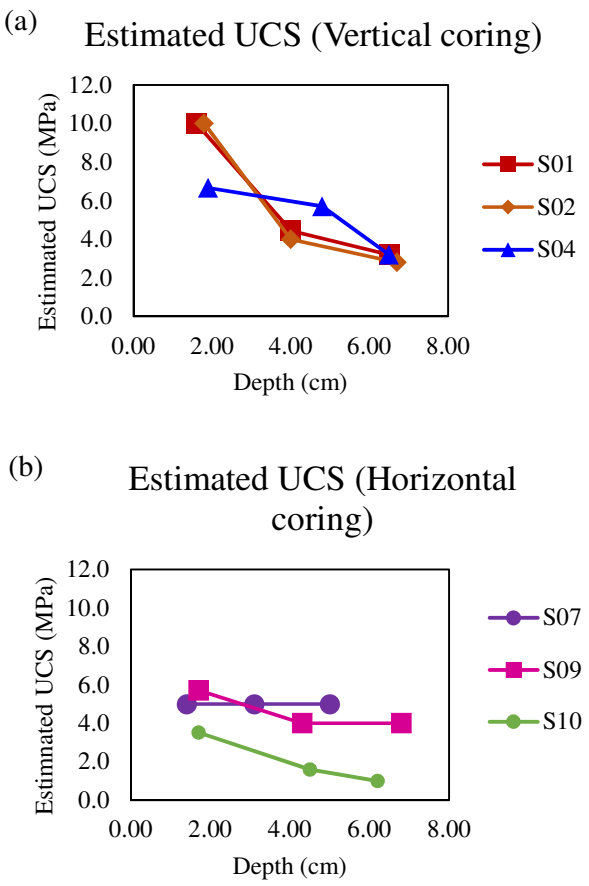

Fig. 5.39: Relationship between estimated UCS and depth of the sample for; (a) vertically cored samples and (b) horizontally cored samples.

Results of XRD observation

The results of XRD observation are shown in Fig. 5.40 and Fig. 5.41. In this study, S02 and S09 samples were used for the experiment (Fig. 5.35). Powder samples were obtained from the top and bottom of the cored sample; S02 and from the sample S09, two powder samples obtained from both edges of the sample. Fig. 5.38 shows that the calcite precipitation was larger at the top of the sample than the bottom of the sample (SiO_2 – 91.5% and $CaCO_3$ – 8.5% at the top and SiO_2 – 96.5% and $CaCO_3$ – 3.5% at the bottom). Nevertheless, calcite precipitation was not so large difference in the samples which were cored horizontally (Fig. 5.41).

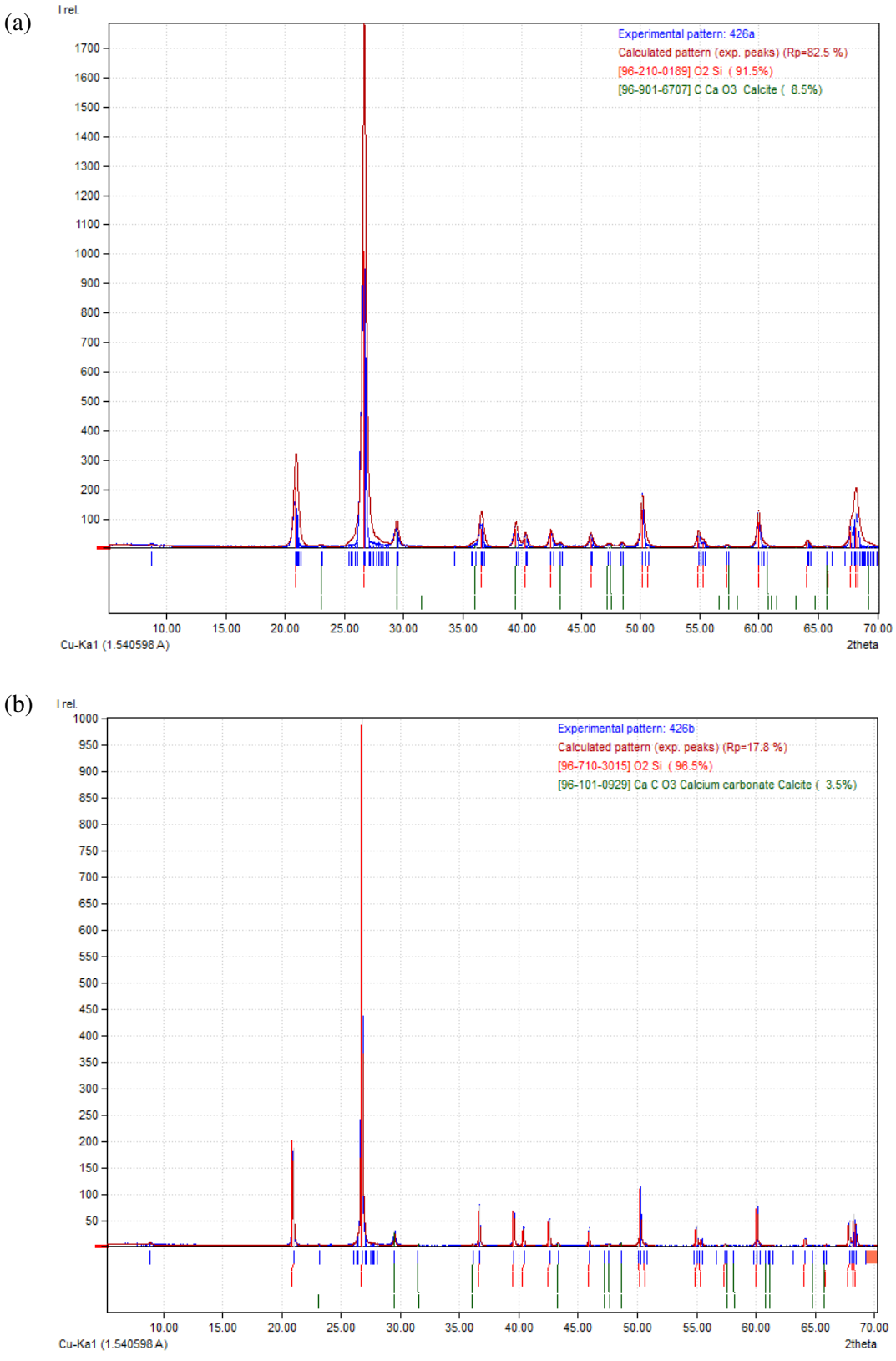

Fig. 5.40: XRD results for vertically cored sample; (a) at the top of the sample and (b) at the bottom of the sample.

(a)

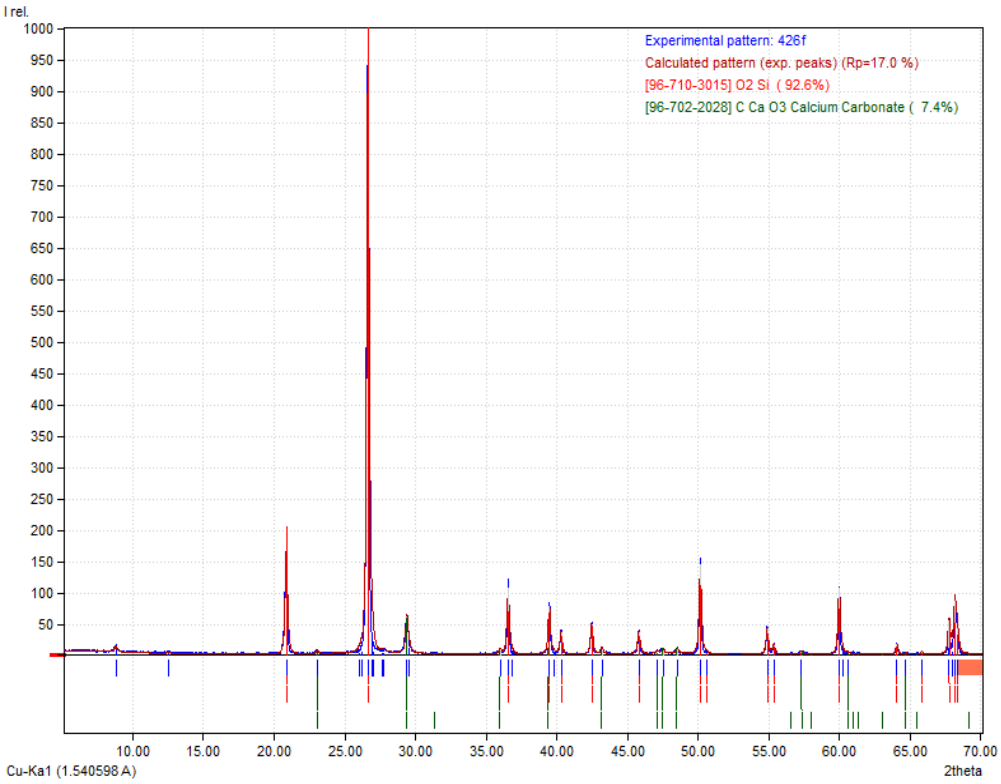

(b)

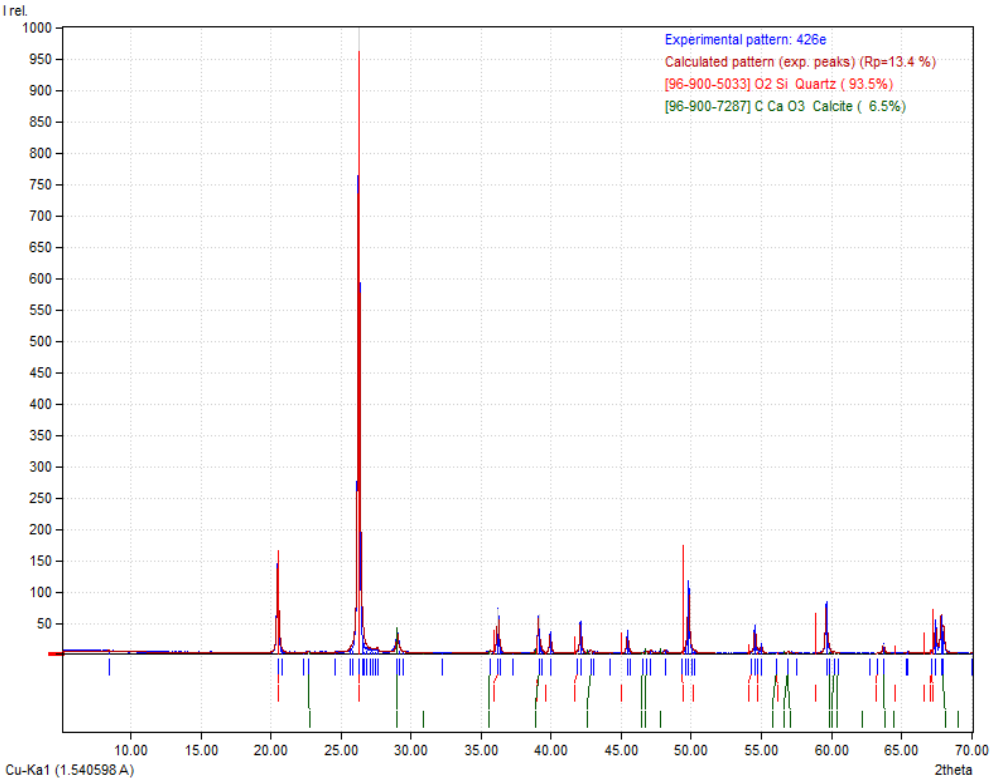

Fig. 5.41: XRD results for horizontally cored sample; (a) at the edge which is near to the outlet of the sample and (b) at the opposite edge of the sample.

5.5 DISCUSSION

5.5.1 Summary of the model test examination

In this study, four testing cases were conducted for obtaining uniformly solidified sample. Following tables (Tables 5.6, 5.7, 5.8, and 5.9) shows the summary of the model tests with results obtained.

Table 5.6: Summary of the testing Case 01.

Testing Case no:	Testing Case 01
Objectives	To identify the possibility of solidifying small scale model test and getting the several MPa of average strength from the solidified sample.
Sample Size	Width: 12.5 cm , Length: 20 cm, and Height: 2 cm
Sand type	Mikawa sand (mean diameter: 0.6 mm)
Curing Time	14 Days
Results obtained	• Obtained uniformly solidified sample after 14 days of curing period. • The average UCS of the sample is about 3 MPa.

Table 5.7: Summary of the testing Case 02.

Testing Case no:	Testing Case 02
Objectives	To obtaining uniformly homogenous sample and getting the several MPa of average strength from the solidified sample.
Sample Size	Width: 12.5 cm , Length: 20 cm, and Height: 9 cm
Sand type	Mikawa sand (mean diameter: 0.6 mm)
Curing Time	14 Days
Results obtained	• Obtained completely solidified sand sample. • Measured the color of the sample during the curing period and obtained the value of color (ΔL*) increase with the time. • The relationship between UCS and Vp, Vs was analyzed. • The relationships between UCS and color (L*) / UCS and wet density were analyzed. • Estimated UCS value of the cored samples were varied from 10 MPa to 3 MPa. • The results of EDX analysis demonstrated that the dominant minerals were SiO_2 and $CaCO_3$, and Ca, O and C were the main elements in the mineral precipitations. • From the XRD analysis, the sample contained with 86.3% of SiO_2 and 13.7% of $CaCO_3$ at the top of the sample. Furthermore, 90.3% of SiO2 and 9.7% of CaCO3 consisted with bottom of the sample. • The strength was large in the top layer and with the depth, the strength (UCS value) intended to decrease with the depth.

Table 5.8: Summary of the testing Case 03.

Testing Case no:	Testing Case 03
Objectives	To obtaining uniform solidified sample by changing the particle size of the sand material and also getting the several MPa of average strength from the solidified sample.
Sample Size	Width: 12.5 cm , Length: 20 cm, and Height: 9 cm
Sand type	Mizunami sand (mean diameter: 1.3 mm)
Curing Time	14 Days
Results obtained	• Using NPT, estimated UCS value was calculated. The average estimated UCS value was 4.4 MPa of the solidified sample. • There is a close relationship in between estimated UCS and color of the sample. $q_{eu} = 0.7669\ L^* - 33.921$ Where; q_{eu} = Estimated UCS (MPa) L^* = Color (L*) • From the results of XRD observation, the sample consisted with SiO_2 79.2 % and $CaCO_3$ 20.8%. Which means, the calcite precipitation was high the Mizunami sand sample than Mikawa sand sample.

Table 5.9: Summary of the testing Case 04.

Testing Case no:	Testing Case 04
Objectives	To obtaining homogeneous solidified sample by re-injecting the bacterial solution after 7 days of curing period and also increasing the curing period up to 21 days. In addition, getting the several MPa of average strength from the solidified sample.
Sample Size	Width: 12.5 cm , Length: 20 cm, and Height: 9 cm
Sand type	Mikawa sand (mean diameter: 0.6 mm)
Curing Time	21 Days
Indexes obtained	• Concentration of Ca^{2+} in outlet solution was small during the curing period because of re-injection of bacteria. • pH value maintained around 7. • Obtained completely solidified sand sample. • Measured the color of the sample during the curing period and obtained the value of color (ΔL^*) increase with the time. • The relationship between UCS and Vp, Vs was analyzed. • The relationships between UCS and color (L^*) / UCS and wet density were analyzed. • Estimated UCS value of the vertically cored samples were varied from 10 MPa to 3 MPa. Estimated UCS value decreased with the depth. • The value of estimated UCS was not so large compliance at any point of the sample which were cored horizontally. • XRD results shows that the calcite precipitation was larger at the top of the sample than the bottom of the sample (SiO_2 – 91.5% and $CaCO_3$ – 8.5% at the top and SiO_2 – 96.5% and $CaCO_3$ – 3.5% at the bottom). Nevertheless, calcite precipitation was not so large difference in the samples which were cored horizontally

5.5.2 $CaCO_3$ content of the model test samples

$CaCO_3$ content was measured for the cored samples in Testing Case 02, 03 and 04. The weight of $CaCO_3$ was measured by adding HCL for the measured weight of the sample. $CaCO_3$ precipitation was more related to the increase of strength of the sample (UCS value). From this study, it is obtained the relationship between $CaCO_3$ content and the UCS values as follows:

$$q_u = 66.6\,x^2 + 3.5287\,x \qquad \text{Eq. (5.2)}$$

Where, q_u = UCS (MPa)

x = $CaCO_3$ content (g / g sand)

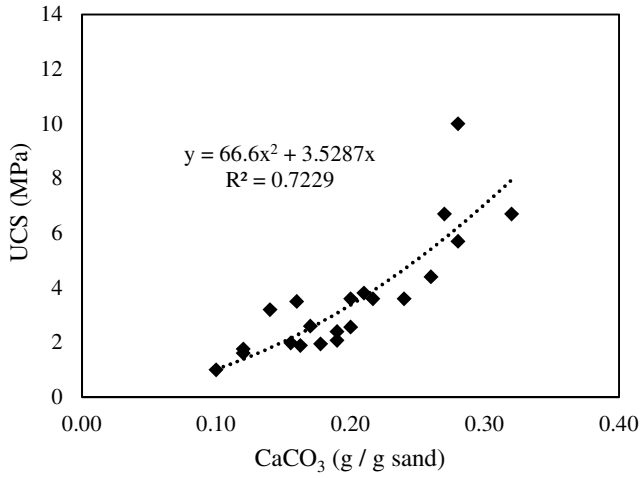

Fig. 5.42: Relationship between UCS and $CaCO_3$ content of samples which were taken from three lab model samples.

Comparison of relationship between UCS and $CaCO_3$ content with previous studies

The results for other bacteria are shown in Fig. 5.43 (Van Paassen et al. 2010, Cheng et al. 2013, and Danjo 2015). *Sporosarcina pasteuriiis* the bacterium that has been most widely applied for investigation of sand improvement using bacteria. *Bacillus sphaericus*was isolated by Al-Thawadi and Cord-Ruwisch (2012). In addition, Danjo (2015) found that the UCS of the specimen prepared using *Pararhodobacter* sp. was higher than that of the

specimen generated using *Sporosarcina pasteurii*, even though these specimens contained the same amount of total $CaCO_3$ precipitation (Fig. 5.43).

The results from this study obtained that the UCS of the specimen using *Pararhodobacter* sp. was less than the UCS of the specimen prepared using same bacteria (Danjo, 2015). However, because these specimens contained different kinds of sand and were cured under different conditions, it is unclear which bacteria is better for sand cementation. Conversely, the different amounts of total precipitation could explain the different UCS of the specimens produced using *Bacillus sphaericus* or the other two bacteria.

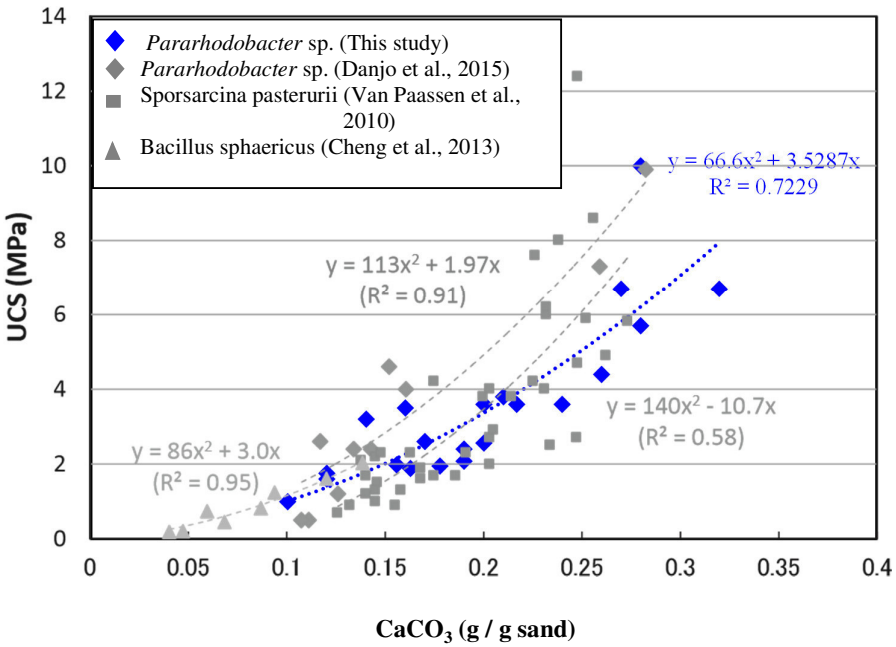

Fig. 5.43: Relationship between UCS and total $CaCO_3$ precipitation content for previous studies.

The results from previous chapter (chapter 4), it measured estimated UCS for the syringe solidification test samples. This study, UCS value was obtained for the cored samples. Fig. 5.44 shows the results obtained by syringe and model test samples. The graphs shows that the rates of increase UCS value are nearly parallel to each other. However, there is a gap between two graphs. This may happens due to an error coefficient between UCS and estimated UCS value. Future experiment is needed to identify the relationship between UCS and Estimated UCS value.

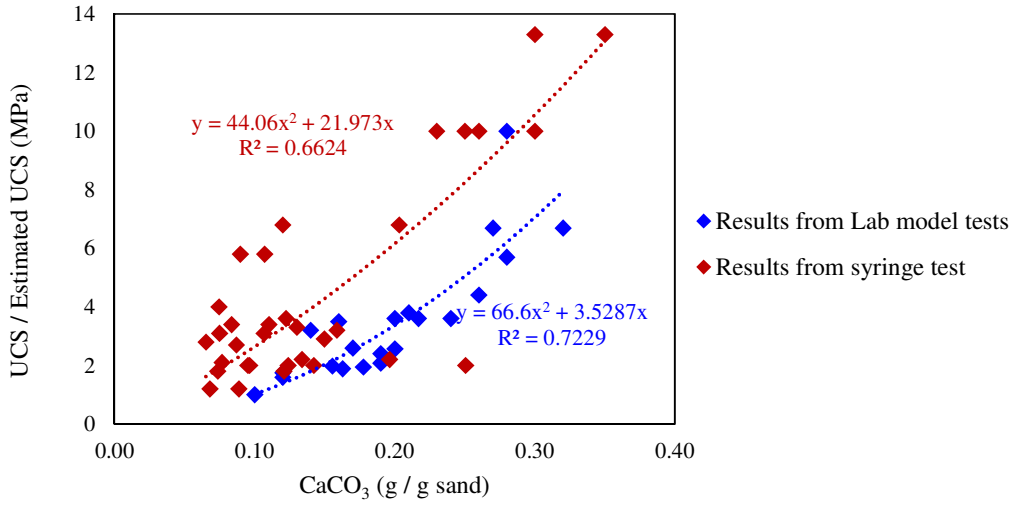

Fig. 5.44: Relationship between estimated UCS / UCS and total $CaCO_3$ precipitation content for syringe test and model test.

5.5.3 X-CT results of the model test samples

The Fig. 5.45 shows clearly that the sand particles bonded with $CaCO_3$ precipitation were large in the top of the sample than middle and bottom. Therefore, the strength decreased with the depth of the sample. Further examination of getting a homogeneous sample is need in future.

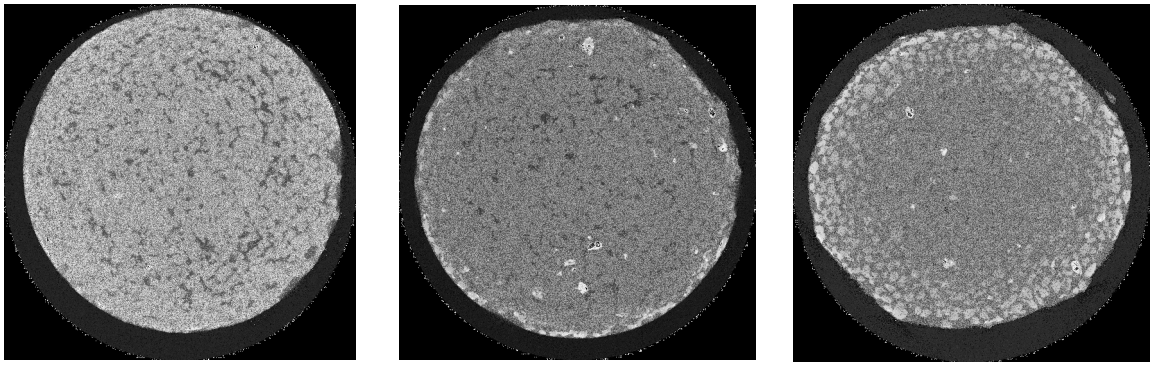

Fig. 5.45: Results of XCT at top, middle and bottom of the sample.

Originality of the model test examination

Many researches were observed sand solidification with MICP method by using common ureolytic bacteria such as *Sporosarcina pasteurii* (formerly *Bacillus pasteurii*) and *Bacillus sphaericus*. From this research study, a new uearlytic bacteria was introduced for the MICP process. The bacterium was *Pararhodobacter* sp. which was found from Okinawa, Japan. It was originality of this research.

Moreover, previous researchers (Danjo, 2015 and Shimazaki, 2015) conducted solidification using *Pararhodobacter* sp. for marine purposes and they used artificial sea water for cultivation of bacteria and solidification process. However, in this research, solidification with *Pararhodobacter* sp. was use for land usage and distilled water was introduced instead of artificial sea water.

5.5.4 Comparison between syringe solidification test and model test

Most studies on MICP soil improvement used cylindrical columns or syringes for sample preparation by pumping or injections methods. In the previous chapter (Chapter 4), it described syringe solidification test. However, it was faced many practical issues. In the syringe test, there can be a possibility of block the bacterial solution and the consolidation solution. This happened, the syringe size was very small and there may be a possibility to happening bio-clogging easily. To avoid this problem, the large size of sample preparation was used. In this chapter, the small size of lab model test was described. The methodology was same as syringe solidification test and here, materials are needed more than compare to the syringe test. In addition, unconfined compressive strength (UCS), X-ray diffraction (XRD), X-CT, primary and secondary wave velocity of the sample (Vp and Vs) and color measurement tests were conducted, which could not be conducted for syringe samples, because the sample size is not matched with the required size for conducting previously mention testing. Therefore, sufficient soil parameters were obtained from the model test.

5.6 CONCLUSION

For obtaining an uniformly homogenous sample and getting the several MPa of average strength from the solidified sample, the small size of lab model tests was conducted as described in this chapter. Unconfined compressive strength (UCS), SEM-EDX, X-CT, Primary and secondary wave velocity of the sample (Vp and Vs), $CaCO_3$ content of the sample and color measurement tests were conducted. Completely solidified samples were obtained by changing different testing conditions; height of the sample (2 cm and 9 cm), particle size of the sand material (mean diameter: 0.6 mm (Mikawa sand) and 1.3 mm (Mizunami sand)), curing time (14 days and 21 days) and re-injection of bacterial solution. The average estimated UCS value varied from 3.1 to 4.4 MPa.

The results indicate that UCS was closely related to $CaCO_3$ weight (g/ g sand) of the sample which means UCS value was increased with the increase of weight of $CaCO_3$ (g/ g sand). From this study, the relationship between $CaCO_3$ content and the UCS values can be derived by following equation.

$$q_u = 66.6\, x^2 + 3.5287\, x$$

Where; q_u = UCS of the sample (MPa)

x = amount $CaCO_3$ (g / g sand)

Moreover, estimated UCS and color (L*) shows a correlation between the parameters. This correlation is valid for Mizunami sand sample only.

$$q_{eu} = 0.7669\, L^* - 33.921$$

Where; q_{eu} = Estimated UCS (MPa)

L^* = Color (L*)).

The results of EDX analysis demonstrated that the dominant minerals were SiO_2 and $CaCO_3$, and Ca, O and C were the main elements in the mineral precipitations. From the X-CT results, percentages of the precipitation of calcite in the solidified samples were obtained.

5.6.1 Future research works

This studies show that the optimization of the MICP process is possible in controlled lab-scale experiments. The applicability of the MICP on the field-scale still requires further investigation. Some common natural conditions like high pore-water pressure, non-uniform flow field, and soil heterogeneity has not received sufficient investigation yet.

This study focused on the assessment of MICP in terms of the precipitation efficiency and the uniformity of precipitation profile. However, further investigation is needed to obtained uniformly solidified sample using *Pararhodobacter* sp. In this study, cementation media and bacterial solution were added using injection method. The sample was saturated all the time of testing period. The solution of cementation media kept around 2 cm from the top of sample. Ca^{2+} concentration and bacteria presence in not only the sample but also the solution which is keep for saturation. Due to the presence of Ca^{2+} concentration and bacteria, the process of calcite precipitation can happen at the top of sample. Therefore, top layer may harden. Cementation media penetration into soil pores under pressure to some extent, the effluent also reduces the number of bacteria as well as a portion of urease produced by bacteria, and the samples may not be uniform along the flow. However, for clarify this matter, further investigation with reducing the cementation media level at the top of sample is needed in future.

MICP is a sustainable and environmentally friendly technique that must be improved both at laboratory and field scales. This technique must be optimized to find the best conditions (pH, soil, temperature, concentration of cementation media etc.) for bacterial activity, and also to get homogeneous distribution in the soil. It is believed that the conditions for bacterial activity were achieved, and therefore future research must be focused on finding efficient injection systems both bacteria and cementation media. Only after solving these problems the UCS from this treatment can be compared with that for soil-cement mixtures, however, it is expected that UCS of cement may be larger.

REFERENCES

Mortensen BM, Haber M J, DeJong J T, Caslake L F, Nelson DC, “Effects of environmental factors on microbial induced calcium carbonate precipitation,” *Journal of Appl. Microbiol.*, Vol. 111(2) 2011, pp. 338–349.

Chou C, Seagren EA, Aydilek AH, Lai M, “Biocalcification of sand through ureolysis,” *Journal of Geotech. Geoenviron. Eng.*, Vol. 10.1061/ (ASCE) GT.1943-5606.0000532, 2011, pp. 1179–1189.

Rebata-Landa V, “Microbial activity in sediments: Effects on soil behavior.” Ph.D. thesis, Georgia Institute of Technology, Atlanta, GA 2007.

Mitchell JK, Santamarina CJ, “Biological considerations in geotechnical engineering.” *Journal of Geotech. Geoenviron. Eng*., Vol. 131(10), 2005, pp. 1222–1233.

Qabany AA, Soga K, Santamarina C, “Factors affecting efficiency of microbially induced calcite precipitation,” *Journal of Geotech. Geoenviron. Eng,* Vol. 138(8), 2012, pp. 992–1001.

Harkes MP, Van Paassen LA, Booster JL, Whiffin VS, Van Loosdrecht MCM, "Fixation and distribution of bacterial activity in sand to induce carbonate precipitation for ground reinforcement," *Ecol. Eng., V*ol. 36, 2010, pp. 112-117.

Ritvo G, Dassa O, Kochba M, "Salinity and pH effect on the colloidal properties of suspended particles in super intensive aquaculture systems," *Aquac.,* Vol. 218, 2003, pp. 379-386.

Torkzaban S, Tazehkand SS, Walker SL, Bradford SA, "Transport and fate of bacteria in porous media: Coupled effects of chemical conditions and pore space geometry," *Water Resour. Res.,* Vol. 44, 2008, pp. W04403.

Danjo T, Kawasaki S, “Microbially induced sand cementation method using Pararhodobacter sp. strain S01, inspired by beachrock formation mechanism, ” Journal of *Materials Transactions*, Vol. 57 (3), 2016, pp. 428-437.

Danjo T, Doctoral Thesis, Hokkaido University, Japan, 2015.

CHAPTER 6

CONCLUSIONS AND FUTURE RESEARCH

6.1 Summary of work presented and main conclusions

This research investigated the sustainability and cost effective techniques for ground improvement. Biochemical methods introduced in this thesis. It consisted of two major sections.

1) Soil Improvement with Calcium Phosphate Compound (CPC)
2) Soil improvement with Microbial Induced Calcite Precipitation (MICP)

In Chapter 1, research background, objectives, and originality of thesis were described. CPC method and MICP method also describe in the Chapter 1. Few studies were done regarding cementation with CPC-Chem and CPC powder method. Therefore, in this study additionally study for identify the best CPC mixture for sand solidification. Moreover, CPC-powder methods were conducted previous researchers and they used chemicals as a powder. But in this thesis bio-mineral was introduced as a powder instead of chemicals. In this research, CPC-powder method was consisted with experiments using scallop cell powder.

Many researches were observed sand solidification with MICP method by using common ureolytic bacteria such as *Sporosarcina pasteurii* (formerly *Bacillus pasteurii*) and *Bacillus sphaericus*. From this research study, we introduced a new uearlytic bacteria for the MICP process. The bacterium was *Pararhodobacter* sp. which was found from Okinawa, Japan. It was originality of this research.

Moreover, previous researchers (Danjo, 2015 and Shimazaki, 2015) conducted solidification using *Pararhodobacter* sp. for marine purposes and they used artificial sea water for cultivation of bacteria and solidification process. However, in this research, solidification with *Pararhodobacter* sp. was use for land usage and distilled water was introduced instead of artificial sea water.

Chapter 2 consisted with soil improvement using CPC-Chem method and Soil improvement using CPC-powder method was viewed in Chapter 3. In Chapter 4, under MICP process, syringe solidification test using MICP method was detailed. Chapter 5 consisted of

model test for sand solidification using MICP method and finally, in Chapter 6 summarized and provided a conclusion that may guide future work.

Calcium phosphate compound (CPC) develops calcium carbonate (CC) precipitation throughout the soil and increase the soil strength. In Chapter 2, the condition for CPC precipitation by using different mixtures of calcium and phosphate stock solutions were investigated and analyzed. For that, Toyoura sand test pieces were cemented by CPC solutions and cured up to 28 days and carried out unconfined compressive strength (UCS) test. The best CPC-Chem mixtures were 1.5 M CA: 3.0 M DPP and 1.5 M CN: 3.0 M DPP with the concentration of Ca/P ratio is 0.5. In addition, the UCS values of Toyoura sand test piece cemented with CA: DPP and CN: DPP were 144.65 kPa and 143.60 kPa respectively. Furthermore, pH concentration and scanning electron microscope (SEM) were observed. The results indicate that the pH concentration was increased with the curing time for the calcium to phosphate molar ratio was 0.5. Wisker-like crystal formation showed the only sample prepared with CA: DPP=0.5 mixture. It has been reported that HA whiskers are formed by adding an acetic acid solution to amorphous calcium phosphate (Toyama et al, 2001). In Portland cement, the formation of ettringite, which shows whisker-like crystals, promotes solidification and increases strength (Sakai E. at al, 2004). Therefore, it is concluded that the CPC mixture of 1.5 M CA: 3.0 M DPP with the concentration of Ca/P ratio = 0.5 is better than other mixtures tested in this study.

Grouting using CPC has been used for a countermeasure for liquefaction in geotechnical engineering applications and it is an economical and environmentally friendly technique that develops to form calcium carbonate precipitation throughout the soil, leading to an increase in soil strength. In Chapter 3, the aim was to improve strength by adding CPC with $CaCO_3$ (commercially found) and scallop shell (naturally found) powder and exceed a maximum UCS of 100 kPa after 28 days of curing, which is the strength required as a countermeasure against soil liquefaction during an earthquake. For that, initially, Toyoura sand test pieces were cemented by CPC solutions only and cured up to 56 days and carried out unconfined compressive strength (UCS) test. Moreover, Toyoura sand test pieces were cemented by CPCs with $CaCO_3$ (CC) powder and CPCs with scallop shell (SS) powder and cured and these specimens also analyzed with UCS tests. The UCS of the sand test pieces cemented by CPC with SS powder and CC powder was higher than that of the test pieces with no added powders. In addition, a series of laboratory experiments were conducted, including pH concentration, scanning electron microscope (SEM) in order to observe the microscopic structure, density before and after curing etc. The results indicate that the density and the pH

concentration of the sand test pieces cemented by CPC with SS powder and CC powder were higher than that of the test pieces with no added powders.

Chapter 4 and 5, describe MICP process. Microbial induced calcite precipitation utilizing urea hydrolysis is a complex biochemical process, especially when it takes place between sand particles for improvement of soil engineering properties. There are many factors that may affect this process. Some of these factors reported in Chapter 4 using syringe solidification test. In the chapter 4, it was described the effect of bacteria concentration, re-injection of bacteria, sand type and particle size of the sample, injection interval of the cementation media, concentration of the cementation media, curing time, temperature, and viscosity of the bacterial solution for the MICP process. The result of estimated UCS value shows that all the studied factors have an obvious effect on the MICP treated sand. More than 3 MPa of estimated UCS value obtained from the solidified samples and also it was obtained more than 10 MPa of estimated UCS value for the testing cases of changing concentration of cementation media and re-injection of the bacterial solution after 7 days of curing period. Multiple regression analysis showed that the relevant conditions for estimated UCS, q_u (MPa), was experimentally determined by following equation (Eq. 6.1). These conditions were selected as explanatory variables, and the UCS of specimens generated at a curing temperature of 30 °C, 1.0 g of bacterial population, and 0.6 mm particle size diameter (Mikawa sand) were used as objective variables.

$$\boldsymbol{q_{eu} = 13.99\, C_{Ca} + 0.37\, D - 0.09} \qquad \text{Eq. 6.1}$$

Where; q_{eu} = Estimated UCS (MPa)

C_{Ca} = Concentration of cementation media (M)

D = Curing time (Days)

Overall, the results of this study were contributed to the application of a new technique for soil improvement and bio-stimulation.

For obtaining an obtaining uniformly homogenous sample and getting the several MPa of average strength from the solidified sample, the small size of lab model tests was conducted as described in chapter 5. Unconfined compressive strength (UCS), SEM-EDX, X-CT, Primary and secondary wave velocity of the sample (Vp and Vs), $CaCO_3$ content of the sample and color measurement tests were conducted. Completely solidified samples were obtained by changing different testing conditions; height of the sample (2 cm and 9 cm), particle size of

the sand material (mean diameter: 0.6 mm (Mikawa sand) and 1.3 mm (Mizunami sand)), curing time (14 days and 21 days) and re-injection of bacterial solution. The average estimated UCS value varied from 3.1 to 4.4 MPa.

The results indicate that UCS was closely related to $CaCO_3$ weight (g/ g sand) of the sample which means UCS value was increased with the increase of weight of $CaCO_3$ (g/ g sand). From this study, the relationship between $CaCO_3$ content and the UCS values can be derived by following equation (Eq. 6.2).

$$q_u = 66.6\,x^2 + 3.5287\,x \qquad \text{Eq. 6.2}$$

Where; q_u = UCS of the sample (MPa)

x = amount $CaCO_3$ (g / g sand)

Moreover, estimated UCS and color (L*) shows a correlation between the parameters (Eq. 6.3). This correlation is valid for Mizunami sand sample only.

$$q_{eu} = 0.7669\,x - 33.921 \qquad \text{Eq. 6.3}$$

Where; q_{eu} = Estimated UCS (MPa)

x = Color (L*)).

The results of EDX analysis demonstrated that the dominant minerals were SiO_2 and $CaCO_3$, and Ca, O and C were the main elements in the mineral precipitations. From the X-CT results, percentages of the precipitation of calcite in the solidified samples were obtained.

The results obtain from each chapter point out that the solidification using CPC method and MICP method stand as promising techniques for soil improvement.

6.2 Future research works

6.2.1 Suggestions for future works in CPC method

Changes in the concentration of the reaction mixture were not reflected proportionally in the strength of the sand test pieces. In the future, additional tests aimed at determining the improvement in the strength by CPC are needed to understand more clearly the underlying mechanical processes and to facilitate practical application. The relationship between the strength and the various CPC precipitation parameters (concentration and pH of reaction mixture, curing time, etc.) should be examined in further detail, as continued research is needed

to identify the process or processes that link crystal precipitation to the increase in strength. Furthermore, shearing and permeability tests using pieces cemented by CPC should be conducted to evaluate the applicability of CPCs for purposes such as permeability control and reinforcement of soil and rock.

6.2.2 Suggestions for future works in MICP method

This studies show that the optimization of the MICP process is possible in controlled lab-scale experiments. The applicability of the MICP on the field-scale still requires further investigation. Some common natural conditions like high pore-water pressure, non-uniform flow field, and soil heterogeneity has not received sufficient investigation yet.

This study focused on the assessment of MICP in terms of the precipitation efficiency and the uniformity of precipitation profile. However, further investigation is needed to obtained uniformly solidified sample using *Pararhodobacter* sp. In this study, cementation media and bacterial solution were added using injection method. The sample was saturated all the time of testing period. The solution of cementation media kept around 2 cm from the top of sample. Ca^{2+} concentration and bacteria presence in not only the sample but also the solution which is keep for saturation. Due to the presence of Ca^{2+} concentration and bacteria, the process of calcite precipitation can happen at the top of sample. Therefore, top layer may harden. Cementation media penetration into soil pores under pressure to some extent, the effluent also reduces the number of bacteria as well as a portion of urease produced by bacteria, and the samples may not be uniform along the flow. However, for clarify this matter, further investigation with reducing the cementation media level at the top of sample is needed in future.

MICP is a sustainable and environmentally friendly technique that must be improved both at laboratory and field scales. This technique must be optimized to find the best conditions (pH, soil, temperature, concentration of cementation media etc.) for bacterial activity, and also to get homogeneous distribution in the soil. It is believed that the conditions for bacterial activity were achieved, and therefore future research must be focused on finding efficient injection systems both bacteria and cementation media. Only after solving these problems the UCS from this treatment can be compared with that for soil-cement mixtures, however, it is expected that UCS of cement may be larger.